Cloning, expression, characterization and applications of cyanase from a thermophilic fungus *Thermomyces lanuginosus* SSBP

BIBHUTI RANJAN

Submitted in fulfillment of the requirements for the degree of

Doctor of Philosophy

In

Biotechnology

Department of Biotechnology and Food Technology, Faculty of Applied Sciences,

Durban University of Technology, Durban, South Africa

2018

Supervisor: Prof. Suren Singh

Co-supervisor: Dr. Santhosh Kumar Kuttan Pillai

Co-supervisor: Prof. Kugenthiren Permaul

DECLARATION

I hereby declare that this dissertation is my own, unaided work. It is being submitted for the award of the Doctor of Philosophy in Biotechnology, to the Durban University of Technology, Department of Biotechnology and Food Technology, Faculty of Applied Sciences, Durban, South Africa. It has not been submitted before for any degree or dissertation to any other institution.

[redacted]

Student:
Mr. Bibhuti Ranjan (M.Sc.)

07/08/2018

Date

[redacted]

Supervisor:
Prof. S. Singh (Ph. D)

7 AUG 2018

Date

[redacted]

Co Supervisor:
Dr. S. Pillai (D. Tech)

07/08/2018

Date

[redacted]

Co Supervisor:
Prof. K. Permaul (Ph. D)

07/08/2018

Date

DEDICATION

Dedicated to God

&

My Family

TABLE OF CONTENTS

ACKNOWLEDGEMENTS

First and foremost, I would like to express my heartfelt gratitude and regards to Prof. Suren Singh, for giving me the opportunity to do research in his group. Without his support, insight and encouragement, this thesis work would be impossible. I am really fortunate to have met and worked with him, and also I am gratefully indebted for the opportunity he has provided me to work in Prof. Liang Tong's Lab at Columbia University during my pursuit of the PhD. My heartfelt thanks must also go to co-supervisors, Dr. Santhosh Kumar Kuttan Pillai and Prof. Kugenthiren Permaul, for their intellect, and timely inputs at crucial junctures right from the commencement of the thesis till the last minute revisions.

My special thanks go to Prof. Liang Tong for allowing to do part of PhD work under his supervision. His limitless help and fruitful discussions aided me overcome every obstacle I encountered during the project. I have also been constantly inspired by his enduring dedication to science and enthusiasm to push forward the frontier of human knowledge. I also want to thank Tong Lab members, for sharing with me their brilliant ideas regarding work, and making the lab such a pleasant place to work in. In particular, I want to thank Dr. Philip H. Choi for training me on every research technique required to thrive in the lab when I knew nearly nothing about structural biology.

I greatly acknowledge the financial support provided by National research foundation (NRF), Durban University of Technology (DUT) and Technology Innovation agency (TIA) that made my PhD work possible.

I would like to extend my special thanks to all staff and post-graduate students in the Department of Biotechnology and Food Technology for their help and assistance throughout the course of this study.

Finally, I would like to thank my parents for all the sacrifices made and being the guiding light in all my pursuits. I also acknowledge the encouragement provided by my family members and boosting my morale when I was in doubt. I deeply appreciate the words of encouragement received from my friends on numerous occasions. I had the privilege of knowing people from diverse cultures and the fun times spent with my labmates.

LIST OF FIGURES

LIST OF TABLES

PUBLICATIONS AND CONFERENCE PRESENTATIONS

Publications in international journals

Ranjan, B., Pillai, S., Permaul, K., and Singh, S. (2018) A novel strategy for the efficient removal of toxic cyanate by the combinatorial use of recombinant enzymes immobilized on aminosilane modified magnetic nanoparticles. *Bioresour. Technol.* **253**: 105–111.

Ranjan, B., Pillai, S., Permaul, K., and Singh, S. (2017) Expression of a novel recombinant cyanate hydratase (rTl-Cyn) in *Pichia pastoris*, characteristics and applicability in the detoxification of cyanate. *Bioresour. Technol.* **238**: 582–588.

Ranjan, B., Pillai, S., Permaul, K., and Singh, S. (2018) Simultaneous removal of heavy metals and cyanate in a wastewater sample using immobilized cyanate hydratase on magnetic-multiwall carbon nanotubes (Accepted: *J. Hazard. Mater.*).

Publications under preparation

Ranjan, B., Choi, P.H., Pillai, S., Permaul, K., Tong, L., and Singh, S. (2018) Crystal structure of a fungal cyanase and implications for catalytic mechanism.

International conferences

Ranjan, B., Pillai, S., Permaul, K., Tong, L., and Singh, S. Exploiting the untapped potential of a fungal cyanase in bioremediation. SIMB Annual Meeting and Exhibition, 12-16 August, 2018, Chicago, LI, USA (Accepted).

Ranjan, B., Pillai, S., Permaul, K., and Singh, S. Integrative approaches for bio-remediation towards environmental sustainability. Sustainable Energy and Environmental Challenges (SEEC), 31 December, 2017- 3 January, 2018, Bangalore, India.

Ranjan, B., Pillai, S., Permaul, K., and Singh, S. A novel recombinant cyanate hydratase (rTl-Cyn) from the thermophilic fungus *Thermomyces lanuginosus* for plant growth promotion. SIMB Annual Meeting and Exhibition, 24-28 July, 2016, New Orleans, LA, USA.

Ranjan, B., Puri, A.K., Tong, L., Permaul, K., Pillai, S., and Singh, S. Crystallization and application of a novel cyanate hydratase for cyanate remediation. International Conference on Strategies for Environmental Protection and Management (ICSEPM-2016), 11-13 December, 2016, New Delhi, India.

National conferences

Ranjan, B., Pillai, S., Permaul, K., and Singh, S. Potential use of immobilized cyanase from *Thermomyces lanuginosus* in bioremediation of wastewater. The South African Society for Microbiology's (SASM), 4-7 April, 2018, Johannesburg, South Africa.

Ranjan, B., Pillai, S., Permaul, K., and Singh, S. Cloning, expression and characterization of cyanate hydratase from the thermophilic fungus *Thermomyces lanuginosus* SSBP. The South African Society for Microbiology's (SASM) 19th Biennial Congress, 17-20 January, 2016, Durban, South Africa.

Ranjan, B., Nekhumb, D., Pillai, S., Permaul, K., and Singh, S. Comparative study of cyanate hydratase production by different strains of thermophilic fungus *Thermomyces lanuginosus*. The South African Society for Microbiology's (SASM) 19th Biennial Congress, 17-20 January, 2016, Durban, South Africa.

Ranjan, B., Pillai, S., Permaul, K., and Singh, S. (2015) Amelioration of toxic soil contaminants using cyanate hydratase from the thermophilic fungus *Thermomyces lanuginosus*. Catalysis Society of South Africa (CATSA), 15-18 November, 2015, Cape Town, South Africa.

ABSTRACT

Rapid industrialization and proliferative development of chemical and mining industries have resulted in increased global pollution and environment deterioration, due to the release of numerous toxic substances. This has extreme relevance in the South African context due to the high amount of cyanide used by local mines in comparison to that utilized globally. This has created the need for the development of novel approaches *viz*., using microbial enzymes for its remediation because of lower process times, lower energy requirements, and their cost-effective, nontoxic and eco-friendly characteristics. From previous work in our lab, the whole genome sequencing and secretome analysis of the industrially-important fungus *Thermomyces lanuginosus* SSBP revealed the presence of a cyanate hydratase gene and enzyme, respectively. Cyanate hydratase detoxifies cyanate in a bicarbonate-dependent reaction to produce ammonia and carbon dioxide. The cyanate hydratase gene (*Tl-Cyn*) from this fungus was therefore cloned, overexpressed, purified, characterized and its potential in cyanate detoxification has also been evaluated. The recombinant cyanate hydratase (rTl-Cyn) showed high catalytic efficiency, suggesting that it could be used for bioremediation applications.

Though, cyanate hydratase catalyzes the decomposition of cyanate, the requirement of bicarbonate is a major drawback for its effective utilization in large-scale applications. Hence, a novel strategy was developed to limit the bicarbonate requirement in cyanate remediation, by the combinatorial use of two recombinant enzymes *viz*., cyanate hydratase (rTl-Cyn) and carbonic anhydrase (rTl-CA) from *T. lanuginosus*. This integrative approach resulted in the complete degradation of cyanate using 80% less bicarbonate, compared to the cyanate hydratase alone. In addition, co-immobilization of these recombinant enzymes onto magnetic nanoparticles and evaluation of their potential in bio-remediation of cyanurated wastes together with their reusability resulted in more than 80% of cyanate detoxification in wastewater samples after 10 cycles.

Another novel strategy was also developed for the simultaneous removal of heavy metals and cyanate from synthetic wastewater samples, by immobilizing the rTl-Cyn on magnetic multi-walled carbon nanotubes (m-MWCNT-rTl-Cyn). The m-MWCNT-rTl-Cyn simultaneously reduced the concentration of chromium (Cr), iron (Fe), lead (Pb) and copper (Cu) by 39.31, 35.53, 34.48 and 29.63%, respectively, as well as the concentration of cyanate by ≥85%.

The crystal structure of Tl-Cyn in complex with inhibitors malonate or formate at 2.2 Å resolution was solved for the first time to elucidate the molecular mechanism of cyanate hydratase action. This structure enabled the creation of a mutant enzyme with ~1.3-fold enhanced catalytic activity as compared to the wild-type Tl-Cyn. In addition, the active site region of Tl-Cyn was found to be highly conserved among fungal cyanases. Information from the 3D structure could enabled the creation of novel fungal cyanases, which may have potential for biotechnological applications, biotransformation and bioremediation.

CHAPTER 1

1. Introduction and Literature Review

Cyanide is a toxic compound which poses a major threat to health and ecosystems. It is produced by several industries such as: electroplating; ore leaching; steel manufacturing; and also by several other anthropogenic activities (Patil and Paknikar, 2000; Hamel, 2011). Cyanide is also applied as an anticaking agent in road salt and fire retardants. In the USA, 10 million tonnes of road salt representing an environmental input of 700 tonnes of cyanide are used annually (Baxter and Cummings, 2006). Besides, at the salt storage depots, runoff from precipitation may result in the leaching of cyanide into surface waters (Paschka *et al.*, 1999). In a similar manner, the use of cyanide compounds in chemical retardants for firefighting results in 400 tonnes of cyanide derivatives being applied annually during forest fire control in the USA (Mudder and Botz, 2004). In addition to this, it is also produced by a number of organisms *viz*., plants, bacteria and fungi (Dubey and Holmes, 1995).

Cyanate is an important derivative of cyanide, which is produced by spontaneous photo-oxidation (Carepo *et al.*, 2004; Malhotra *et al.*, 2005) and chemical-oxidation of cyanide (Barakat *et al.*, 2004; Baxter and Cummings, 2006). It is also produced naturally from the dissociation of urea and carbamoylphosphate (Qian *et al.*, 1997; Purcarea *et al.*, 2003). Currently, cyanate has been used in agriculture as a pesticide and fungicide (Elmore *et al.*, 2015). Pesticides used in agriculture has resulted in an increase in production, however, only 5% of the total chemicals applied reach the intended targets (Kookana *et al.*, 1998; Nawaz *et al.*, 2011), and the remainder enters into soil and water and causes environmental pollution (Barriuso and Koskinen, 1996; Liu *et al.*, 2001; Lai, 2017; Clasen *et al.*, 2018). Notably, main concerns associated with cyanide or cyanate is their prospective toxicity, which is generated predominantly through anthropogenic activity and also as an outcome of cyanogenic activity by a number of organisms.

1.1 Naturally occurring sources of cyanide/cyanogenic compounds in the environment

Among living organisms, cyanide compounds are produced by many taxa, including higher plants (Jones, 1998; Pičmanová *et al*., 2015; Rajniak *et al*., 2015; van Ohlen *et al*., 2017; Bjarnholt

et al., 2018), arthropods (Eisner *et al.*, 1996; Zagrobelny *et al.*, 2008), fungi (Dubey and Holmes, 1995; Baxter and Cummings, 2006; Spiteller, 2015), algae (Dubey and Holmes, 1995; Wolfe *et al.*, 2001) and bacteria (Dubey and Holmes, 1995; Blumer and Haas, 2000; Zdor, 2015). Plants produce cyanide compounds in the form of cyanogenic glucosides (bitter tasting) as a defense against herbivores and pathogens (Jones, 1998; Pičmanová *et al.*, 2015; Rajniak *et al.*, 2015; Bjarnholt *et al.*, 2018). Such plants include mainly alfalfa, sorghum and cassava. Cyanide is also present in many seeds, nuts, fruits and vegetables, which include: apricots; bean sprouts; cashews; cherries; chestnuts; corn; kidney beans; lentils; nectarines; peaches; peanuts; pecans; pistachios; potatoes; soybeans; and walnuts. Conversely, a number of fungi and bacteria utilize the toxicity of cyanide compounds in a more obvious way by generating cyanide-containing antibiotic compounds to inhibit competitive organisms. For example, *Chromobacterium violaceum* ATCC 53434 produces the isonitrile antibiotic, aerocyanidin, that is mainly active against Gram-positive bacteria (Parker *et al.*, 1988), and the fungus *Trichoderma harzianum* produces homothallin II, a nitrile with an extensive activity against fungi and bacteria. In nutrient-limited environments such as soil, or where competition for resources is extreme, as in the rhizosphere, these compounds apparently increase the competitive advantage of the cyanogenic organisms (Baxter and Cummings, 2006).

1.2 Anthropogenic sources of cyanide/cyanogenic compounds in the environment

There are a number of significant anthropogenic inputs of cyanide into the soil and water environment (Ubalua, 2010; Kwaansa-Ansah *et al.*, 2017; Priestley *et al.*, 2018; Tapia *et al.*, 2018). Possibly, the most significant is the discharge of municipal wastewater by sewage treatment plants, predominantly from industrialized areas, where cyanide can reach concentrations of upto 65 000 mg/L (Machingura *et al.*, 2016). Despite its toxicity, there is a substantial demand for cyanide in many processes.

1.2.1 Electroplating industries

Electroplating is a procedure that uses electric current to minimize dissolved metal cations, so that they form a thin coherent metal coating on an electrode. It is mainly used for: (i) to alter their appearance; (ii) to provide a protective coating; (iii) to give them special surface properties; and (iv) to give them engineering or mechanical properties. Discharges from electroplating industries are one of the key concerns of the present world due to the hazardous nature of its wastes

(Orescanin *et al.*, 2009, 2018; Naim *et al.*, 2010). The effluent released from these industries can pollute water, resulting in toxic effects to human health and ecosystems due to their prospective of bioaccumulation. The effluent wastewater from the electroplating industries contain; chromium, cyanide, nickel, copper, zinc and lead (Jeon *et al.*, 2001; Naim *et al.*, 2010; Bhateria and Dhaka, 2017; Orescanin *et al.*, 2018).

1.2.2 Coal-gasification/Coal-coking plants

Coal gasification is the method of producing syngas, a mixture comprising primarily of carbon monoxide (CO), hydrogen (H_2), carbon dioxide (CO_2), methane (CH_4), and water vapour (H_2O) from coal, water, and oxygen. Recently, large-scale use of coal gasification is primarily for electricity generation (Zuldian *et al.*, 2017), such as in integrated gasification combined cycle power plants (Chen *et al.*, 2015; Prabu, 2015), for the production of chemical feedstocks, or for the production of synthetic natural gas (Guo *et al.*, 2015; Man *et al.*, 2016; Xiang *et al.*, 2018). Historically, the main coal refining processes in the USA have been linked with coal coking for the manufacture of metallurgical coke and for the production of by-products (Luthy, 1981). Cyanide, sulphide, and thiocyanate are major pollutants in industrial wastewaters from coke-plants, iron-production, coal-gasification and liquefaction (Luthy and Bruce Jr., 1979; Wang *et al.*, 2012; Ji *et al.*, 2016). The existence of these pollutants in coal-coking wastes results from the pyrolysis of coal at high temperature. Coke is manufactured in by-product regaining ovens, where coal is heated under vacuum at temperatures ranging from 1500 to 2000°F. In addition, ammonia is also produced as a result of the release of amino or substituted amino type side chains from the coal structure (Jeremiáš *et al.*, 2014). However, it is also believed that ammonia released from coal may be converted into cyanide under the situations existing during coal carbonization and gasification (Luthy and Bruce Jr., 1979). Hydrogenation during gasification also results in the formation of ammonia and further into cyanide, as a secondary reaction. It may also be produced in small amounts by pyrolysis of nitrogenous products, obtained as a result of coal decomposition, such as from pyridine (Luthy and Bruce Jr., 1979; Hansson *et al.*, 2003). It is well-known that cyanide can react with oxidized products of sulphide to produce thiocyanate in the aqueous phase (Luthy and Bruce Jr., 1979). Moreover, it was found that, the association between simple and complex cyanide species in industrial wastes is not consistent. For example, the complex forms of cyanide found in wastes from the chemical manufacturing plants can be either 0% or 100% of the

total cyanide content (Dash *et al.*, 2009). However, it generally appears that the cyanide in industrial wastes are found mostly in complexed species. Thiocyanate is one of the most important cyanide-complexing compounds present in industrial effluents.

1.2.3 Recovery of precious metals

Cyanide leaching has been an effective technology applied globally for the recovery of valuable metals (especially Au and Ag) from ores/concentrates/waste materials (Montero *et al.*, 2012; Akcil *et al.*, 2015; Johnson, 2015). On the other hand, cyanide is constantly favoured over other chemical compounds because of its potential to deliver high recovery at a reduced cost (Akcil *et al.*, 2015). Chemical alternates for cyanide have been explored for decades; however, cyanide remains the high-class lixiviant of choice in the mining industry, because of its availability, efficiency and economics. Remarkably, about 90% of the gold manufacturing processes worldwide utilize cyanide for its extraction (Mudder and Botz, 2004). The commercial introduction of cyanide was initially started in New Zealand over a century ago, and subsequently it has been used worldwide for the extraction of gold, silver and other metals. The use of cyanide in the world mines is shown in Fig. 1.1, which indicates that Africa is the highest cyanide user (27%) in the world and mine-related pollution in the central rand goldfield, South Africa is shown in Fig. 1.2.

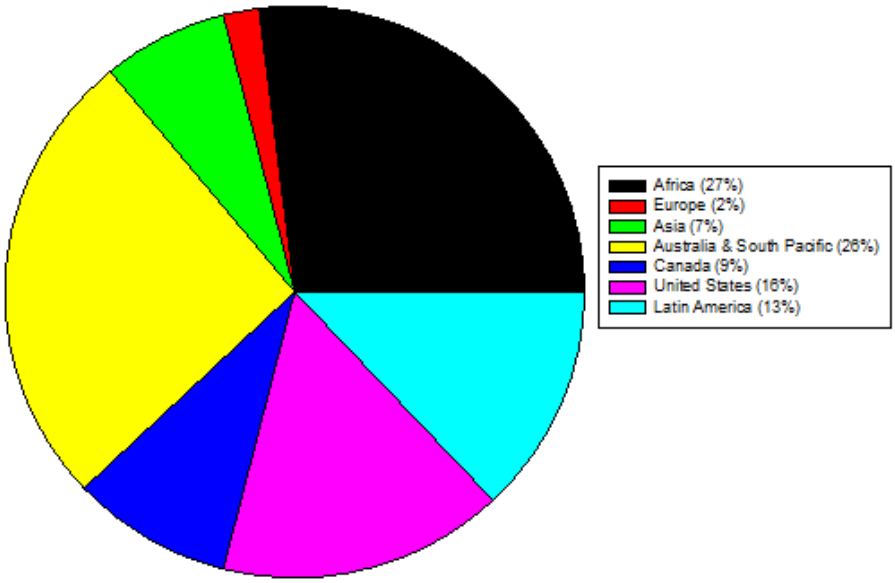

Fig. 1.1 World-wide distribution of cyanide use in mines (Mudder and Botz, 2004).

The demand for sodium cyanide worldwide is about 360000 tonnes per annum of which about 120000 tonnes (one-third) is used in the recovery of gold and silver. In addition, mining uses 18% of the total cyanide produced globally (https://miningfocus.squarespace.com/s/ICMMCY1.PDF) (Fig. 1.3). Cyanide effectively and efficiently extracts gold from ore. Although, a number of other chemicals can extract gold, such as halogens, thiourea, and thiosulphate, these form less stable complexes with gold and thus need more destructive conditions and oxidants to dissolve the gold. The use of alternative chemicals are limited because of its high risk to health and the environment compared to cyanide (Akcil, 2010).

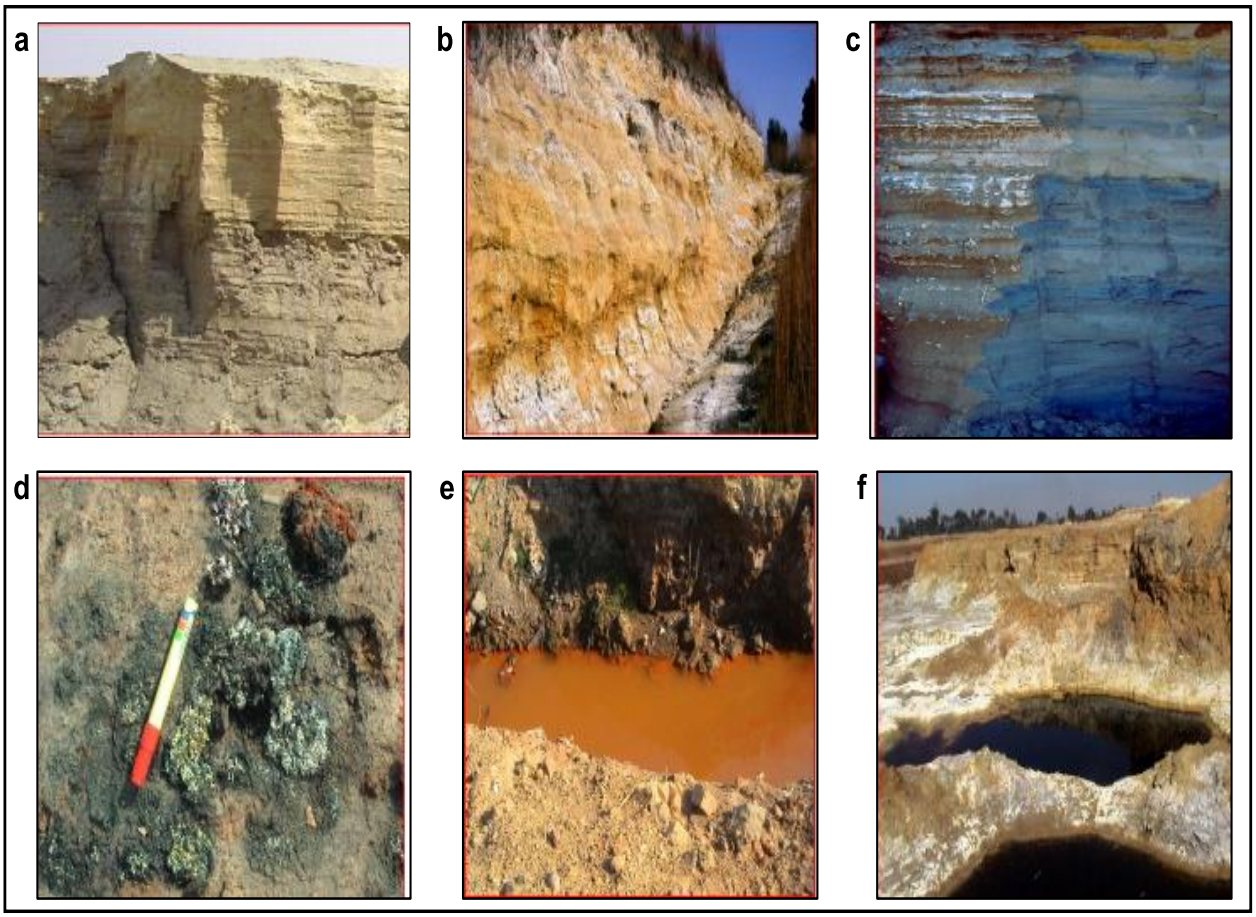

Fig. 1.2 Mine-related pollution in the central rand goldfield of South Africa showing: **(a)** slimes dump oxidation front; **(b)** slimes dump showing efflorescent crust on the lower slope; **(c)** slimes dump showing precipitation of ferric hydroxide in a paddock at the foot; **(d)** and **(e)** various colours of efflorescent crusts around a paddock at the foot of a slimes dump; **(f)** polluted water pond in a domestic ground (Tutu *et al.*, 2008).

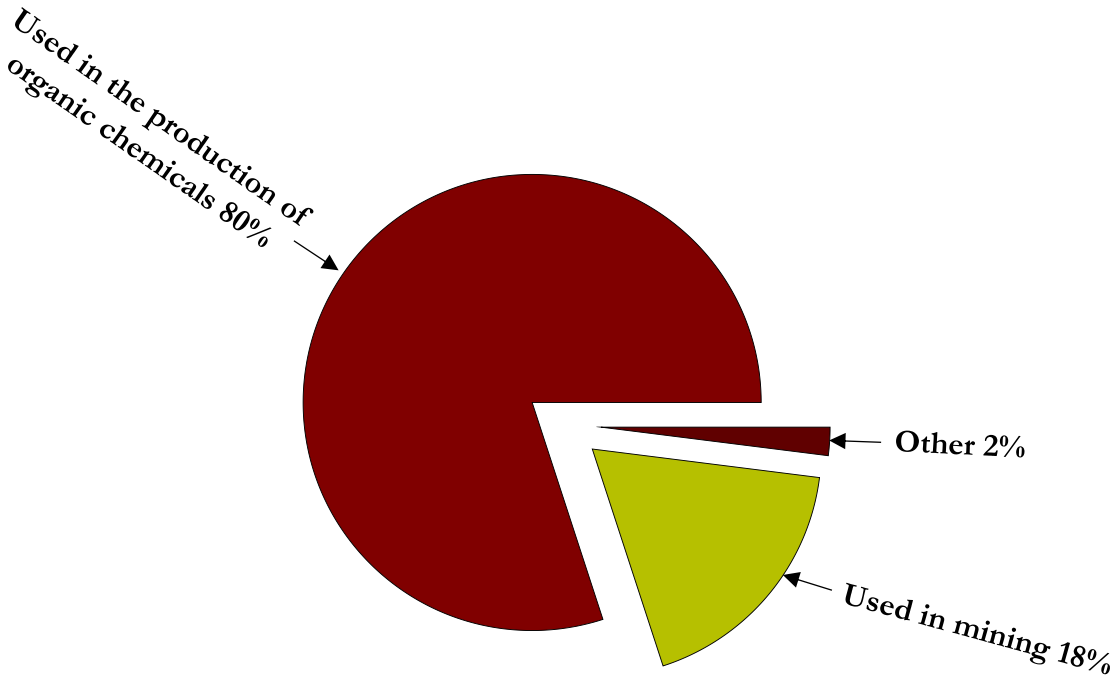

Fig. 1.3 World-wide industrial uses of cyanide. About 80% of the total is used in organic chemical manufacturing, 18% in mining and 2% in other industries.

The mining-industry continues to hunt for cost-effective and eco-friendly substitutes to cyanide. Although, they have investigated alternative lixivants from several decades, no chemical system has been developed thus far, which is safer, from an environmental and worker perspective, as well as cost-effective and efficient. Therefore, irrespective of the perceived or real risks associated with cyanide usage, it is being permitted for mining operations. It is far superior and safer for society and the environment compared to the use of mercury for the extraction of gold (Mudder and Botz, 2004). Environmental issues due to mining operations are often accredited to cyanide, whether it is involved or not. This situation arises from the perception that mining and cyanide are synonymous, or a simple desire to depict mining in a negative light (Mudder and Botz, 2004).

Gold cyanidation is an electrochemical process which depend on the fact that gold dissolves in the alkaline cyanide solution and forms gold cyanide complex ($Au(CN)_2^-$) in the so called anodic reaction (Senanayake, 2008; Bas *et al.*, 2017; Asamoah *et al.*, 2018) (Fig. 1.4).

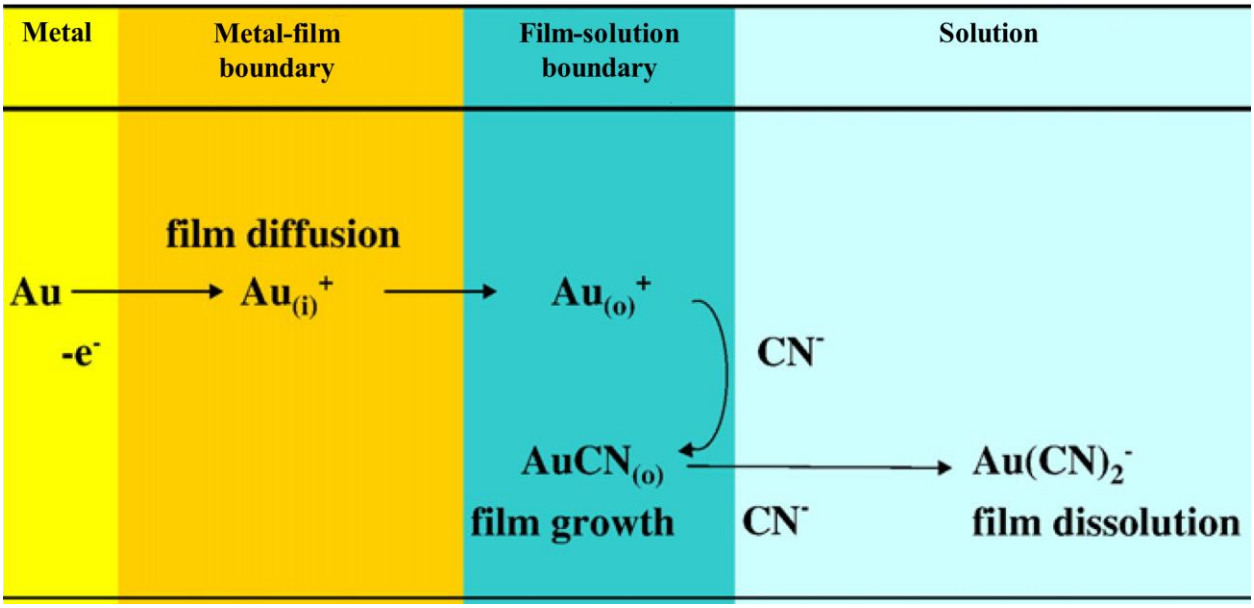

Fig. 1.4 Anodic cyanidation model for gold; boundary i: gold-film interface, boundary o: film-solution interface (Senanayake, 2008).

1.2.4 Surface coating industries

According to Alkaya and Demirer (2014), over the years, small- and medium-sized enterprises (SMEs) in surface coating industry have shown noteworthy progress toward resource-efficient and environmentally aware production. However, the potential environmental innovation in this sector has not yet been fully exploited. Still, high energy and water consumption, low efficiency, costly wastewater treatment, high volatile organic carbon (VOC) emissions, excessive solvent use, corrosive fluoride and toxic lead, as well as highly toxic cadmium and cyanide contaminated wastes are among the foremost environmental issues which need to be undertaken via cost-effective measures. Due to these environmental issues and stringent legislative restrictions on the use of certain toxic chemicals/metals (e.g., chromium, cadmium, and cyanide), surface coating industry is facing a structural technological change (Alkaya and Demirer, 2014). Cadmium electroplating is one of the noteworthy examples among various surface coating sub-sectors, from which renovation should be practiced towards more eco-friendly and resource-efficient technologies (Merrikhpour and Jalali, 2013; Senthilnathan and Rajam, 2014). According to EU

Water Framework Directive "cadmium and its components" are listed among 33 priority hazardous substances, which are targeted for advanced reduction and subsequent termination in the European market. Moreover, cyanide, which is used extensively in cadmium plating, was listed both among main pollutants and substances matter to review for possible identification as priority hazardous substances (http://ec.europa.eu/smartregulation/impact/ia_carried_out/docs/ia_2012/com_2011_076_en.pdf). Cyanide is extensively used in all these processes, owing to its strong complexing capability, ready availability, relatively low-cost and well-known chemistry. Because of the potential hazards associated with cyanide, it is necessary to find the removal process, which can remediate cyanide-contamination. Various methods have been employed for the removal of cyanide or cyanate, as outlined below.

1.3 Physical methods for the removal of cyanide

Physical methods for cyanide removal include adsorption, membrane, hydrolysis/distillation, flotation, resins and photolysis. Adsorption is the most common physical treatment method used for the removal of cyanide (Naveen *et al.*, 2011).

1.3.1 Adsorption

Different bio-sorbents have been used for the removal of cyanide complexes. Such bio-sorbents are: agricultural waste, industrial waste, municipal solid waste components, fungal and bacterial waste, algal biomass, plant waste, and charcoal. The amount of cyanide complexes removed using these sorbents ranges from 1.95-3.65 µmol/g biomass (Patil, 2012). Among all materials tested for the sorption of cyanide complex, rice husk (3.65 µmol/g) and *Eichornia* roots (3.56 µmol/g) showed the most efficient bio-sorption, other than activated charcoal (selected as a reference material). Apart from the removal of cyanide complex, these low-cost materials were also used for the treatment of metal-contaminated wastewater worldwide, such as in India (Ajmal *et al.*, 2001), Nigeria (Abia *et al.*, 2003), Italy (Abollino *et al.*, 2003) and USA (Yu *et al.*, 2003). In addition to these bio-sorbents, several other materials such as, zero-valent iron (Tyagi *et al.*, 2018); different nanomaterials (Khataee *et al.*, 2017; Uppal *et al.*, 2017) have also been employed for the removal of cyanide from wastewater.

Despite the low-cost and eco-friendly nature of sorbents, it has certain limitations, such as their adsorption capacity is dependent on the pH. Increasing or decreasing the pH will affect their

removal efficiency, due to the change in adsorption capacity of materials. In addition, adsorption methods also generate toxic by-products which further requires treatment (Mudder *et al.*, 1991; Young and Jordan, 1995). Apart from sorption, other physical methods have been employed for cyanide removal, such as reverse osmosis (Young and Jordan, 1995; Patil and Paknikar, 2000), hydrolysis/distillation (Akcil, 2003), flotation (Young and Jordan, 1995), resin (Bose *et al.*, 2002; Fernando *et al.*, 2002) and photolysis (Peral and Domenech, 1992; Young and Jordan, 1995; Kim *et al.*, 2003).

1.4 Chemical methods for the removal of cyanide

Several chemical methods have been employed for the degradation of cyanide. Among them alkaline chlorination, peroxide oxidation and ozonation technologies are well-established (Dzombak *et al.*, 2006; Acheampong *et al.*, 2010).

1.4.1 Alkaline chlorination

Alkaline breakpoint chlorination [Equation (1a, b)] is a commonly-used chemical oxidation method for cyanide removal (Baxter and Cummings, 2006).

$$Cl_2 + CN^- \longrightarrow CNCl + Cl^- \quad (1a)$$

$$CNCl + H_2O \longrightarrow OCN^- + Cl^- + 2H^+ \quad (1b)$$

However, this method has significant disadvantages as it needs special requirements for waste disposal, releases more toxic chemical agents (such as OCN^-) and the potential formation of chlorinated organic compounds (Huertas *et al.*, 2010). Furthermore, it is ineffective with metal-cyanide complexes because of its low reactivity.

1.4.2 Peroxide oxidation

Hydrogen peroxide (H_2O_2) has been used for the removal of cyanide since 1980s. Firstly, it was used for full-scale treatment by Degussa at the Ok Tedi Mining Limited gold mine in Papua New Guinea. Total cyanide concentration was reduced to 10 mg/L after treatment with H_2O_2 (Griffiths *et al.*, 1987). H_2O_2 oxidizes cyanide to produce cyanate which subsequently hydrolyses, if there is an excess of H_2O_2, to give nitrite and carbonate [Equation 2a, b] (Mudder *et al.*, 1991; Young and Jordan, 1995; Chergui *et al.*, 2015).

$$CN^- + H_2O_2 \longrightarrow OCN^- + H_2O \quad (2a)$$

$$OCN^- + 3H_2O_2 + H_2O \longrightarrow NO_2^- + CO_3^{2-} + 2H_2O + 2H^+ \quad (2b)$$

H_2O_2 has also been used for cyanide treatment in the presence of homo- or heterogeneous catalysts, such as Ru/MgO (Pak and Chang, 1997), cadmium (Taylor *et al.*, 2004), and copper (Kitis *et al.*, 2005; Chen *et al.*, 2014). However, this method is expensive and requires special equipment and maintenance, and also needs accurate measurement of chemical dose (Huertas *et al.*, 2010). The presence of suspended solids in wastewater also limits the percentage removal of cyanide (Pueyo *et al.*, 2016). In addition, other alternative chemical treatment has also been used such as the SO_2/air (INCO) process. This involves combining sulphur dioxide with oxygen and cyanide compounds in the presence of a copper catalyst [Equation (3a)] and the oxidation of cyanide compounds using hydrogen peroxide [Equation (3b)], which also results in the formation of cyanate (Baxter and Cummings, 2006).

$$CN^- + SO_2 + O_2 + H_2O \xrightarrow{Cu^{2+}\ catalyst} OCN^- + H_2SO_4 \quad (3a)$$

$$CN^- + H_2O_2 \xrightarrow{Cu^{2+}\ catalyst} OCN^- + H_2O \quad (3b)$$

The disadvantage associated with this process is the need for sulphates addition to the treated water, and some of the reagent savings are offset by license/royalty payments (Dash *et al.*, 2009).

1.4.3 Ozonation

Ozone is a powerful oxidizing agent with no secondary product formation during the cyanide removal from wastewater (Parga *et al.*, 2003). Concentrations of ozone varies from 5-25 mg/L of air, depending on the ozone generator parameters, such as, air flow, generator power etc. (Van Leeuwen *et al.*, 2003). Ozone has also been used in combination with H_2O_2 (Monteagudo *et al.*, 2004), and UV radiation (Kim *et al.*, 2003; Mudliar *et al.*, 2009) for the removal of cyanide. Despite its advantages, ozone has certain limitations such as, inadequate oxidation ability to remove ozonated by-products (Chang *et al.*, 2008), and also requires high cost, due to the use of external energy, chemicals, and operators (Mudder *et al.*, 1991). Apart from this, other chemical methods have also been used for the removal of cyanide, which are shown in Table 1.1.

Table 1.1 Advantages and disadvantages associated with various chemical methods used for cyanide removal

Chemical methods	Advantages	Disadvantages	References
Anodic oxidation	Treat all cyanide baths regardless of concentration.	Require post treatment by a number of oxidation method	(Ho *et al.*, 1990; Lin *et al.*, 1992; Ögütveren *et al.*, 1999)
Electrodialysis	Efficient in treatment.	Costly and only applicable to certain type of wastes	(Young and Jordan, 1995)
Electrowinning	Performs well in concentrated solution and also useful in gold processing.	Proper controlled condition require and can't be directly used for removal. Technology is not properly established. Thiocyanate does not respond. Free cyanide liberated and not useful at low concentration.	(Mosher and Figueroa, 1996)
Acidification/volatilization and reneutralisation (AVR)	Reduced energy consumption and increased volatilization.	High acid consumption. Sludge of gypsum is high. Require specially designed reactor.	(Young and Jordan, 1995; Mosher and Figueroa, 1996; Akcil, 2003)
Iron cyanide precipitation	Widely used as a polishing process and suitably used for mining industry.	Suitability is limited to situations, such as work only with low concentration of cyanide and also need to maintain the pH. Special requirements for the disposal of precipitate.	(Young and Jordan, 1995; Sharma *et al.*, 1998; Ghosh *et al.*, 1999)
Caro's acid	Useful on site treatment and also used where SO_2/air process is not suitable.	Difficulty in handling as it readily decomposes to oxygen and sulfuric acid. It is also not applicable for all type of site.	(Young and Jordan, 1995; Akcil, 2003)

Even though physical and chemical methods can be used to degrade cyanide and its allied compounds, their expensive nature and complex operation is a major concern for application. An alternative to these processes is biological treatment, which usually depends on the enhancement of indigenous microbes and their enzymes. Biodegradation of cyanide or cyanogenic compounds has been offered as a potentially economical and eco-friendly alternative to conventional processes (Dash *et al.*, 2008).

1.5 Biological methods for the removal of cyanide

Biological methods of cyanide removal can be less expensive than physical and chemical methods (Dash *et al.*, 2009). The biodegradation of cyanide and cyanate by microorganisms or microbial enzymes have revealed the feasibility for concomitant generation of biogas (Ebbs, 2004), and its utilization as an alternative energy source (Palatinszky *et al.*, 2015), which is possibly an economic benefit of the biological process. These methods satisfy the need for an eco-friendly bio-remediation process which has been applied on a large-scale in several systems (Akcil, 2003). There are four common pathways for the bioremediation of cyanogenic compounds such as, hydrolytic, oxidative, reductive, and substitution/transfer (Fig. 1.5), which has been reported in several literature (Knowles and Bunch, 1986; Raybuck, 1992; Dubey and Holmes, 1995; Luque-Almagro *et al.*, 2008). Enzymes involved in this bioremediation processes for different reactions are, hydrolytic reactions: cyanide hydratase; nitrile hydratase; cyanidase; nitrilase, oxidative reactions: cyanide monoxygenase; cyanide dioxygenase, reductive reaction: nitrogenase, substitution/transfer reactions: cyanoalanine synthase; cyanide sulphurtransferase, and oxidative/ substitution/transfer reactions: thiocyanate hydrolase; cyanase. Fungi are the main source for cyanide hydratase (Barclay *et al.*, 2002), and bacteria for cyanidase (cyanide dihydratase) (Ebbs, 2004).

It has been shown that cyanide hydratase and cyanidase have structural similarity with nitrilase and nitrile hydratase enzymes (O'Reilly and Turner, 2003). Nitrilase and nitrile hydratase has shown less substrate specificity compared to cyanide hydratase and cyanidase. Moreover, cyanide hydratase also showed nitrilase activity, when cyanide hydratase gene from *Fusarium lateritium* was expressed in *E. coli*, which facilitated their growth on nitriles as the sole nitrogen source. Further, cyanide hydratase and nitrilase activities were abolished by mutating the active site of the gene via site-directed mutagenesis (Nolan *et al.*, 2003). The wide-range of catalytic activity and

substrate specificities of these enzymes, offer significant opportunity for biotechnological development, including bio-remediation (Rezende *et al.*, 2000; Dias *et al.*, 2001). Cyanide biodegradation by oxidative reactions formed ammonia and carbon dioxide (Fig. 1.5).

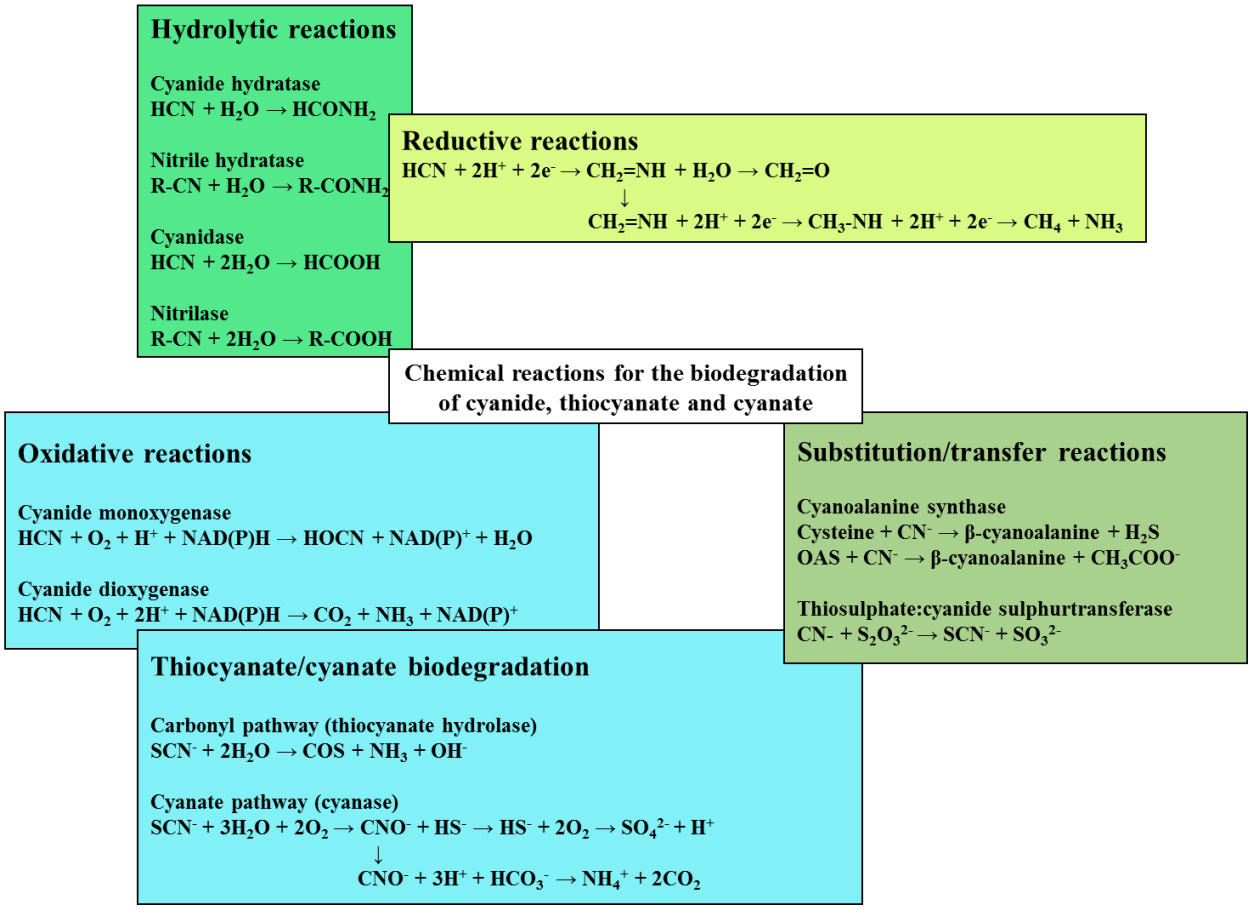

Fig. 1.5 The general types of chemical reactions responsible for the biodegradation of cyanide and cyanate. For the hydrolytic reaction involving nitriles, R represents either an aliphatic or aromatic group. The substitution/transfer reaction catalyzed by cyanoalanine synthase can also use O-acetylserine (OAS) as a substrate. The cyanate formed by cyanide monoxygenase is converted to NH_4^+ and CO_2 by the same pathway as the cyanate from thiocyanate. Also, cyanate is directly converted into NH_4^+ and CO_2 by cyanase in the presence of bicarbonate. The reductive pathway is derived from the action of nitrogenase and the products resulting from the transfer of pairs of electrons [Source: (Ebbs, 2004) with slight modification].

In addition, cyanide oxidation also forms cyanate, which is an important cyanide derivative (Luque-Almagro *et al.*, 2016). Cyanide monoxygenase converts cyanide to cyanate, which is further converted into ammonia and carbon dioxide by cyanase, in a bicarbonate dependent manner. Cyanases have been identified in many bacteria, fungi, plants and animals. However, phytoremediation is seemingly inefficient, as it is time consuming and takes several years to halve the contamination (Peuke and Rennenberg, 2005). Thus, the bio-remediation process principally depends on the microorganisms (Karigar and Rao, 2011), which enzymatically degrade the pollutants and converts them to harmless products or even economically valuable products (Ebbs, 2004). Microbial enzymes have also gained interest over the plant and animal enzymes, because of their ease of production and optimization, which makes them suitable for their widespread use in industries (Whitlock and Whitlock, 2001; Singh *et al.*, 2016).

Several microorganisms have been utilized for the bio-remediation of cyanide and other cyanogenic compounds (Table 1.2). However, the complex nature of industrial effluents, primarily the high concentrations of cyanide or cyanate and heavy metals limit the utilization of microorganisms, due to poor viability (Papadimitriou *et al.*, 2009; Sharma and Philip, 2014). At high concentrations, these toxic compounds alter the conformation of nucleic acids and proteins and also interfere with oxidative phosphorylation and osmotic balance, resulting in low viability (Bruins *et al.*, 2000). In contrast to the microbial cells, enzymes produced from them have known to play a major role in the detoxification of environmental pollutants, as they have showed higher efficiency in a short span of time (Gianfreda and Rao, 2004; Sutherland *et al.*, 2004).

1.5.1 Microbial enzymes

Enzyme driven processes are promptly gaining interest owing to lowered process-time, requirement of lower-energy, cost-effective, nontoxic and eco-friendly characteristics (Li *et al.*, 2012; Choi *et al.*, 2015). Moreover, with the introduction of genetic- and protein- engineering, microorganisms can be manipulated and cultivated at large-scale for the production of new enzymes with improved catalytic properties to meet the industrial demand (Liu *et al.*, 2013). Some of the factors which prompted the use of microbial enzymes in industrial processes are: need of cost reduction; depletion of natural resources; and environmental safety (Choi *et al.*, 2015). In addition to this, microbial enzymes from different sources, work well under a wide range of physical and chemical conditions (Singh *et al.*, 2016).

Table 1.2 Bioremediation of cyanide/cyanate and other cyanogenic compounds using microorganisms or microbial enzymes

Compound	**Microorganism/ Enzyme**	**Optimum conditions**		**References**
		pH	**Temp. (°C)**	
Cyanides	*Pseudomonas* sp.(CM5, MN2)	9.2-11.4	30	(Akcil *et al.*, 2003)
Ferrous(II) cyanides complex	*Pseudomonas fluorescens* immobilized on calcium alginate	4.0-7.0	25-35	(Dursun and Aksu, 2000)
Potassium cyanide	*Klebsiella oxytoca*	7.0	30	(Kao *et al.*, 2003)
Nitriles	*K. oxytoca*	7.0	30	(Kao *et al.*, 2006)
Cyanides and formamide	*Fusarium oxysporum* immobilized on sodium alginate, *Methylobacterium* sp.	8.0	25-30	(Campos *et al.*, 2006)
Metallo-cyanide	Strains of *Trichoderma* spp.	6.5	25	(Ezzi and Lynch, 2005)
Phenol and cyanides	*P. putida* immobilized on Ultrafiltration membranes	-	27	(Kowalska *et al.*, 1998)
Cyanide and phenol	*Aspergillus niger* K10 (cyanide hydratase) and *Agaricus bisporus* (tyrosinase)	7.0-8.0	25-30	(Martínková and Chmátal, 2016)
Copper and zinc cyanide	*Citrobacter* sp., *Pseudomonas* sp.	7.5	35	(Patil and Paknikar, 2000)
Tetra-cyano-nickelate(II)	*P. fluorescens* immobilized on zeolite	-	30	(Suh *et al.*, 1994)
Potassium cyanide	*Burkholderia cepatia* stain C-3	8.0-10.0	30	(Adjei and Ohta, 2000)
Iron/nickel CN $K_2Ni(CN)_4K_4Fe(CN)_6$	Mix of (1) *F. solani*, *T. polysporum* (2) *F. oxyspoum, Scytalidium themophilum, Pencillium miczynski*	4.0 and 7.0	25	(Barclay *et al.*, 1998)

Compound	Microorganism/ Enzyme	Optimum conditions		References
		pH	Temp. (°C)	
Potassium cyanide	*Klebsiella oxytoca* immobilized on alginate and cellulose triacetate	7.0	30	(Chen *et al.*, 2008)
Potassium cyanide	*Pseudomonas stutzeri* AK61 (cyanidase)	7.6	30	(Watanabe *et al.*, 1998)
Sodium cyanide	*Pseudomonas pseudoalcaligenes* CECT5344	9.5	30	(Huertas *et al.*, 2010)
Tetra-cyano-nickelate(II)	*Cryptococcus humicolus* MCN2	7.5	25	(Kwon *et al.*, 2002)
Potassium cyanide	*Trichoderma harzianum T. pseudokoningi*	8.5	30	(Ezzi and Lynch, 2002)
Soil cyanide	*Pseudomonas stutzeri Bacillus subtilis*	-	30±2	(Nwokoro and Dibua, 2014)
Copper cyanide, Nickel cyanide	*Cladosporium cladosporioides*	7.5	30-35	(Patil and Paknikar, 1999)
Cyanide from gold mining wastewater	*Pseudomonas pseudoalcaligenes* strain W2	-	30	(Tiong *et al.*, 2015)
Potassium cyanate	*Nitrososphaera gargensis*	-	37	(Palatinszky *et al.*, 2015)
Potassium cyanate	*Synechocystis sp. strain* PCC 6803 and *Synechococcus sp* strain PCC 7942	7.0	26-30	(Harano *et al.*, 1997)
Potassium cyanate	*Sordaria macrospora*	7.6	27	(Elleuche and Pöggeler, 2008)
Potassium cyanate	*Arabidopsis thaliana* and *Oryza sativa*	7.7	27	(Qian *et al.*, 2011)
Sodium cyanide, cyanates and thiocyanates	*P. putida* immobilized on sodium alginate	7.5	25	(Chapatwala *et al.*, 1998)

The global market for industrial enzymes was about $4.2 billion in 2014 and predicted to develop at a compound annual growth rate (CAGR) of approximately 7% over the period from 2015-2020, to reach nearly $6.2 billion (http://www.pharmaion.com/report/india-industrial-enzymes-market-forecast-and-opportunities-2020/10.html). Enzymes are specific and they accelerate the rate of reaction by lowering the activation energy without any permanent change into them; hence, it has a vital role to support life (Freeman, 1985; Piccolino, 2000; Aldridge, 2013). It usually requires milder conditions of temperature and pressure for catalyzing reactions, and therefore, are used as an alternative to harmful chemical pollutants (Mojsov, 2011; Illanes *et al.*, 2012).

1.5.2 *Thermomyces lanuginosus* as a source for enzyme production

T. lanuginosus is a thermophilic filamentous fungus, commonly found in composting environments. It is well-known for the production of several robust and thermostable enzymes with potential industrial applications (Puchart *et al.*, 1999; Singh *et al.*, 2000, 2003; Shrivastava *et al.*, 2013; Khan *et al.*, 2015; Kumar *et al.*, 2016; Sikandar *et al.*, 2017). The whole genome sequencing and seceretome analysis of a *T. lanuginosus* SSBP has revealed the presence of several industrially important enzymes, many for the first time (Mchunu *et al.*, 2013; Winger *et al.*, 2014). Enzymes produced by this fungus include: amylase, chitinase, cyanate hydratase, carbonic anhydrase, glucoamylase, lipase, phytase, protease, xylanase, etc. In addition, it has a ubiquitin degradation pathway which plays an essential role in response to various stress, such as nutrient limitation, heat shock, and heavy metal exposure (Mchunu *et al.*, 2013). Due to these requisite properties, this fungus has been identified as one of the organisms of choice for industrial applications and has provided the foundation to explore these novel enzymes.

1.5.2.1 Cyanate hydratase

Cyanate hydratase (Cyn, EC 4.2.1.104) (also known as cyanate lyase or cyanase) catalyzes the bicarbonate-dependent decomposition of cyanate into ammonium and carbon dioxide. Cyanases are found in bacteria (Anderson, 1980; Johnson and Anderson, 1987; Sung *et al.*, 1987), fungi (Elleuche and Pöggeler, 2008) and plants (Qian *et al.*, 2011), where they have important roles for nitrogen assimilation or cyanate detoxification. Despite these important functions, the production of this enzyme is low by most known organisms (Anderson, 1980; Harano *et al.*, 1997; Elleuche and Pöggeler, 2008; Qian *et al.*, 2011). In general, several microorganisms are known to

produce high amounts of enzymes, however, the enzyme production by wild type strain is low for its commercial utilization (Punt *et al.*, 2002). Therefore, strain improvement using genetic- and protein- engineering approaches are essential for application. Additionally, most of the enzymes used in industries are recombinant, which is produced by bacteria and fungi, as the production level by wild-strain is low (Adrio and Demain, 2014).

1.5.2.2 Carbonic anhydrase

Carbonic anhydrase (CA, EC 4.2.1.1) (also known as carbonate dehydratase) catalyzes the interconversion between carbon dioxide and bicarbonate: $CO_2 + H_2O \leftrightarrow HCO_3^- + H^+$. Carbonic anhydrases are involved in several physiologic processes, such as photosynthesis, respiration, CO_2 transport, as well as metabolism of xenobiotics (Capasso and Supuran, 2015). Thus far six families of carbonic anhydrases are known *viz*., α-, β-, γ-, δ-, ζ- and η-CAs (Supuran, 2016). In particular, the product of this enzyme i.e. bicarbonate, is one of the substrates for cyanate hydratase to convert cyanate into ammonium and carbon dioxide (Fig. 1.6) (Elmore *et al.*, 2015). So clustering of these two genes (cyanate hydratase and carbonic anhydrase) or encoding these enzymes may enhance the cyanate detoxification capacity with low dependence on bicarbonate.

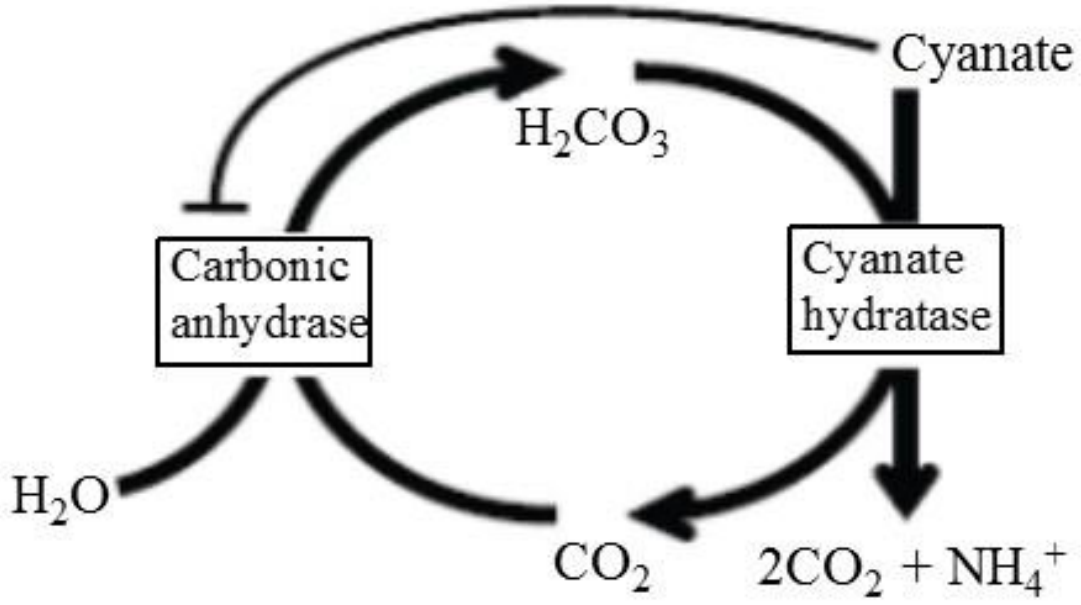

Fig. 1.6 Cyanate hydratase converts the toxic compound cyanate into nontoxic ammonia and carbon dioxide. Carbonic anhydrase converts carbon dioxide and water into bicarbonate, which cyanate hydratase requires in order to convert cyanate to ammonia and carbon dioxide (Elmore *et al.*, 2015).

1.6 Strategies to improve microbial enzyme production by different hosts

The progress of sophisticated molecular approaches such as recombinant DNA technology has established a new stepping stone towards the goal of using an efficient and scale-up expression systems for enzyme production (Punt *et al.*, 2002; Adrio and Demain, 2014). Some industrially known organisms such as, *E. coli*, *Bacillus subtilis* and other species of *Bacillus, Ralstonia eutropha*, *Pseudomonas fluorescens*, *Saccharomyces cerevisiae*, *Pichia pastoris*, *Hansenula polymorpha*, and species of *Aspergillus and Trichoderma,* are used for the production of enzymes from industrially unknown microorganisms (Demain and Vaishnav, 2009). Approximately 90% of the industrial enzymes are recombinant.

1.6.1 *E. coli* as a recombinant host for microbial enzyme production

E. coli has been extensively used as a recombinant host for enzyme production because of several reasons: easy to modify the genome; short generation time; reduced protease activity; and ease to grow in cheap culture media. It can accumulate up to 80% of recombinant proteins of its dry cell weight (Adrio and Demain, 2014). However, it has certain disadvantages such as, lack of post-translational modifications, presence of toxic cell wall pyrogens or formation of inclusion bodies, which results in the formation of insoluble heterologous proteins. Despite of all this, several proteins have been heterologously expressed in *E. coli* with high levels of production.

1.6.2 *S. cerevisiae* as a recombinant host for microbial enzyme production

S. cerevisiae as a cloning host offers some benefits over bacteria (Romanos *et al.*, 1992), *viz*., grows well on simple media and reaches high cell density, produces heterologous proteins extracellularly, and also has a more advanced and better understood genetics than other eukaryotes (http://www.yeastgenome.org/). Regardless of all these advantages, it has been observed that *S. cerevisiae* is not an optimal host for large-scale production, because of hyperglycosylation, and lack of strong and tightly-regulated promoters (Demain and Vaishnav, 2009).

1.6.3 *P. pastoris* as a recombinant host for microbial enzyme production

P. pastoris is one the most widely used and established expression systems (Higgins and Cregg, 1998; Demain and Vaishnav, 2009; Ahmad *et al.*, 2014; Zahrl *et al.*, 2017). In this heterologous expression system, around 22 g/L of proteins has been intracellularly expressed (Hasslacher *et al.*, 1997) and 14.8 g/L extracellularly (Werten *et al.*, 1999). Apart from this, it has been observed that up to 30 g/L of recombinant proteins can also be produced from this host (Morrow, 2007). This methylotrophic expression host has certain advantages over *S. cerevisiae* such as the presence of tightly-regulated methanol promoter (AOX1); less extensive glycosylation; generation of high-copy number and integration of foreign DNA into the chromosomal DNA; which makes stable transformants, high-density growth and easy to scale-up (Romanos, 1995; Ahmad *et al.*, 2014; Safder *et al.*, 2018; Theron *et al.*, 2018).

Apart from protein expression using different hosts, some other techniques have also been used for the rapid development of bio-catalysis, such as, directed evolution, metabolic engineering and

structural biology (Ran *et al.*, 2008; Bornscheuer *et al.*, 2012). The production and properties of enzymes can be improved according to the need by all these techniques, however, the high cost of downstream processing of enzymes and difficulty in separation from the reaction mixture for subsequent reuse may discourage their uses from the economic prospect (Datta *et al.*, 2013). Consequently, enzyme immobilization offers an alternative to resolve the challenges associated with the reusability of free enzymes coupled with several other advantages such as enhanced thermal stability and ease of separation (Dehnavi *et al.*, 2015; Zhou *et al.*, 2017).

1.7 Enzyme immobilization

Immobilization of enzymes on random carrier/support may decrease the enzyme stability, if the carrier and enzyme has undesired interactions (Mateo *et al.*, 2007).To develop an efficient bio-catalyst capable of performing in a broad spectrum of operating conditions after immobilization, needs a suitable carrier and immobilization technique for a particular enzyme (Oliveira *et al.*, 2015).

1.7.1 Carrier selection for enzyme immobilization

Numerous carriers and techniques have been applied to improve the traditional enzyme immobilization with the aim of enhancing enzyme loading, activity and stability at reduced cost for industrial applications. Several carriers have been used for the immobilization of enzymes (Table 1.3), however, nanomaterials serve as an ideal supporting carrier for immobilization (Wang, 2006; Fortes *et al.*, 2017; Wong *et al.*, 2017). Such carriers include nanoparticles, nanotubes, nanofibers, nanocomposites and graphene (Puri *et al.*, 2013; Heidarizadeh *et al.*, 2017; Kim *et al.*, 2017; Xu *et al.*, 2017; Benucci *et al.*, 2018). Nanomaterials provide high surface areas, large surface-to-volume ratios, mass transfer resistance, and effective enzyme loading in contrast to other planar 2-dimensional surfaces (Ahmed and Husain, 2012). It also possess a combination of the precise physical, chemical, optical and electrical properties with the specific recognition of biomolecules, which prompted their occurrence in countless novel biotechnological applications.

Table 1.3 Different carrier/support used for the immobilization of enzymes

Carrier/supports	Enzymes	References
Natural polymer as a carrier		
Alginate	Urease and tannase	(Elçin, 1995; Flores-Maltos *et al.*, 2011)
Chitosan and chitin	Xylanase	(Kapoor and Kuhad, 2007)
Carrageenan	Lipase	(Tümtürk *et al.*, 2007)
Gelatin	β-galactosidase	(Shen *et al.*, 2011)
Cellulose	β-galactosidase	(Klein *et al.*, 2011)
Starch	Peroxidase	(Matto and Husain, 2009)
Pectin	Invertase	(Gómez *et al.*, 2006)
Sepharose	Luciferase	(Hosseinkhani *et al.*, 2003)
Synthetic polymer as a carrier		
Amberlite	α-amylase	(Kumari and Kayastha, 2011)
Polyvinyl chloride	Cyclodextrin glucosyltransferase	(Abdel-Naby, 1999)
Polyurethane microparticles	α-amylase and maltogenase	(Kahraman *et al.*, 2007; Romaskevic *et al.*, 2010)
Polyaniline	Lipase	(Pahujani *et al.*, 2008)
Inorganic materials as a carrier		
Zeolites	Cutinase and α-chymotrypsin	(Serralha *et al.*, 1998; Xing *et al.*, 2000)
Ceramics	Lipase	(Magnan *et al.*, 2004; Huang and Cheng, 2008)
Celite	Oxidase and β-galactosidase	(Khan *et al.*, 2006; Ansari and Husain, 2012)
Silica	Urease and α-amylase	(Pogorilyi *et al.*, 2007; Soleimani *et al.*, 2012)
Glass	Nitrite reductase and urease	(Rosa *et al.*, 2002; Sahney *et al.*, 2005)
Activated carbon	Cellulase and lipase	(Daoud *et al.*, 2010; Ramani *et al.*, 2012)
Charcoal	Urease and amyloglucosidase	(Kibarer and Akovali, 1996; Rani *et al.*, 2000)

1.7.2 Techniques for enzyme immobilization

The commonly used techniques for enzyme immobilization are adsorption, entrapment, cross-linking and covalent bonding.

1.7.2.1 Adsorption

It is a simple and straightforward enzyme immobilization technique, in which, enzymes are physically attached onto the carrier material (Mohamad *et al.*, 2015). In addition, it is a chemical-free enzyme binding technique (Chronopoulou *et al.*, 2011), which is another advantage over other techniques. However, no permanent bond formation occurs between enzymes and carrier; only weak bonds such as van der Waals, hydrophobic interactions and hydrogen bonds that stabilize the enzymes to the support (Jegannathan *et al.*, 2008). Due to the weak bond formation, enzyme leaches from the immobilized enzyme preparation after few cycles which limit its applications.

1.7.2.2 Entrapment

It is caging of enzymes inside a porous matrix or fibers by covalent or non-covalent bonds (Chiang *et al.*, 1997). This method is fast, cheap and easy to practice at small-scale, however, leakage of enzyme and pore diffusion limitation, is a major drawback of its large-scale utilization http://www.easybiologyclass.com/enzyme-cell-immobilization-techniques/.

1.7.2.3 Covalent bonding

Covalent bonding is one of the most extensively used techniques for irreversible enzyme immobilization (Mohamad *et al.*, 2015). This technique involves the biding of amino acid residues *via* side chains such as, ε-amino group of lysine, thiol group of cysteine, and carboxylic group of aspartic and glutamic acids (Tran and Balkus, 2011). It also yields relatively stable immobilized enzyme preparations with more reusability, as compared to the physical adsorption techniques (Georgakilas *et al.*, 2005; Ahmed and Husain, 2012).

1.7.3 Effect of immobilization on enzyme activity

It has been observed that enzyme immobilized on nanoparticles showed higher thermal stability and broader working pH range, compared to the native enzymes (Husain, 2010). Immobilization also enhances the enzyme activity, due to the mobility of nanoparticles which

enhances substrate-to-enzyme interactions *via* Brownian motion (Jia *et al.*, 2003). In addition to this, various factors *viz*., binding modes, change in conformations, diffusion effects, etc. are also responsible for the improvement of immobilized enzymes activity (Datta *et al.*, 2013). Immobilization of enzymes on nanoparticles also offers some important features as compared to other conventional immobilization methods, such as easy to synthesize nano-enzyme particles without the use of surfactants and toxic reagents. Thick enzyme-shell can be attained due to well defined core-shell nanoparticles (Singh *et al*., 2014). Nanoparticle size can be suitably customized within convenience limit. Further, with the increasing consideration paid towards enzymatic cascade reactions, it is possible to achieve the co-immobilization of multiple enzymes on these nanoparticles, which will offer considerable advantages in biotechnological applications.

1.8 Purpose of the study

In view of green chemistry as the forerunner in all eco-friendly managing strategies, application of enzymes in bio-remediation is a critical event for a sustainable environment (Nair and Jayachandran, 2017). Microbial enzymes are rapidly gaining interest in the bio-remediation process because of their short process time, low energy requirement, cost-effective, nontoxic and eco-friendly characteristics. In view of these considerations, *T. lanuginosus*, a thermophilic fungus that produces a high amount of hydrolyzing enzymes and is well-known as an organisms of choice for industrial applications (Singh *et al.*, 2003) could be a viable alternative. Furthermore, whole-genome sequencing and secretome analysis of *T. lanuginosus* (Mchunu *et al.*, 2013; Winger *et al.*, 2014), revealed the presence of a cyanate hydratase, which prompted for further investigation on this enzyme. The present investigation therefore focused on following objectives:

- To clone and express the cyanate hydratase gene from *T. lanuginosus* into prokaryotic and eukaryotic hosts;
- To purify and characterize the recombinant cyanate hydratase (rTl-Cyn);
- To immobilize the rTl-Cyn on several matrices;
- To apply the rTl-Cyn in bio-remediation; and
- To determine the crystal structure of Tl-Cyn and its implications for a catalytic mechanism.

CHAPTER 2

Expression of a novel recombinant cyanate hydratase (rTl-Cyn) in *Pichia pastoris,* its characteristics and applicability in the detoxification of cyanate

(*Published: Ranjan, B., Pillai, S., Permaul, K., and Singh, S. (2017) Expression of a novel recombinant cyanate hydratase (rTl-Cyn) in Pichia pastoris, characteristics and applicability in the detoxification of cyanate. Bioresource Technology. **238**: 582-588*).

2.1 Introduction

Cyanate is a toxic compound produced by industries and also formed from some metabolites, such as urea and carbamoylphosphate (Outer and Protein, 1987). Cyanate hydratase catalyzes the decomposition of cyanate into ammonium and carbon dioxide in a bicarbonate-dependent reaction. Bicarbonate acts as a nucleophilic reactant, which helps in the breakdown of cyanate, with carbamate as an unstable intermediate (Anderson, 1980). At least three biological roles have been allied with cyanate hydratase activity *viz*., nitrogen assimilation, cyanate detoxification and metabolism regulation (Luque-Almagro *et al.*, 2008). Since cyanate hydratase catalyzes the decomposition of cyanate into ammonium, this allows some bacteria (Luque-Almagro *et al.*, 2008) and certain marine cyanobacteria (Rocap *et al*., 2003; Kamennaya and Post, 2013), to utilize cyanate as a nitrogen source. It is also found in a variety of other bacteria and archaea, which play a role in nitrogen assimilation or detoxification, as cyanate chemically alters proteins through carbamylation (Kamennaya *et al.*, 2008; Luque-Almagro *et al.*, 2008). In addition, some organisms utilizes ammonium and carbon dioxide produced from cyanate, as a nitrogen and carbon source, respectively (Kunz and Nagappan, 1989; Espie *et al.*, 2007). Nitrifying microbes are commonly considered to be highly devoted chemolithoautotrophs, that oxidize either ammonia or nitrite to produce energy (as a nitrogen source) and reductant for growth, and uses carbon dioxide as a carbon source (Palatinszky *et al.*, 2015). However, the growth of microorganisms and plants which lack cyanate hydratase are inhibited in the presence of cyanate (Qian *et al.*, 2011).

Whole genome sequencing and secretome analysis of the thermophilic fungus *T. lanuginosus* SSBP has revealed the presence of a cyanate hydratase gene and protein (Mchunu *et al.*, 2013; Winger *et al.*, 2014). Since *T. lanuginosus* SSBP is a hyper-xylanase producer with good pH and temperature stability, has prompted further exploration of the fungus for cyanate hydratase. As the production of cyanate hydratase by *T. lanuginosus* SSBP (wild-type) is low, it was required to clone and overexpress the cyanate hydratase encoding gene heterologously into *P. pastoris*. *P. pastoris* is a methylotrophic yeast, where proteins can be heterologously expressed either constitutively or inducibly. Heterologous proteins can be produced extracellularly using an expression plasmid with the α-factor secretory signal sequence (Ranjan and Satyanarayana, 2016).

Thus far, numerous genes have been successfully expressed in *P. pastoris* (Cregg *et al.*, 2000), however, no attempts have been made to express the *Tl-Cyn* gene. In this chapter, the research work focused on cloning and expression of the cyanate hydratase gene heterologously in *P. pastoris*, followed by characterization of the recombinant cyanate hydratase (rTl-Cyn) and finally evaluation of its potential in cyanate detoxification was assessed.

2.2 Materials and Methods

2.2.1 *T. lanuginosus* SSBP, *P. pastoris* strain and vectors

The thermophilic fungus *T. lanuginosus* SSBP used in this study was deposited in the Industrial Biotechnology MIRCEN Culture Collection, Bloemfontein, South Africa (Accession number PRI 0226) (Singh *et al.*, 2000). *P. pastoris* GS115 (Invitrogen) was used as an expression host for the production of rTl-Cyn. The expression cassette containing the inducible promoter *AOX1* was used for protein expression. The plasmid pPICZαA was used for the cloning of *Tl-Cyn* gene (Fig. 2.1). Restriction sites, *Eco*RI and *Kpn*I were added to the sense and antisense primers, respectively, for the cloning of *Tl-Cyn* in pPICZαA vector. Cloning steps were accomplished in *E. coli* DH5α (Invitrogen).

2.2.2 Suitability of the *Tl-Cyn* gene for expression in *P. pastoris*

Before commencing *Tl-Cyn* expression studies in the eukaryotic host *P. pastoris*, the cyanate hydratase open reading frame (ORF) from *T. lanuginosus* SSBP was analyzed for codon bias. The percentage usage of different codons for a particular amino acid was calculated and compared with codon usage in *P. pastoris* (Ranjan and Satyanarayana, 2016).

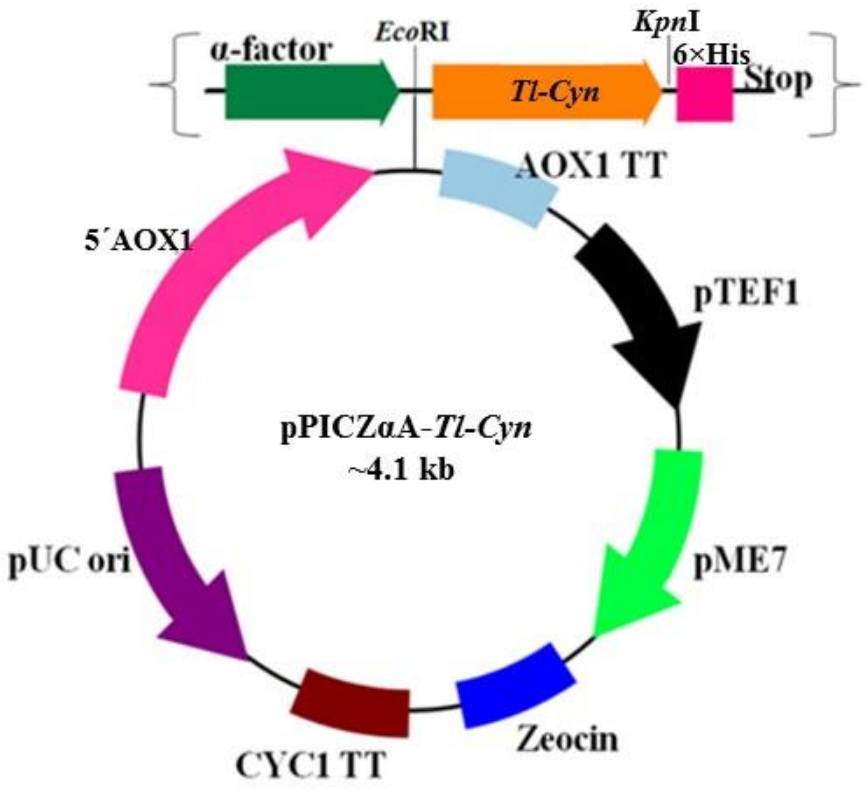

Fig. 2.1 Pictorial representation of the pPICZαA-*Tl-Cyn* construct. 5´ AOX1, alcohol oxidase (inducible) promoter; α-factor, secretory signal sequence; *Tl-Cyn*, *T. lanuginosus* cyanate hydratase; 6×His, histidine tag for rapid purification; AOX1 TT, alcohol oxidase transcription termination region; PTEF1, yeast promoter for zeocin; PEM7, bacterial promoter for zeocin; Zeocin, a zeocin resistance gene; CYC1 TT, cytochrome c1 transcription termination region; pUC ori, bacterial origin of replication.

2.2.3 RNA isolation

RNA was isolated from *T. lanuginosus* SSBP mycelium after 5 days of incubation (50°C and 150 rpm), at the time of maximum cyanate hydratase activity. The mycelium was frozen in liquid nitrogen and ground with a mortar and pestle until a floury consistency was attained. RNA was isolated using the RNeasy Mini Kit (Qiagen).

2.2.4 cDNA synthesis

cDNA synthesis was carried out using the Maxima H Minus First Strand cDNA Synthesis Kit (Thermo Fisher Scientific), as per the manufacturer's instructions.

2.2.5 Construction of *rTl-Cyn*

The cyanate hydratase gene was amplified from the cDNA, using primers P1 and P2 containing flanking regions for *Eco*RI and *Kpn*I restriction sites, respectively (Table 2.1). PCR conditions was as follows: denaturation at 95°C for 5 min; 25 cycles of (denaturation at 95°C for 30 s, annealing at 58°C for 30 s, elongation at 72°C for 60 s) and a final elongation step at 72°C for 5 min. The 500 bp PCR product obtained and plasmid pPICZαA were digested with *Eco*RI and *Kpn*I restriction enzymes and were ligated to make the pPICZαA-*Tl-Cyn* construct (Fig. 2.1). In this construct, the *Tl-Cyn* ORF was fused in-frame with the α-factor secretory signal sequence, and the *myc* epitope and 6×His-tag from the vector at the N- and C-termini, respectively. The construct was confirmed by double digestion with *Eco*RI and *Kpn*I. The presence and precise positioning of the insert was confirmed by DNA sequencing.

Table 2.1 Primers used in this study

Primers	**Oligonucleotide sequence (5′→3′)**
P1	CGGAATTCATGGCTGATATCGCAACCC
P2	GGTTGGTACCTTGAATCGACTGTATGGCAA

GAATTC- restriction site for *Eco*RI; GGTACC- restriction site for *Kpn*I.

2.2.6 Sequence alignment

The nucleotide and protein sequences were compared with the NCBI nucleotide/protein database using the BLASTN and BLASTP algorithms, respectively. Multiple sequence alignment of protein sequences were performed at http://www.ebi.ac.uk/Tools/msa/clustalw2/ with the proteins available in the databases using ClustalW2.

2.2.7 Transformation of *P. pastoris* with *Tl-Cyn*

The pPICZαA-*Tl-Cyn* construct was linearized with *Sac*I for transformation into *P. pastoris*. Chemically competent *P. pastoris* cells were prepared for the transformation of linearized pPICZαA-*Tl-Cyn* by electroporation. Approximately 10 µg of linearized pPICZαA-*Tl-Cyn* was mixed with competent cells and the mixture was transferred to a 0.2 cm pre-chilled electroporation cuvette and incubated on ice for 5 min. Electroporation conditions were as follows:

voltage (1.5 kV), capacitance (25 µF) and resistance (200 Ω). One mL of ice-cold sorbitol (1.0 M) was immediately added to the cuvette after electroporation, and the mixture was spread on YPD agar medium (g L^{-1}: yeast extract 10, peptone 20 and dextrose 20, agar 15), supplemented with 1.0 M sorbitol containing different concentrations of zeocin (100, 200, 500, 1000 and 1500 µg mL^{-1}). The plates were incubated at 30°C until single distinct colonies appeared. Colony PCR was performed to identify the positive clones harbouring cyanate hydratase genes. Spheroplasting of *P. pastoris* was done before colony PCR by mixing single yeast colony in 30 µL buffer containing 1 U of lyticase (Sigma) for 30 min. After spheroplasting, 5 µL of the suspension was used as template DNA in the PCR mix and PCR was performed using primers P1 and P2 (Table 2.1). The positive transformants with fastest growth rates on YPD agar plates (supplemented with 1.0 M sorbitol) containing the highest concentration of zeocin were screened for the production of enzyme, rTl-Cyn. These clones were first grown in YPD broth and then inoculated into Yeast extract-Peptone (YP) medium containing 0.5% (v/v) methanol (Ranjan and Satyanarayana, 2016). The cyanate hydratase production levels by different clones were determined by performing the enzyme assay as described below.

2.2.8 Cyanate hydratase assay

Cyanate hydratase assays were performed according to the modified method of Anderson (1980). The reaction mixture contained 0.1 mL appropriately diluted rTl-Cyn, 0.5 mL Tris-HCl buffer (50 mM, pH 8.0), 0.2 mL of potassium cyanate (2 mM) and 0.2 mL of sodium bicarbonate (6 mM) and incubated at 60°C for 10 min. One mL of Nessler's reagent was added to the reaction mixture to terminate the reaction. The amount of ammonia released was measured spectrophotometrically at 420 nm. One unit (U) of cyanate hydratase was defined as the amount of enzyme required to liberate 1 µmol of ammonia per minute under the standard assay conditions.

2.2.9 Purification of rTl-Cyn

The cell-free culture supernatant was filtered through 10 kDa ultrafiltration membrane cartridges (Millipore). Desalting and reconcentration was carried out for three cycles using the same membrane cartridges with Tris-HCl buffer (20 mM, pH 8.0). The concentrated enzyme was further purified by a fast protein liquid chromatography (FPLC) system (ÄKTApurifier 100, GE Healthcare Bio-Sciences) using a HiTrap Capto Q column (GE Healthcare Bio-Sciences) and the bound protein was eluted with a linear gradient of 0-1 M NaCl in Tris-HCl buffer (20 mM, pH

8.0) at a flow rate of 1.0 mL min^{-1}. The fractions having cyanate hydratase activity were pooled and dialyzed against Tris-HCl buffer (20 mM, pH 8.0) and concentrated using a vacuum concentrator (Eppendorf). The concentrated enzyme was loaded on a gel filtration chromatography column [Sephacryl S-200HR(16/60)] and eluted with 20 mM Tris-HCl buffer (pH 8.0) containing 50 mM NaCl at a flow rate of 0.4 mL min^{-1}. The fractions having cyanate hydratase activity were collected and their purity was analyzed by SDS-PAGE.

2.2.10 Biochemical characterization of rTl-Cyn

The optimum pH for the activity of rTl-Cyn was determined by performing enzyme assays using different buffers [Sodium acetate buffer 20 mM (pH 4.0-5.0), Tris-HCl buffer 20 mM (pH 6.0-8.0) and glycine-NaOH buffer 20 mM (pH 9.0-10.0)] at 60°C. Similarly, the optimum reaction temperature was determined by conducting rTl-Cyn assays at various temperatures (40-80°C) at pH 8.0. The effect of various modulators on rTl-Cyn activity was assessed by performing enzyme assays in the presence of modulators such as, metal ions (As^{3+}, Cr^{2+}, Cd^{2+}, Cu^{2+}, Hg^{2+}, Na^{+}, Ni^{2+}, Pb^{2+}, Zn^{2+}), and inhibitors (azide, nitrite, nitrate, NaCN, β-Mercaptoethanol).

2.2.11 Enzyme kinetics and thermal deactivation of rTl-Cyn

rTl-Cyn activity was assayed at various concentrations of potassium cyanate (ranging from 0.1 to 3.0 mM). The K_m and V_{max} values were graphically determined from the Lineweaver-Burk plot. Activation energy (E_a) was calculated according to the protocol described by Ranjan *et al*. (2015). The efficiency of ammonia liberation by the enzyme action was calculated from the V_{max}/K_m ratio. The energy of deactivation (E_d) of the rTl-Cyn was calculated from the residual activity at different temperatures, by incubating the enzyme solution in 20 mM Tris-HCl buffer (pH 8.0) at various temperatures (60-80°C) in the absence of substrate. Aliquots were drawn from the incubated samples at specific time intervals, cooled on ice for 30 min and cyanate hydratase assays were performed to calculate the residual activity. The inactivation rate constants (K_d) and energy of deactivation (E_d) were calculated according to Ranjan and Satyanarayana (2016).

The effect of temperature on the rate of reaction was expressed in terms of temperature quotient (Q_{10}), which is the factor by which the rate increases when the temperature is raised by 10°C. Temperature quotient (Q_{10}) was calculated by rearranging the equation of Dixon and Webb (1979):

$$Q_{10} = \text{antilog}\ (E_a \times 10/RT^2) \qquad (1)$$

where, E_a = activation energy, R is the universal gas constant and T is the absolute temperature.

2.2.12 Thermodynamic parameters of rTl-Cyn

Thermodynamics of irreversible inactivation of the rTl-Cyn was determined by rearranging the Eyring's absolute rate equation derived from the transition state theory:

$$K_d = (K_bT/h)\, e^{(-\Delta H/RT)}\, e^{(-\Delta S/RT)} \qquad (2)$$

ΔH (change in enthalpy of deactivation), ΔG (change in free energy of inactivation), and ΔS (change in entropy of inactivation) for irreversible inactivation were calculated as follows:

$$\Delta H = E_d - RT \qquad (3)$$

$$\Delta G = -RT \ln (K_dh/K_bT) \qquad (4)$$

$$\Delta S = (\Delta H - \Delta G)/ T \qquad (5)$$

where K_b is the Boltzmann's constant =1.38 x 10-23 J K^{-1}, K_d is the deactivation constant, T is the absolute temperature (K), h the Planck's constant = 6.626 x 10^{-34} J s, R is the gas constant = 8.314 J K^{-1} mol^{-1}.

2.2.13 Fourier transform infrared (FTIR) spectroscopy analysis for cyanate degradation

Samples were prepared for FTIR spectroscopy analysis according to Bryan *et al*. (1994). The reaction mixture containing 0.1 mL of appropriately diluted rTl-Cyn, 0.5 mL Tris-HCl buffer (50 mM, pH 8.0), 0.2 mL of potassium cyanate (2 mM) and 0.2 mL of sodium bicarbonate (6 mM) was incubated at 60°C for 10 min. Reaction mixtures without rTl-Cyn served as control. Absorbance were measured on KBr sample pellets (samples with and without rTl-Cyn) to determine the degradation of cyanate and liberation of ammonia.

2.2.14 Cyanate detoxification by rTl-Cyn in wastewater samples

Samples were collected from the influent of an industrial wastewater treatment plant in KwaZulu Natal, South Africa. rTl-Cyn (30 U) was added to 1 mL of wastewater sample supplemented with varying concentrations of cyanate (5-20 mM) and the reactions were carried out for 10 min at 60°C, in a reciprocating water bath at 100 rpm. Similarly, another set of experiments were also performed, except that the wastewater sample was replaced with Tris-HCl buffer (50 mM, pH 8.0). After 10 min of incubation, samples were centrifuged and analyzed for

cyanate degradation via release of ammonia using a spectrophotometer. In a separate experiment, heavy metals (Ag^{+}, Au^{3+}, Cr^{2+}, Cd^{2+}, Cu^{2+}, Fe^{2+}, Pb^{2+}, and Zn^{2+}) were added to both wastewater and buffered samples, and thereafter observed for cyanate degradation by rTl-Cyn. In addition, the presence of heavy metals in wastewater samples (spiked and un-spiked) were analyzed using atomic absorption spectroscopy (AAS) (Srikanth *et al.*, 2013).

2.3 Results and Discussion

2.3.1 Construction of rTl-Cyn

To achieve the expression of cyanate hydratase, differences in the relative codon frequency between *T. lanuginosus* SSBP and *P. pastoris* were analyzed using codon analysis tool (http://www.genscript.com/cgi-bin/tools/rare_ codon_analysis) and compared with the wild-type gene. The codon usage frequency for wild-type and optimized gene were found to be 46 and 38%, respectively, for its expression in *P. pastoris*. Since the codon usage of optimized gene (predicted by analysis tool) was lower than that of the native gene, the native gene was used for expression. The construction of pPICZαA-*Tl-Cyn* was confirmed by colony PCR (Fig. 2.2a) and double digestion with *Eco*RI and *Kpn*I (Fig. 2.2b).

2.3.2 Sequence alignment

Multiple amino acid sequence alignments of the rTl-Cyn with known cyanases from NCBI showed an identity of 84, 84, 82, 82, 83, 83, 82 and 83% to the cyanases from *Rasamsonia emersonii* CBS 393.64 (XP_013324462.1), *Talaromyces cellulolyticus* (GAM35076.1), *Talaromyces stipitatus* ATCC 10500 (XP_002486940.1), *Talaromyces marneffei* ATCC 18224 (XP_002145582.1), *Aspergillus oryzae* RIB40 (XP_001822419.1), *Aspergillus flavus* NRRL3357 (XP_002382512.1), *Penicillium oxalicum* (EPS32828.1), and *Aspergillus fischeri* NRRL 181 (XP_001261116.1), respectively (Fig. 2.3).

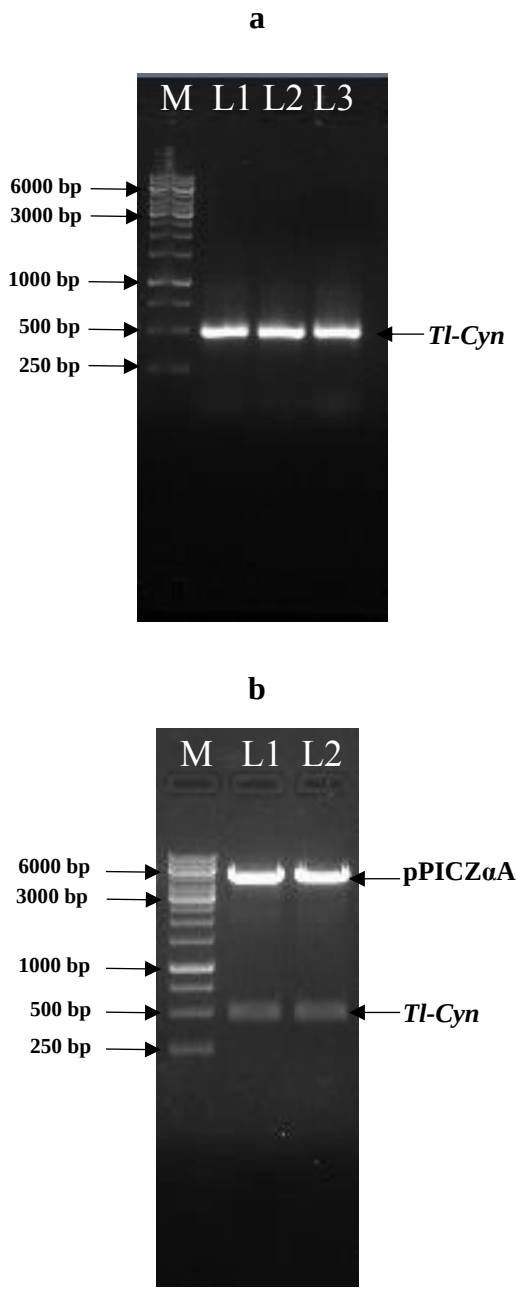

Fig. 2.2 Confirmation of pPICZαA-*Tl-Cyn* construction using agarose gel electrophoresis by colony PCR and restriction endonuclease digested products **(a)** colony PCR products: lanes 1-3, random colonies and **(b)** restriction endonuclease products after digestion with *Eco*RI and *Kpn*I: lanes 1-2 double digested pPICZαA-*Tl-Cyn*, lane M- 1kb ladder.

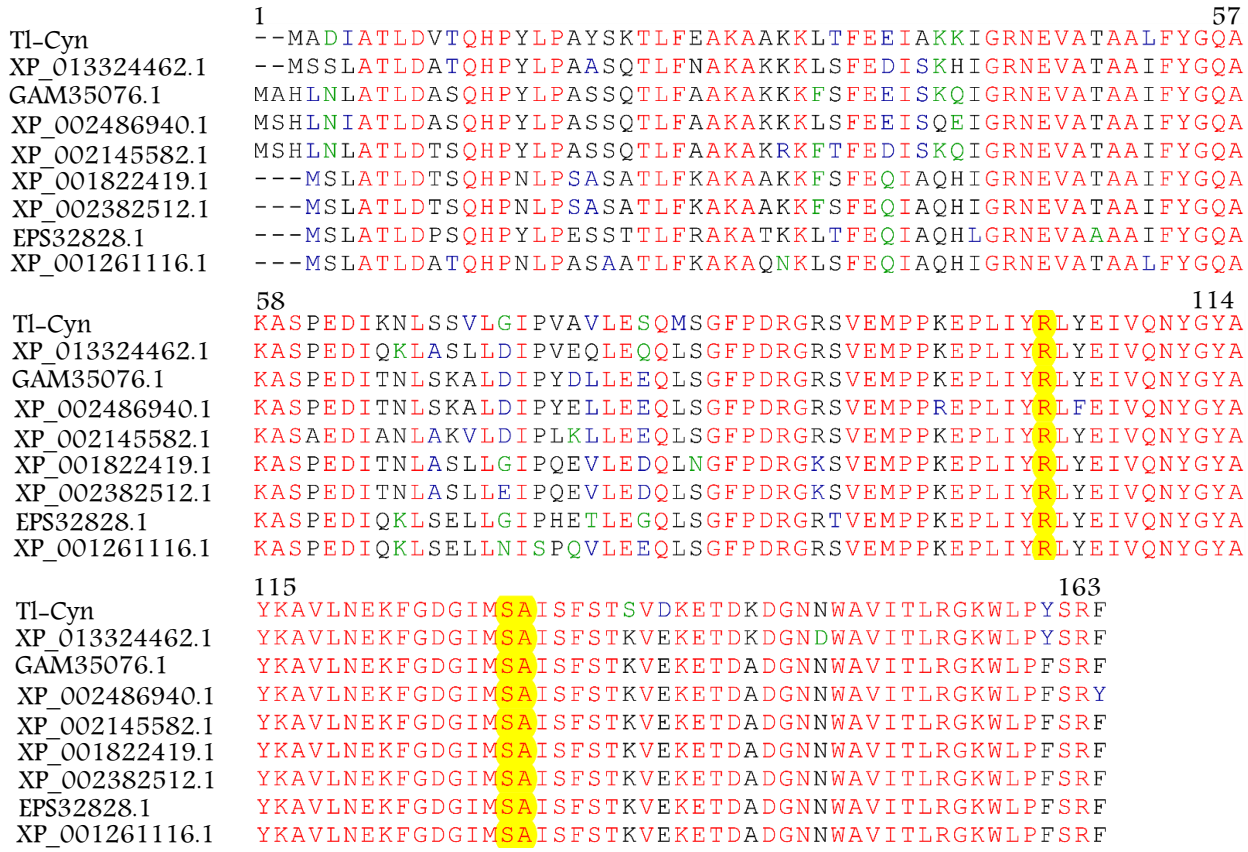

Fig. 2.3 Multiple amino acid sequence alignment of cyanases from *Rasamsonia emersonii* CBS 393.64 (XP_013324462.1), *Talaromyces cellulolyticus* (GAM35076.1), *Talaromyces stipitatus* ATCC 10500 (XP_002486940.1), *Talaromyces marneffei* ATCC 18224 (XP_002145582.1), *Aspergillus oryzae* RIB40 (XP_001822419.1), *Aspergillus flavus* NRRL3357 (XP_002382512.1), *Penicillium oxalicum* (EPS32828.1), and *Aspergillus fischeri* NRRL 181 (XP_001261116.1). Fully conserved residues are shown in red, block of similar residues are in blue, and weakly similar residues are in green. The R, S, and A residues of the catalytic triad are shown in red with yellow background.

2.3.3 rTl-Cyn activity and purification

Of the >100 clones screened for high titre of cyanate hydratase production, clone 26 displayed the highest extracellular rTl-Cyn activity (100±13 U mL^{-1}) and was selected for further investigation. No cell bound rTl-Cyn activity was observed in clone 26 which indicated efficient

functioning of the α-factor secretory signal sequence. A ~10-fold improvement in cyanate hydratase production was achieved by the recombinant *P. pastoris* compared with the wild-type *T. lanuginosus*. The rTl-Cyn was purified to homogeneity, in three steps *viz.*, ultrafiltration, ion-exchange chromatography and gel-filtration chromatography. The purity of rTl-Cyn was confirmed by SDS-PAGE as a single band corresponding to ~20 kDa (Fig. 2.4). The purified rTl-Cyn displayed a 34.66 fold increase in activity with a specific activity of 84545.45 U mg^{-1} (Table 2.2).

Table 2.2 Summary of rTl-Cyn purification from the recombinant *P. pastoris*

Purification step	**Total activity (U mL^{-1})**	**Total protein (mg mL^{-1})**	**Specific activity (U mg^{-1})**	**Purification fold**
Cell-free supernatant	100	0.041	2439	1
Ultrafiltration	209	0.076	2750	1.13
Anion exchange	185	0.0038	48684.21	19.96
Gel filtration	93	0.0011	84545.45	34.66

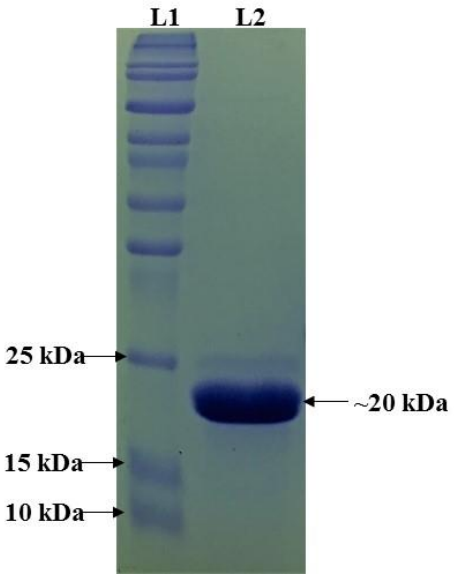

Fig. 2.4 SDS-PAGE analysis profile of rTl-Cyn. Lane 1: protein marker, lane 2: purified rTl-Cyn.

2.3.4 Biochemical characterization of rTl-Cyn

The optimum temperature and pH for rTl-Cyn activity were 60°C and pH 8, respectively (Fig. 2.5). In addition, rTl-Cyn displayed ~60% of its activity at pH 5.0-7.0 and more than 60% at pH 9.0. Similarly, it showed ~80% activity at 40°C and ~95% at 50°C, 70°C and 80°C. It was also observed that the optimum pH of rTl-Cyn was similar to that of the other known cyanases reported in literature (Elleuche and Pöggeler, 2008; Luque-Almagro *et al.*, 2008). Furthermore, the rTl-Cyn activity was marginally stimulated by Na^+ while other metal ions slightly inhibited or did not influence the activity (Table 2.3). In addition, rTl-Cyn activity was remarkably inhibited by azide (~44%), because it is a cyanide and cyanate analog. Conversely, the enzyme activity was not inhibited by cyanide, urea, nitrite, EDTA, or dithioerythritol up to 10 mM concentrations. Similar results were observed with cyanase from *Pseudomonas pseudoalcaligenes* CECT5344 (Luque-Almagro *et al.*, 2008). The reducing agent, β-mercaptoethanol displayed no effect on the rTl-Cyn activity, signifying that -SH groups had no role in the catalytic activity or rTl-Cyn does not have any free and accessible -SH groups. The chelating agent EDTA also had no effect on the rTl-Cyn activity, indicating that it did not require any cations for activity. Similar effects were observed with other enzyme where EDTA had no effect on enzymatic activity (Ranjan and Satyanarayana, 2016).

a

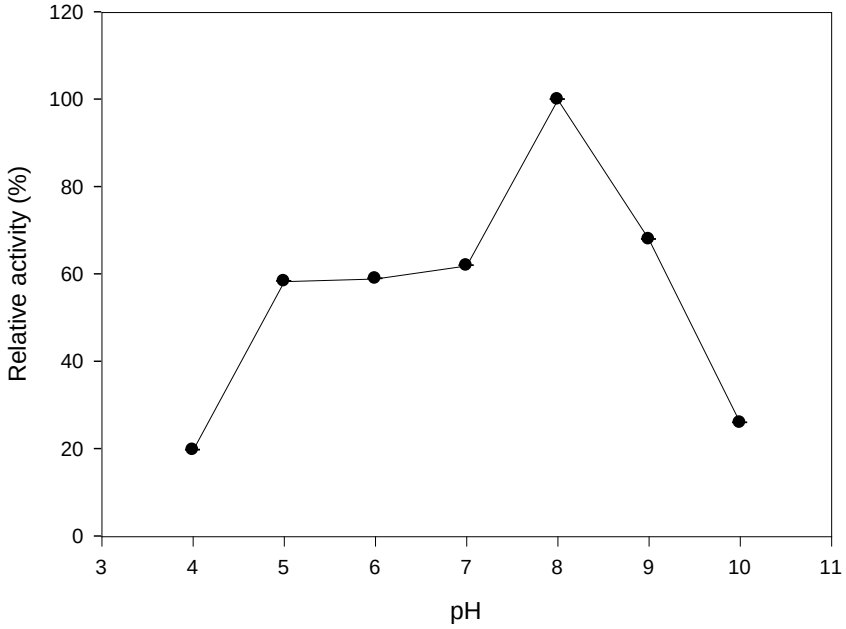

b

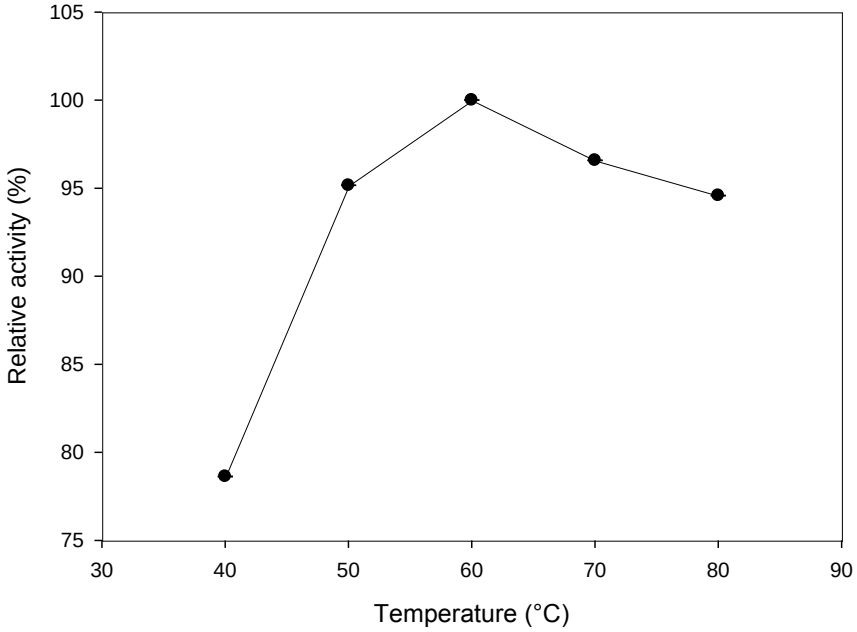

Fig. 2.5 Influence of temperature **(a)** and pH **(b)** on rTl-Cyn activity. For optimum pH rTl-Cyn activity was performed at 60°C and for optimum temperature rTl-Cyn activity was performed at pH 8.0.

Table 2.3 Effect of different metal ions on rTl-Cyn activity at 60°C for 10 min

Metal ions	Relative enzyme activity (%)	
	Metal ion concentration	
	2 mM	5 mM
As^{3+}	96 ± 0.93	93 ± 0.79
Cr^{2+}	92.6 ± 0.82	88.8 ± 0.84
Cd^{2+}	98 ± 0.72	97 ± 0.79
Cu^{2+}	97 ± 0.92	95 ± 0.86
Hg^{2+}	92 ± 0.89	89 ± 0.90
Na^{+}	102 ± 0.63	106 ± 0.68
Ni^{2+}	99.2 ± 0.82	97.4 ± 0.79
Pb^{2+}	93 ± 0.94	89 ± 0.83
Zn^{2+}	100 ± 0.39	99.8 ± 0.48

Control (no metal ions) = 100 ± 0.87

2.3.5 Kinetic parameters and thermodynamics of rTl-Cyn

The Michaelis constant (K_m) and maximum velocity (V_{max}) of rTl-Cyn were 0.34 mM and 2857.14 µmoles $mg^{-1}min^{-1}$, respectively. The turnover number (k_{cat}) and specificity constant (k_{cat}/K_m) of the rTl-Cyn were 2.14 x 10^4 s^{-1} and 6.3 x 10^7 M^{-1} s^{-1}, respectively, which was remarkably higher than that of the other known cyanases (Anderson *et al.*, 1994; Luque-Almagro *et al.*, 2008). A larger k_{cat} value of the rTl-Cyn suggests that only low amount of enzyme is required for its applications.

The deactivation constant (K_d) was calculated from the plot of ln[Et/Eo] vs time for rTl-Cyn (Fig. 2.6a). This value of K_d was substituted in Eq. (2) to calculate $T_{1/2}$ of the rTl-Cyn. The $T_{1/2}$ values of the rTl-Cyn at 60°C and 80°C were 16.16 and 2.6 h, respectively. An Arrhenius plot of the deactivation constant at different temperatures was plotted for calculating the deactivation energy (E_d) of rTl-Cyn (Fig. 2.6b), which was 91.73 kJ mol^{-1}. In addition, the activation energy of rTl-Cyn was also calculated and found to be 41.5 kJ mol^{-1}, further this value was substituted in Eq. (1) to calculate the temperature quotient (Q_{10}), and was 1.57.

a

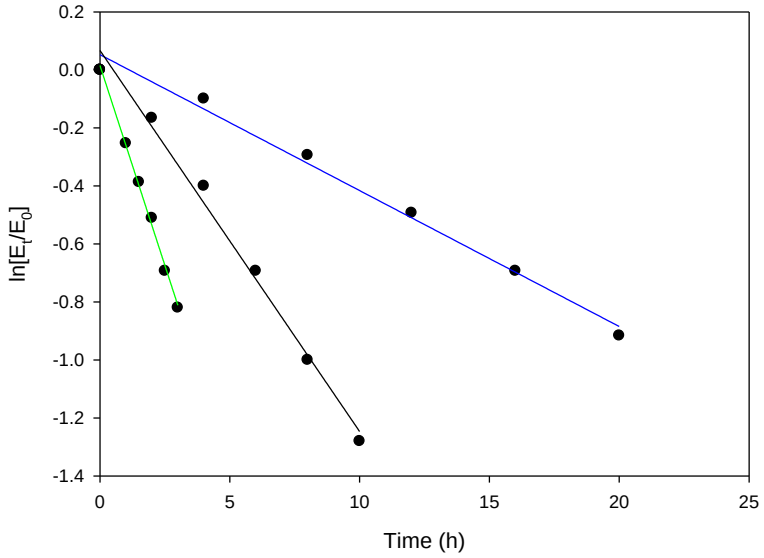

b

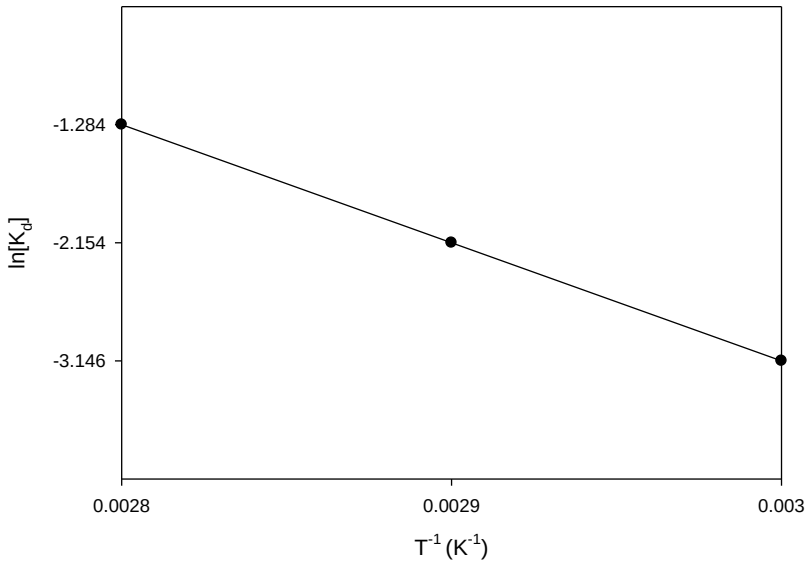

Fig. 2.6 Determination of thermodynamic parameters for the rTl-Cyn. **(a)** Plot of ln[E_t/E_0] vs time (h) for the calculation of deactivation constant (K_d) and $T_{1/2}$ of rTl-Cyn at different temperature [60°C (blue line), 70°C (black line), 80°C (green line)]. **(b)** Arrhenius plot of rTl-Cyn for the calculation of deactivation energy [E_d].

Thermodynamic parameters of thermal inactivation was calculated for rTl-Cyn by applying the first order kinetics to the thermal inactivation data. The overall ΔG, ΔH and ΔS values for thermal inactivation of rTl-Cyn were positive (Table 2.4). The enthalpy change (ΔH) represents the energy required for thermal denaturation of the protein. A large ΔH value signifies that high energy is required for breaking covalent bonds during thermal inactivation of rTl-Cyn. Free energy change (ΔG) was positive for rTl-Cyn, which indicates that the thermal denaturation of recombinant enzyme was non-spontaneous as reported for other enzymes (Ranjan *et al.*, 2015; Parashar and Satyanarayana, 2016; Ranjan and Satyanarayana, 2016). Also, the viability of any chemical reaction is mostly determined by the measurement of change in Gibbs free energy (ΔG), more precisely for the transformation of E-S complex into products. The lower the ΔG, the more viable is the reaction. Enzyme denaturation is also accompanied by an increase in the conformational disorder of the enzyme structure, which can be measured as entropy change (ΔS). Thus, ΔS values decreases with increasing enzyme stability (Yadav *et al.*, 2018).

Table 2.4 The thermodynamic parameters of rTl-Cyn measured during thermal deactivation at various temperatures

Temp (K)	**K_d (h^{-1})**	**$T_{1/2}$ (h)**	**ΔH (kJ mol^{-1})**	**ΔG(kJ mol^{-1})**	**ΔS (J mol^{-1} K^{-1})**
333.15	0.043	16.16	88.96	52.33	110.00
343.15	0.113	6.14	88.88	51.23	109.78
353.15	0.266	2.6	88.79	50.29	109.07

2.3.6 FTIR spectroscopy analysis

Complete degradation of cyanate and liberation of ammonia after the addition of rTl-Cyn in the reaction mixture was confirmed by FTIR analysis (Fig. 2.7). A characteristic peak in the range of 3400 and 3320 cm^{-1} was observed for ammonia and in contrast, a peak in the range of 2300-2100 cm^{-1} was observed for cyanate, in the control experiment (Fig. 2.7). Similar peaks were observed by Morimoto *et al*. (1976) for ammonia and by Alwis *et al*. (2015) for cyanate.

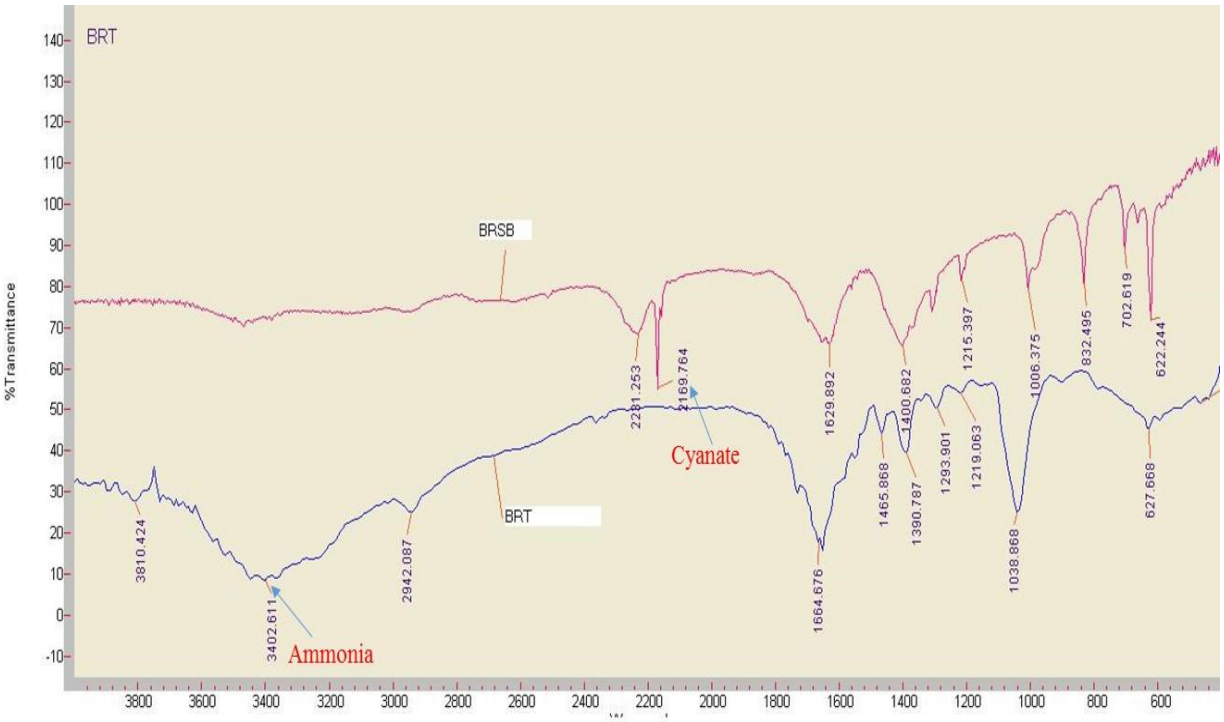

Fig. 2.7 FTIR analysis to assess the liberation of ammonia and complete degradation of cyanate using rTl-Cyn [red line- reaction mixture without rTl-Cyn (control) and blue line with rTl-Cyn].

2.3.7 Cyanate detoxification by rTl-Cyn

The degradation potential of rTl-Cyn was assessed in wastewater as well as in buffered (control) samples supplemented with 5-20 mM cyanate. Complete degradation of cyanate (10 mM concentration) was achieved in buffered sample (control) and 90% in a wastewater sample, within 10 min of incubation. Moreover, more than 80% of cyanate degradation was achieved, upto 20 mM cyanate concentration, in wastewater and control samples under the same conditions (Fig. 2.8). A similar study showed that 80% of cyanide (20 mM, KCN) degradation was achieved using cell-free extracts of *Rhodococcus* UKMP-5M in 80 min (Nallapan Maniyam et al., 2015). In addition, the concentration of heavy metals were also examined by AAS in wastewater samples under spiked and un-spiked conditions (Table 2.5). These findings revealed that the presence of heavy metals in the reaction mixture had no substantial effect on the catalytic activity of rTl-Cyn, achieving ~95% cyanate degradation compared to un-spiked samples. Furthermore, it was also noticed that the degradation of cyanate was lower in a wastewater sample compared to buffered

sample. This could be due to the fact that wastewater contains many impurities which might have inhibited the proper binding of rTl-Cyn to cyanate.

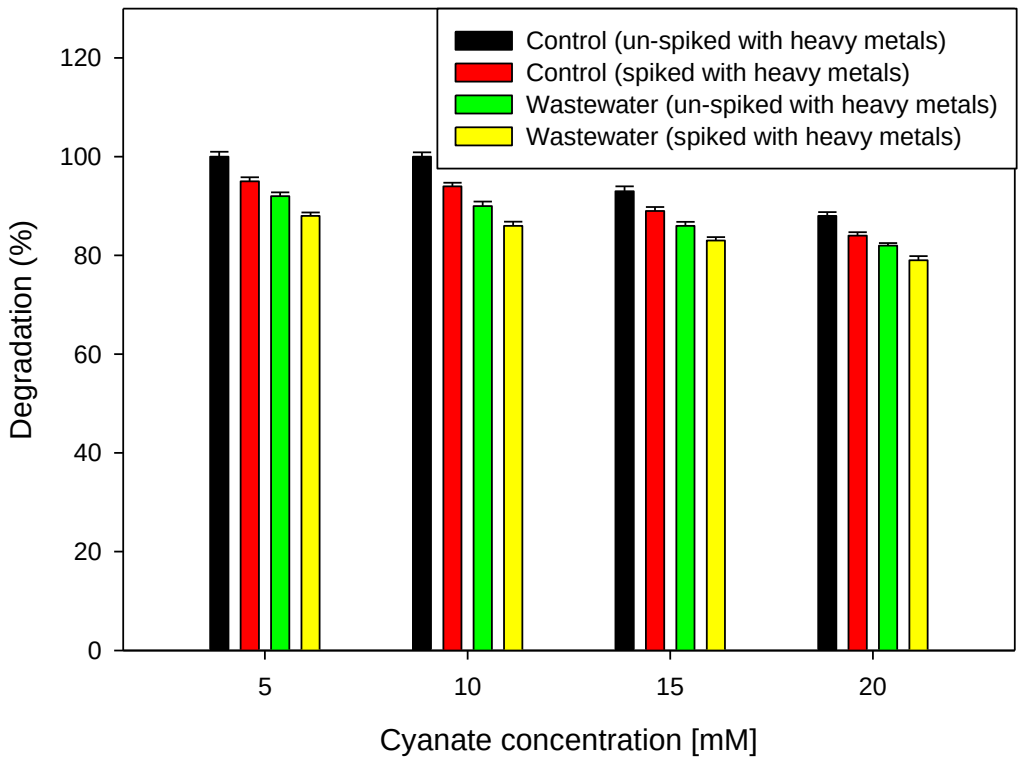

Fig. 2.8 Degradation of cyanate in wastewater and control samples using rTl-Cyn. Control= Tris-HCl buffer (50 mM, pH 8.0).

Table 2.5 Heavy metal analysis of a wastewater sample under spiked and un-spiked conditions using atomic absorption spectroscopy

Metals	**Spiked with metals [mg L^{-1}]**	**Not spiked with metals [mg L^{-1}]**
Ag^{+}	0.32	0.01
Au^{3+}	1.77	0.16
Cd^{2+}	574	0.01
Cr^{2+}	61.2	0.01
Cu^{2+}	263	<0.01
Fe^{2+}	167.5	<0.01
Pb^{2+}	20.8	0.49
Zn^{2+}	319	<0.01

2.4 Conclusions

The cyanate hydratase gene of *T. lanuginosus* SSBP was successfully expressed in *P. pastoris*. The recombinant *P. pastoris* produced ~10-fold higher titre of cyanate hydratase activity compared with the original host. The high thermostability, catalytic-efficiency and metal-tolerance of rTl-Cyn makes it a good biocatalyst for cyanate detoxification.

CHAPTER 3

A novel strategy for the efficient removal of toxic cyanate by the combinatorial use of recombinant enzymes immobilized on aminosilane modified magnetic nanoparticles

(*Published: Ranjan, B., Pillai, S., Permaul, K., and Singh, S. (2018) A novel strategy for the efficient removal of toxic cyanate by the combinatorial use of recombinant enzymes immobilized on aminosilane modified magnetic nanoparticles. Bioresource Technology.* ***253****: 105-111*).

3.1 Introduction

Cyanide is one of the most toxic chemicals widely used in mining industries for the extraction of metals and electroplating (Barakat *et al.*, 2004; Luque-Almagro *et al.*, 2016). The mining industry discharges several billion pounds of toxic wastewaters, which in addition to cyanide, contains silver, gold, cadmium, chromium, copper, iron, lead, zinc etc. (Luque-Almagro *et al.*, 2011). Cyanide is also applied as an anticaking agent in road salt and fire retardants. Cyanate (OCN^-) is an important cyanide derivative formed by its oxidation (Luque-Almagro *et al.*, 2016), and is present in cyanide contaminated environments. The application of pesticides and fungicides in agriculture also results in the accumulation of cyanate in the environment (Elmore *et al.*, 2015).

The treatment of cyanurated wastewaters has been performed using several physical, chemical and biological methods or combinations of them (Papadimitriou *et al.*, 2006; Sharma *et al.*, 2012; Pal and Kumar, 2013; Glanpracha and Annachhatre, 2016). Alkaline breakpoint chlorination [Equation (1a, b)] is a commonly used chemical oxidation method for cyanide removal (Barakat *et al.*, 2004; Baxter and Cummings, 2006).

$$Cl_2 + CN^- \longrightarrow CNCl + Cl^- \quad (1a)$$

$$CNCl + H_2O \longrightarrow OCN^- + Cl^- + 2H^+ \quad (1b)$$

However, this method has substantial disadvantages as it needs special requirements for waste removal, releases more toxic chemical agents (such as OCN^-) and the potential formation of

chlorinated organic compounds (Huertas *et al.*, 2010). Alternate chemical treatments such as the SO_2/air (INCO) process have also been used, which involves combining sulphur dioxide with oxygen and cyanide compounds in the presence of a copper catalyst [Equation (2)] and the oxidation of cyanide compounds using hydrogen peroxide [Equation (3)], which also results in the formation of cyanate (Baxter and Cummings, 2006).

$$CN^- + SO_2 + O_2 + H_2O \xrightarrow{Cu^{2+}\ catalyst} OCN^- + H_2SO_4 \qquad (2)$$

$$CN^- + H_2O_2 \xrightarrow{Cu^{2+}\ catalyst} OCN^- + H_2O \qquad (3)$$

Due to the several disadvantages allied with chemical treatments for cyanide removal, eco-friendly technologies by means of activated sludge (Papadimitriou *et al.*, 2009; Ryu *et al.*, 2017) or microbes (Ebbs, 2004) have been employed. However, the complex nature of polluted wastewaters, and the high concentrations of cyanide or cyanate in industrial effluents, may weaken the sustainability and activity of microorganisms (Papadimitriou *et al.*, 2009; Sharma and Philip, 2014). In contrast, the cyanate hydrolyzing enzyme, cyanate hydratase (also called as cyanase), detoxifies cyanate by transforming it to ammonium (NH_4^+) and carbon dioxide (CO_2) in a bicarbonate-dependent reaction (Johnson and Anderson, 1987). Since bicarbonate is required to facilitate the reaction, a novel strategy was developed to limit the dependency on exogenous bicarbonate by the combinatorial use of two recombinant enzymes, rTl-Cyn and recombinant carbonic anhydrase (rTl-CA) for cyanate removal.

The use of free enzymes have some limitations such as, large consumption, difficulty in separation and recycling, which are key factors for their effective utilization at industrial scale (Madhavan *et al.*, 2017). Enzyme immobilization offers an alternative to resolve the challenges associated with the reusability of enzymes coupled with numerous advantages, such as, enhanced thermal stability and ease of separation (Dehnavi *et al.*, 2015; Zhou *et al.*, 2017). Immobilization methods generally include adsorption (Wu *et al.*, 2014), combination (Karimi *et al.*, 2014), and entrapment (Kovalenko *et al.*, 2013). Due to the increasing demands for enzyme applications in various industrial processes, there is a constant search for new materials to be used for immobilization. Among these, magnetic nanoparticles (MNPs) are deemed appropriate for enzyme

immobilization owing to their small size, high surface area, superparamagnetism, low toxicity and good catalytic properties (Xu and Wang, 2012; Pereira *et al.*, 2017).

The use of surface functionalization of MNPs increases their stability in solution which prevents the formation of agglomerates due to magnetic dipole interactions (Villa *et al.*, 2016). Surface functionalization also facilitates the attachment of anchoring mediates and subsequent grafting of acidic, basic, hydrophilic or hydrophobic functional groups. This contributes to an engineered surface with selective affinity towards diverse bio-compounds which are amenable to biocompatibility measures (Kovalenko *et al.*, 2013; Dehnavi *et al.*, 2015). Silanization is one of the most widely-used techniques for introducing functional groups on the surface of MNPs (Faridi *et al.*, 2017).

In this chapter, the detoxification of cyanate was assessed by the combinatorial use of recombinant enzymes, rTl-Cyn and rTl-CA. As the ability of rTl-Cyn for cyanate detoxification has been described in the previous chapter, this chapter focuses on: (i) to evaluate the synergistic effect of rTl-Cyn and rTl-CA on the degradation potential of cyanate at varying concentrations of bicarbonate; (ii) to determine the influence of rTl-CA on the efficacy of cyanate degradation under the same conditions; (iii) to immobilize the rTl-Cyn and rTl-CA on silanized MNPs and assess their reusability in cyanate degradation; (iv) to characterize the free and immobilized MNPs using FTIR spectroscopy, FE-SEM, and XRD analysis.

3.2 Materials and Methods

3.2.1 Strains and reagents

All plasmid constructions were performed using *E. coli* DH5α as the host and *E. coli* BL21 (DE3) (Invitrogen) was used as the expression host. The pJET1.2/blunt vector (Thermo Scientific) was used as the cloning vector for nucleotide sequence determination. pET28a(+) (Novagen) vector was used for the cloning and expression of *Tl-Cyn* and *Tl-CA* genes. Ni^{2+}-NTA agarose resin (Qiagen) was used for protein purification. Restriction enzymes were procured from New England Biolabs (NEB). Primers used in this study were procured from Integrated DNA Technologies (IDT). Wastewater samples were collected from the influent of an industrial wastewater treatment plant in KwaZulu-Natal, South Africa.

3.2.2 RNA isolation, cDNA synthesis and construction of *Tl-Cyn* and *Tl-CA* plasmids

RNA isolation and cDNA synthesis from *T. lanuginosus* SSBP were performed as described previously in chapter 2. Cyanate hydratase and carbonic anhydrase genes were amplified from cDNA using primers P1/P2 and P3/P4, respectively (Table 3.1), containing *Eco*RI and *Hin*dIII restriction sites. PCR conditions used in this study were as follows: denaturation at 95°C for 1 min; 25 cycles (denaturation at 95°C for 40 s, annealing at 58°C for 30 s, elongation 72°C for 60 s) and final elongation at 72°C for 8 min, for the amplification of *Tl-Cyn* and *Tl-CA* genes. PCR products of 500 bp and 583 bp for *Tl-Cyn* and *Tl-CA*, respectively were obtained and digested with *Eco*RI and *Hin*dIII restriction enzymes and cloned into the plasmid pET28a(+) vector to make pET28a-*Tl-Cyn* and pET28a-*Tl-CA* constructs. The constructs were confirmated by double digestion with *Eco*RI and *Hin*dIII. The presence and precise positioning of the inserts were confirmed by DNA sequencing.

Table 3.1 Primers used in this study

Primers	Oligonucleotide sequence (5′→3′)
P1	CGGAATTCATGGCTGATATCGCAACCC
P2	GGTTAAGCTTTTAGAATCGACTGTATGGC
P3	CGGAATTCATGGGTTTCCGCATTTATGGC
P4	GGTTAAGCTTTTATGTGCACACCTCCGGATCAAC

GAATTC– restriction site for *Eco*RI; AAGCTT– restriction site for *Hin*dIII.

3.2.3 Expression and purification of rTl-Cyn and rTl-CA

Plasmids isolated from both the positive clones, pET28a-*Tl-Cyn* and pET28a-*Tl-CA* were transformed into *E. coli* BL21 (DE3), and the transformants were cultured at 37°C for 16-18 h in LB medium supplemented with kanamycin (50 µg/mL). LB-kanamycin medium (100 mL) was inoculated with *E. coli* BL21 (DE3) and cultivated at 37ºC until the absorbance (A_{600}) reached 0.5 to 0.7 (Ranjan *et al.*, 2015). The expression of *Tl-Cyn* and *Tl-CA* genes under the control of the T7 promoter was induced by adding 0.8 mM isopropyl-β-D-thiogalactopyranoside (IPTG) with further incubation at 25ºC for 8 h. The cells were harvested by centrifugation (13000 × g for 20

min) and cell pellets were resuspended in Tris-HCl buffer (50 mM, pH 8.0). Resuspended cells were sonicated using 2 s pulses for 10 min at 21% amplitude in a ultrasonic sonicator (Sonics Vibra-cell), to release the intracellular proteins. Thereafter, sonicated samples were centrifuged (13000 × g for 20 min) to remove cell debris, and the supernatant was evaluated for enzyme activity. Recombinant cyanate hydratase and carbonic anhydrase were purified as described by Parashar and Satyanarayana (2016).

3.2.4 Enzyme assays

Cyanate hydratase activity was determined as previously described in chapter 2. One unit (U) of cyanate hydratase was defined as the amount of enzyme that liberates 1 µmol of ammonium per minute under the standard assay conditions.

Carbonic anhydrase activity was analyzed by a modified protocol of Khalifah (1971). The assay was carried out at 4°C by adding 0.1 mL of rTl-CA to 3.0 mL of Tris-HCl buffer (20 mM, pH 8.0). Thereafter, the reaction was initiated by the addition of ice-cold CO_2-saturated water (2.0 mL). The time interval for the pH to decrease by 1 unit (from 8.0 to 7.0) due to the release of protons during CO_2 hydration was measured. One unit of rTl-CA activity was defined as the amount of enzyme required to reduce pH of the buffer from 8.0 to 7.0, and expressed as Wilbur-Anderson (WA) units per unit volume.

3.2.5 Biodegradation of cyanate by rTl-Cyn

rTl-Cyn (20 U) was added to reaction mixtures (1 mL total volume) containing Tris-HCl buffer (50 mM, pH 8.0), $NaHCO_3$ (3 mM), KOCN (4 mM), and was incubated at 60°C for 10 min in a reciprocating water bath at 100 rpm. The stability of rTl-Cyn in the presence of heavy metal ions such as Ag^{+}, Au^{3+}, Cd^{2+}, Cr^{2+}, Cu^{2+}, Fe^{2+}, Pb^{2+}, and Zn^{2+} was also assessed. In addition, the buffered sample was replaced with an industrial wastewater sample (1 mL total volume) spiked with cyanate (4 mM). Thereafter, samples were incubated for 10 min and centrifuged at 10000 × g for 10 min. The resulting supernatants were analyzed spectrophotometrically for the product released at 420 nm. Samples were also analyzed by Fourier transform infrared spectroscopy (FTIR) for the presence of ammonia and cyanate, as previously described in chapter 2. The concentration of different heavy metals in the wastewater sample was analyzed by atomic absorption spectroscopy (AAS) (Srikanth *et al.*, 2013).

3.2.6 Biodegradation of cyanate by rTl-Cyn and rTl-CA and optimization of their concentrations

rTl-Cyn (20 U) was added to reaction mixtures (1 mL total volume) containing Tris-HCl buffer (50 mM, pH 8.0), $NaHCO_3$ (3 mM) and KOCN (4 mM). Incubation of the reaction mixtures were carried out for 10 min at 60°C in a shaking water bath at 100 rpm, and the liberation of ammonia was measured by a colorimetric method. $NaHCO_3$ at different concentrations (0.3-3.0 mM) were also added to the buffered samples at the above conditions and ammonia release was analyzed. rTl-Cyn and rTl-CA were also mixed together, and incubated at the above conditions and was evaluated for cyanate degradation. Buffered samples were replaced with industrial wastewater and the reaction was carried out under the same conditions. Varying concentrations of rTl-CA were used in combination with rTl-Cyn, together with different concentrations of $NaHCO_3$, to determine the minimum amount of rTl-CA required for cyanate degradation.

3.2.7 Synthesis of MNPs

A chemical co-precipitation method was used for the preparation of MNPs (Can *et al.*, 2009), wherein a 1.75:1 molar ratio of Fe^{3+}:Fe^{2+} was dissolved in 320 mL of Milli-Q water. The mixture was stirred vigorously under N_2 at 80°C for 1 h. Aqueous ammonia solution (25%) was added to the mixture to raise the pH to ~10, and continuously stirred for another 1 h under N_2-sparging and cooled to room temperature. The black magnetic slurry was collected by a magnet and thereafter washed several times with ethanol followed by several cycles of washes with Milli-Q water. Finally, MNPs were dispersed by sonication for 15 min and the precipitates were removed and dried under vacuum at 60°C overnight.

3.2.8 Silanization of MNPs by (3-aminopropyl)-triethoxysilane (APTES)

The MNPs obtained from co-precipitation (1.0 g) were dispersed in a solution of APTES (20%) and glycerol (4.0 mL) and the mixture was heated for 2 h at 90°C with simultaneous N_2-sparging and mechanical stirring, as previously described (Faridi *et al.*, 2017). The solution was cooled to room temperature and the modified MNPs were sonicated for 10 min, collected with a magnet followed by several washings with ethanol and Milli-Q water and dried under vacuum at 60°C overnight.

3.2.9 Immobilization of rTl-Cyn and rTl-CA on modified MNPs

Prior to immobilization on modified MNPs, carboxyl groups of rTl-Cyn and rTl-CA were pre-treated with 3-(3 dimethylaminopropyl) N′-ethylcarbodiimide (EDC) and N-hydroxysuccinimide (NHS) as described previously (Faridi *et al.*, 2017). EDC (4 mg) was added to a 10 mL solution of rTl-Cyn:rTl-CA (1:0.75; v/v), incubated at room temperature for 1 h with gentle shaking, followed by the addition of NHS (5 mg). The pre-treated enzymatic solution was then added to MNPs (20 mg) and incubated at room temperature for 3 h with gentle shaking. A schematic illustration of the MNPs synthesis, their modification and immobilization of rTl-Cyn/rTl-CA is shown in Fig. 3.1.

3.2.10 Determination of the binding efficiency of rTl-Cyn and rTl-CA onto silanized MNPs

MNPs (5 mg) were mixed with the recombinant enzyme (1-10 mg) for 3 h. After immobilization, the amount of free enzyme in the supernatant was measured by the Lowry method (Lowry *et al.*, 1951), using bovine serum albumin as the standard. The binding capacity of the MNPs against varied concentrations of enzyme was determined by the difference in concentration of the free enzyme after immobilization against the initial enzyme concentration (Faridi *et al.*, 2017).

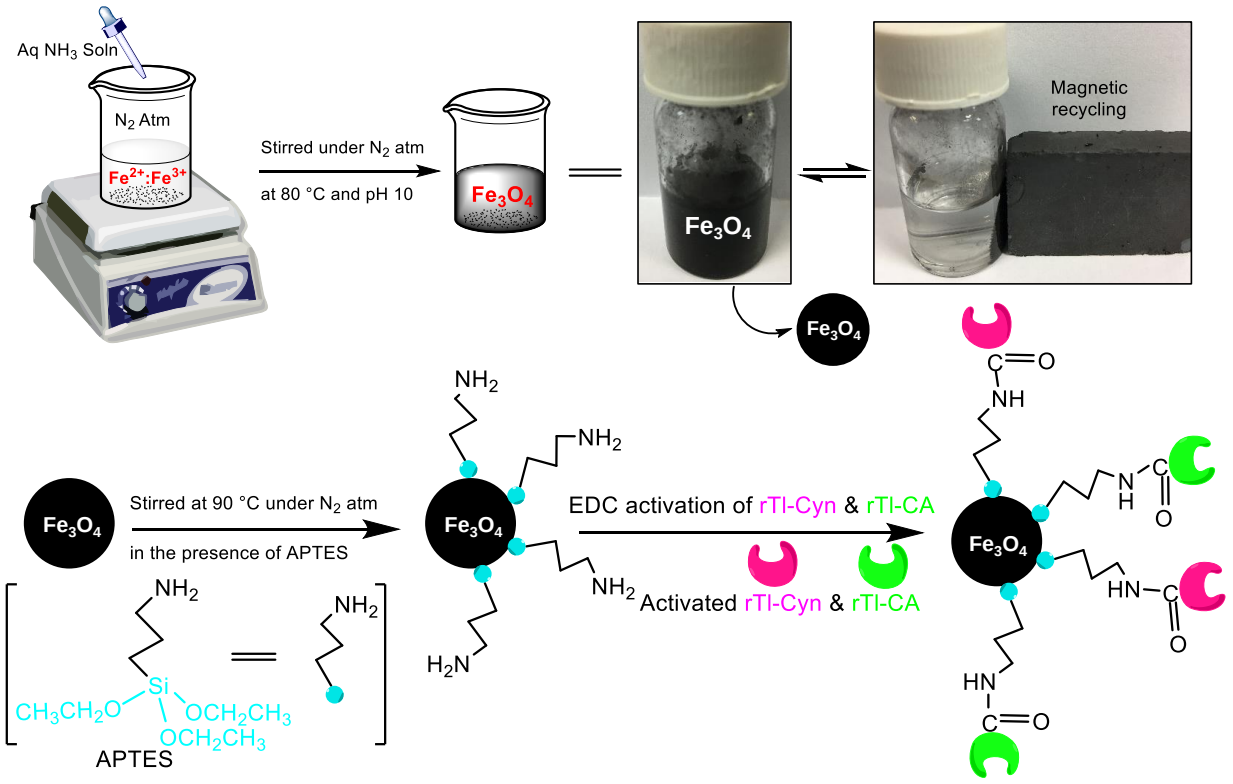

Fig. 3.1 Schematic illustration of magnetic nanoparticles synthesis modified with APTES for rTl-Cyn/rTl-CA immobilization.

3.2.11 Characterization of nanoparticles

Adsorption of functional groups on the surface of MNPs were confirmed by infrared spectra of the nanoparticles recorded on FTIR spectroscopy (Perkin Elmer). Field emission scanning electron microscopy (FE-SEM) was performed to study the morphology of MNPs using a Zeiss Gemini instrument. The crystalline structure and phase purity of the MNPs prepared were identified by X-ray diffraction (Philips PW1830).

3.2.12 Reusability of the immobilized enzyme

To study the reusability of Fe_3O_4/APTES-rTl-Cyn-rTl-CA, the immobilized enzyme was recovered by magnetic separation after each batch reaction. The recovered immobilized-enzyme was washed several times with Tris-HCl buffer (20 mM, pH 8.0) to prepare for the subsequent batch reaction.

3.3 Results and Discussion

3.3.1 Construction, expression and purification of rTl-Cyn and rTl-CA

Tl-Cyn and *Tl-CA* genes were constructed from the cDNA of *T. lanuginosus* SSBP and the generated constructs, pET28a-*Tl-Cyn* and pET28a-*Tl-CA*, were confirmed by colony PCR and double digestion (using *Eco*RI and *Hin*dIII restriction enzymes).

The expression of rTl-Cyn and rTl-CA were confirmed by investigating the whole-cell protein profiles of the induced cultures (Fig. 3.2a). rTl-Cyn and rTl-CA were further purified to homogeneity, and the purity of recombinant enzymes were confirmed by SDS-PAGE analysis. The bands for rTl-Cyn and rTl-CA corresponding to ~18 kDa and ~22 kDa, respectively, were visualized on SDS-PAGE (Fig. 3.2b). The sizes of rTl-Cyn and rTl-CA were comparable to those reported for *E. coli* K12 (17 kDa) (Sung and Fuchs, 1988) and *E. coli* (24 kDa) (Guilloton *et al.*, 1992), respectively.

3.3.2 Effect of industrial wastewater components on cyanate degradation

The effect of industrial wastewater components, especially heavy metals, were evaluated with purified rTl-Cyn in Tris-HCl buffer (50 mM, pH 8.0) containing 4 mM of cyanate. Complete (100%) cyanate degradation was attained in buffered conditions (without the addition of heavy metals) with 20 U of rTl-Cyn after 10 min. This was confirmed by UV-vis spectrophotometry and also by FTIR spectroscopy. However, in other studies, nearly 60% of cyanide degradation was observed using cyanide hydratase (Martínková and Chmátal, 2016), and the concentration of cyanide was decreased by 50% using cell-free extracts of *Rhodococcus* UKMP-5M (Nallapan Maniyam *et al.*, 2015).

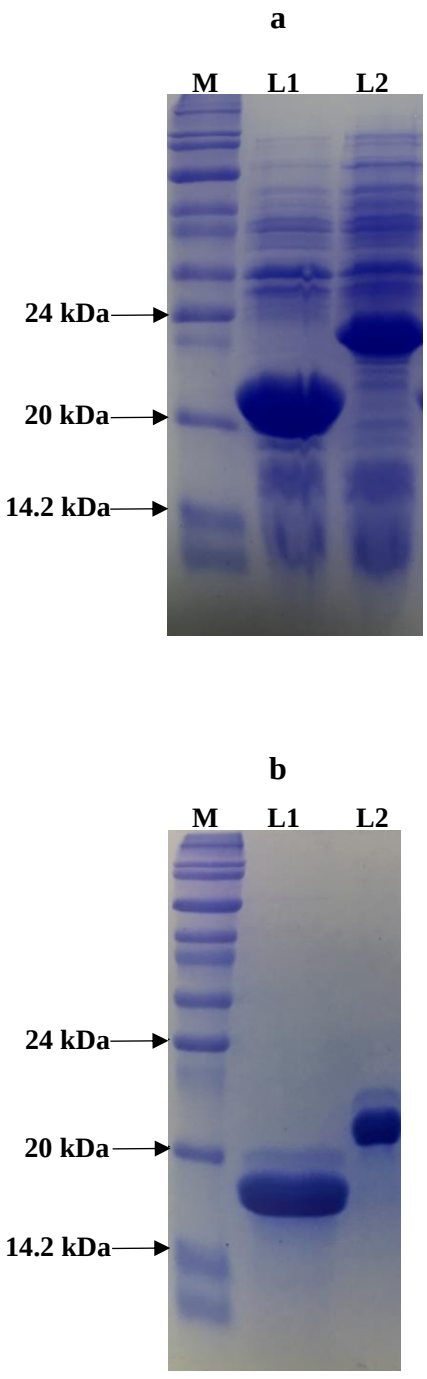

Fig. 3.2 SDS-PAGE analysis profile of rTl-Cyn and rTl-CA. **(a)** whole-cell protein profile, **(b)** purified protein profile: M- protein marker; L1- rTl-Cyn; L2- rTl-CA.

The effect of individual heavy metals (Ag^{+}, Au^{3+}, Cd^{2+}, Cr^{2+}, Cu^{2+}, Fe^{2+}, Pb^{2+} or Zn^{2+}) on rTl-Cyn activity was assessed. It was observed that heavy metals when applied individually was not inhibitory to rTl-Cyn, as the enzyme displayed >91% of its initial activity. A 10% reduction in enzyme activity was noticed when all the heavy metals were applied together. The concentration of cyanate did not decrease in control experiments without rTl-Cyn. Since, degradation of cyanate by rTl-Cyn was not affected by the addition of heavy metals, this suggests that the enzyme is reasonably robust.

3.3.3 Application of rTl-Cyn in industrial wastewaters

rTl-Cyn was able to degrade 90% of cyanate in industrial wastewater samples, not spiked with heavy metals, and 85% of cyanate degradation when samples were spiked with heavy metals. In addition, the concentration of heavy metals were examined by AAS in wastewater samples under spiked and un-spiked conditions (Table 3.2). Cyanate was completely degraded in a buffered sample within 10 min following the addition of rTl-Cyn. Cyanate degradation was also confirmed by FTIR spectroscopy, with peaks in the range of 3400-3320 cm^{-1} for ammonia and 2300-2100 cm^{-1} for cyanate in control experiments (Fig. 3.3).

Table 3.2 Heavy metal analysis of industrial wastewater samples under spiked and un-spiked conditions using atomic absorption spectroscopy

Metals	**Spiked with metals [mg L^{-1}]**	**Not spiked with metals [mg L^{-1}]**
Ag^{+}	0.42	0.04
Au^{3+}	2.21	0.28
Cd^{2+}	627	0.02
Cr^{2+}	77.4	0.03
Cu^{2+}	301.5	0.08
Fe^{2+}	16.5	<0.01
Pb^{2+}	21.9	0.94
Zn^{2+}	351	0.03

a

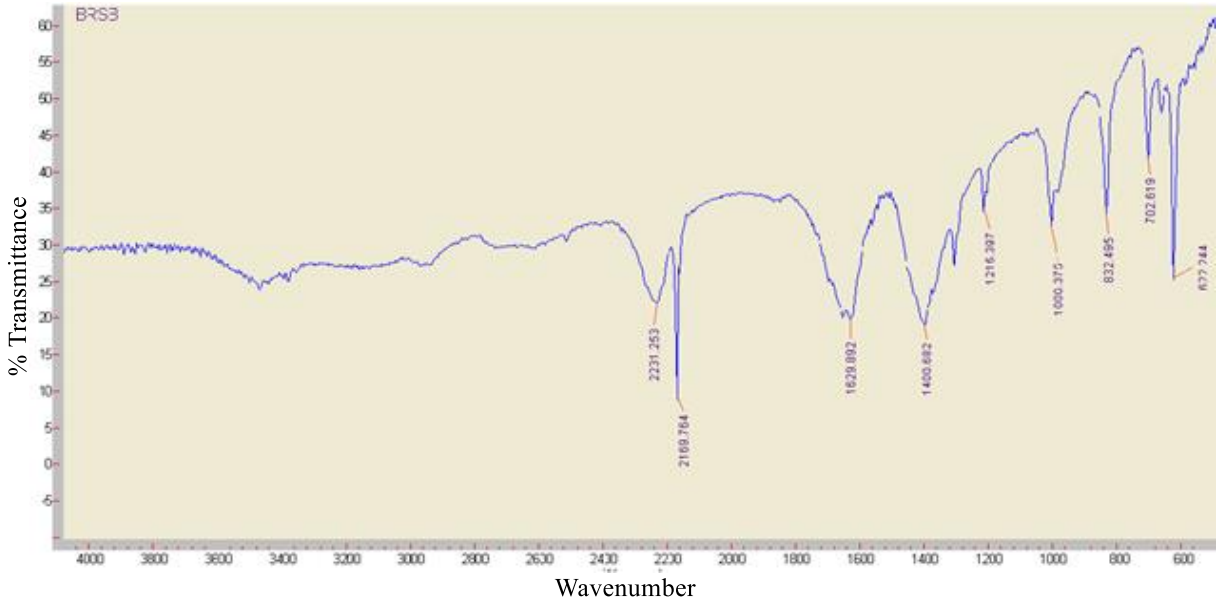

b

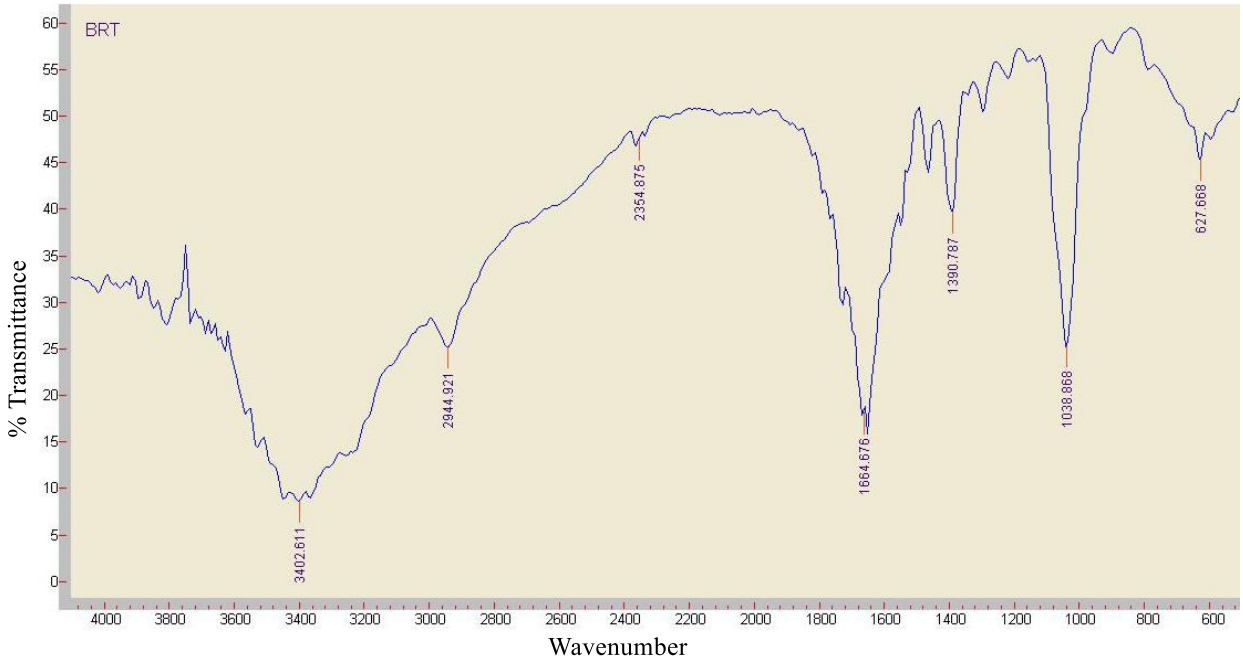

Fig. 3.3 FTIR spectra showing degradation of cyanate and release of ammonia. **(a)** Reaction mixture without rTl-Cyn, **(b)** reaction mixture with rTl-Cyn.

Until now, only rTl-Cyn was used for the removal of cyanate from the industrial wastewater sample (Chapter 2). Moreover, other close comparison is the cyanide hydratase expressed in *E. coli* from *A. niger* K10, showed 80% degradation of cyanide (Rinágelová *et al.*, 2014). Although, rTl-Cyn is able to degrade cyanate in wastewater samples, there is a dependency on bicarbonate for its effective degradation and this is a hurdle for any large-scale application. To overcome this bottleneck, rTl-Cyn were complemented with rTl-CA from *T. lanuginosus* SSBP.

3.3.4 Combinatorial effect of rTl-Cyn and rTl-CA in industrial wastewater bioremediation

Cyanate degradation by rTl-Cyn was increased from 30 to 100% with increasing concentrations of $NaHCO_3$ from 0.3 to 3 mM (Fig. 3.4a). In comparison, the combined application of rTl-Cyn and rTl-CA, resulted in complete cyanate degradation with 0.6 mM $NaHCO_3$ (Fig. 3.4b). It was noted that, the combined use of rTl-Cyn and rTl-CA resulted in a 3-fold increase in cyanate degradation in the presence of 0.6 mM $NaHCO_3$, where rTl-CA contributing to an overall enhancement of 64%. This clearly shows that the synergy of rTl-Cyn and rTl-CA enhanced cyanate degradation even at low bicarbonate concentration in comparison to rTl-Cyn alone. Three different ratios of rTl-CA were tested, while rTl-Cyn was kept constant, in the presence of different concentrations of $NaHCO_3$ (Fig. 3.4b, c, d), and observed that a rTl-Cyn:rTl-CA ratio of 1.0:0.75 was optimum for efficient cyanate degradation (Fig 3.4c). This optimized enzyme combination was further used for the degradation of cyanate as well as for immobilization experiments. Although, other cyanases have been previously reported (Elleuche and Pöggeler, 2008; Luque-Almagro *et al.*, 2008; Qian *et al.*, 2011) their potential for the bioremediation of cyanurated wastewaters has not been explored. The closest comparison to this study was the application of cyanide hydratase and tyrosinase in a two-step process for phenol degradation (Martínková and Chmátal, 2016). Therefore, the combinatorial use of rTl-Cyn and rTl-CA opens up new prospects for the efficient biodegradation of cyanurated industrial wastes. A schematic illustration of the process for the expression of rTl-Cyn and rTl-CA and their combinatorial use to reduce bicarbonate utilization in cyanate removal is shown in Fig. 3.5.

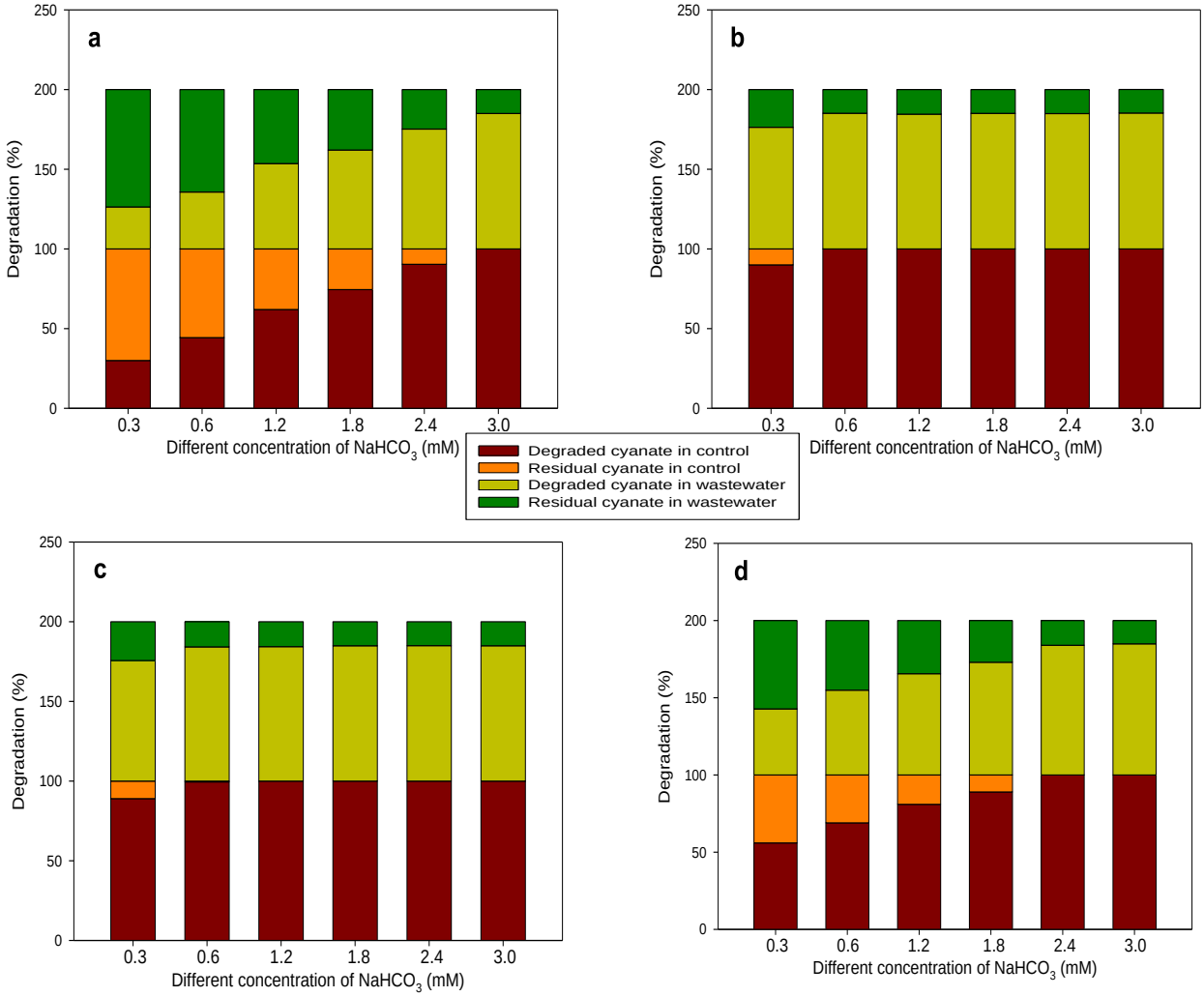

Fig. 3.4 Degradation of cyanate in control and industrial wastewater at different concentrations of $NaHCO_3$ by **(a)** rTl-Cyn, **(b)** rTl-Cyn:rTl-CA (1:1), **(c)** rTl-Cyn:rTl-CA (1:0.75), **(d)** rTl-Cyn:rTl-CA (1:0.5). Control= buffered conditions without heavy metals. Industrial wastewater samples were spiked with cyanate and different heavy metals.

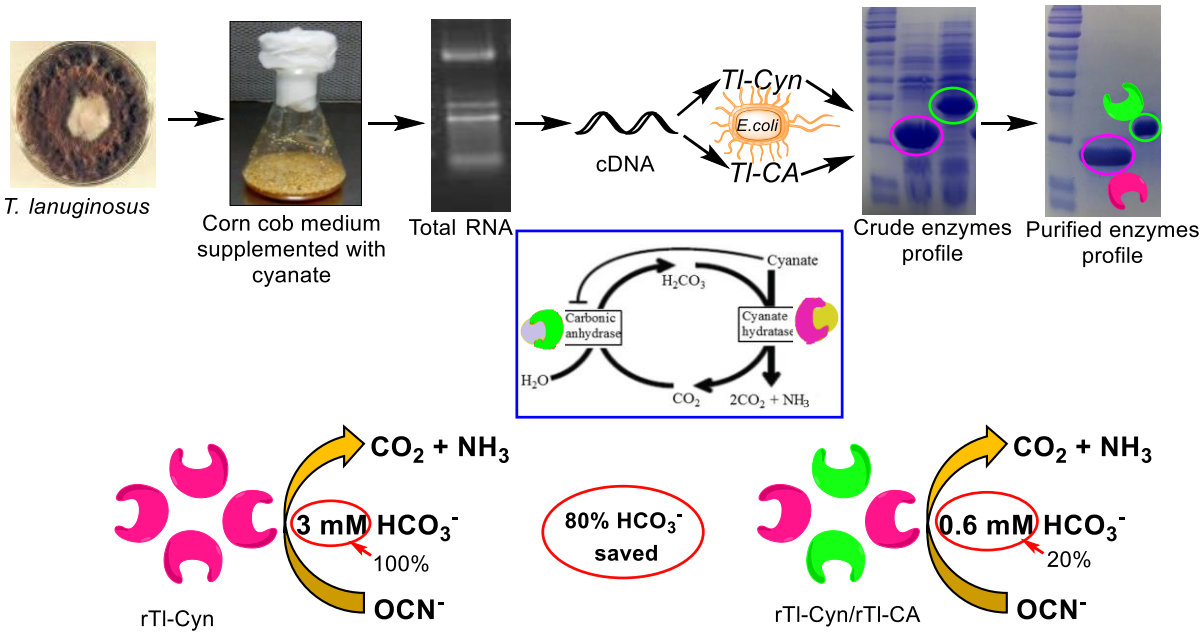

Fig. 3.5 Schematic demonstration of rTl-Cyn; rTl-CA expression and a strategy for the efficient removal of cyanate by their combinatorial use to save the bicarbonate utilization.

3.3.5 Characterization of nanoparticles

FE-SEM images of Fe_3O_4 and Fe_3O_4/APTES nanoparticles revealed that the Fe_3O_4 nanoparticles had a diameter in the range of 50 to 200 nm (Fig 3.6). Morphological changes were not evident for the APTES-grafted samples (Fig 3.6b) compared to their bare counterparts (Fig 3.6a).

a

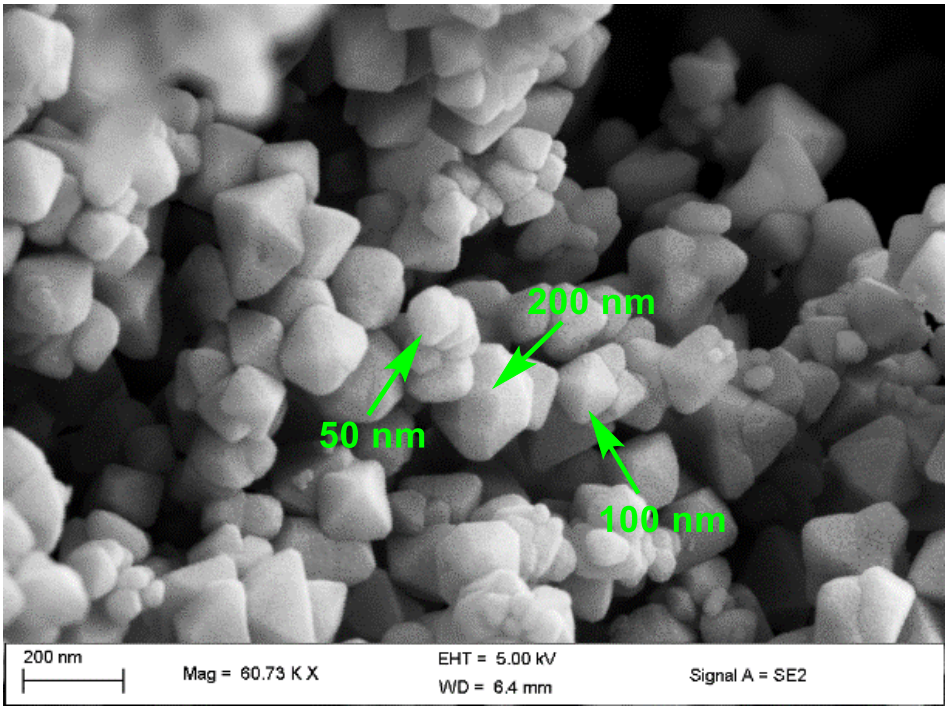

b

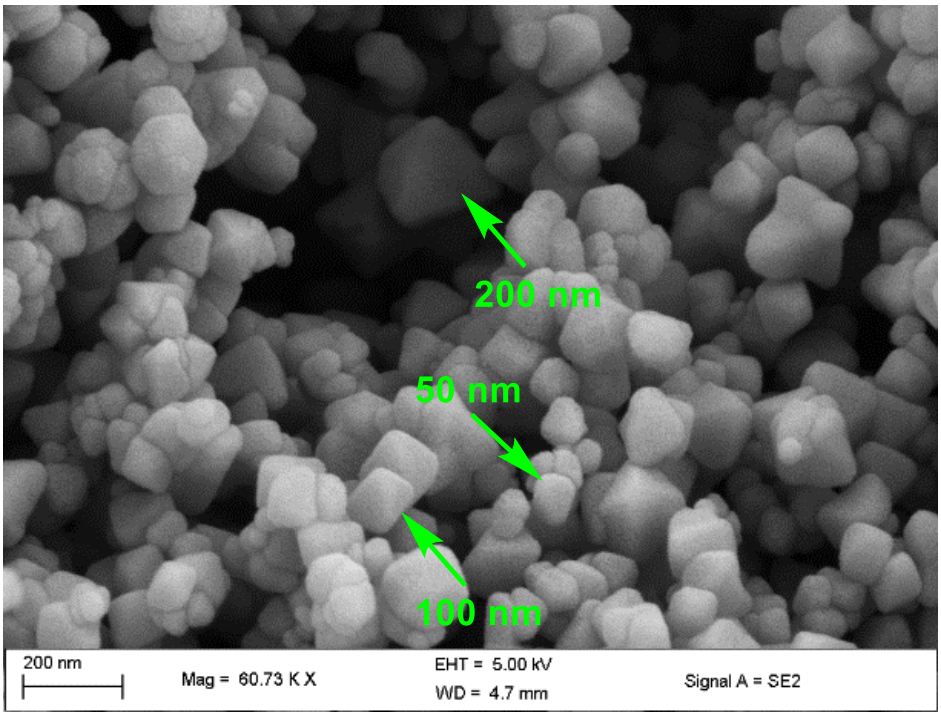

Fig. 3.6 FE-SEM images of bare Fe_3O_4 **(a)** and APTES grafted Fe_3O_4 **(b)** nanoparticles.

FTIR spectra showed characteristic peaks for Fe_3O_4, Fe_3O_4/APTES and Fe_3O_4/APTES-rTl-Cyn-rTl-CA nanoparticles (Fig. 3.7). A peak at 589 cm^{-1} was associated with the Fe-O functional groups (Fig. 3.7a) as demonstrated by the characteristic peak for Fe_3O_4 (Zhang *et al.*, 2007). The grafting of APTES to the surface of Fe_3O_4 nanoparticles were confirmed by the presence of a band around 1055 cm^{-1}, which is assigned to the Si-O groups (Kumar and Cabana, 2016; Faridi *et al.*, 2017). The peak detected near 1637 cm^{-1} for the Fe_3O_4 nanoparticles was due to the adsorption of water molecules to the surface via hydrogen bonds (Faridi *et al.*, 2017). A broad peak acquired at 3200-3500 cm^{-1} in all of the spectra, originated from the hydroxyl group present on the surface of the nanoparticles, uncondensed silanol groups present in the coating layer, and water on the surfaces of the Fe_3O_4 nanoparticles adsorbed physically and chemically (Ma *et al.*, 2003). Thus, peaks displayed by FTIR confirmed the synthesis of Fe_3O_4 nanoparticles and the grafting of APTES on its surface. Some peaks were common in Fe_3O_4, Fe_3O_4/APTES and Fe_3O_4/APTES-rTl-Cyn-rTl-CA nanoparticles, however, the peak intensity of Fe_3O_4 grafted with APTES or APTES/enzymes decreased noticeably, confirming that functional groups and enzymes were successfully introduced onto the surface of nanoparticles. Similar results were observed with the functionalization of Fe_3O_4 nanoparticles, as reported by Song *et al*. (2016). XRD analysis confirmed the crystalline structure and phase purity of the Fe_3O_4 nanoparticles, which had six characteristic peaks 2θ=35.25°, 41.55°, 50.62°, 63.11°, 67.57° and 74.49 (Fig. 3.8) that matched well with the standard data of Fe_3O_4 (JCPDS 19-629).

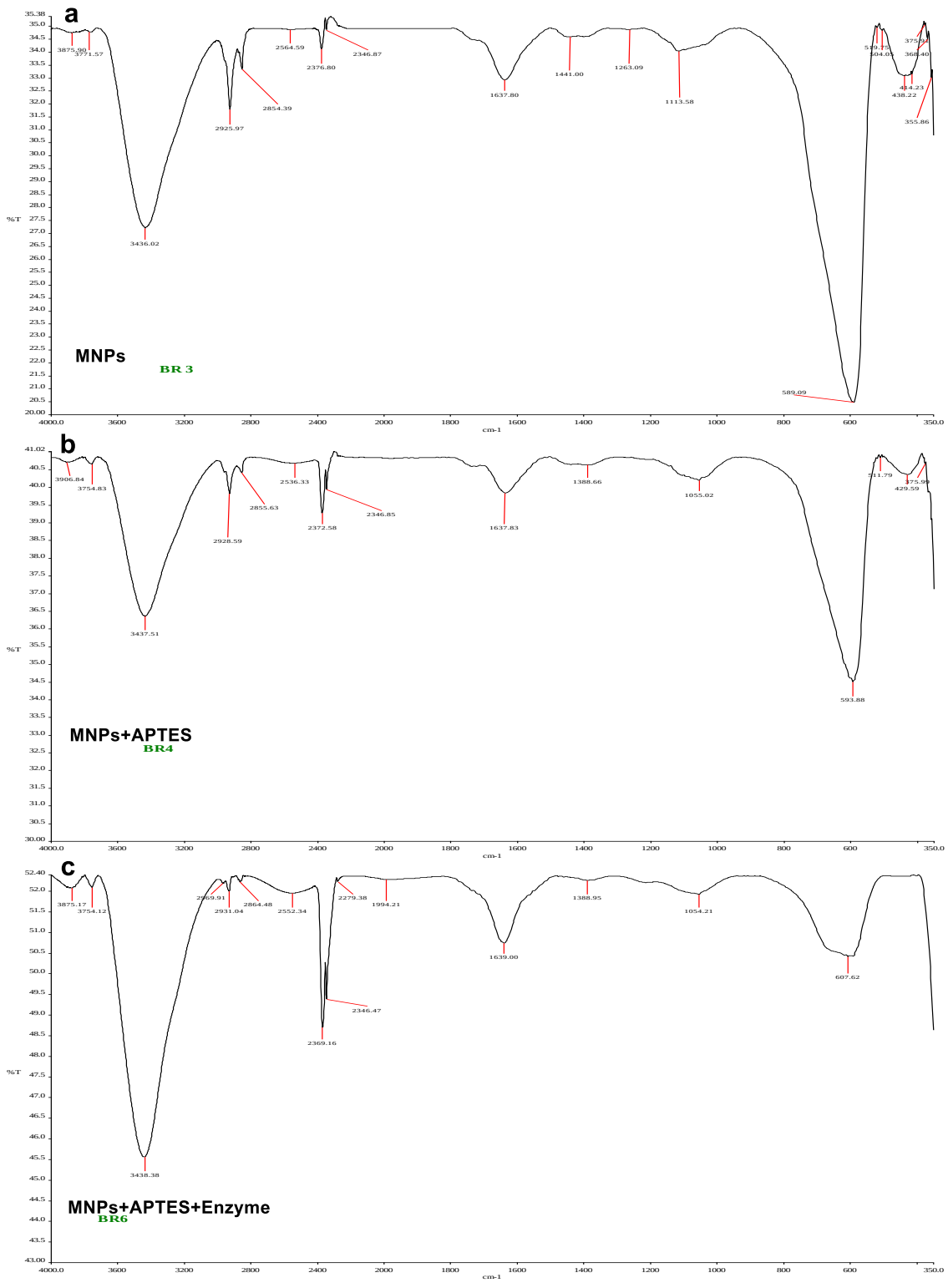

Fig. 3.7 FTIR spectra of **(a)** MNPs, **(b)** MNPs/APTES, **(c)** MNPs/APTES/enzyme.

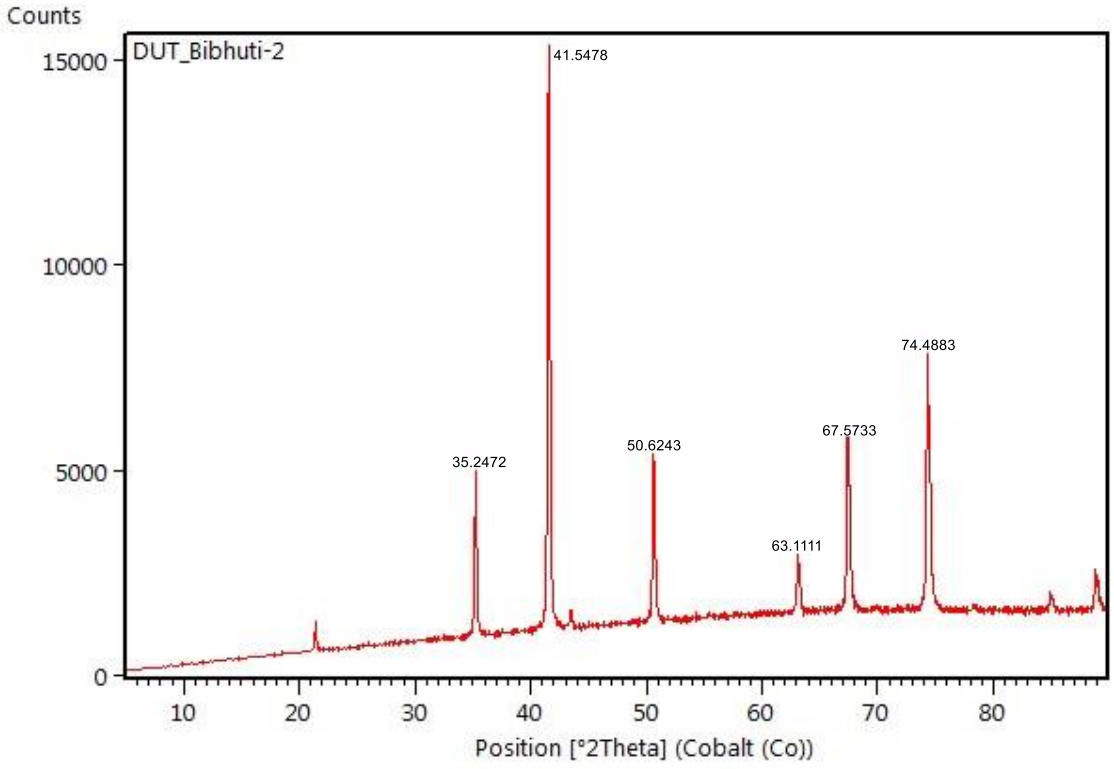

Fig. 3.8 XRD patterns of Fe_3O_4 nanoparticles.

3.3.6 Application of immobilized enzyme in cyanate remediation

Approximately 90% cyanate degradation was observed by Fe_3O_4/APTES-rTl-Cyn in industrial wastewater sample and complete degradation (100%) was achieved with buffered sample at a $NaHCO_3$ concentration of 3 mM. Decreasing $NaHCO_3$ concentrations resulted in less cyanate degradation (Fig. 3.9a). Surprisingly, the combination of rTl-Cyn and rTl-CA nanoparticles also attained a 100% degradation of cyanate at 0.6 mM $NaHCO_3$ concentration (Fig. 3.9b).

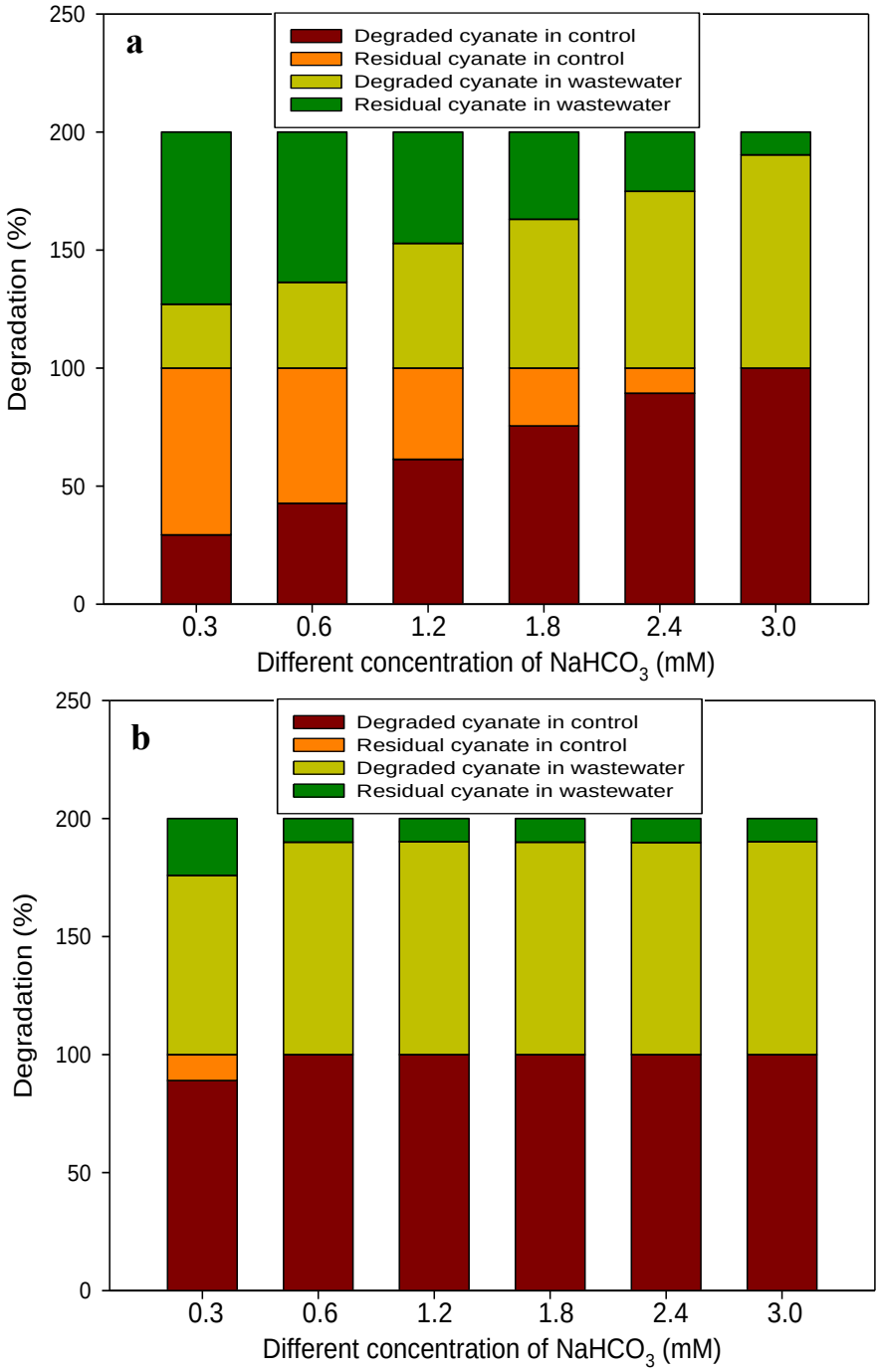

Fig. 3.9 Degradation of cyanate in control and industrial wastewater at different concentration of $NaHCO_3$ using **(a)** Fe_3O_4/APTES-rTl-Cyn, **(b)** Fe_3O_4/APTES-rTl-Cyn-rTl-CA. Control= buffered conditions without heavy metals. Industrial wastewater samples spiked with cyanate and different heavy metals.

3.3.7 Determination of binding and storage stability of the immobilized enzyme

The economic viability of industrial enzyme applications are dependent on the cost of enzyme production, therefore, enzymes with long-term reusability and storage stability are preferred (Alex *et al.*, 2014; Faridi *et al.*, 2017). To this end, immobilization and storage stability of Fe_3O_4/APTES-rTl-Cyn and Fe_3O_4/APTES-rTl-Cyn-rTl-CA were evaluated by incubating them in Tris-HCl buffer (20 mM, pH 8.0) at 4°C, and assessed for the release of free enzyme into the supernatant after magnetic settlement. No free enzymes were detected in the supernatant over a 30-day incubation period from Fe_3O_4/APTES-rTl-Cyn and Fe_3O_4/APTES-rTl-Cyn-rTl-CA (Fig 3.10a). Similarly, enzymes stored at 4°C were analyzed every 5^{th} day for enzyme activity over a period of 30 days. The storage stability of the immobilized enzymes were satisfactorily stable and retained almost 100% of their catalytic activity (Fig 3.10b), which highlighted its potential for large-scale application.

3.3.8 Reusability of the immobilized enzyme

In an industrial bioremediation process, reusability of the immobilized enzyme is crucial, as it determines the biodegradation potential after sequential reuses (Jiang *et al.*, 2016). Consequently, one of main aims was to use an immobilized enzyme with efficient bio-catalytic properties and that can be easily recovered and reused. Reusability of immobilized enzymes in this investigation was verified by the presence of more than 80% of residual activity in a wastewater sample and 90% in a buffered sample after 10 cycles (Fig. 3.11).

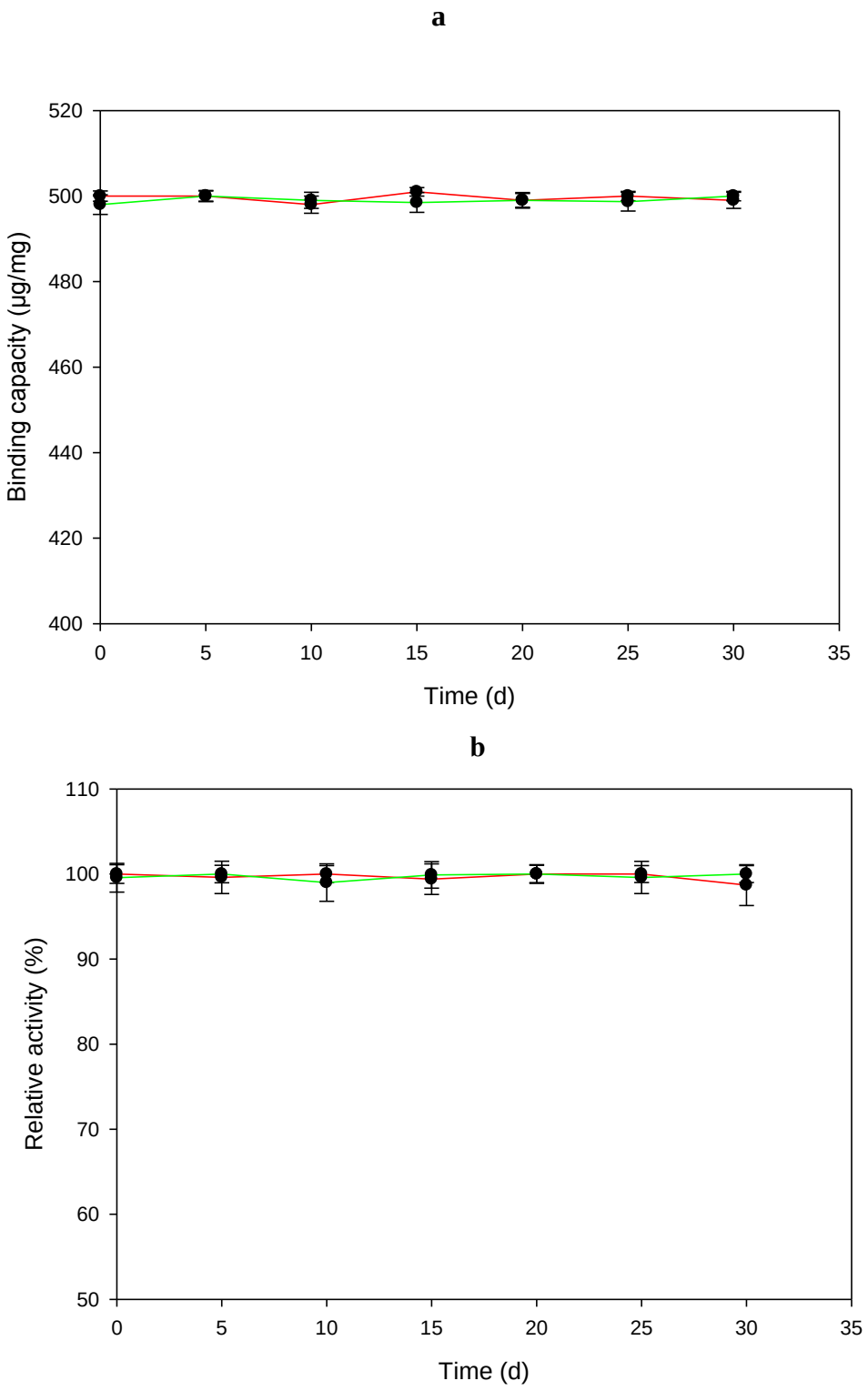

Fig. 3.10 Time-dependent stability studies of the immobilized Fe_3O_4/APTES-rTl-Cyn (—●—) and Fe_3O_4/APTES-rTl-Cyn-rTl-CA (—●—). **(a)** Immobilization stability and **(b)** storage stability at 4°C.

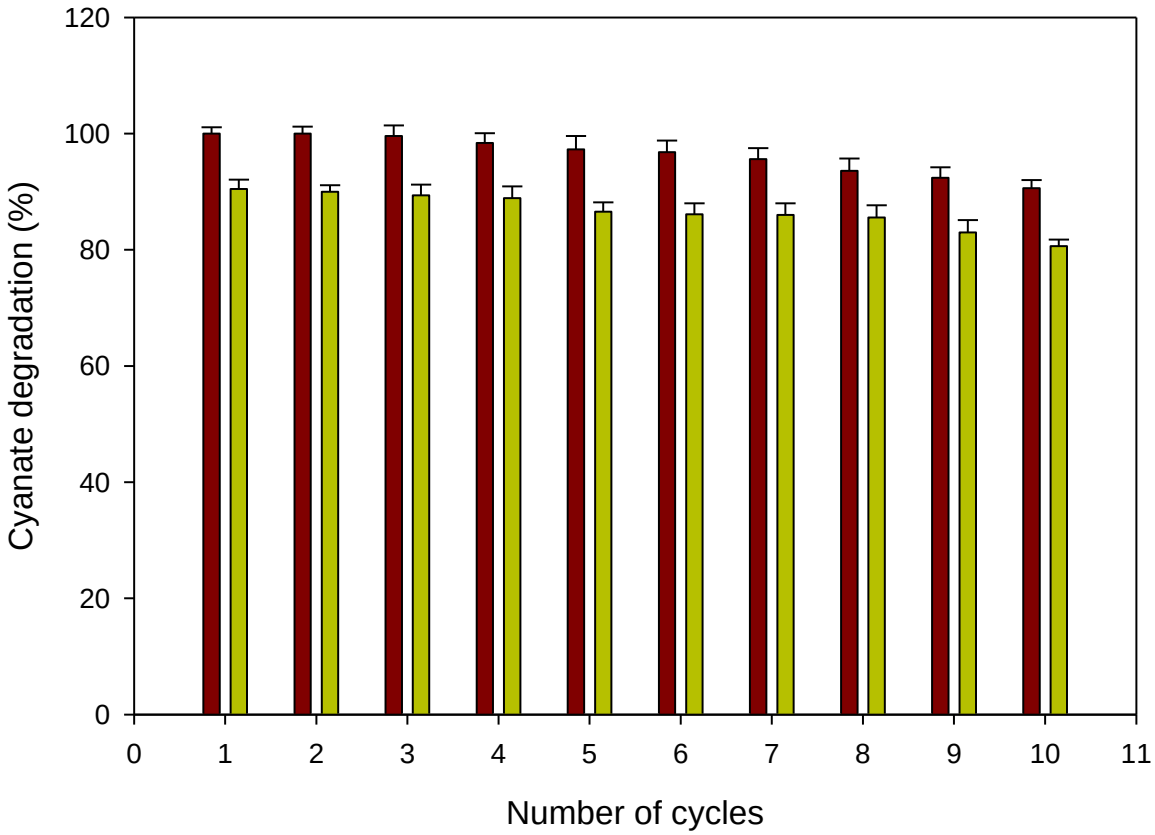

Fig. 3.11 Reusability of Fe_3O_4/APTES-rTl-Cyn-rTl-CA for cyanate degradation in control ( ) and industrial wastewater sample ( ).

3.4 Conclusions

This study revealed that the combinatorial use of recombinant enzymes, rTl-Cyn and rTl-CA, reduced the $NaHCO_3$ dependency by 80% as compared to rTl-Cyn alone for cyanate remediation. In addition, the recombinant enzymes were successfully co-immobilized on magnetic nanoparticles, with high stability retaining 100% of the catalytic activity over a period of 30 days. More than 80% of the residual activity in wastewater and buffered samples was also retained after 10 catalytic cycles with this co-immobilized system. This unique and novel enzyme combination clearly demonstrates its great potential for the bioremediation of cyanurated wastes on a large-scale.

CHAPTER 4

Simultaneous removal of heavy metals and cyanate in a wastewater sample using immobilized cyanate hydratase on magnetic-multiwall carbon nanotubes

(*Accepted: Ranjan, B., Pillai, S., Permaul, K., and Singh, S. (2018) Simultaneous removal of heavy metals and cyanate in a wastewater sample using immobilized cyanate hydratase on magnetic-multiwall carbon nanotubes. Journal of Hazardous Materials*).

4.1 Introduction

Increasing global pollution by numerous toxic substances (cyanide, cyanate, heavy metals etc.) as a result of mining, electroplating and several other industries, is a major threat to health and ecosystems (Luque-Almagro *et al.*, 2008; Dash *et al.*, 2009; Huertas *et al.*, 2010). This warrants the need for efficient processes that are eco-friendly and cost-effective in bio-remediation. The use of enzymatic bio-catalysis can be employed for sustainable remediation (Mirizadeh *et al.*, 2014; Sheldon and Woodley, 2017). However, the practical use of free enzymes as bio-catalysts are limited, because of their instability, high costs of production and difficulty in separation from the reaction mixture, for subsequent reuse (Tran and Balkus, 2011; Subrizi *et al.*, 2014). Consequently, enzyme immobilization offers an alternative to resolve these challenges associated with free enzymes and making them industrially and commercially feasible (Feng and Ji, 2011; Tran and Balkus, 2011; Sheldon and Woodley, 2017). Nanomaterials serve as ideal support for enzyme immobilization as they provide high surface areas, large surface-to-volume ratios, mass transfer resistance, and effective enzyme loading (Wang, 2006). A variety of structural forms, such as nanoparticles, nanofibres, nanotubes, and nanocomposites have been used to immobilize enzymes to improve their catalytic performance (Ahmed and Husain, 2012; Ke *et al.*, 2014). Carbon nanotubes (CNTs) serve as excellent immobilization matrices as they possess unique structural, mechanical, thermal and biocompatibility properties (Verma *et al.*, 2013; Modugno *et al.*, 2016). However, their potential use for bioremediation is limited, owing to agglomeration from the strong attraction between the tiny carbon particles, which decreases their effective surface area (Abo-Hamad *et al.*, 2017). To address this limitation, CNTs can be further processed by surface modification to reduce agglomeration and increase the available surface area

(Johnson *et al.*, 2011; Abo-Hamad *et al.*, 2017). In addition, the efficiency of CNTs can be improved by surface functionalization, which introduces chemical functional groups onto their surface to obtain CNTs with desired properties (Shim *et al.*, 2002; Pavlidis *et al.*, 2010).

Enzyme immobilization onto the surface of CNTs can be achieved using physical adsorption or covalent bonding (Pavlidis *et al.*, 2010). Adsorption is a relatively simple method as it is a chemical free enzyme binding process (Chronopoulou *et al.*, 2011), however, leaching of the enzyme from the immobilized carrier after a few catalytic cycles has limited its application (Sheldon and Woodley, 2017). This could be overcome by covalent-binding of the enzyme to the support matrix via reaction with amino acid functional groups (-NH_2, -COOH and -SH) (Tran and Balkus, 2011). Cross linkers such as glutaraldehyde have also been used for the covalent immobilization of enzymes (Puri *et al.*, 2005; Pavlidis *et al.*, 2012; Subrizi *et al.*, 2014). Studies have shown that covalent binding methods yield relatively stable immobilized enzyme preparations with more reusability than physical adsorption (Ahmed and Husain, 2012; Lal *et al.*, 2012). However, recovery of the CNTs-immobilized enzymes from the reaction mixture for repeated use remains a major challenge. An effective solution for this is to develop CNTs with magnetic properties (Georgakilas *et al.*, 2005).

Thus far, several enzymes have been immobilized on magnetic CNTs, however, no attempts have been made for the immobilization of cyanase to this carrier, although, the efficacy of rTl-Cyn for cyanate detoxification has been described in Chapter 2. Therefore, in this chapter, characterization and covalent immobilization of magnetic-multiwall carbon nanotubes (m-MWCNTs) with rTl-Cyn for the simultaneous removal of cyanate and heavy metals from wastewater sample has been described. In addition, stability and reusability of the immobilized enzyme was also evaluated.

4.2 Materials and Methods

4.2.1 Enzymes and chemicals

Multi-walled carbon nanotubes (6-13 nm outer diameter × 2.5-20 µm length, >98% carbon), ethylenediamine (EDA), O-(7-Azabenzotriazol-1-yl)-N,N,N',N'-tetramethyluronium hexafluoro- phosphate (HATU) and glutaraldehyde were purchased from Sigma-Aldrich. All other

chemicals used for the modification of MWCNTs were purchased from Merck. The rTl-Cyn was produced and purified as reported in chapter 2.

4.2.2 Modification of MWCNTs

The MWCNTs (1 g) were treated with a 3:1 (v/v) mixture of concentrated H_2SO_4 and concentrated HNO_3 in a screw cap bottle, and refluxed at 120°C for 30 min (Verma *et al.*, 2013). The MWCNTs suspension was cooled at room temperature, vacuum-filtered with a 0.22 µm pore polytetrafluoroethylene (PTFE) membrane and washed with Milli-Q water until a neutral pH was achieved. The oxidized nanotubes (ox-MWCNTs) were vacuum dried at 80°C for 8 h and the dry powder was stored at room temperature.

4.2.3 Preparation of magnetic MWCNTs

Iron-oxide nanoparticles were synthesized by chemical co-precipitation as described by Faridi *et al*. (2017). m-MWCNTs were prepared according to the method of Juan and Xin (2012) with minor modification. ox-MWCNTs and iron-oxide with a ratio of 4:1 (w/w) was dispersed in a solution of Milli-Q water and ethanol (1:1, v/v). The mixture was sonicated for 2 h, stirred at room temperature for 96 h, filtered using a 0.22 µm PTFE membrane, and vacuum dried at 60°C for 16 h.

4.2.4 Amino-functionalization of m-MWCNTs

m-MWCNTs (100 mg) were dispersed in ethylenediamine (EDA, 60 mL) for amino-functionalization. The coupling agent, HATU (8 mg) was added to increase the reaction yield and the mixture was sonicated for 4 h at 40°C. The samples were thereafter diluted in absolute methanol (300 mL) and filtered using a 0.22 µm PTFE membrane filter. The filtrate was washed several times with methanol and vacuum dried at 60°C for 8 h.

4.2.5 Characterization of MWCNTs and m-MWCNTs

Scanning electron microscopy (SEM) was carried out on the pristine MWCNTs and ox-MWCNTs using a Zeiss GeminiSEM equipped with a field emission electron gun. Micrographs were taken at 5 kV and composites were coated with gold before analysis. High-resolution transmission electron microscopy (HRTEM) was carried out using a JEOL JEM-2100 instrument operating at 200 kV. The crystalline structure and phase purity of the samples were analyzed by

X-ray diffraction using X'Pert Pro diffractometer (PANalytical) with a Co anode at 40 kV and a wavelength 0.179 nm. Data was collected in the range of 2θ = 5-90°. Fourier transform infrared (FTIR) spectra was recorded on a Perkin Elmer instrument after dispersing the samples in a KBr pellet as described previously in chapter 2, to confirm the presence of amino groups in the functionalized carbon nanotubes.

4.2.6 Enzyme immobilization onto functionalized m-MWCNTs

The amino-functionalized m-MWCNTs (5 mg) were dispersed in Tris-HCl (50 mM, pH 8.0) buffer (10 mL) and sonicated for 30 min to achieve a homogenous dispersion. Glutaraldehyde (1 M) was thereafter added to the solution for the surface activation of nanotubes (Verma *et al.*, 2013), followed by gentle shaking at room temperature for 1 h. m-MWCNTs were magnetically separated and washed several times with Milli-Q water to remove excess glutaraldehyde followed by washing with buffers of different pH values [(Tris-HCl buffer (50 mM, pH 7.0-8.0) and glycine-NaOH buffer (50 mM, pH 9.0)], to confirm the optimum pH for immobilization. Varying amounts of rTl-Cyn (ranging from 0.2 to 1 mg; total volume of 5 mL) were immobilized onto surface-activated m-MWCNTs (1 mg) by gentle shaking overnight. The excess enzyme was separated by collecting the m-MWCNTs using a magnetic field, and the supernatant was assayed for enzyme activity to calculate the immobilization efficiency (Subrizi *et al.*, 2014). The immobilized m-MWCNT-rTl-Cyn was washed several times with respective buffers (used for immobilization) to confirm the complete removal of unbound enzyme. The amount of enzyme in the supernatant after each wash cycle was quantified to determine the total amount of free enzyme leached. The absence of enzyme in the washing buffer was confirmed by standard enzyme and protein assays.

4.2.7 Determination of rTl-Cyn activity

The activity of native and immobilized cyanase was measured as previously described in chapter 2.

4.2.8 Biochemical characterization of free and immobilized rTl-Cyn

The optimum pH for free and immobilized rTl-Cyn was determined by conducting enzyme assays at different pH values (7 to 9) using Tris-HCl buffer (50 mM, pH 7.0-8.0) and glycine-NaOH buffer (50 mM, pH 9.0) at 60°C. Similarly, the optimum reaction temperature was determined by performing cyanate hydratase assays at various temperatures (40 to 80°C) at pH

8.0. Relative activity of the free and immobilized rTl-Cyn at a selected range of pH and temperature was also determined.

4.2.9 Determination of kinetic constants

The kinetic constants of immobilized m-MWCNT-rTl-Cyn were determined by measuring the initial rates of the reaction with different cyanate concentrations, ranging from 0.1 to 3 mM, in Tris-HCl buffer (50 mM, pH 8.0) at 60°C. The K_m and V_{max} values were calculated after plotting data in a Lineweaver-Burk plot. All experiments were performed in triplicate using native and immobilized rTl-Cyn.

4.2.10 Storage stability

The storage stability of free and immobilized m-MWCNT-rTl-Cyn was carried out by storing in Tris-HCl buffer (50 mM, pH 8.0) at 4°C over a period of 30 days. Sampling was done over 5 day intervals and enzyme activity was expressed as the relative activity with respect to time zero (representing 100%).

4.2.11 Enzyme recycling

The reusability of immobilized m-MWCNT-rTl-Cyn was assessed at 60°C by determining the degradation of cyanate in the control and wastewater samples, as described previously for the free enzyme in chapter 2. After each cycle, the immobilized m-MWCNT-rTl-Cyn was recovered by magnetic separation, washed several times, and reused. For each run, the cyanase activity was expressed as the percent relative activity with respect to the first run (considered as 100%).

4.2.12 Simultaneous removal of cyanate and heavy metals from wastewater sample

The cyanate and heavy metal removal tests were performed by the addition of m-MWCNT-rTl-Cyn (1 mg) in synthetic wastewater samples (20 mL) supplemented with cyanate (4 mM) and heavy metals (5 mM each; lead, chromium, copper and iron), followed by shaking at 100 rpm for 30 min. The heavy metal removal was assessed by atomic absorption spectrophotometry (AAS) and the residual cyanate concentration was analyzed by a colorimetric method. A schematic representation for the simultaneous removal of cyanate and heavy metals from wastewater sample by m-MWCNT-rTl-Cyn is shown in Fig. 4.1.

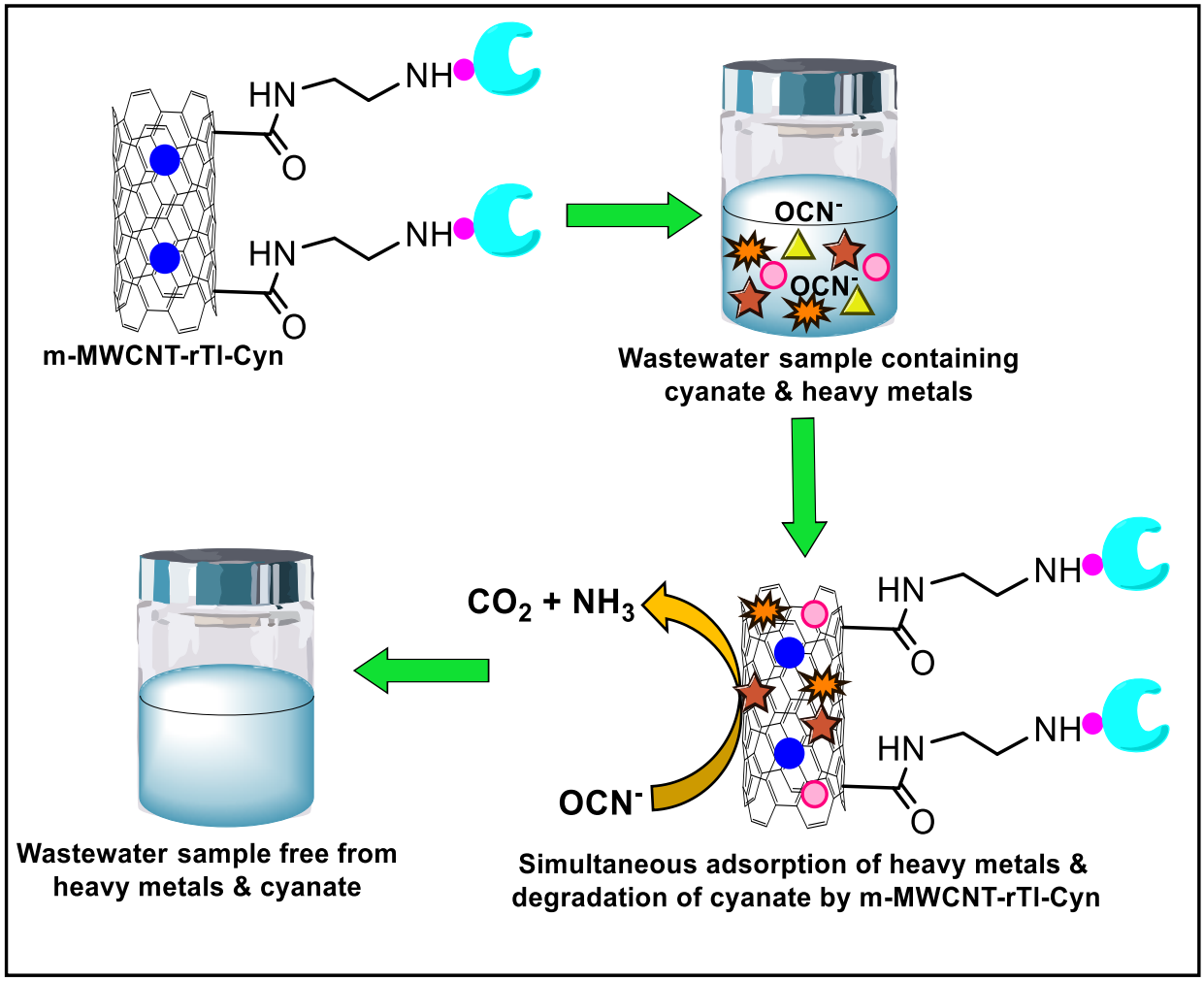

Fig. 4.1 A schematic representation for the simultaneous removal of cyanate and heavy metals from wastewater sample by m-MWCNT-rTl-Cyn.

4.3 Results and Discussion

4.3.1 Modification, functionalization and characterization of MWCNTs and m-MWCNTs

To develop efficient enzyme immobilization supports, studies were carried out with MWCNTs because of their low cost and greater commercial availability (Subrizi *et al.*, 2014). However, the low dispersibility of MWCNTs in aqueous solutions even after prolonged sonication (Fig. 4.2a), results in the lack of available surfaces for enzyme immobilization. MWCNTs were oxidized by refluxing at 120°C in a mixture of concentrated sulfuric and nitric acids (3:1, v/v) for

30 min, followed by repeated washing with Milli-Q water until the pH became neutral. This treatment has allowed for the removal of impurities and increased the dispersibility of MWCNTs in aqueous solution (Fig. 4.2b), by introducing carboxyl and hydroxyl groups (Modugno *et al*., 2016). The resulting ox-MWCNTs suspension (Fig. 4.2b) showed minimal flocculation even after storing for 2 weeks in aqueous solution, thus opening the possibility for long-term application. Increased dispersion of ox-MWCNTs was also verified by spectroscopy (A_{500}) and a linear relationship between absorbance and concentration of ox-MWCNTs was observed, indicating that the particles were evenly dispersed. These changes in the properties of ox-MWCNTs could be attributed to the introduction of oxygenated functional groups onto their surface, which form hydrogen bonds with water thereby increasing their dispersibility (Asuri *et al.*, 2006; Umbuzeiro *et al.*, 2011; Subrizi *et al.*, 2014).

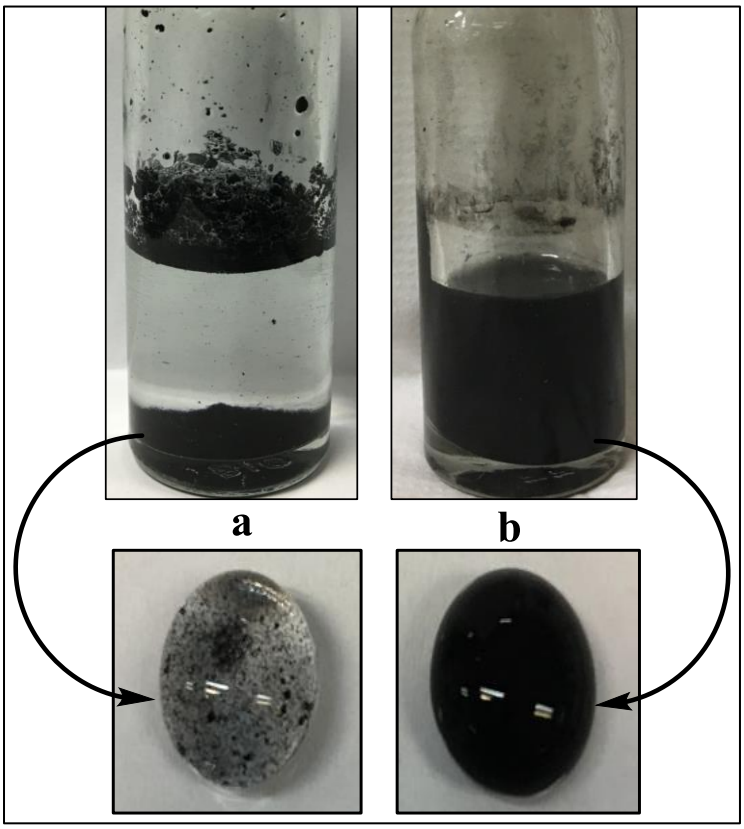

Fig. 4.2 Aqueous dispersion test of pristine **(a)** and oxidized **(b)** MWCNTs.

In addition, FEG-SEM analysis was carried out to demonstrate the effect of oxidation on the morphological changes of MWCNTs. The smooth appearance of the well-separated pristine MWCNTs (Fig. 4.3a) has changed to more dense structure, after oxidation (Fig. 4.3b). This has probably resulted from the successful introduction of acid functional groups onto the MWCNTs surface, which is in accordance with the report by Mubarak *et al*. (2014), wherein functionalized multiwall carbon nanotubes was used for the immobilization of cellulase.

m-MWCNTs were prepared and their magnetic properties were initially tested by the application of a magnetic field (Fig. 4.4). HRTEM images has revealed the presence of MWCNTs filled with iron-oxide nanoparticles (Fig. 4.5). The absence of iron-oxide nanoparticles on the HRTEM carbon film suggests that nanoparticles have successfully entered the tubes and unattached nanoparticles were completely removed from the m-MWCNTs. Furthermore, powder XRD revealed the presence of the typical peaks for both iron-oxide and MWCNTs in m-MWCNTs (Fig. 4.6), indicating that the phase remained unchanged during the preparation process, and also confirmed the attachment of iron-oxide nanoparticles onto the MWCNTs. This is in accordance with the results from previous studies, where it was observed that the characteristic peaks of MWCNTs remain unchanged in the presence of magnetic phase in the composites (Xiu-juan and Xin, 2012; Fan *et al.*, 2017).

FTIR analysis has confirmed the presence of amino groups in the functionalized carbon nanotubes (Fig. 4.7). IR spectra showed the presence of amine and ester groups with symmetric and asymmetric stretching vibration of $-CH_2$ groups at 2924 and 2848 cm^{-1}, respectively. The absorption peak at 1638 cm^{-1} is attributed to the stretching vibration of C=O in the amide group. Also, the broad band which appeared at 3430 cm^{-1} was due to the hydroxyl stretching vibration, as reported in the literature (Pavlidis *et al.*, 2010; Verma *et al.*, 2013). However, these bands did not appear in the spectra of pristine nanotubes, which suggests that organic groups were successfully attached to the surface of functionalized nanotubes. This result is in accordance with a previous report, wherein no peaks were observed for pristine carbon nanotubes (Verma *et al.*, 2013).

a

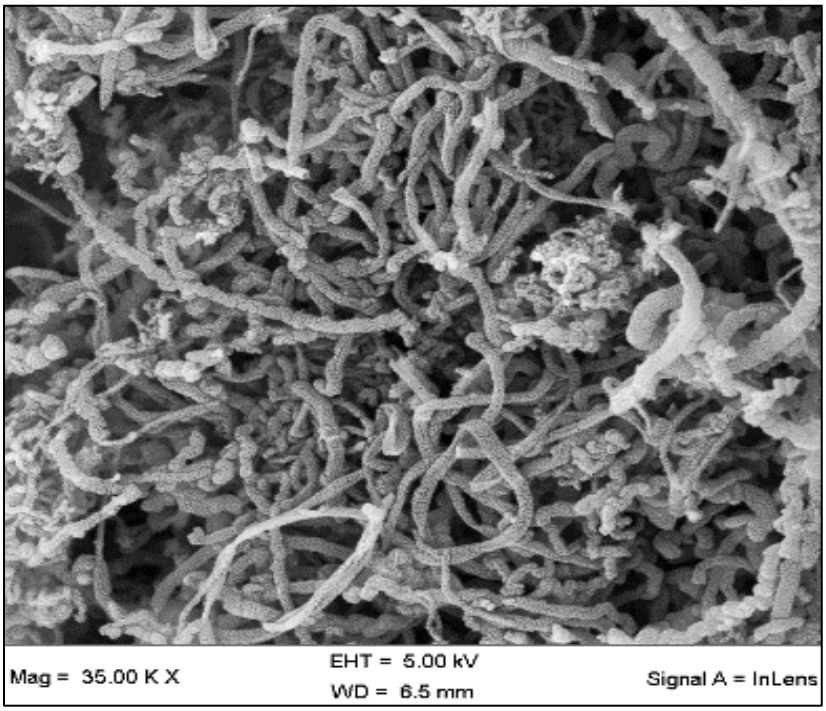

b

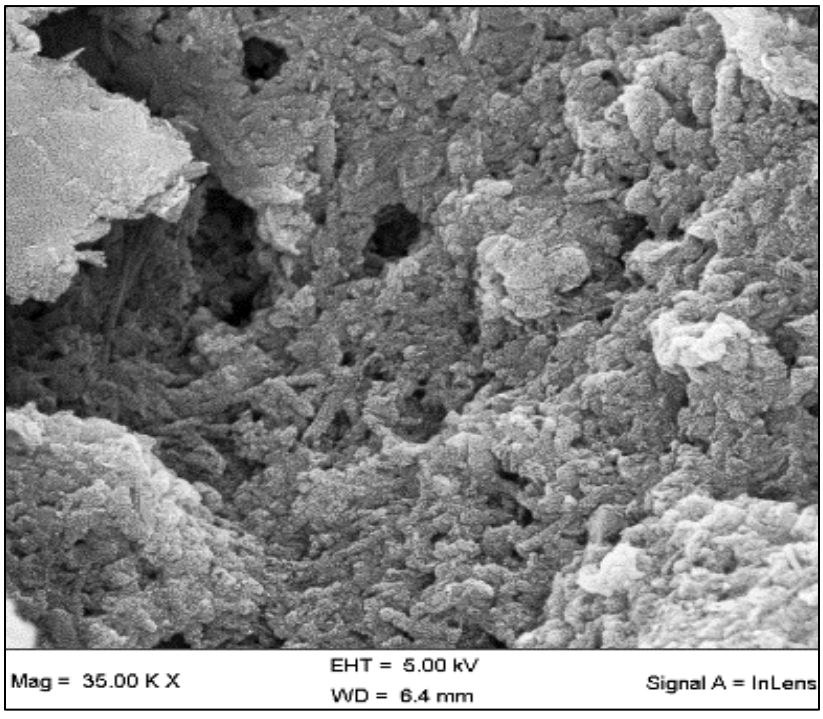

Fig. 4.3 FEG-SEM images showing the change in surface morphology after oxidation of pristine **(a)** and oxidized **(b)** MWCNTs.

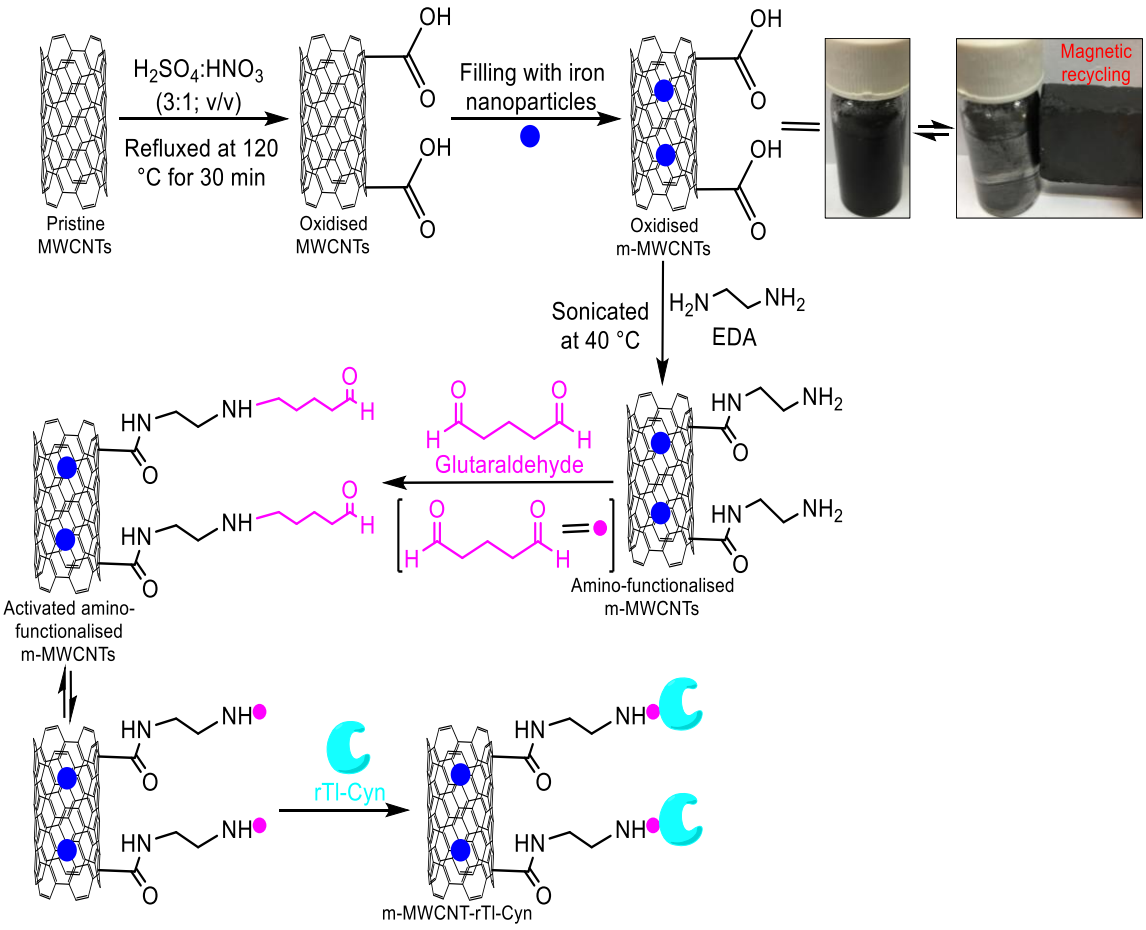

Fig. 4.4 Schematic illustration of the synthesis process to produce m-MWCNTs and their activation for rTl-Cyn immobilization.

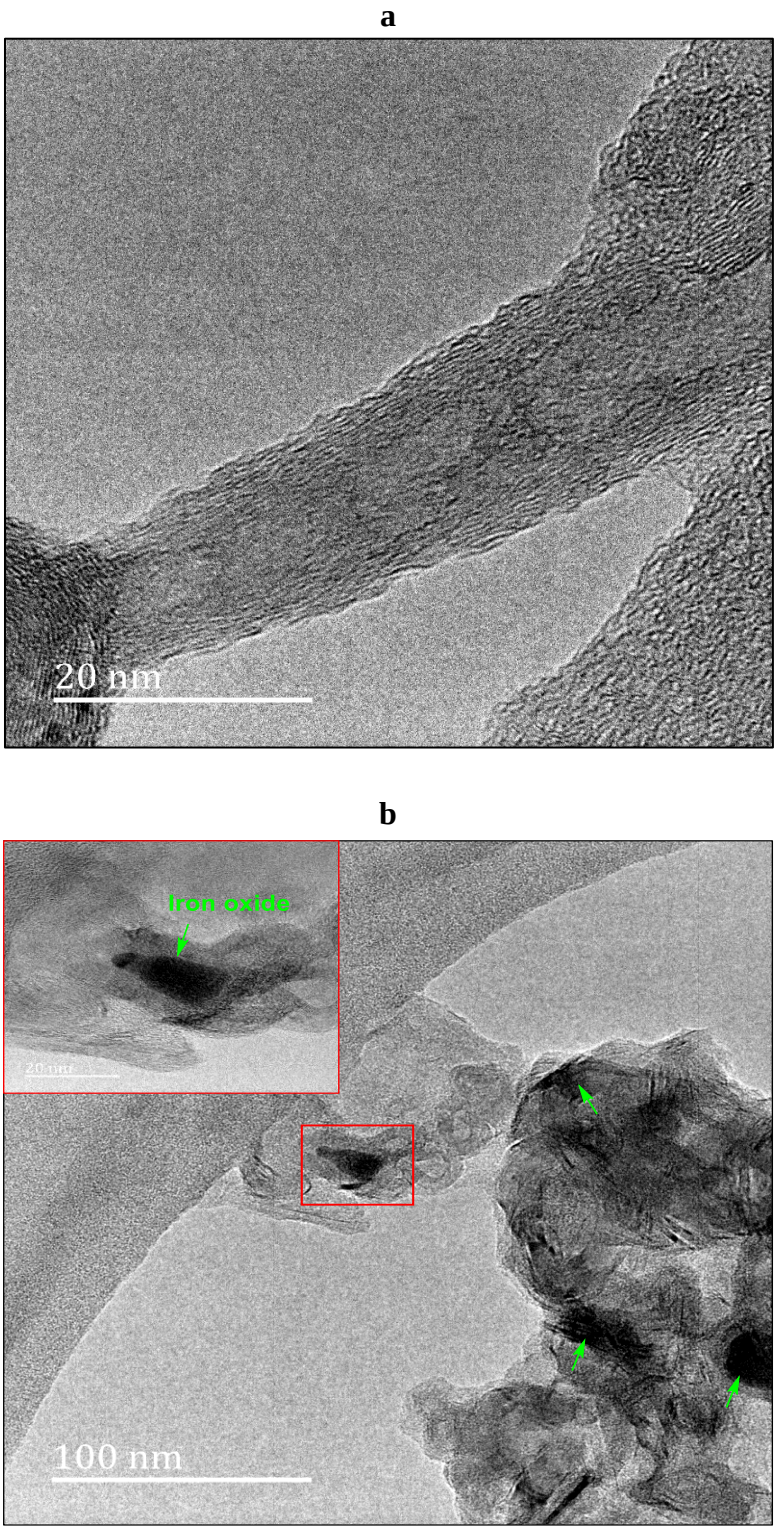

Fig. 4.5 HRTEM micrographs of **(a)** MWCNT and **(b)** m-MWCNT, showing entrapped iron-oxide within an internal cavity of tubes; *inset* shows a zoomed-in image of entrapped iron-oxide.

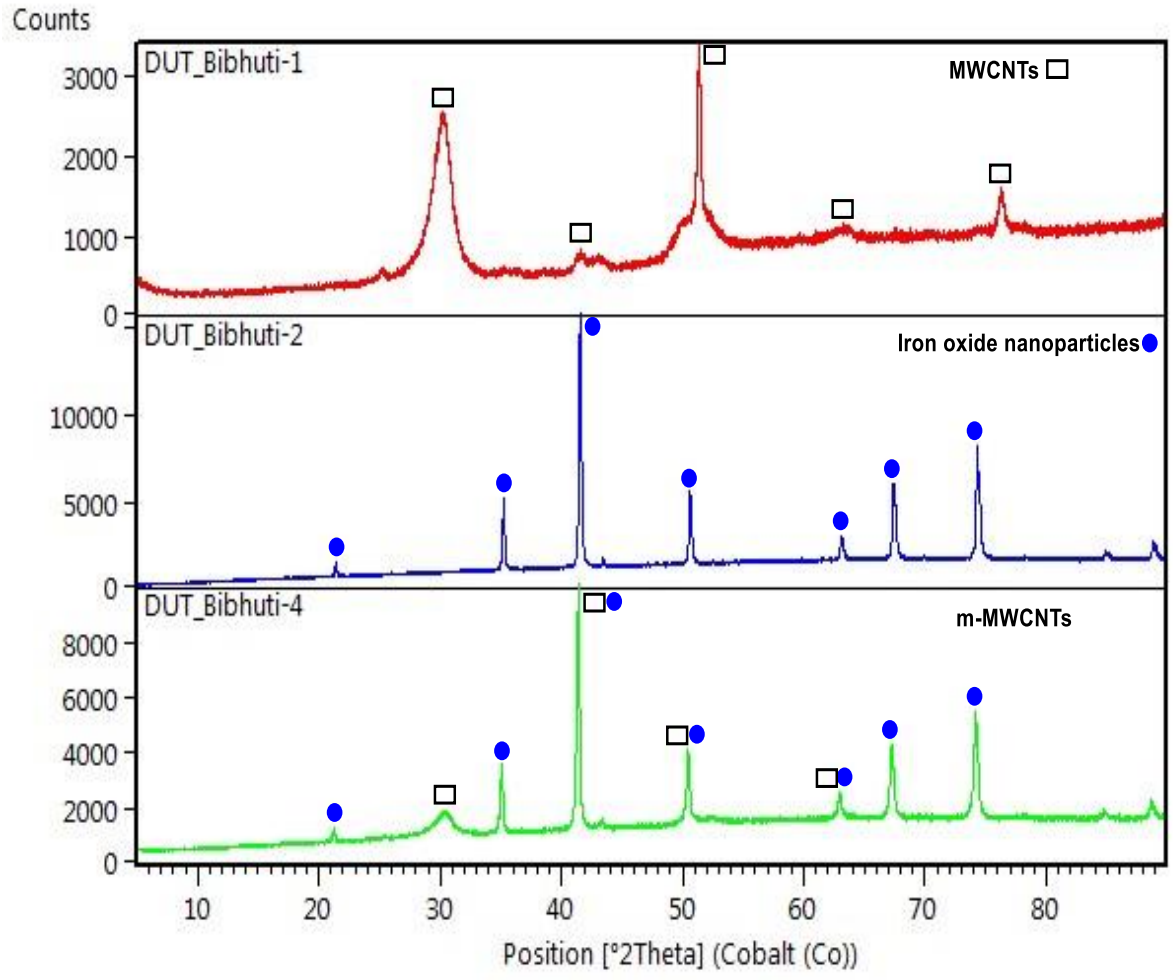

Fig. 4.6 XRD pattern of the MWCNTs (▭), iron-oxide nanoparticles (•) and iron-oxide filled MWCNTs (m-MWCNTs; ▭ •). m-MWCNTs: shows the characteristic peaks for both iron-oxide and MWCNTs.

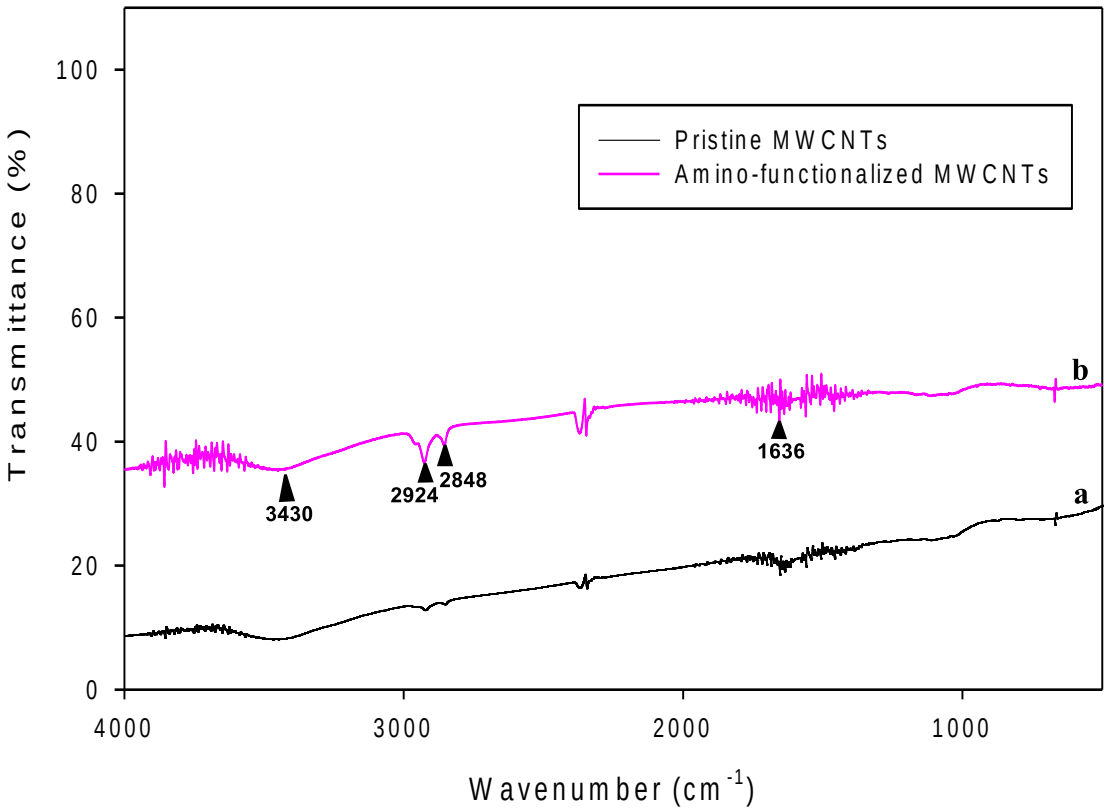

Fig. 4.7 FTIR spectra of MWCNTs showing the characteristic peaks after amino-functionalization. **(a)** Pristine MWCNTs (——) **(b)** amino-functionalized MWCNTs (——).

4.3.2 Immobilization of rTl-Cyn onto m-MWCNTs

4.3.2.1 Effect of pH on rTl-Cyn immobilization

pH is a critical factor in many enzyme-driven reactions as well as in the immobilization process (Ke *et al.*, 2014). It was noted that alkaline conditions were most-suited for the immobilization process of rTl-Cyn (Fig. 4.8a). The increase in immobilization yield at pH 8.0 might have favoured the Schiff base reaction between ε-NH_2 groups on the surface of rTl-Cyn and m-MWCNTs activated by glutaraldehyde. In another study, it was also observed that an alkaline pH was beneficial for the Schiff base reaction for the immobilization of lipase (Fan *et al.*, 2017).

Although several enzymes have been immobilized on a carrier activated by glutaraldehyde, there are no reports on the immobilization of cyanate hydratase.

4.3.2.2 Effect of rTl-Cyn concentrations on immobilization

The rTl-Cyn activity and immobilization yield gradually increased with the increase of enzyme concentrations up to 0.6 mg, beyond which both declined (Fig. 4.8b). It can be concluded that the low concentration of enzyme during the immobilization process would have increased the bonding between enzyme and linker, leading to enhanced activity and immobilization yield. Thus, a rTl-Cyn concentration of 0.6 mg was selected for immobilization.

4.3.3 Effect of pH and temperature on the catalytic activity of free and immobilized rTl-Cyn

The optimum pH for the catalytic activity of both free and immobilized enzymes was pH 8.0 (Fig. 4.9a). However, the immobilized enzyme was more active at higher pH in comparison to the free enzyme (Fig. 4.9a). This could be advantageous for cyanurated waste remediation, as the nature of these wastes are usually alkaline, which is a major bottleneck for most of the enzymatic bio-remediation process (Huertas *et al.*, 2010). The change in activity could be attributed to the improvement in enzyme stability through covalent immobilization onto the carrier.

The optimum temperature for both the enzymes was 60°C and it was observed that temperature variations had minimal effect on the immobilized enzyme activity in comparison to the free enzyme (Fig. 4.9b).

a

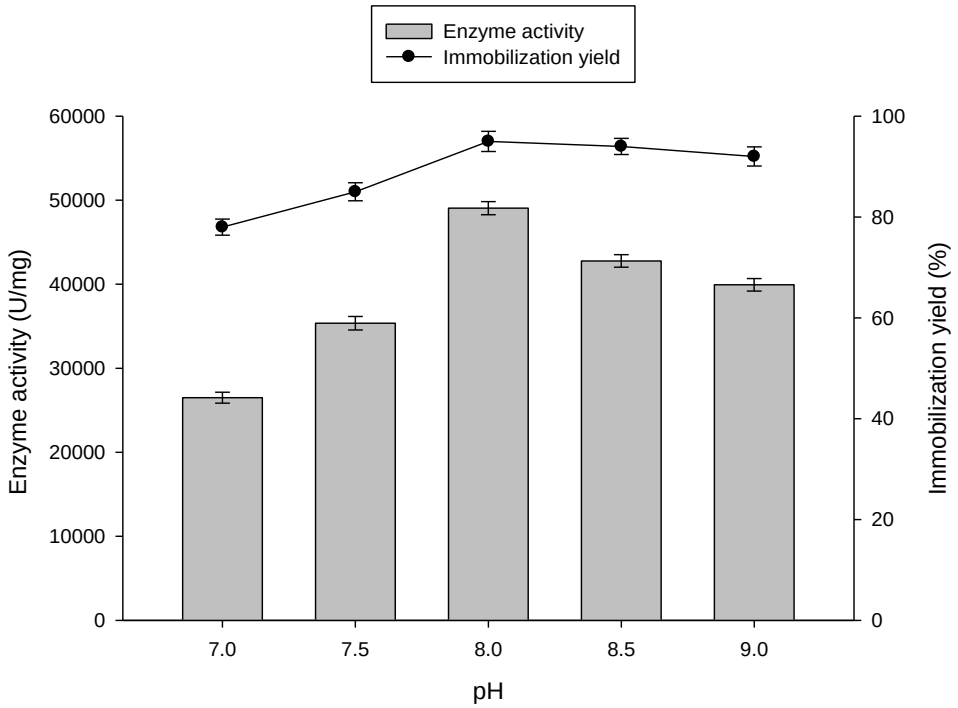

b

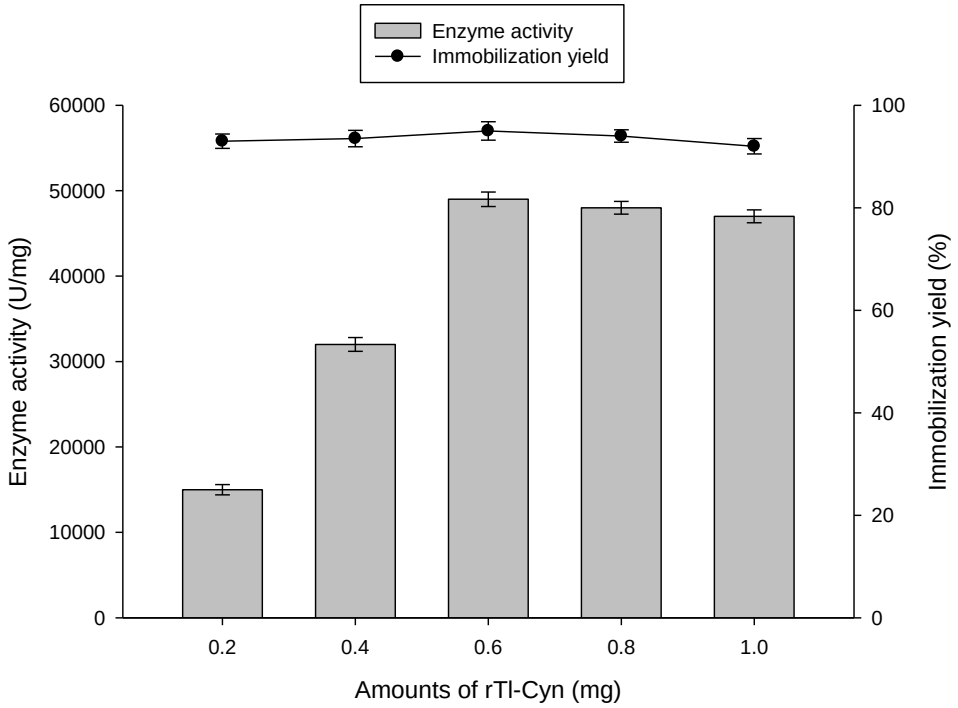

Fig. 4.8 Effect of pH **(a)** and concentration **(b)** on the immobilization yield of rTl-Cyn.

a

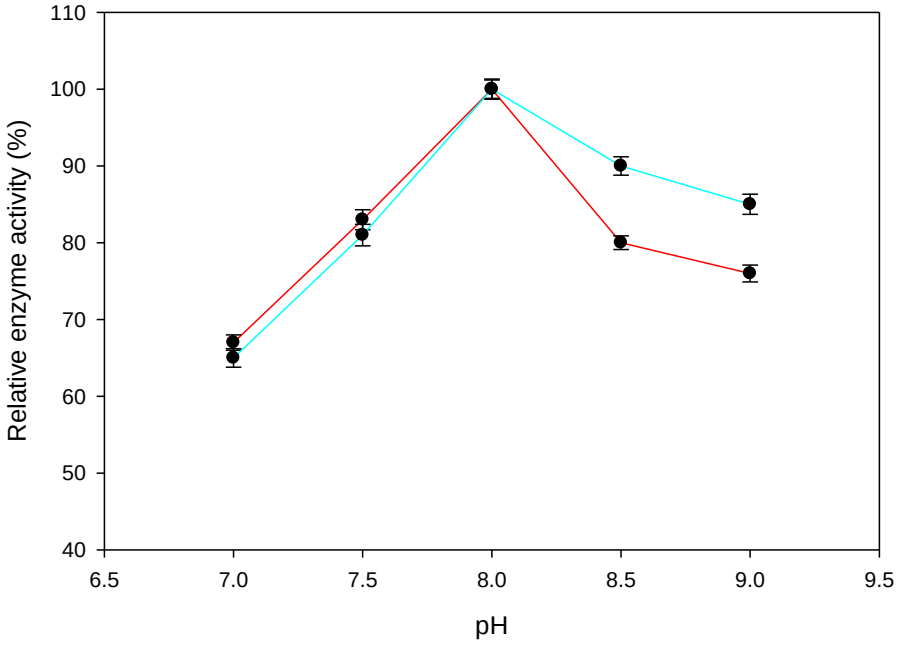

b

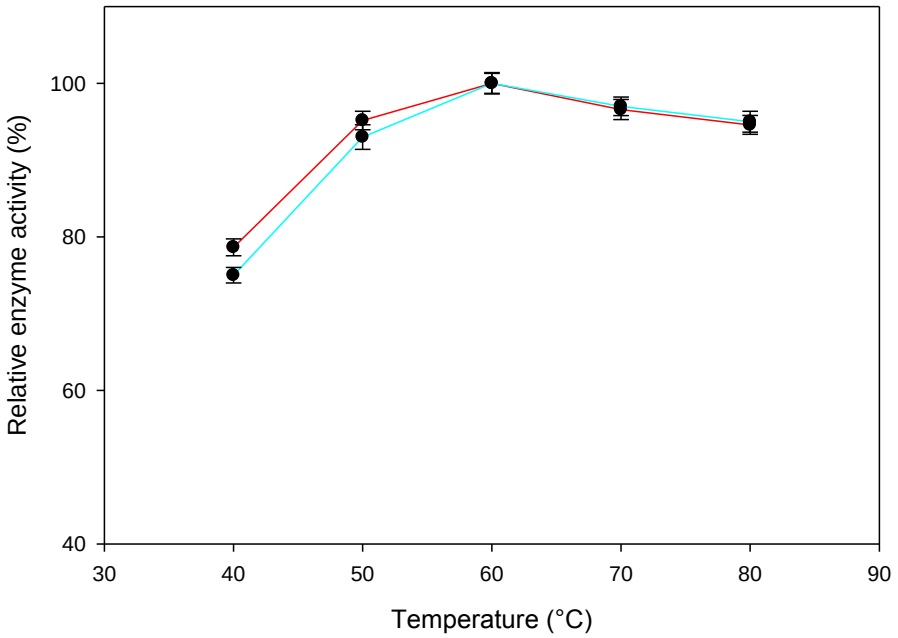

Fig. 4.9 Effect of pH **(a)** and temperature **(b)** on the catalytic efficiency of free (—●—) and immobilized (—●—) rTl-Cyn.

4.3.4 Determination of the kinetic constants

The Michaelis constant (K_m) and maximum velocity (V_{max}) for free and immobilized enzymes were 0.34 and 0.51 mM and 2857.14 and 3141.72 µmoles mg^{-1} min^{-1}, respectively. The 1.5 fold increase (0.51 mM) in the K_m for immobilized enzyme was possibly due to the diffusional limitation, which resulted in a lower enzyme-substrate complex formation. However, a 4-fold increase in the K_m value was reported for an immobilized lipase from *T. lanuginosus* in comparison to the free enzyme (Sörensen *et al.*, 2010). Irrespective of the K_m, m-MWCNT-rTl-Cyn showed a V_{max} of 3141.72 µmoles mg^{-1} min^{-1}, which is 1.1 fold higher than free rTl-Cyn, indicating a better efficiency of the immobilized enzyme.

4.3.5 Storage stability and reusability properties

Major advantages of immobilized enzymes is their increased stability and reusability (Subrizi *et al.*, 2014). The storage stability of free and immobilized enzymes were evaluated and showed that almost 100% of initial activity was retained over 30 days (Fig. 4.10a). This confirms that covalent immobilization of rTl-Cyn to m-MWCNTs did not affect the enzyme stability and also prevented the leaching of the enzyme from the immobilized carrier.

The reusability of m-MWCNT-rTl-Cyn was assessed in a batch operation mode for 10 cycles during the degradation of cyanate at 60°C with each cycle lasting for 10 min (Fig. 4.10b). Strikingly, the m-MWCNT-rTl-Cyn retained >94% of its initial activity after 10 consecutive cycles. However, in another study MWCNT-cellulase retained only 52% of its initial activity after 6 catalytic cycles (Mubarak *et al.*, 2014). This small loss in activity (<5%) of m-MWCNT-rTl-Cyn, might be due to the deactivation of the enzyme during repeated use. Thus, the preservation of the catalytic activity of m-MWCNT-rTl-Cyn during 10 successive reactions, along with their outstanding storage stability, with an activity retention of 100% over 30 days, emphasizes its potential in large-scale and economically-feasible remediation processes.

a

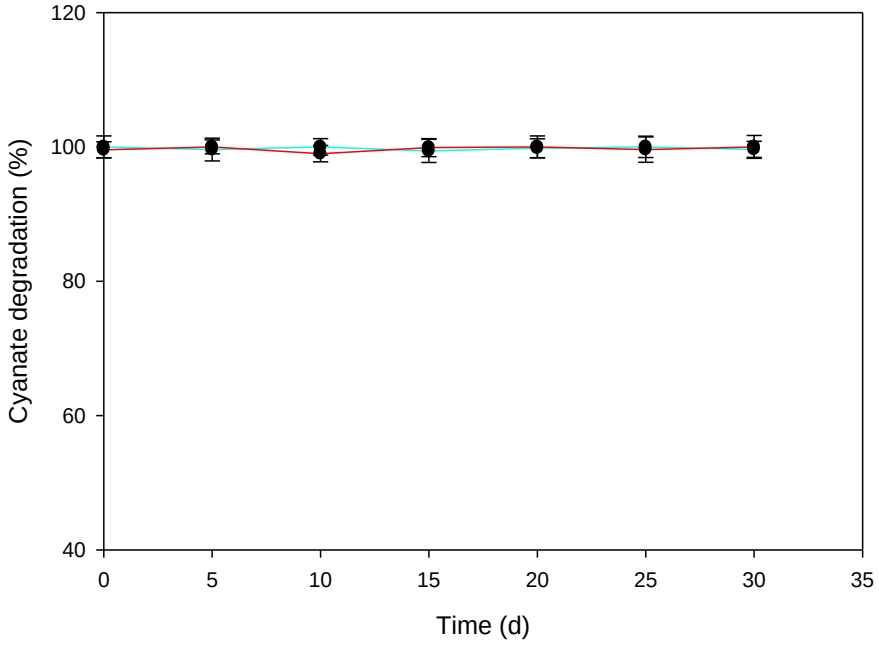

b

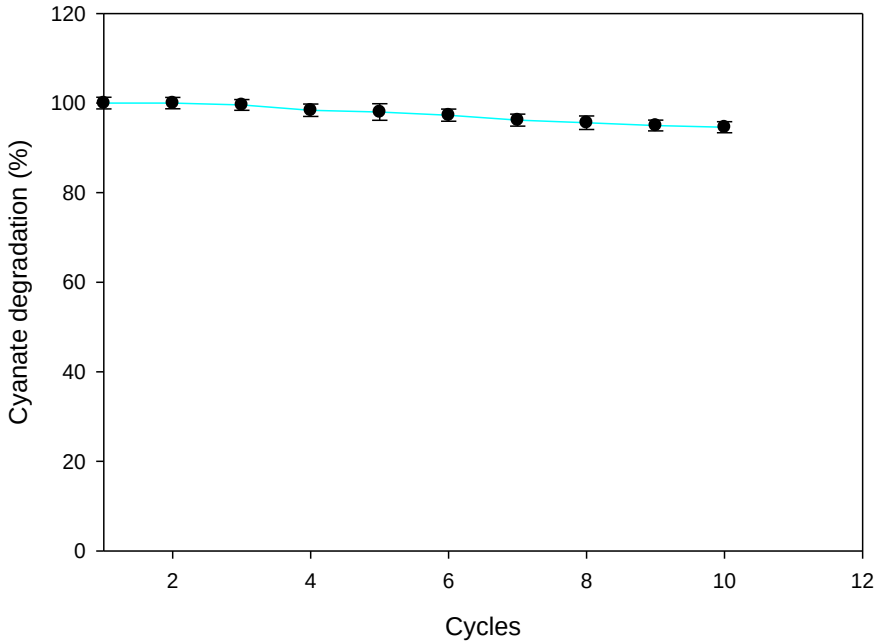

Fig. 4.10 (a) Storage stability at 4°C of the free (rTl-Cyn; —●—) and immobilized (m-MWCNT-rTl-Cyn; —●—) enzyme **(b)** Reuse of m-MWCNT-rTl-Cyn in the degradation of cyanate.

4.3.6 Simultaneous removal of cyanate and heavy metals

CNTs have proven to be an efficient, economical and eco-friendly adsorbent for the removal of a number of heavy metals from water, due to their van der Waals forces and π-π interaction (Ihsanullah *et al.*, 2016). The degradation of cyanate in wastewater is previously reported in chapter 2. In this chapter, the simultaneous removal of heavy metals and cyanate using m-MWCNT-rTl-Cyn in a synthetic wastewater sample was assessed. The removal of heavy metals was observed in the supernatant obtained after magnetic separation of the m-MWCNT-rTl-Cyn, and their concentrations were analyzed using AAS. In addition, control samples were also used for different heavy metals and the concentration of the respective metal in control sample was considered as 100%. Based on this, the relative percentage of test samples were evaluated. Interestingly, it was observed that, 39.31, 35.53, 34.48 and 29.63% of chromium (Cr^{+2}), iron (Fe^{+2}), lead (Pb^{+2}) and copper (Cu^{+2}), respectively were removed using 1 mg of the immobilized carrier (m-MWCNT-rTl-Cyn) (Fig. 4.11). However, in another study, 1 g of carrier (MWCNTs) was used to remove 55.74 and 70% of Pb and Fe, respectively (Jagadish *et al.*, 2016). In the present investigation, a ≥84% of cyanate degradation was simultaneously achieved in the presence of all heavy metals tested (Fig. 4.11). It was also observed that, while increasing adsorption of these heavy metals on m-MWCNT-rTl-Cyn, the extent of cyanate degradation has decreased. This could be due to the increase in concentration of metals adsorbed onto the surface of m-MWCNT-rTl-Cyn, probably hindered the binding of cyanate to the active site of rTl-Cyn. Moreover, similar observations were noticed for the free enzyme (r-Tl-Cyn), wherein cyanate degradation was inhibited by ~ 4%, when heavy metal concentrations were increased from 2 to 5 mM (Chapter 2). This bi-functionality of the m-MWCNT-rTl-Cyn bio-composites shows remarkable potential for synthetic wastewater treatment.

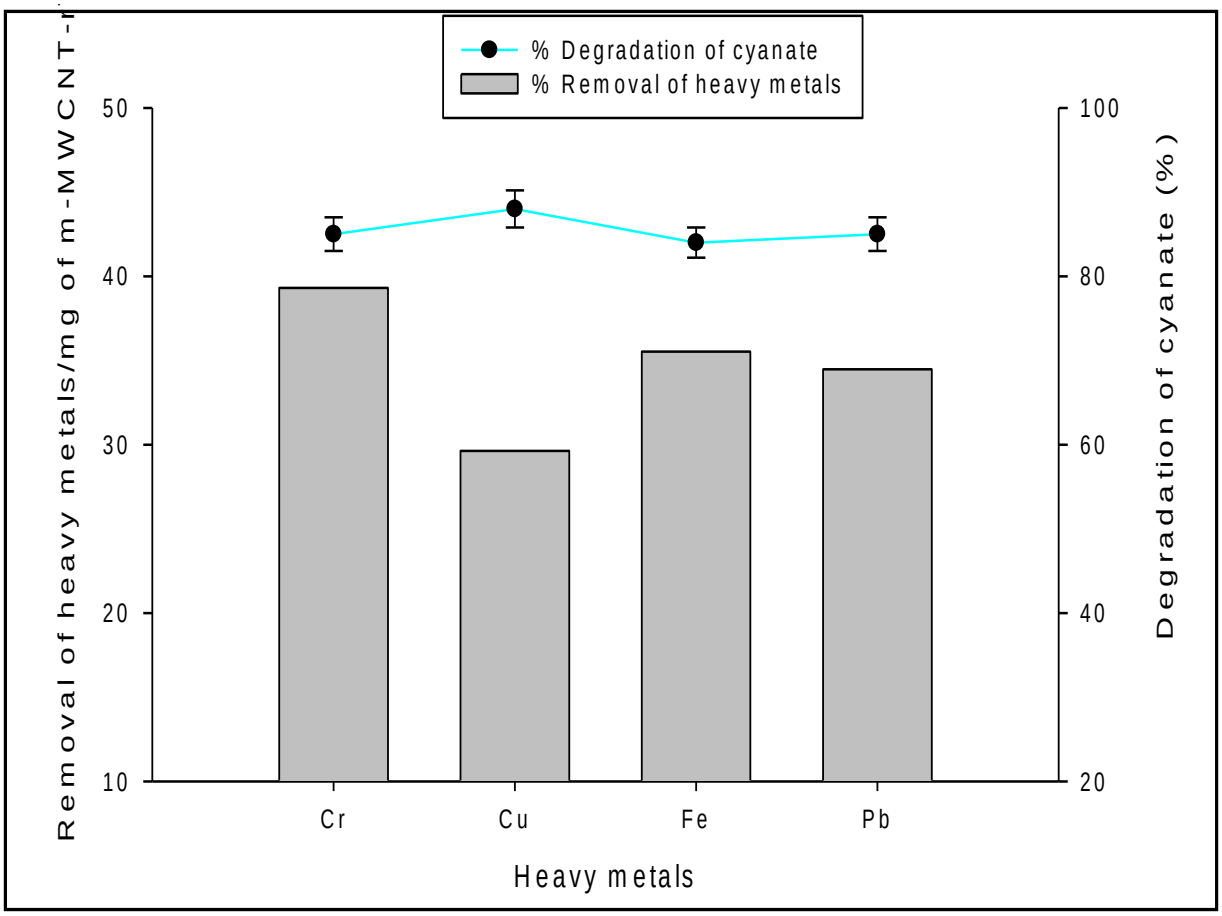

Fig. 4.11 Simultaneous removal of heavy metals and cyanate in a synthetic wastewater sample.

4.4. Conclusions

The immobilization of rTl-Cyn on m-MWCNTs was accomplished for the first time, and their bi-functionality in a synthetic wastewater remediation was evaluated. The potential for the simultaneous removal of heavy metals and cyanate from a synthetic wastewater sample in a single step was clearly highlighted with the immobilized enzyme (m-MWCNT-rTl-Cyn). Due to the increasing demands for enzymatic cascade reactions geared towards bio-remediation, the contributions from this work would open up new approaches for economical, efficient and sustainable bio-catalytic processes.

CHAPTER 5

Crystal structure of a fungal cyanase and implications for catalytic mechanism

5.1 Introduction

Cyanate is a toxic compound produced by industry (Luque-Almagro *et al.*, 2008), but also generated spontaneously from urea and carbamoyl phosphate (Qian *et al.*, 1997; Purcarea *et al.*, 2003). The toxicity of cyanate possibly arises from its reactivity with amino, sulfhydryl, carboxyl, phenolic hydroxyl, imidazole, and phosphate groups in proteins (Stark, 1967). Additionally, cyanate is widely used to inhibit the physiological reactions in plants as a herbicide (Koshiishi *et al.*, 1997) and in mammals as an uremic toxin (Kraus and Kraus Jr., 1998). In contrast, cyanate has been assumed to serve as a nitrogen source for the growth of certain microorganisms (having a functional cyanase) under nitrogen limitation (Rocap *et al.*, 2003; Palatinszky *et al.*, 2015). However, microbes lacking a cyanase gene are not able to grow in the presence of cyanate (Anderson *et al.*, 1990; Kozliak *et al.*, 1995).

Cyanase (also known as cyanate hydratase and cyanate lyase) catalyzes the decomposition of cyanate into ammonium and CO_2. Cyanases are found in bacteria (Anderson, 1980; Johnson and Anderson, 1987; Sung *et al.*, 1987), fungi (Elleuche and Pöggeler, 2008) and plants (Qian *et al.*, 2011), where they have important roles for nitrogen assimilation or cyanate detoxification. Despite these important functions, the production of this enzyme is low by most known organisms (Anderson, 1980; Harano *et al.*, 1997; Elleuche and Pöggeler, 2008; Qian *et al.*, 2011). Although cyanase from bacteria has been characterized in detail and its structure is also known (Walsh *et al.*, 2000; Butryn *et al.*, 2015), no attempt has been made to enhance its production.

T. lanuginosus, a thermophilic fungus, has been known to produce the highest amount of xylanase and also produces several other hydrolytic enzymes (Singh *et al.*, 2003). In addition, it has a ubiquitin degradation pathway which plays an essential role in response to various stress, such as nutrient limitation, heat shock, and heavy metal exposure (Mchunu *et al.*, 2013). Owing to these requisite properties, this fungus has been identified as one of the organisms of choice for industrial applications. Furthermore, whole genome sequencing and secretome analysis of

T. lanuginosus (Mchunu *et al.*, 2013; Winger *et al.*, 2014) has revealed the presence of a cyanase (*Tl-Cyn*) and its potential in cyanate detoxification has been presented in previous chapters.

To get a better understanding of Tl-Cyn function and a deeper insight into its molecular mechanism, structural information on this enzyme is required. To date, biochemical and structural studies have been limited to bacterial cyanases and no structural information is available on fungal cyanases. In this chapter, the crystal structure of the cyanase (Tl-Cyn) from *T. lanuginosus* is reported. Also, the binding modes of substrate-analog inhibitors in the active site of Tl-Cyn was determined and characterized their inhibition of the enzyme by kinetic studies. Furthermore, mutation studies were performed to confirm the structural observations and also to enhance the catalytic activity of the Tl-Cyn.

5.2 Materials and Methods

5.2.1 Protein expression and purification

Tl-Cyn gene was sub-cloned into the pET28a vector (Novagen), which introduced an N-terminal hexa-histidine tag. The recombinant protein was over-expressed in *E. coli* BL21 Star (DE3) cells (Novagen), which were induced with 0.8 mM IPTG and allowed to grow at 20°C for 16 h. The protein was extracted as described previously in chapter 3. The soluble protein was purified by nickel-charged immobilized-metal affinity chromatography (Qiagen) followed by gel filtration chromatography (Sephacryl S-300, GE Healthcare). The purified protein was concentrated to 13 mg/mL in a buffer containing 20 mM Tris-HCl (pH 8.0) and 150 mM NaCl, flash-frozen in liquid nitrogen and stored at –80°C. The N-terminal hexa-histidine tag was not removed for crystallization.

5.2.2 Thermal shift assay

The thermal stability of the Tl-Cyn at 10 µM concentration was analyzed at various temperatures using the Mx3005P Real-Time PCR system (Stratagene). The Tl-Cyn was mixed with the fluorescence dye (SYPRO orange; Invitrogen) for monitoring protein unfolding. All assays were performed in duplicate in a buffer comprising of 20 mM Tris-HCl (pH 8.0) and 150 mM NaCl. The temperature was increased from 25 to 99°C at 1°C intervals over a 75 min period. Fluorescence values for the curve were normalized to the maximum and the minimum of the curve (Zhang *et al.*, 2017).

5.2.3 Protein crystallization

Crystals were grown by the sitting-drop vapour diffusion method at 20°C (Maderbocus *et al.*, 2017). The protein was at 13 mg/mL concentration. The reservoir solution contained 2% (v/v) Tacsimate (pH 8.0), 0.1 M Tris (pH 8.5), and 16% (w/v) PEG 3350. Fully-grown crystals were obtained one day after set-up. The crystals were initially observed under microscope and are shown in Fig. 5.1. The crystals were then cryo-protected in the reservoir solution supplemented with 20% (v/v) glycerol and flash-frozen in liquid nitrogen for data collection at 100 K.

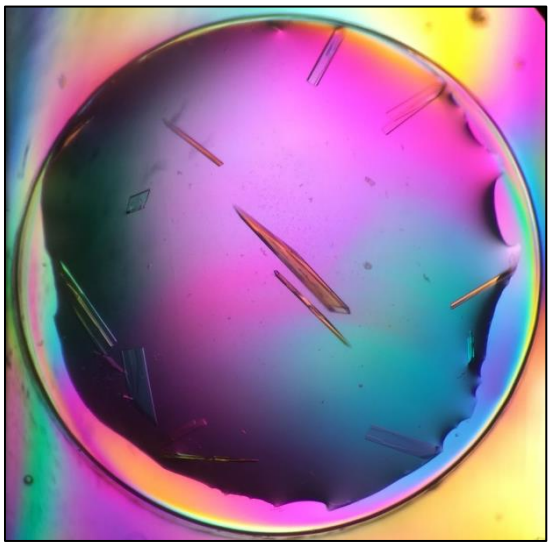

Fig. 5.1 Microscopic view of Tl-Cyn crystals under polarized light.

5.2.4 Data collection and processing

X-ray diffraction data were collected at the Advanced Photon Source beamline NE-CAT 24-ID-E using an ADSC Q315r detector (Argonne National Laboratory, USA) and at X25 beamline at the National Synchrotron Light Source at Brookhaven National Laboratory using a Pilatus 6M detector. The diffraction images were processed and scaled with the HKL2000 package (Otwinowski *et al.*, 1997).

5.2.5 Structure determination and refinement

The structure of Tl-Cyn was solved by the molecular replacement method with the programme Phaser (McCoy *et al.*, 2007), using the structure of *E. coli* cyanase (PDB code 1dw9) as the search model (Walsh *et al.*, 2000). Manual model rebuilding was carried out with Coot (Emsley and Cowtan, 2004) and refinement with the programme Refmac (Murshudov *et al.*, 1997).

5.2.6 Site directed mutagenesis

Mutants were made by PCR-based site directed mutagenesis using the Phusion High-Fidelity DNA Polymerase (Thermo Scientific) and confirmed by sequencing. A set of overlapping oligonucleotide primer pairs with the desired mutations were designed to generate the mutant constructs (Table 5.1). The recombinant vector (pET28a(+)-Cyn) was used as a template. Approximately 100 ng of template was used for the amplification of the mutant constructs in a thermocycler (GeneAmp PCR System 9700, Applied Biosystems) in 50 μL reaction mixtures according to the following PCR conditions: denaturation at 98°C for 1 min; 25 cycles (denaturation at 98°C for 30 s, annealing at 60°C for 30 s, elongation 68°C for 6 min) and final elongation at 68°C for 10 min. PCR products were digested with *Dpn*I at 37°C for 4 h and digested products were transformed into *E. coli* DH5α. The plasmid constructs isolated from the transformants were sequenced for the confirmation of the mutated nucleotide(s). For generating double mutants, confirmed single mutant plasmids were used as a template for the second mutagenesis.

5.2.7 Cyanase assay

Cyanase assays were performed as previously described in chapter 2.

5.2.8 Kinetic studies

The enzyme kinetics studies were performed by determining the velocities of the enzyme reactions at different concentrations (0.05 to 3.0 mM) of potassium cyanate (Sigma). The apparent Michaelis constant (K_m) and the maximal velocity (V_{max}) of the enzyme activities were calculated by fitting the initial velocities and substrate concentrations into the Lineweaver-Burk plots. The catalytic efficiency of the enzymes were estimated as k_{cat}/K_m ratios.

Table 5.1 Primer sequences for site directed mutagenesis

Primer	Sequence (5′→3′)*
BRF_Y14	GACGTCACTCAGCATCCA**GC**TCTACCCGCCTACTCCAA
BRR_Y14	TTGGAGTAGGCGGGTAGA**GC**TGGATGCTGAGTGACGTC
BRF_R101	AAGGAACCCTTGATTTAT**AA**ATTGTATGAGATTGTGCA
BRR_R101	TGCACAATCTCATACAAT**TT**ATAAATCAAGGGTTCCTT
BRF_E104	GATTTATCGATTGTATGA**C**ATTGTGCAGAATTATGGA
BRR_E104	TCCATAATTCTGCACAAT**G**TCATACAATCGATAAATC
BRF_S127	TCGGGGACGGTATCATGA**C**TGCGATCAGCTTTTCAAC
BRR_S127	GTTGAAAAGCTGATCGCA**G**TCATGATACCGTCCCCGA
BRF_A128	GGGACGGTATCATGAGTG**T**GATCAGCTTTTCAACGTC
BRR_A128	GACGTTGAAAAGCTGATC**A**CACTCATGATACCGTCCC

*Substituted nucleotides are indicated in bold.

5.2.9 Inhibition kinetics by formate and malonate

To characterize the nature of the inhibition by formate and malonate, kinetic assays were carried out with varying concentrations of cyanate and bicarbonate along with different concentration of inhibitors (one at a time). The inhibitory constants for uncompetitive and mixed inhibitions were analyzed by equations 1, 2 and 3, 4, respectively.

$$Km_{app} = Km/(1+[I]/K_{ib}) \quad \text{(Eq. 1)}$$

$$Vmax_{app} = Vmax/(1+[I]/K_{ib}) \quad \text{(Eq. 2)}$$

$$Km_{app} = Km(1+[I]/K_{ia})/(1+[I]/K_{ib}) \quad \text{(Eq. 3)}$$

$$Vmax_{app} = Vmax/(1+[I]/K_{ib}) \quad \text{(Eq. 4)}$$

where Km_{app} is the apparent Michaelis constant (measured values of Km in the presence of inhibitor), [I] the inhibitor concentration, K_{ia} and K_{ib} are the inhibitory constants for binding to

the free enzyme and enzyme-substrate complex, respectively, and $V_{max_{app}}$ is the apparent maximal velocity (measured values of V_{max} in the presence of inhibitor). SigmaPlot 10.0 was used to generate the plots.

5.2.10 Sequence alignment

Alignment of selected sequences of cyanase was produced with Clustal Omega (https://www.ebi.ac.uk/Tools/msa/clustalo/), and modified manually to include additional information.

5.3 Results and Discussion

5.3.1 Overall structure of Tl-Cyn

To gain insight into the Tl-Cyn structure, activity and enable its rational design, the crystal structure of Tl-Cyn at 2.2 Å resolution was solved using *E. coli* cyanase as the model. The full-length *Tl-Cyn* gene was expressed in *E. coli* BL21 Star (DE3) and purified using established protocols (Huang *et al.*, 2010; Choi *et al.*, 2016) (Fig. 5.2a). In addition, stability of the purified Tl-Cyn was evaluated using the thermal shift assay (TSA) (Fig. 5.2b). TSA allows for the assessment of multiphasic unfolding behavior of the protein, which commonly interferes with crystallization (Geders *et al.*, 2012). Therefore, it has been commonly used to improve the purification and crystallization conditions of protein.

a

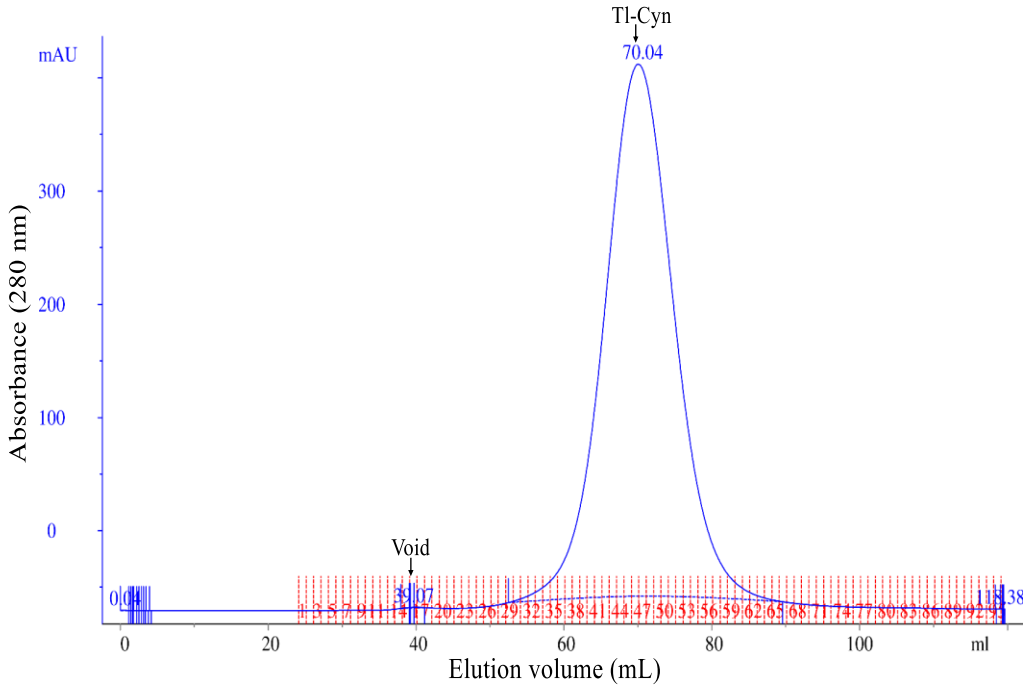

b

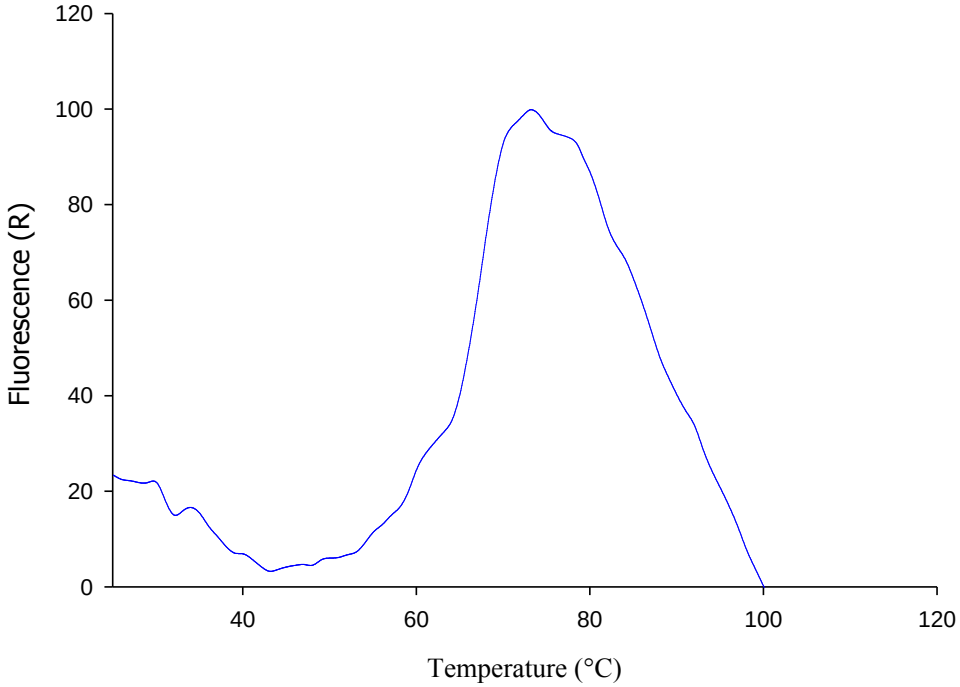

Fig. 5.2 Purification and thermal unfolding analysis of Tl-Cyn. **(a)** Gel filtration chromatogram of the purified Tl-Cyn. **(b)** Thermal shift assay to measure the thermostability of Tl-Cyn.

The refined structure has excellent agreement with the crystallographic data and the expected bond lengths, bond angles, and other geometric parameters (Table 5.2). A total of 99.4% of the residues are in the favoured region of the Ramachandran plot, and none are in the disallowed region.

Table 5.2 Crystallographic data collection and refinement statistics

Structure	**Tl-Cyn**
Data collection	
Space group	$P2_12_12_1$
Cell dimensions	
a, b, c (Å)	75.37, 157.64, 163.87
α, β, γ (°)	90, 90, 90
Resolution (Å)	50.00 - 2.20 (2.28 – 2.20)*
R_{merge}	9.6 (38.1)
Completeness (%)	99.90 (99.50)
Redundancy	4.4 (4.3)
Refinement	
Resolution (Å)	50.00 - 2.20 (2.28 – 2.20)
R_{work}/ R_{free}	15.44 / 20.18
R.m.s deviations	
Bond lengths (Å)	0.018
Bond angles (°)	1.9
Ramachandran plot statistics	
Most favoured regions (%)	99
Additionally allowed regions (%)	1
Outliers (%)	0.0

*Highest resolution shell is shown in parenthesis.

The structure of cyanase contains an N-terminal α-helical domain (residues 1-91; helices H1-H5) and a C-terminal α+β domain (residues 92-161; two antiparallel β-strands S1-S2 and a helix H6) (Fig. 5.3a). There are extensive interactions between the C-terminal domains of two subunits of a dimer, which together form a four-stranded anti-parallel β-sheet that is flanked on one face with the two H6 helices (Fig. 5.3a).

A decamer of Tl-Cyn is formed by a pentamer of these dimers, with intimate contacts among them (Fig. 5.4a-d). The interfaces in this decamer primarily involve the N-terminal domain and the H6 helix, while the four-stranded β-sheet in the center of the dimer interface is located near the 'equator' of the decamer. There is a small channel through the entire decamer, along its five-fold symmetry axis (Fig. 5.4d).

The structure of Tl-Cyn shows substantial differences to that of the *E. coli* cyanase (Fig. 5.3b). With the C-terminal domains of the two structures in overlay, large differences in the positions of the helices in the N-terminal domain are observed. Especially, the N-terminal segment of the two enzymes run in nearly opposite directions. On the other hand, the overall appearance of the two decamers is similar (Fig. 5.5a, b).

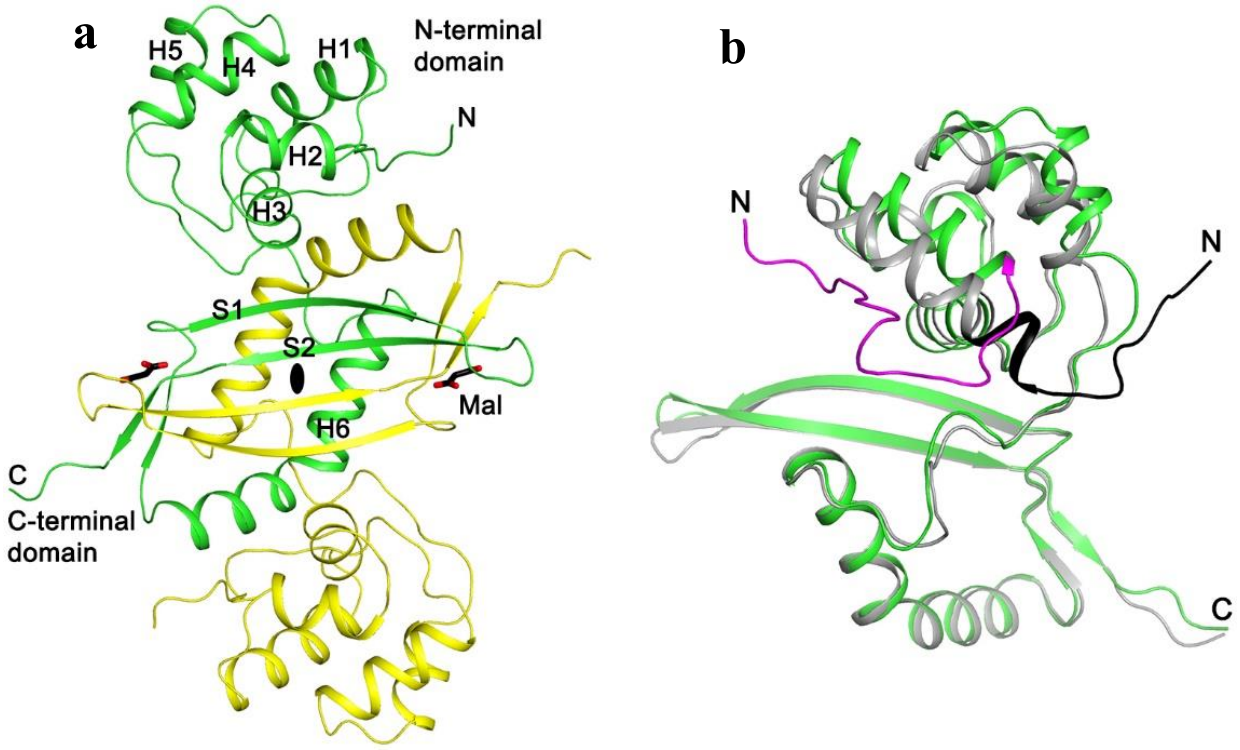

Fig. 5.3 Structure of fungal cyanase dimer. **(a)** An intertwined C-terminal domain (residues 92-160) in the dimer structure (green and yellow) of *T. lanuginosus* cyanase (Tl-Cyn). The two monomers are coloured in yellow and green, and the two-fold axis of the dimer is indicated by the black oval. The two malonate molecules bound to the active sites of the dimer are shown as sticks, colored according to atom types (carbon black, and oxygen red) and labelled Mal. **(b)** Overlay of the structure of Tl-Cyn monomer (green) with that of *E. coli* cyanase (gray). Large structural differences are seen for the N-terminal domain. Especially, the N-terminal segments run in opposite directions in the two structures and are highlighted in magenta and black. The structure figures were produced using PyMOL (http://www.pymol.org).

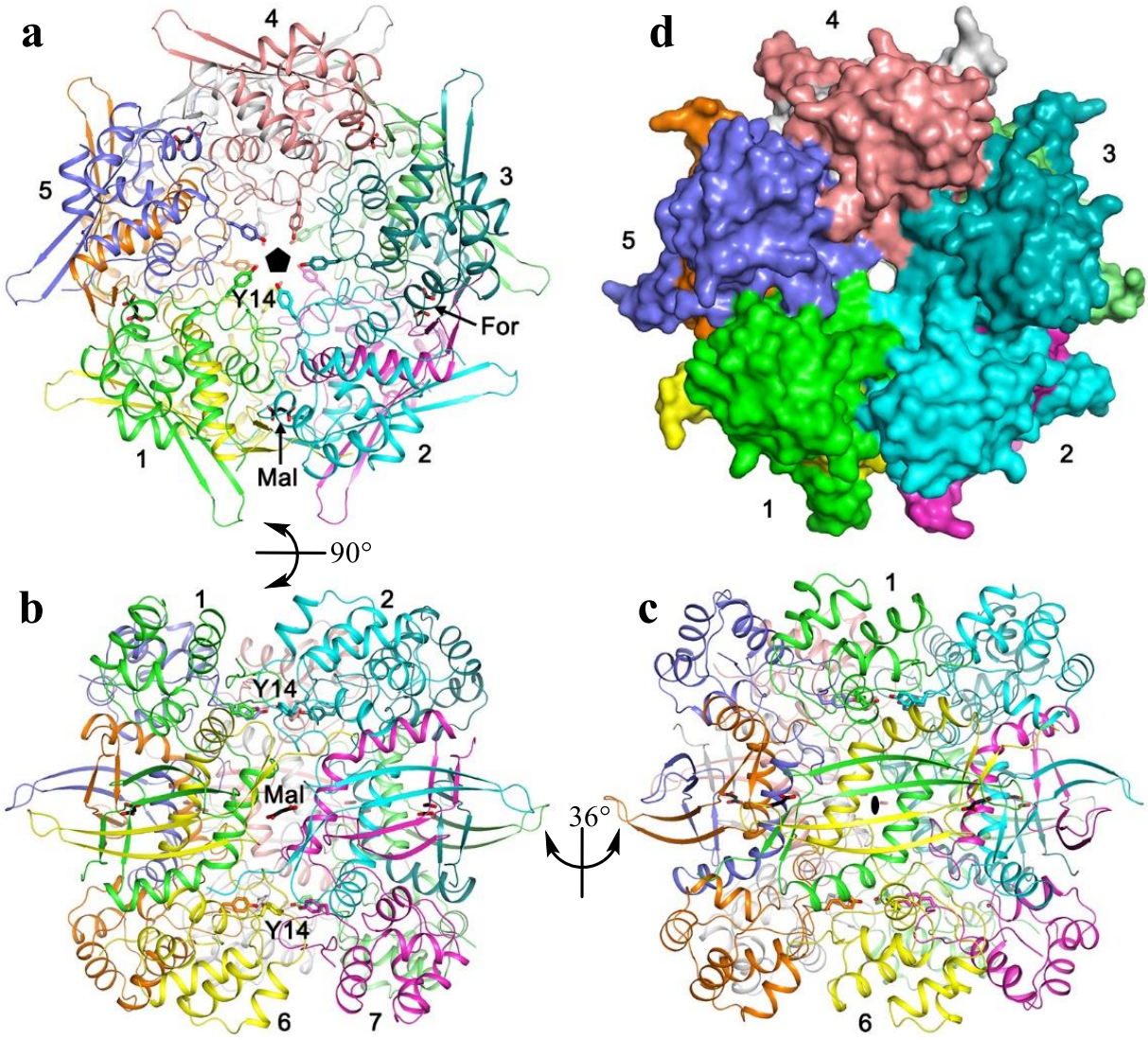

Fig. 5.4 Crystal structure of the fungal cyanase decamer. **(a)** Overall structure of the Tl-Cyn decamer (top view). Each monomer is depicted in a different color. The side chains of Y14 are shown as sticks, pointing towards the center of the structure. The malonate (labeled Mal) and formate (labeled For) molecules bound to the active sites of the decamer are shown as sticks. The five-fold symmetry axis of the decamer is indicated with the black pentagon. **(b)** Overall structure of the Tl-Cyn decamer viewed after a 90° rotation around the horizontal axis. **(c)** Overall structure of the Tl-Cyn viewed after a 36° rotation around the vertical axis from panel **b**. A two-fold axis of the decamer is indicated with the black oval. **(d)** Molecular surface of the Tl-Cyn decamer, viewed in the same orientation as in **a**.

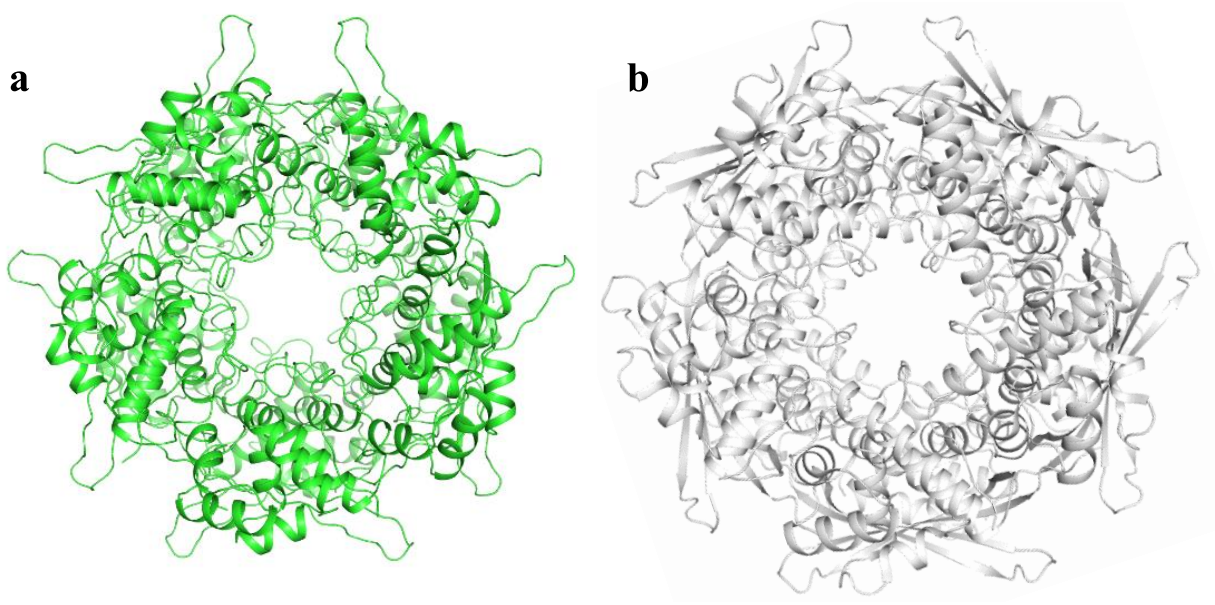

Fig. 5.5 Overall appearance of the two cyanase decamers. **(a)** Tl-Cyn. **(b)** *E. coli* cyanase.

5.3.2 Active site of Tl-Cyn

The active site of Tl-Cyn is located in the C-terminal domain (Fig. 5.3a), at the interface between neighbouring dimers of the decamer (Fig. 5.4a). This suggests that Tl-Cyn needs to be a decamer to be active. Malonate, which was distinct components of the crystallization buffer, is situated on a two-fold symmetry axis of the decamer, and its carboxylate groups are recognized by six hydrogen bonds from residues of four monomers (Fig. 5.6a,b). Specifically, the carboxylate is hydrogen-bonded to the side chain of Ser127 and the main-chain amide of Ala128 from one monomer (Fig. 5.6a). One of the carboxylate oxygen atoms is also hydrogen-bonded to the side chain of Arg101 from another monomer, which is also involved in a bidentate ion-pair with Glu104 from a third monomer.

Residues in the active site region of Tl-Cyn are highly conserved among fungal cyanases, sharing 100% amino-acid sequence identity (Fig. 5.6c). Thus, elucidation of the Tl-Cyn structure would be beneficial to improve the catalytic properties of fungal cyanases and also allow for the creation of novel enzymes for biotechnological applications.

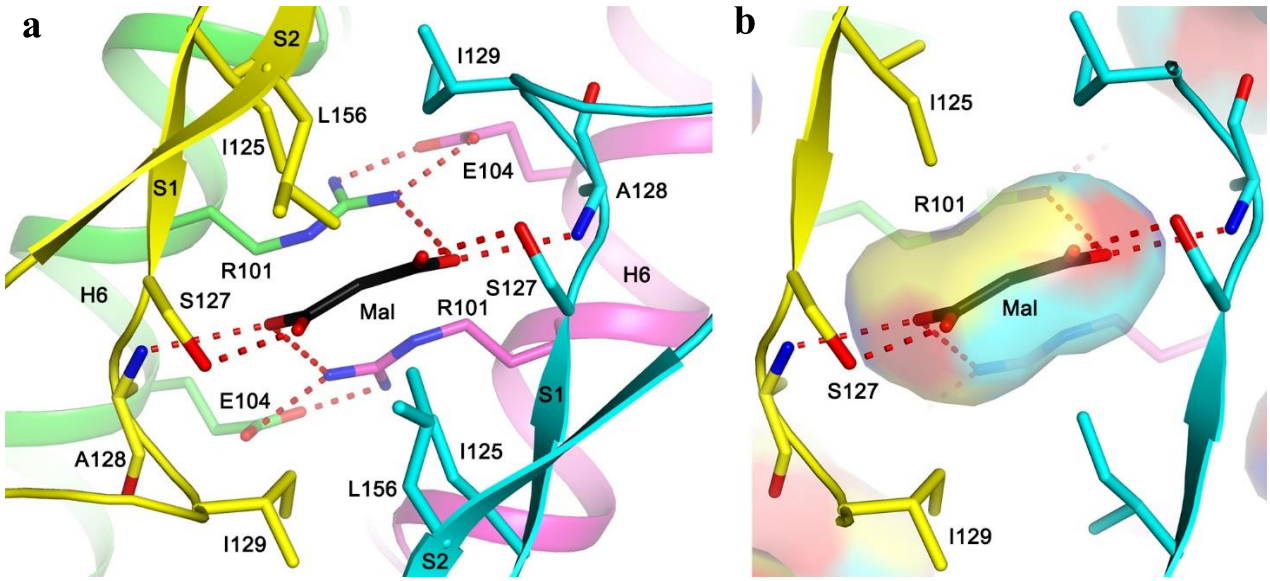

c

Tl-Cyn	100	YRLYEIVQNYGYAYKAVLNEKFGDGIMSAIS	130
Af-Cyn	99	YRLYEIVQNYGYAYKAVLNEKFGDGIMSAIS	129
Ps-Cyn	99	YRLYEIVQNYGYAYKAVLNEKFGDGIMSAIS	129
Pc-Cyn	99	YRLYEIVQNYGYAYKAVLNEKFGDGIMSAIS	129
Fp-Cyn	99	YRLYEIVQNYGYAYKAVLNEKFGDGIMSAIS	129
Rm-Cyn	99	YRLYEIVQNYGYAYKAVLNEKFGDGIMSAIS	129

Fig. 5.6 Structural insights into the catalytic mechanism of Tl-Cyn. **(a)** Schematic drawing of the detailed interactions between Tl-Cyn and the malonate molecule bound in the active site (sticks model and labeled Mal). Hydrogen-bonding interactions with the malonate are indicated with dashed lines (red). **(b)** Close-up view to that in **a**, and the internal cavity for malonate is shown with semi-transparent surface. **(c)** Conserved sequence near the active site region of the C-terminal domain in fungal cyanases are shown in cyan. Residues that interact with Mal are shown with yellow background. Tl: *T. lanuginosus*, Af: *A. flavus*, Ps: *Penicillium subrubescens*, Pc: *Phaeomoniella chlamydospora*, Fp: *Fonsecaea pedrosoi*, Rm: *Rhinocladiella mackenziei*.

5.3.3 Mutagenesis studies to provide insights into the catalytic mechanism

A series of point mutations were designed that are expected to perturb the hydrogen-bonding interactions with Mal based on the structural observations and evaluated their effects on catalysis (Fig. 5.7a). When the arginine (R101) and serine (S127) residues (in Tl-Cyn) were mutated to lysine and threonine, respectively, the catalytic activity was completely abolished (Fig. 5.7a). It was also found that the A128V and E104D mutations greatly reduced the catalytic activity by 77 and 74%, respectively, compared with wild-type (Fig. 5.7a). The Glu104 residue is not directly involved in the hydrogen-bonding interactions with Mal; however, it stabilizes the catalytic residue Arg101. As expected, it was observed that, the A128V/R101K double mutation completely abolished the catalytic activity of the enzyme. These data strongly support the structural observation on the active site of Tl-Cyn in which Arg101, Ser127, and Ala128 residues are involved in the interaction with inhibitor (Mal) residue by hydrogen bonds (Fig. 5.6a). Based on this mutagenesis studies, it is clear that Arg101 and Ser127 is crucial for the catalytic activity of Tl-Cyn, which is also highlighted from the structural observations (Fig. 5.6a, b). This is supported a by previous report wherein it has been shown that, Ser122 is responsible for the binding of substrates (OCN^- and HCO_3^-) and guanidinium group of the Arg96 stabilizing the negative charge of the substrates (Walsh *et al.*, 2000), which is corresponding to a Ser127 and Arg101 in the Tl-Cyn structure.

In addition, a unique feature of Tl-Cyn is the Tyr14 residue (Fig. 5.7b), which is located in the center of the structure and helps to reduce the size of the central channel (Fig. 5.4a). Surprisingly, the Y14A mutant displayed ~1.3 fold higher catalytic activity as compared with wild-type Tl-Cyn (Fig. 5.7a). This could be due to the bulky side chain of Tyr14 residue sterically hindering substrate access to the active site of the Tl-Cyn, while mutating Tyr14 to smaller amino acid (Ala) might have facilitated more substrate binding to the active site of the mutant. In addition, further mutagenesis studies are needed to enhance the substrate specificity of fungal cyanases, and Tl-Cyn structure would provide insights on the effect of mutations on substrate binding.

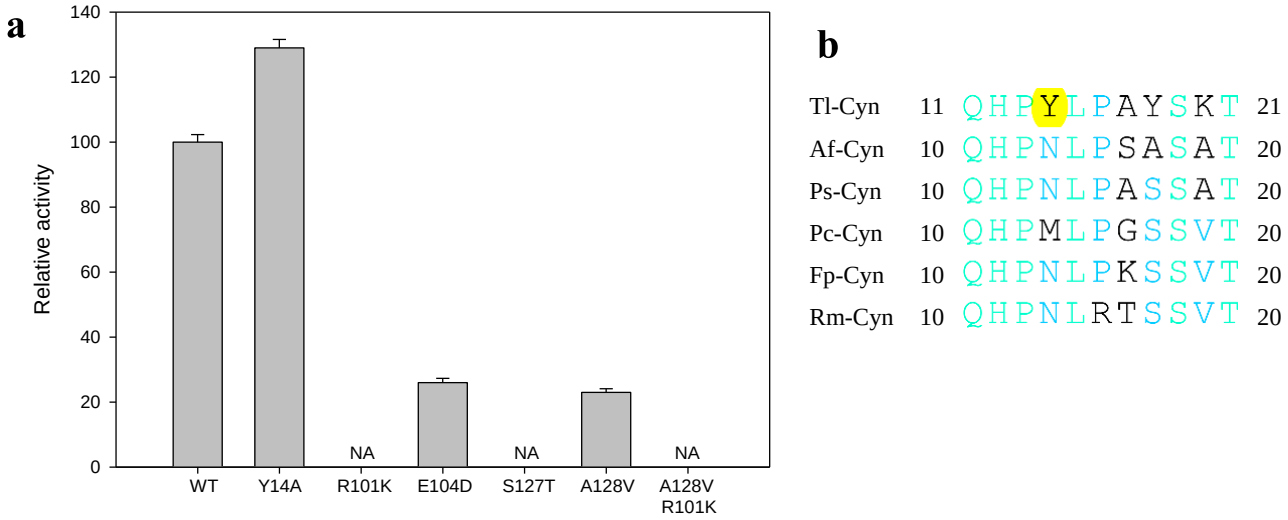

Fig. 5.7 Mutagenesis studies and their effects on catalytic activities. **(a)** Catalytic activities of wild-type (WT) and mutant Tl-Cyn. The cyanate concentration is at 2 mM. The error bars represent the standard deviation from three independent measurements. NA, no activity observed under the condition tested. **(b)** Sequence alignment in between the N-terminal domain region of the fungal cyanases. Conserved residues are in cyan and a unique Y14 residue is shown with yellow background.

To further characterize the effect of mutations on the catalytic efficiency (k_{cat}/K_m) of these enzymes, kinetic experiments were performed. It was observed that, the catalytic efficiency of the E104D and A128V mutants was $2.79 \pm 0.025 \times 10^7\ s^{-1}\ M^{-1}$ and $2.93 \pm 0.12 \times 10^7\ s^{-1}\ M^{-1}$, which is ~3.5- and ~3.3-fold lower than that for the wild-type enzyme, respectively (Table 5.3). In contrast, the catalytic efficiency of the Y14A mutant was $12.04 \pm 0.69 \times 10^7\ s^{-1}\ M^{-1}$, which is ~1.2-fold higher compared to the wild-type enzyme ($9.8 \pm 0.4 \times 10^7\ s^{-1}\ M^{-1}$).

Table 5.3 Summary of kinetic data for wild-type and mutant cyanases

Protein	**k_{cat} (s^{-1})**	**K_m (mM) (for cyanate)**	**k_{cat}/K_m (s^{-1} M^{-1})**
Wild-type	$3.56 \pm 0.19 \times 10^4$	0.36 ± 0.04	$9.8 \pm 0.4 \times 10^7$
Y14A	$4.81 \pm 0.11 \times 10^4$	0.40 ± 0.01	$12.04 \pm 0.69 \times 10^7$
R101K	NA[α]	NA[α]	NA[α]
E104D	$5.84 \pm 0.026 \times 10^3$	0.21 ± 0.003	$2.79 \pm 0.025 \times 10^7$
S127T	NA[α]	NA[α]	NA[α]
A128V	$5.72 \pm 0.029 \times 10^3$	0.20 ± 0.007	$2.93 \pm 0.12 \times 10^7$
A128V/ R101K	NA[α]	NA[α]	NA[α]

[α]No activity was observed under the same conditions.

5.3.4 Malonate and formate are cyanase inhibitors

In order to confirm the structural observations that malonate and formate are fortuitously present in the active site of Tl-Cyn (Fig. 5.6a, b), kinetic experiments were performed to determine the inhibition mechanisms. The data are plotted in the form of $1/v_0$ against 1/[S], where v_0 is the initial velocity of an enzyme-catalyzed reaction (μmoles mg^{-1} min^{-1}) and [S] is the substrate concentration (mM) (Fig. 5.8). On the basis of the double-reciprocal plots, formate and malonate have direct inhibitory effect on the catalysis of Tl-Cyn. Furthermore, the point of intersections observed in the double-reciprocal plots showed that it is a mixed-type of inhibition with respect to the HCO_3^- (Fig. 5.8a, b). In contrast, no point of intersections were observed with respect to the OCN^-, and the presence of parallel lines in the double-reciprocal plots are indicative of the uncompetitive inhibitions (Fig. 5.8c, d).

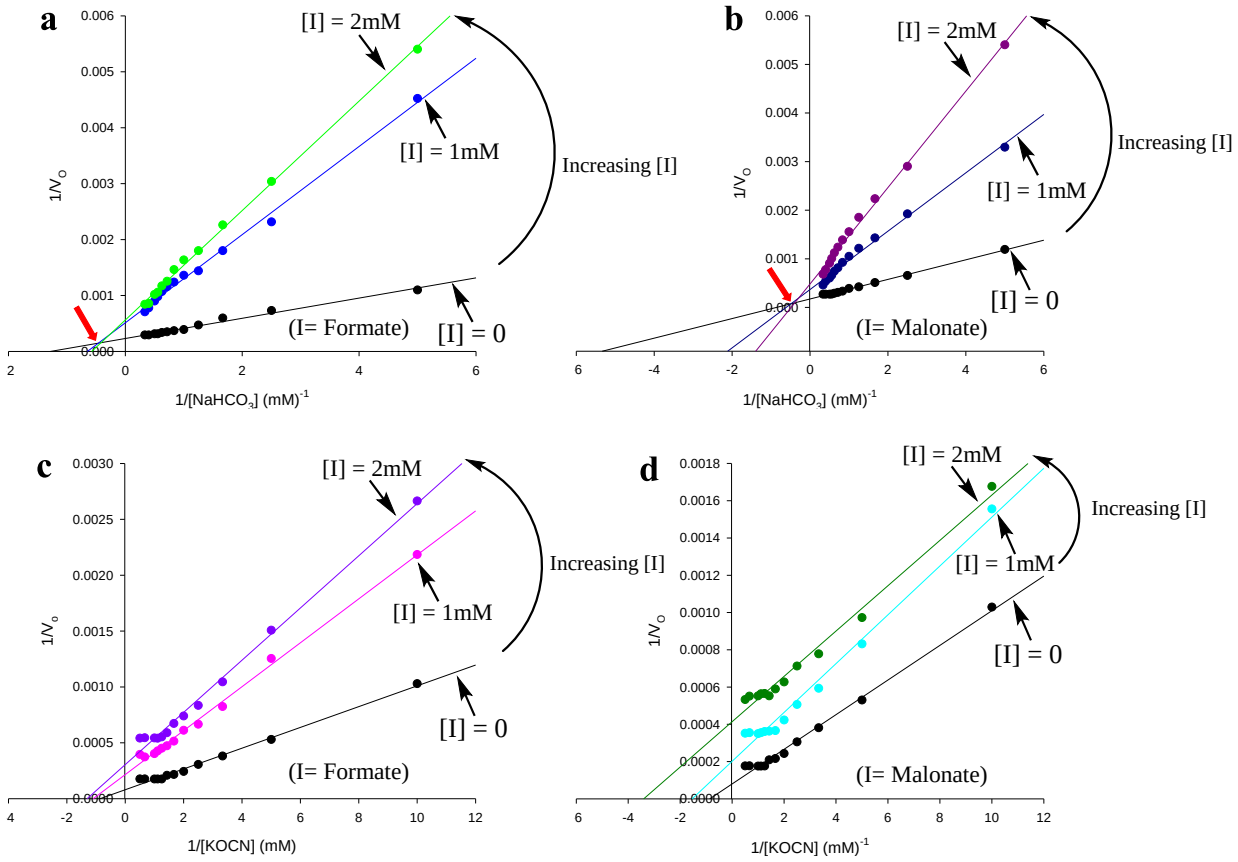

Fig. 5.8 Kinetic studies on the inhibition of Tl-Cyn by malonate and formate. **(a)** and **(b)** A set of double-reciprocal plots, one obtained in the absence of inhibitor and two at different concentrations of inhibitor, formate and malonate, respectively in the presence of varying concentrations of $NaHCO_3$. The location of the intersection point of the lines is indicated with the red arrow. **(c)** and **(d)** A set of double-reciprocal plots, one obtained in the absence of inhibitor and two at different concentrations of inhibitor, formate and malonate, respectively in the presence of varying concentrations of KOCN. Data points are means taken from three representative set of experiments.

The inhibitory constants (K_i) for malonate and formate were determined (Table 5.4), and these values provide information on the inhibitory potency of the compounds. These kinetic results confirmed that formate and malonate could inhibit the catalytic activity of Tl-Cyn by hindering substrate binding, which further supports the structural observations. Overall, mutagenesis and kinetic studies confirmed the presence of inhibitor at the active site of the Tl-Cyn. A possible mechanism was proposed for the decomposition of cyanate and kinetic inhibition of the Tl-Cyn (Fig. 5.9a, b). A similar mechanism for the decomposition of cyanate has been proposed on the basis of the kinetic studies of *E. coli* cyanase (Johnson and Anderson, 1987). Although there is no direct inhibition (uncompetitive-type) observed with respect to cyanate by these inhibitors, however, it showed competitive- as well as uncompetitive- inhibition with respect to bicarbonate. Moreover, it has been found that bicarbonate is necessary for the binding of cyanate to the active site of cyanase for its degradation (Kozliak *et al.*, 1995). Thus, inhibition of bicarbonate leads to the inhibition of cyanate binding at the active site of Tl-Cyn. Notably, it has also been observed that bicarbonate and cyanate has a competitive relationship for the catalytic binding site (Kozliak *et al.*, 1995). In addition, inhibition of cyanase activity by malonate molecule in *E. coli* was also previously reported (Anderson *et al.*, 1987). Finally, this structural analysis has laid the foundations for future protein engineering to design biocatalysts with enhanced catalytic properties, which would be valuable for industries focused on sustainable bio-remediation.

Table 5.4 Summary of inhibition kinetics of Tl-Cyn

Substrate	**Inhibitor**	**Type of inhibition**	**Inhibitory constant (K_i)**	
			K_{ia}^{β}	**K_{ib}^{γ}**
KOCN	Formate	Uncompetitive	-	0.70 ± 0.06
KOCN	Malonate	Uncompetitive	-	0.54 ± 0.12
$NaHCO_3$	Formate	Mixed	0.41 ± 0.11	1.19 ± 0.39
$NaHCO_3$	Malonate	Mixed	0.23 ± 0.01	1.08 ± 0.20

$^{\beta}$The K_i for binding to the free enzyme. $^{\gamma}$The K_i for binding to the enzyme-substrate complex.

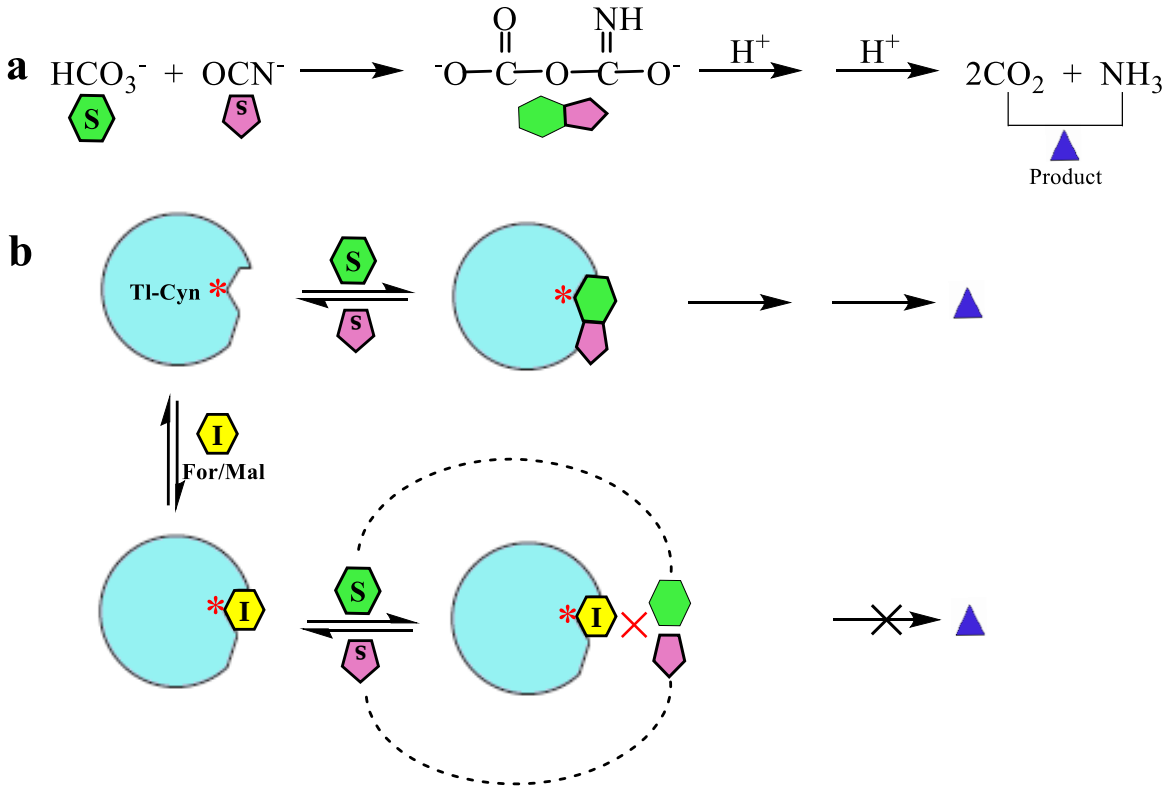

Fig. 5.9 Possible mechanism of the Tl-Cyn catalysis and inhibition. **(a)** Schematic drawing for the mechanism of cyanate decomposition catalyzed by cyanase. The substrates are shown with different colors and shapes, bicarbonate green hexagon, and cyanate purple pentagon. **(b)** A cartoon representation for the catalysis and kinetic inhibition of the Tl-Cyn. The active site is indicated with the red *asterisk*. The presence of the inhibitor at the active site of the Tl-Cyn has hindered substrate binding. The substrates are given separate colors as in **a**. The inhibitor molecule is shown in yellow hexagon.

5.4 Conclusions

The crystal structure of cyanase from the thermophilic fungus *T. lanuginosus* (Tl-Cyn) was solved. This structural, biochemical, kinetic and mutagenesis studies also revealed the molecular mechanism of Tl-Cyn action. The structure has also aided the creation of a mutant enzyme with enhanced catalytic activity. In addition, the active site region of Tl-Cyn are highly conserved among fungal cyanases, so Tl-Cyn structure would be beneficial to improve the catalytic properties of fungal cyanases and also allow for the creation of novel enzymes for biotechnological applications, including biotransformation and bioremediation.

6. CONCLUDING REMARKS

The thermophilic fungus *T. lanuginosus* SSBP has been known to produce the highest titre of xylanase together with several other hydrolytic enzymes of industrial interest (Singh *et al.*, 2003). Of note is that apart from xylanase, other associated hemicellulases are secreted at extremely low levels (Singh *et al.*, 2000). This has been an evolutionary phenomenon across various other strains that were evaluated (Singh *et al.*, 2003; Xiong *et al.*, 2004; Li *et al.*, 2005). In addition, it has a ubiquitin degradation pathway which plays an essential role in response to various stress factors, such as nutrient limitation, heat shock, and heavy metal exposure (Staszczak, 2008). Based on these characteristics outlined above, this fungus has been identified as an organism of choice for industrial applications.

The advent of fungal genomics has resulted in a massive influx of data, which provides an unparalleled opportunity to gain insight into the industrially and environmentally relevant enzymes. In this regard, the whole genome sequence analysis of *T. lanuginosus* SSBP (23.3 Mb) has predicted the presence of 5,105 genes, of which 224 genes belongs to the Carbohydrate Active EnZymes (CAZy) family (Mchunu *et al.*, 2013). Several of these genes have been cloned, expressed, and characterized, *viz.*, xylanase (Birijlall *et al.*, 2011), chitinase (Khan *et al.*, 2015; Zhang *et al.*, 2015), β-xylosidase (Gramany *et al.*, 2016), oligo-1, 6-glucosidases (Dong *et al.*, 2018) and many more genes are yet to be explored. Application of these recombinant enzymes were also evaluated in various sectors such as, xylanase in biobleaching of bagasse pulp (Birijlall *et al.*, 2011), chitinase in antifungal activity against *P. verrucosum* and *A. niger* (Zhang *et al.*, 2015), and oligo-1, 6-glucosidases for the production of glucose from starch (Dong *et al.*, 2018).

Another approach is to assess the fungal secretome, which consists of a repertoire of secreted proteins and enzymes which are necessary for vital biological processes, *viz.*, cell-cell communication, differentiation, morphogenesis, survival, defense etc. (Ganesan, 2016). Profiling of the secretome of *T. lanuginosus* SSBP (grown on corn cob medium) was done by shotgun proteomics, which revealed the presence of several industrially important enzymes. This revealed a total of 74 extracellular proteins, among them xylanase GH11, β-xylosidase GH43, β-glucosidase GH3, α-galactosidase GH36, trehalose hydrolase GH65, β-xylosidase,

α-galactosidase, α-arabinosidase and β-mannosidase belongs to glycoside hydrolases. In addition, lipase and amylase were also identified from *Thermomyces*, which are commercially available. Other industrially important enzymes *viz.*, glutaminase, fructose bisphosphate aldolase and cyanate hydratase, were also identified (Winger *et al.*, 2014).

The contamination of water and soil due to rapid industrialization and proliferative development of chemical and mining industries is a serious environmental challenge. The use of cyanide in mining industries for the extraction of precious metals has resulted in the deterioration of environmental quality. This is relevant in the South African context due to the high amount of cyanide used by the mining industries compared to the global mining sector (Mudder and Botz, 2004). The development of novel approaches or strategies towards remediation is therefore of extreme significance.

Several bacteria, fungi, and algae have been documented for their ability to bio-transform detrimental environmental wastes. Fungi are well known to play a crucial role in the decomposition of waste matter, and are critical constituents of the soil food web, providing sustenance for the other biota that live in the soil (Rhodes, 2013). In addition, fungi play an imperative role in industrial biotechnology as well as contributing the highest percentage of extracellular enzymes which includes, amylases, cellulases, hemicellulases, inulinases, lipases, pectinases and proteases which are utilized in the food and feed industry (Pel *et al.*, 2007). Fungi also play a key role in bioremediation and are regarded as the most sustainable green technology for the cleanup of hazardous wastes (Czaplicki *et al.*, 2016; Deshmukh *et al.*, 2016; Spina *et al.*, 2018).

The bioconversion can be classified into two main types: (i) use of whole-cells; and (ii) biocatalysts (Woodley *et al.*, 2013). However, microbial growth is impeded due to toxic environments which impacts on bio-remediation process (Sharma and Philip, 2014). In addition, microbial cells need to be metabolically active in extreme environments, such as wide ranges of pH, temperature, heavy metal tolerance, etc. In this regard, biocatalysts produced from extremophiles, especially, fungi could be an alternative, as they can thrive under harsh conditions (Neifar *et al.*, 2015). Similarly, the cyanate hydratase from *T. lanuginosus* SSBP expressed in *P. pastoris* demonstrated high catalytic efficiency along with a remarkable potential for the remediation of cyanurated industrial wastewater. It also displayed good thermostability and pH stability, as well as insensitivity towards heavy metals, which makes it a suitable candidate for

bioremediation. However, the drawback associated with free enzymes are: large consumption, difficulty in separation and recycling, which restricts their use at industrial scale (Das *et al.*, 2018).

Current approaches highlight the use of immobilization for the improvement of biocatalytic properties such as stability and reusability (Das *et al.*, 2018; Zdarta *et al.*, 2018). Apart from this, another important advantage associated with immobilized biocatalysts is their absence from the product stream (DiCosimo *et al.*, 2013). Various techniques have been employed for the immobilization of biocatalysts, *viz*. adsorption, covalent binding, cross-linking, encapsulation and entrapment (Sheldon, 2007). However, covalent binding of biocatalysts onto the support matrix is more appropriate for industrial applications (DiCosimo *et al.*, 2013; Barbosa *et al.*, 2015; Hosseini *et al.*, 2018). The type of matrices used for immobilization processes also play a critical role in catalysis (Zdarta *et al.*, 2018). The use of nanomaterials are gaining much attention due to their small size, high surface to volume ratio, aqueous dispersibility, thermal stability, and chemical inertness (Singh *et al.*, 2014; Patila *et al.*, 2016). Immobilized biocatalysts have also been justified, both from an economic and eco-friendly viewpoint, due to these requisite properties (Bilal *et al.*, 2017). This then prompted the use of nanomaterials for the immobilization of rTl-Cyn. In this regard, the immobilization of rTl-Cyn on m-MWCNTs displayed >94% of initial activity after ten cycles and also showed bi-functionality in removal of cyanate and heavy metals from industrial wastewater. A secondary approach of co-immobilization of multiple enzymes on nanomaterials was also a focus of this study. Hence, rTl-Cyn and rTl-CA were co-immobilized to reduce the dependence on bicarbonate and this resulted in the complete degradation of cyanate using 80% less bicarbonate, compared to rTl-Cyn alone. This suggested that the immobilized biocatalyst can be applied on a large-scale, especially for the bioremediation of cyanurated wastes.

The final goal of protein science is to reveal the 3D structure of proteins to predict the binding of ligands, and elucidate structure-function relationships. The development of protein structures has also led to rapid drug discovery with the aid of computational methods (Śledź and Caflisch, 2018). In addition to drug designing, the generation of accurate protein models will also assist in the creation of novel bio-catalysts via site-directed mutagenesis and this would provide deeper insight into their molecular mechanisms of action. Similarly, the generation of the Tl-Cyn crystal structure with the aid of site directed mutagenesis has enabled the creation of a novel

biocatalyst with ~1.3-fold enhanced catalytic activity and also provided information on their molecular mechanism of catalytic action.

6.1 Future prospects

Based on the above future research will focus on:

i) Enhance production of cyanase using dual promoter system *viz*., constitutive and inducible
ii) Expression of cyanase and carbonic anhydrase together in *P. pastoris*
iii) Site directed mutagenesis to enhance the substrate specificity as well as other properties
iv) Large-scale remediation of cyanurated waste
v) Use of cyanate generated ammonia as an alternative energy source for algal growth and concomitant production of biofuels

The biocatalysts and strategies developed in this study will provide a foundation for the widespread application of cyanases in sustainable bioremediation of cyanate-contaminated environments.

REFERENCES

Abdel-Naby, M.A. (1999) Immobilization of *Paenibacillus macerans* NRRL B-3186 cyclodextrin glucosyltransferase and properties of the immobilized enzyme. *Process Biochem.* **34**: 399–405.

Abia, A.A., Horsfall, M., and Didi, O. (2003) The use of chemically modified and unmodified cassava waste for the removal of Cd, Cu and Zn ions from aqueous solution. *Bioresour. Technol.* **90**: 345–348.

Abo-Hamad, A., Hayyan, M., AlSaadi, M.A.H., Mirghani, M.E.S., and Hashim, M.A. (2017) Functionalization of carbon nanotubes using eutectic mixtures: A promising route for enhanced aqueous dispersibility and electrochemical activity. *Chem. Eng. J.* **311**: 326–339.

Abollino, O., Aceto, M., Malandrino, M., Sarzanini, C., and Mentasti, E. (2003) Adsorption of heavy metals on Na-montmorillonite. Effect of pH and organic substances. *Water Res.* **37**: 1619–1627.

Acheampong, M.A., Meulepas, R.J.W., and Lens, P.N.L. (2010) Removal of heavymetals and cyanide from gold mine wastewater. *J. Chem. Technol. Biotechnol.* **85**: 590–613.

Adjei, M.D. and Ohta, Y. (2000) Purification and properties of a cyanide-degrading enzyme from *Burkholderia cepacia* C-3. *World J. Microbiol. Biotechnol.* **16**: 171–175.

Adrio, J.L. and Demain, A.L. (2014) Microbial enzymes: Tools for biotechnological processes. *Biomolecules* **4**: 117–139.

Ahmad, M., Hirz, M., and Pichler, H. (2014) Protein expression in *Pichia pastoris*: Recent achievements and perspectives for heterologous protein production. *Appl. Microbiol. Biotechnol.* **98**: 5301–5317.

Ahmed, S. and Husain, Q. (2012) Potential applications of enzymes immobilized on/in nano materials: A review. *Biotechnol. Adv.* **30**: 512–523.

Ajmal, M., Rao, R.A.K., Ahmad, R., Ahmad, J., and Rao, L.A.K. (2001) Removal and recovery of heavy metals from electroplating wastewater by using kyanite as an adsorbent. *J. Hazard. Mater.* **87**: 127–137.

Akcil, A. (2010) A New Global Approach of cyanide management: International cyanide management code for the manufacture, transport, and use of cyanide in the production of gold. *Miner. Process. Extr. Metall. Rev.* **31**: 135–149.

Akcil, A. (2003) Destruction of cyanide in gold mill effluents: Biological versus chemical treatments. *Biotechnol. Adv.* **21**: 501–511.

Akcil, A., Erust, C., Gahan, C.S., Ozgun, M., Sahin, M., and Tuncuk, A. (2015) Precious metal recovery from waste printed circuit boards using cyanide and non-cyanide lixiviants- A review. *Waste Manag.* **45**: 258–271.

Akcil, A., Karahan, A.G., Ciftci, H., and Sagdic, O. (2003) Biological treatment of cyanide by natural isolated bacteria (*Pseudomonas* sp.). *Miner. Eng.* **16**: 643–649.

Aldridge, S. (2013) Industry backs biocatalysis for greener manufacturing. *Nat. Biotechnol.* **31**: 95–96.

Alex, D., Mathew, A., and Sukumaran, R.K. (2014) Esterases immobilized on aminosilane modified magnetic nanoparticles as a catalyst for biotransformation reactions. *Bioresour. Technol.* **167**: 547–550.

Alkaya, E. and Demirer, G.N. (2014) Improving resource efficiency in surface coating/painting industry: Practical experiences from a small-sized enterprise. *Clean Technol. Environ. Policy* **16**: 1565–1575.

Alwis, L.K.H.K., Mucalo, M.R., Ingham, B., and Kappen, P. (2015) A combined SNIFTIRS and XANES study of electrically polarized copper electrodes in DMSO and DMF solutions of cyanate (NCO^-), thiocyanate (NCS^-) and selenocyanate ($NCSe^-$) ions. *J. Electrochem. Soc.* **162**: H434–H448.

Anderson, P.M. (1980) Purification and properties of the inducible enzyme cyanase. *Biochemistry* **19**: 2882–2888.

Anderson, P.M., Johnson, W. V., Endrizzi, J.A., Little, R.M., and Korte, J.J. (1987) Interaction of mono- and di-anions with cyanase: Evidence for apparent half-site binding. *Biochemistry* **26**: 3938–3943.

Anderson, P.M., Korte, J.J., Holcomb, T.A., Cho, Y.G., Son, C.M., and Sung, Y.C. (1994) Formation of intersubunit disulfide bonds and properties of the single histidine and cysteine residues in each subunit relative to the decameric structure of cyanase. *J. Biol. Chem.* **269**: 15036–15045.

Anderson, P.M., Sung, Y., and Fuchs, J.A. (1990) The cyanase operon and cyanate metabolism. *FEMS Microbiol. Lett.* **87**: 247–252.

Ansari, S.A. and Husain, Q. (2012) Lactose hydrolysis from milk/whey in batch and continuous processes by concanavalin a-celite 545 immobilized *Aspergillus oryzae* β-galactosidase. *Food Bioprod. Process.* **90**: 351–359.

Asamoah, R.K., Skinner, W., and Addai-Mensah, J. (2018) Alkaline cyanide leaching of refractory gold flotation concentrates and bio-oxidised products: The effect of process variables. *Hydrometallurgy*.

Asuri, P., Karajanagi, S.S., Sellitto, E., Kim, D.-Y., Kane, R.S., and Dordick, J.S. (2006) Water-soluble carbon nanotube-enzyme conjugates as functional biocatalytic formulations. *Biotechnol. Bioeng.* **95**: 804–811.

Baker, S.E., Thykaer, J., Adney, W.S., Brettin, T.S., Brockman, F.J., D'haeseleer, P., Martinez, A.D., Miller, R.M., Rokhsar, D.S., Schadt, C.W., Torok, T., Tuskan, G., Bennett, J., Berka, R.M., Briggs, S.P., Heitman, J., Taylor, J., Turgeon, B.G., and Himmel, M.E. (2008) Fungal genome sequencing and bioenergy. *Fungal Biol. Rev.* **22**: 1–5.

Barakat, M.A., Chen, Y.T., and Huang, C.P. (2004) Removal of toxic cyanide and Cu(II) ions from water by illuminated TiO_2 catalyst. *Appl. Catal. B Environ.* **53**: 13–20.

Barbosa, O., Ortiz, C., Berenguer-Murcia, Á., Torres, R., Rodrigues, R.C., and Fernandez-Lafuente, R. (2015) Strategies for the one-step immobilization-purification of enzymes as industrial biocatalysts. *Biotechnol. Adv.* **33**: 435–456.

Barclay, M., Day, J.C., Thompson, I.P., Knowles, C.J., and Bailey, M.J. (2002) Substrate-regulated cyanide hydratase (chy) gene expression in *Fusarium solani*: The potential of a transcription-based assay for monitoring the biotransformation of cyanide complexes. *Environ. Microbiol.* **4**: 183–189.

Barclay, M., Hart, A., Knowles, C.J., Meeussen, J.C.L., and Tett, V.A. (1998) Biodegradation of metal cyanides by mixed and pure cultures of fungi. *Enzyme Microb. Technol.* **22**: 223–231.

Barriuso, E. and Koskinen, W.C. (1996) Incorporating nonextractable atrazine residues into soil size fractions as a function of time. *Soil Sci. Soc. Am. J.* **60**: 150–157.

Bas, A.D., Ghali, E., and Choi, Y. (2017) A review on electrochemical dissolution and passivation of gold during cyanidation in presence of sulphides and oxides. *Hydrometallurgy* **172**: 30–44.

Baxter, J. and Cummings, S.P. (2006) The current and future applications of microorganism in the bioremediation of cyanide contamination. *Antonie van Leeuwenhoek, Int. J. Gen. Mol. Microbiol.* **90**: 1–17.

Benucci, I., Liburdi, K., Cacciotti, I., Lombardelli, C., Zappino, M., Nanni, F., and Esti, M. (2018) Chitosan/clay nanocomposite films as supports for enzyme immobilization: An innovative green approach for winemaking applications. *Food Hydrocoll.* **74**: 124–131.

Bhateria, R. and Dhaka, R. (2017) Impact of electroplating effluent on growth of *Triticum aestivum* and *Hordeum vulgare*. *Environ. Technol. Innov.* **8**: 389–398.

Bilal, M., Iqbal, H.M.N., Hu, H., Wang, W., and Zhang, X. (2017) Development of horseradish peroxidase-based cross-linked enzyme aggregates and their environmental exploitation for bioremediation purposes. *J. Environ. Manage.* **188**: 137–143.

Birijlall, N., Manimaran, A., Santhosh Kumar, K., Permaul, K., and Singh, S. (2011) High level expression of a recombinant xylanase by *Pichia pastoris* NC38 in a 5L fermenter and its efficiency in biobleaching of bagasse pulp. *Bioresour. Technol.* **102**: 9723–9729.

Bjarnholt, N., Neilson, E.H.J., Crocoll, C., Jørgensen, K., Motawia, M.S., Olsen, C.E., Dixon, D.P., Edwards, R., and Møller, B.L. (2018) Glutathione transferases catalyze recycling of auto-toxic cyanogenic glucosides in sorghum. *Plant J.* 1–17. Doi: 10.1111/tpj.13923.

Blumer, C. and Haas, D. (2000) Mechanism, regulation, and ecological role of bacterial cyanide biosynthesis. *Arch. Microbiol.* **173**: 170–177.

Bornscheuer, U.T., Huisman, G.W., Kazlauskas, R.J., Lutz, S., Moore, J.C., and Robins, K. (2012)

Engineering the third wave of biocatalysis. *Nature* **485**: 185–194.

Bose, P., Aparna Bose, M., and Kumar, S. (2002) Critical evaluation of treatment strategies involving adsorption and chelation for wastewater containing copper, zinc and cyanide. *Adv. Environ. Res.* **7**: 179–195.

Bruins, M.R., Kapil, S., and Oehme, F.W. (2000) Microbial resistance to metals in the environment. *Ecotoxicol. Environ. Saf.* **45**: 198–207.

Bryan, S.A., Pool, K.H., Bryan, S.L., Sell, R.L., and Thomas, L.M.P. (1994) Ferrocyanide safety project cyanide speciation studies FY Annual Report; PNL-8887; Pacific Northwest Laboratory: Richland, WA.

Butryn, A., Stoehr, G., Linke-Winnebeck, C., and Hopfner, K.P. (2015) Serendipitous crystallization and structure determination of cyanase (CynS) from *Serratia proteamaculans*. *Acta Crystallogr. Sect. FStructural Biol. Commun.* **71**: 471–476.

Campos, M.G., Pereira, P., and Roseiro, J.C. (2006) Packed-bed reactor for the integrated biodegradation of cyanide and formamide by immobilised *Fusarium oxysporum* CCMI 876 and *Methylobacterium* sp. RXM CCMI 908. *Enzyme Microb. Technol.* **38**: 848–854.

Can, K., Ozmen, M., and Ersoz, M. (2009) Immobilization of albumin on aminosilane modified superparamagnetic magnetite nanoparticles and its characterization. *Colloids Surfaces B Biointerfaces* **71**: 154–159.

Capasso, C. and Supuran, C.T. (2015) An overview of the alpha-, beta- and gamma-carbonic anhydrases from bacteria: Can bacterial carbonic anhydrases shed new light on evolution of bacteria? *J. Enzyme Inhib. Med. Chem.* **30**: 325–332.

Carepo, M.S.P., De Azevedo, J.S.N., Porto, J.I.R., Bentes-Sousa, A.R., Da Silva Batista, J., Da Silva, A.L.C., and Schneider, M.P.C. (2004) Identification of *Chromobacterium violaceum* genes with potential biotechnological application in environmental detoxification. *Genet. Mol. Res.* **3**: 181–194.

Chang, E.E., Hsing, H.J., Chiang, P.C., Chen, M.Y., and Shyng, J.Y. (2008) The chemical and biological characteristics of coke-oven wastewater by ozonation. *J. Hazard. Mater.* **156**: 560–567.

Chapatwala, K.D., Babu, G.R., Vijaya, O.K., Kumar, K.P., and Wolfram, J.H. (1998) Biodegradation of cyanides, cyanates and thiocyanates to ammonia and carbon dioxide by immobilized cells of *Pseudomonas putida*. *J. Ind. Microbiol. Biotechnol.* **20**: 28–33.

Chen, C.Y., Kao, C.M., and Chen, S.C. (2008) Application of *Klebsiella oxytoca* immobilized cells on the treatment of cyanide wastewater. *Chemosphere* **71**: 133–139.

Chen, F., Zhao, X., Liu, H., and Qu, J. (2014) Reaction of $Cu(CN)_3^{2-}$ with H_2O_2 in water under alkaline conditions: Cyanide oxidation, Cu^+/Cu^{2+} catalysis and H_2O_2 decomposition. *Appl. Catal. B Environ.* **158**–**159**: 85–90.

Chen, S., Lior, N., and Xiang, W. (2015) Coal gasification integration with solid oxide fuel cell and chemical looping combustion for high-efficiency power generation with inherent CO_2 capture. *Appl. Energy* **146**: 298–312.

Chergui, S., Yeddou, A.R., Chergui, A., Halet, F., Amaouche, H., Nadjemi, B., and Ould-Dris, A. (2015) Removal of cyanide in aqueous solution by oxidation with hydrogen peroxide in presence of activated alumina. *Toxicol. Environ. Chem.* **97**: 1289–1295.

Chiang, C.-J., Hsiau, L.-T., and Lee, W.-C. (1997) Immobilization of cell-associated enzymes by entrapment in polymethacrylamide beads. *Biotechnol. Tech.* **11**: 121–125.

Choi, J.M., Han, S.S., and Kim, H.S. (2015) Industrial applications of enzyme biocatalysis: Current status and future aspects. *Biotechnol. Adv.* **33**: 1443–1454.

Choi, P.H., Jo, J., Lin, Y.-C., Lin, M.-H., Chou, C.-Y., Dietrich, L.E.P., and Tong, L. (2016) A distinct holoenzyme organization for two-subunit pyruvate carboxylase. *Nat. Commun.* **7**: 12713.

Chronopoulou, L., Kamel, G., Sparago, C., Bordi, F., Lupi, S., Diociaiuti, M., and Palocci, C. (2011) Structure–activity relationships of *Candida rugosa* lipase immobilized on polylactic acid nanoparticles. *Soft Matter* **7**: 2653.

Clasen, B., Loro, V.L., Murussi, C.R., Tiecher, T.L., Moraes, B., and Zanella, R. (2018) Bioaccumulation and oxidative stress caused by pesticides in *Cyprinus carpio* reared in a rice-fish system. *Sci. Total Environ.* **626**: 737–743.

Cregg, J.M., Cereghino, J.L., Shi, J., and Higgins, D.R. (2000) Recombinant protein expression in *Pichia pastoris*. *Mol. Biotechnol.* **16**: 23–52.

Czaplicki, L.M., Cooper, E., Ferguson, P.L., Stapleton, H.M., Vilgalys, R., and Gunsch, C.K. (2016) A new perspective on sustainable soil remediation-Case study suggests novel fungal genera could facilitate in situ biodegradation of hazardous contaminants. *Remediat. J.* **26**: 59–72.

Daoud, F.B.O., Kaddour, S., and Sadoun, T. (2010) Adsorption of cellulase *Aspergillus niger* on a commercial activated carbon: Kinetics and equilibrium studies. *Colloids Surfaces B Biointerfaces* **75**: 93–99.

Das, R., Talat, M., Srivastava, O.N., and Kayastha, A.M. (2018) Covalent immobilization of peanut β-amylase for producing industrial nano-biocatalysts: A comparative study of kinetics, stability and reusability of the immobilized enzyme. *Food Chem.* **245**: 488–499.

Dash, R.R., Balomajumder, C., and Kumar, A. (2008) Treatment of metal cyanide bearing wastewater by simultaneous adsorption and biodegradation (SAB). *J. Hazard. Mater.* **152**: 387–396.

Dash, R.R., Gaur, A., and Balomajumder, C. (2009) Cyanide in industrial wastewaters and its removal: A review on biotreatment. *J. Hazard. Mater.* **163**: 1–11.

Datta, S., Christena, L.R., and Rajaram, Y.R.S. (2013) Enzyme immobilization: an overview on techniques and support materials. *3 Biotech* **3**: 1–9.

Dehnavi, S.M., Pazuki, G., and Vossoughi, M. (2015) PEGylated silica-enzyme nanoconjugates: a new frontier in large scale separation of α-amylase. *Sci. Rep.* **5**: 18221.

Demain, A.L. and Vaishnav, P. (2009) Production of recombinant proteins by microbes and higher organisms. *Biotechnol. Adv.* **27**: 297-.

Deshmukh, R., Khardenavis, A.A., and Purohit, H.J. (2016) Diverse metabolic capacities of fungi for bioremediation. *Indian J. Microbiol.* **56**: 247–264.

Dias, J.C.T., Rezende, R.P., and Linardi, V.R. (2001) Bioconversion of nitriles by *Candida guilliermondii* CCT 7207 cells immobilized in barium alginate. *Appl. Microbiol. Biotechnol.*

56: 757–761.

DiCosimo, R., McAuliffe, J., Poulose, A.J., and Bohlmann, G. (2013) Industrial use of immobilized enzymes. *Chem. Soc. Rev.* **42**: 6437.

Dixon, M., & Webb, E.C. (1979) Enzyme kinetics. In: Dixon M, Webb EC (eds) Enzymes academic press, New York.

Dong, Z., Hao, X., Pokhrel, D.S., Chen, X., Liu, X., Mchunu, N.P., Permaul, K., Singh, S., Niu, D., and Wang,Z. (2018) Molecular cloning and biochemical characterization of two novel oligo 1,6-glucosidases from *Bacillus mycoides* and *Thermomyces lanuginosus*. *Starch* **70**: 1700093.

Dubey, S.K. and Holmes, D.S. (1995) Biological cyanide destruction mediated by microorganisms. *World J. Microbiol. Biotechnol.* **11**: 257–265.

Dursun, A.Y. and Aksu, Z. (2000) Biodegradation kinetics of ferrous(II) cyanide complex ions by immobilized *Pseudomonas fluorescens* in a packed bed column reactor. *Process Biochem.* **35**: 615–622.

Dzombak, D.A., Ghosh, R.S., and Wong-Chong, G.M. (2006) Cyanide in water and soil: chemistry, risk and management. CRC Press.

Ebbs, S. (2004) Biological degradation of cyanide compounds. *Curr. Opin. Biotechnol.* **15**: 231–236.

Eisner, T., Eisner, M., and Deyrup, M. (1996) Millipede defense: use of detachable bristles to entangle ants. *Proc. Natl. Acad. Sci. U. S. A.* **93**: 10848–10851.

Elçin, Y.M. (1995) Encapsulation of urease enzyme in xanthan-alginate spheres. *Biomaterials* **16**: 1157–1161.

Elleuche, S. and Pöggeler, S. (2008) A cyanase is transcriptionally regulated by arginine and involved in cyanate decomposition in *Sordaria macrospora*. *Fungal Genet. Biol.* **45**: 1458–1469.

Elmore, M.H., McGary, K.L., Wisecaver, J.H., Slot, J.C., Geiser, D.M., Sink, S., O'Donnell, K., and Rokas, A. (2015) Clustering of two genes putatively involved in cyanate detoxification

evolved recently and independently in multiple fungal lineages. *Genome Biol. Evol.* **7**: 789–800.

Emsley, P. and Cowtan, K. (2004) Coot: Model-building tools for molecular graphics. *Acta Crystallogr. Sect. D Biol. Crystallogr.* **60**: 2126–2132.

Espie, G.S., Jalali, F., Tong, T., Zacal, N.J., and So, A.K. (2007) Involvement of the cynABDS operon and the CO_2-concentrating mechanism in the light-dependent transport and metabolism of cyanate by cyanobacteria. *J. Bacteriol.* **189**: 1013–1024.

Ezzi, M.I. and Lynch, J.M. (2005) Biodegradation of cyanide by *Trichoderma* spp. and *Fusarium* spp. *Enzyme Microb. Technol.* **36**: 849–854.

Ezzi, M.I. and Lynch, J.M. (2002) Cyanide catabolizing enzymes in *Trichoderma* spp. *Enzyme Microb. Technol.* **31**: 1042–1047.

Fan, Y., Su, F., Li, K., Ke, C., and Yan, Y. (2017) Carbon nanotube filled with magnetic iron oxide and modified with polyamidoamine dendrimers for immobilizing lipase toward application in biodiesel production. *Sci. Rep.* **7**: 45643.

Faridi, S., Bose, H., and Satyanarayana, T. (2017) Utility of immobilized recombinant carbonic anhydrase of *Bacillus halodurans* TSLV1 on the surface of modified iron magnetic nanoparticles in carbon sequestration. *Energy & Fuels* **31**: 3002–3009.

Feng, W. and Ji, P. (2011) Enzymes immobilized on carbon nanotubes. *Biotechnol. Adv.* **29**: 889–895.

Fernando, K., Tran, T., Laing, S., and Kim, M.J. (2002) The use of ion exchange resins for the treatment of cyanidation tailings Part 1- Process development of selective base metal elution. *Miner. Eng.* **15**: 1163–1171.

Flores-Maltos, A., Rodríguez-Durán, L. V, Renovato, J., Contreras, J.C., Rodríguez, R., and Aguilar, C.N. (2011) Catalytical properties of free and immobilized *Aspergillus niger* tannase. *Enzyme Res.* **2011**: 768183.

Fortes, C.C.S., Daniel-da-Silva, A.L., Xavier, A.M.R.B., and Tavares, A.P.M. (2017) Optimization of enzyme immobilization on functionalized magnetic nanoparticles for laccase

biocatalytic reactions. *Chem. Eng. Process. Process Intensif.* **117**: 1–8.

Freeman, W.H. (1985) Enzyme structure and mechanism. In, *New York.*, p. 475.

Ganesan, B. (2016). *Aspergillus* Secretome: An overview. In *New and Future Developments in Microbial Biotechnology and Bioengineering*. p. 69-77.

Geders, T.W., Gustafson, K., and Finzel, B.C. (2012) Use of differential scanning fluorimetry to optimize the purification and crystallization of PLP-dependent enzymes. *Acta Crystallogr. Sect. F Struct. Biol. Cryst. Commun.* **68**: 596–600.

Georgakilas, V., Tzitzios, V., Gournis, D., and Petridis, D. (2005) Attachment of magnetic nanoparticles on carbon nanotubes and their soluble derivatives. *Chem. Mater.* **17**: 1613–1617.

Ghosh, R.S., Dzombak, D.A., and Luthy, R.G. (1999) Equilibrium precipitation and dissolution of iron cyanide solids in water. *Environ. Eng. Sci.* **16**: 293–313.

Gianfreda, L. and Rao, M.A. (2004) Potential of extra cellular enzymes in remediation of polluted soils: A review. *Enzyme Microb. Technol.* **35**: 339–354.

Glanpracha, N. and Annachhatre, A.P. (2016) Anaerobic co-digestion of cyanide containing cassava pulp with pig manure. *Bioresour. Technol.* **214**: 112–121.

Gómez, L., Ramírez, H.L., Neira-Carrillo, A., and Villalonga, R. (2006) Polyelectrolyte complex formation mediated immobilization of chitosan-invertase neoglycoconjugate on pectin-coated chitin. *Bioprocess Biosyst. Eng.* **28**: 387–395.

Gramany, V., Khan, F.I., Govender, A., Bisetty, K., Singh, S., and Permaul, K. (2016) Cloning, expression, and molecular dynamics simulations of a xylosidase obtained from *Thermomyces lanuginosus*. *J. Biomol. Struct. Dyn.* **34**: 1681–1692.

Griffiths, A., Knorre, H., Gos, S., and Higgins, R. (1987) The detoxification of gold-mill tailings with hydrogen peroxide. *J. South African Inst. Min. Metall.* **87**: 279–283.

Guilloton, M.B., Korte, J.J., Lamblin, A.F., Fuchs, J.A., and Anderson, P.M. (1992) Carbonic anhydrase in *Escherichia coli*. *J. Biol. Chem.* **267**: 3731–3734.

Guo, L.J., Jin, H., Ge, Z.W., Lu, Y.J., and Cao, C.Q. (2015) Industrialization prospects for

hydrogen production by coal gasification in supercritical water and novel thermodynamic cycle power generation system with no pollution emission. *Sci. China Technol. Sci.* **58**: 1989–2002.

Hamel, J. (2011) A review of acute cyanide poisoning with a treatment update. *Crit. Care Nurse* **31**: 72–82.

Hansson, K.M., Åmand, L.E., Habermann, A., and Winter, F. (2003) Pyrolysis of poly-L-leucine under combustion-like conditions. *Fuel* **82**: 653–660.

Harano, Y., Suzuki, I., Maeda, S., Kaneko, T., Tabata, S., and Omata, T. (1997) Identification and nitrogen regulation of the cyanase gene from the cyanobacteria *Synechocystis* sp. PCC6803 and *Synechococcus* sp. PCC7942. *J. Bacteriol.* **179**: 5744–5750.

Hasslacher, M., Schall, M., Hayn, M., Bona, R., Rumbold, K., Lückl, J., Griengl, H., Kohlwein, S.D., and Schwab, H. (1997) High-level intracellular expression of hydroxynitrile lyase from the tropical rubber tree *Hevea brasiliensisin* microbial hosts. *Protein Expr. Purif.* **11**: 61–71.

Heidarizadeh, M., Doustkhah, E., Rostamnia, S., Rezaei, P.F., Harzevili, F.D., and Zeynizadeh, B. (2017) Dithiocarbamate to modify magnetic graphene oxide nanocomposite (Fe_3O_4-GO): A new strategy for covalent enzyme (lipase) immobilization to fabrication a new nanobiocatalyst for enzymatic hydrolysis of PNPD. *Int. J. Biol. Macromol.* **101**: 696–702.

Higgins, D.R. and Cregg, J.M. (1998) Introduction to *Pichia pastoris*. *Methods Mol. Biol.* **103**: 1–15.

Ho, S., Wang, Y., and Wan, C. (1990) Electrolytic decomposition of cyanide effluent with an electrochemical reactor packed with stainless steel fiber. *Water Res.* **24**: 1317–1321.

Hosseini, S.H., Hosseini, S.A., Zohreh, N., Yaghoubi, M., and Pourjavadi, A. (2018) Covalent immobilization of cellulase using magnetic poly(ionic liquid) support: Improvement of the enzyme activity and stability. *J. Agric. Food Chem.* **66**: 789–798.

Hosseinkhani, S., Szittner, R., Nemat-Gorgani, M., and Meighen, E.A. (2003) Adsorptive immobilization of bacterial luciferases on alkyl-substituted Sepharose 4B. *Enzyme Microb. Technol.* **32**: 186–193.

Huang, C.S., Sadre-Bazzaz, K., Shen, Y., Deng, B., Zhou, Z.H., and Tong, L. (2010) Crystal structure of the $\alpha_6\beta_6$ holoenzyme of propionyl-coenzyme A carboxylase. *Nature* **466**: 1001–1005.

Huang, L. and Cheng, Z.M. (2008) Immobilization of lipase on chemically modified bimodal ceramic foams for olive oil hydrolysis. *Chem. Eng. J.* **144**: 103–109.

Huertas, M.J., Sáez, L.P., Roldán, M.D., Luque-Almagro, V.M., Martínez-Luque, M., Blasco, R., Castillo, F., Moreno-Vivián, C., and García-García, I. (2010) Alkaline cyanide degradation by *Pseudomonas pseudoalcaligenes* CECT5344 in a batch reactor. Influence of pH. *J. Hazard. Mater.* **179**: 72–78.

Husain, Q. (2010) Beta galactosidases and their potential applications: A review. *Crit. Rev. Biotechnol.* **30**: 41–62.

Ihsanullah, Abbas, A., Al-Amer, A.M., Laoui, T., Al-Marri, M.J., Nasser, M.S., Khraisheh, M., and Atieh, M.A. (2016) Heavy metal removal from aqueous solution by advanced carbon nanotubes: Critical review of adsorption applications. *Sep. Purif. Technol.* **157**: 141–161.

Illanes, A., Cauerhff, A., Wilson, L., and Castro, G.R. (2012) Recent trends in biocatalysis engineering. *Bioresour. Technol.* **115**: 48–57.

Jagadish, K., Chandrashekar, B.N., Byrappa, K., and Rangappa, K.S. (2016) Simultaneous removal of dye and heavy metals in a single step reaction using PVA/MWCNT composites. *Anal. Methods* **8**: 2408–2412.

Jegannathan, K.R., Abang, S., Poncelet, D., Chan, E.S., and Ravindra, P. (2008) Production of biodiesel using immobilized lipase- A critical review. *Crit. Rev. Biotechnol.* **28**: 253–264.

Jeon, C., Park, J.Y., and Yoo, Y.J. (2001) Removal of heavy metals in plating wastewater using carboxylated alginic acid. *Korean J. Chem. Eng.* **18**: 955–960.

Jeremiáš, M., Pohořelý, M., Bode, P., Skoblia, S., Beňo, Z., and Svoboda, K. (2014) Ammonia yield from gasification of biomass and coal in fluidized bed reactor. *Fuel* **117**: 917–925.

Ji, Q., Tabassum, S., Hena, S., Silva, C.G., Yu, G., and Zhang, Z. (2016) A review on the coal gasification wastewater treatment technologies: Past, present and future outlook. *J. Clean.*

Prod. **126**: 38–55.

Jia, H., Zhu, G., and Wang, P. (2003) Catalytic behaviors of enzymes attached to nanoparticles: The effect of particle mobility. *Biotechnol. Bioeng.* **84**: 406–414.

Jiang, B., Shi, S., Song, L., Tan, L., Li, M., Liu, J., and Xue, L. (2016) Efficient treatment of phenolic wastewater with high salinity using a novel integrated system of magnetically immobilized cells coupling with electrodes. *Bioresour. Technol.* **218**: 108–114.

Jiang, B., Tan, L., Ning, S., and Shi, S. (2016) A novel integration system of magnetically immobilized cells and a pair of graphite plate-stainless iron mesh electrodes for the bioremediation of coking wastewater. *Bioresour. Technol.* **216**: 684–690.

Johnson, C.A. (2015) The fate of cyanide in leach wastes at gold mines: An environmental perspective. *Appl. Geochemistry* **57**: 194–205.

Johnson, P.A., Park, H.J., and Driscoll, A.J. (2011) Enzyme nanoparticle fabrication: magnetic nanoparticle synthesis and enzyme immobilization. *Methods Mol Biol* **679**: 183–191.

Johnson, W. V. and Anderson, P.M. (1987) Bicarbonate is a recycling substrate for cyanase. *J. Biol. Chem.* **262**: 9021–9025.

Jones, D.A. (1998) Why are so many food plants cyanogenic? *Phytochemistry* **47**: 155–162.

Kahraman, M.V., Bayramoğlu, G., Kayaman-Apohan, N., and Güngör, A. (2007) UV-curable methacrylated/fumaric acid modified epoxy as a potential support for enzyme immobilization. *React. Funct. Polym.* **67**: 97–103.

Kamennaya, N.A., Chernihovsky, M., and Post, A.F. (2008) The cyanate utilization capacity of marine unicellular cyanobacteria. *Limnol. Oceanogr.* **53**: 2485–2494.

Kamennaya, N.A. and Post, A.F. (2013) Distribution and expression of the cyanate acquisition potential among cyanobacterial populations in oligotrophic marine waters. *Limnol. Oceanogr.* **58**: 1959–1971.

Kao, C.M., Chen, K.F., Liu, J.K., Chou, S.M., and Chen, S.C. (2006) Enzymatic degradation of nitriles by *Klebsiella oxytoca*. *Appl. Microbiol. Biotechnol.* **71**: 228–233.

Kao, C.M., Liu, J.K., Lou, H.R., Lin, C.S., and Chen, S.C. (2003) Biotransformation of cyanide to

methane and ammonia by *Klebsiella oxytoca*. *Chemosphere* **50**: 1055–1061.

Kapoor, M. and Kuhad, R.C. (2007) Immobilization of xylanase from *Bacillus pumilus* MK001 and its application in production of xylo-oligosaccharides. *Appl. Biochem. Biotechnol.* **142**: 125–138.

Karigar, C.S. and Rao, S.S. (2011) Role of microbial enzymes in the bioremediation of pollutants: A review. *Enzyme Res.* doi: 10.4061/2011/805187.

Karimi, M., Chaudhury, I., Jianjun, C., Safari, M., Sadeghi, R., Habibi-Rezaei, M., and Kokini, J. (2014) Immobilization of endo-inulinase on non-porous amino functionalized silica nanoparticles. *J. Mol. Catal. B Enzym.* **104**: 48–55.

Ke, C., Li, X., Huang, S., Xu, L., and Yan, Y. (2014) Enhancing enzyme activity and enantioselectivity of *Burkholderia cepacia* lipase via immobilization on modified multi-walled carbon nanotubes. *RSC Adv.* **4**: 57810–57818.

Khalifah, R.G. (1971) The carbon dioxide hydration activity of carbonic anhydrase. *J. Biol. Chem.* **246**: 2561–2573.

Khan, A.A., Akhtar, S., and Husain, Q. (2006) Direct immobilization of polyphenol oxidases on Celite 545 from ammonium sulphate fractionated proteins of potato (*Solanum tuberosum*). *J. Mol. Catal. B Enzym.* **40**: 58–63.

Khan, F.I., Bisetty, K., Singh, S., Permaul, K., and Hassan, M.I. (2015) Chitinase from *Thermomyces lanuginosus* SSBP and its biotechnological applications. *Extremophiles* **19**: 1055–1066.

Khan, F.I., Govender, A., Permaul, K., Singh, S., and Bisetty, K. (2015) Thermostable chitinase II from *Thermomyces lanuginosus* SSBP: Cloning, structure prediction and molecular dynamics simulations. *J. Theor. Biol.* **374**: 107–114.

Khataee, A., Bayat, G., and Azamat, J. (2017) Separation of cyanide from an aqueous solution using armchair silicon carbide nanotubes: insights from molecular dynamics simulations. *RSC Adv.* **7**: 7502–7508.

Kibarer, G. and Akovali, G. (1996) Optimization studies on the features of an activated charcoal-

supported urease system. *Biomaterials* **17**: 1473–1479.

Kim, B.C., Lee, I., Kwon, S.J., Wee, Y., Kwon, K.Y., Jeon, C., An, H.J., Jung, H., Ha, S., Dordick, J.S., and Kim, J. (2017) Fabrication of enzyme-based coatings on intact multi-walled carbon nanotubes as highly effective electrodes in biofuel cells. *Sci. Rep.* **7**: 1–10.

Kim, Y.J., Qureshi, T.I., and Min, K.S. (2003) Application of advanced oxidation processes for the treatement of cyanide containing effluent. *Environ. Technol.* **24**: 1269–1276.

Kitis, M., Akcil, A., Karakaya, E., and Yigit, N.O. (2005) Destruction of cyanide by hydrogen peroxide in tailings slurries from low bearing sulphidic gold ores. *Miner. Eng.* **18**: 353–362.

Klein, M.P., Scheeren, C.W., Lorenzoni, A.S.G., Dupont, J., Frazzon, J., and Hertz, P.F. (2011) Ionic liquid-cellulose film for enzyme immobilization. *Process Biochem.* **46**: 1375–1379.

Knowles, C.J. and Bunch, A.W. (1986) Microbial cyanide metabolism. *Adv. Microb. Physiol.* **27**: 73–111.

Kookana, R.S., Baskaran, S., and Naidu, R. (1998) Pesticide fate and behaviour in Australian soils in relation to contamination and management of soil and water: A review. *Aust. J. Soil Res.* **36**: 715–764.

Koshiishi, I., Mamura, Y., and Imanari, T. (1997) Cyanate causes depletion of ascorbate in organisms. *Biochim. Biophys. Acta* **1336**: 566–574.

Kovalenko, G.A., Beklemishev, A.B., Perminova, L. V, Mamaev, A.L., Rudina, N.A., Moseenkov, S.I., and Kuznetsov, V.L. (2013) Immobilization of recombinant *E. coli* thermostable lipase by entrapment inside silica xerogel and nanocarbon-in-silica composites. *J. Mol. Catal. B, Enzym.* **98**: 78–86.

Kowalska, M., Bodzek, M., and Bohdziewicz, J. (1998) Biodegradation of phenols and cyanides using membranes with immobilized microorganisms. *Process Biochem.* **33**: 189–197.

Kozliak, E.I., Fuchs, J.A., and Guilloton, M.B. (1995) Role of bicarbonate/CO_2 in the inhibition of *Escherichia coli* growth by cyanate. *J. Bacteriol.* **177**: 3213–3219.

Kraus, L.M. and Kraus, A.P. (1998) The search for the uremic toxin: the case for carbamoylation of amino acids and proteins. *Wien Klin Wochenschr* **110**: 521–530.

Kumar, V., Marín-Navarro, J., and Shukla, P. (2016) Thermostable microbial xylanases for pulp and paper industries: trends, applications and further perspectives. *World J. Microbiol. Biotechnol.* **32**: 1–10.

Kumar, V.V. and Cabana, H. (2016) Towards high potential magnetic biocatalysts for on-demand elimination of pharmaceuticals. *Bioresour. Technol.* **200**: 81–89.

Kumari, A. and Kayastha, A.M. (2011) Immobilization of soybean (*Glycine max*) α-amylase onto chitosan and amberlite MB-150 beads: Optimization and characterization. *J. Mol. Catal. B Enzym.* **69**: 8–14.

Kunz, D.A. and Nagappan, O. (1989) Cyanase-mediated utilization of cyanate in *Pseudomonas fluorescens* NCIB 11764. *Appl. Environ. Microbiol.* **55**: 256–258.

Kwaansa-Ansah, E.E., Amenorfe, L.P., Armah, E.K., and Opoku, F. (2017) Human health risk assessment of cyanide levels in water and tuber crops from Kenyasi, a mining community in the brong ahafo region of Ghana. *Int. J. Food Contam.* **4**: (26 October 2017)-(26 October 2017).

Kwon, H.K., Woo, S.H., and Park, J.M. (2002) Degradation of tetracyanonickelate(II) by *Cryptococcus humicolus* MCN2. *FEMS Microbiol. Lett.* **214**: 211–216.

Lai, W. (2017) Pesticide use and health outcomes: Evidence from agricultural water pollution in China. *J. Environ. Econ. Manage.* **86**: 93–120.

Lal, M., James, C., Kennedy, J.F., and Puri, M. (2012) Immobilization of β-D- galactosidase from *Kluyveromyces lactis* on functionalized silicon dioxide nanoparticles: Characterization and lactose hydrolysis. *Int. J. Biol. Macromol.* **50**: 432–437.

Van Leeuwen, J., Badriyha, B., and Vaczi, S. (2003) Investigation into ozonation of coal coking processing wastewater for cyanide, thiocyanate and organic removal. *Ozone Sci. Eng.* **25**: 273–283.

Li, S., Yang, X., Yang, S., Zhu, M., and Wang, X. (2012) Technology prospecting on enzymes: application, marketing and engineering. *Comput. Struct. Biotechnol. J.* **2**: e201209017.

Li, X.T., Jiang, Z.Q., Li, L.T., Yang, S.Q., Feng, W.Y., Fan, J.Y., and Kusakabe, I. (2005)

Characterization of a cellulase-free, neutral xylanase from *Thermomyces lanuginosus* CBS 288.54 and its biobleaching effect on wheat straw pulp. *Bioresour. Technol.* **96**: 1370–1379.

Lin, M.L., Wang, Y.Y., and Wan, C.C. (1992) A comparative study of electrochemical reactor configurations for the decomposition of copper cyanide effuent. *J. Appl. Electrochem.* **22**: 1197–1200.

Liu, L., Yang, H., Shin, H.D., Chen, R.R., Li, J., Du, G., and Chen, J. (2013) How to achieve high-level expression of microbial enzymes: Strategies and perspectives. *Bioengineered* **4**: 212–223.

Liu, Y.H., Chung, Y.C., and Xiong, Y. (2001) Purification and characterization of a dimethoate-degrading enzyme of *Aspergillus niger* ZHY256, isolated from sewage. *Appl. Environ. Microbiol.* **67**: 3746–3749.

Lowry, O.H., Rosebrough, N.J., Farr, A.L., and Randall, R.J. (1951) Protein measurement with the folin phenol reagent. *J. Biol. Chem.* **193**: 265–275.

Luque-Almagro, V.M., Blasco, R., Martínez-Luque, M., Moreno-Vivián, C., Castillo, F., and Roldán, M.D. (2011) Bacterial cyanide degradation is under review: *Pseudomonas pseudoalcaligenes* CECT5344, a case of an alkaliphilic cyanotroph. *Biochem. Soc. Trans.* **39**: 269–74.

Luque-Almagro, V.M., Huertas, M.J., Sáez, L.P., Luque-Romero, M.M., Moreno-Vivián, C., Castillo, F., Roldán, M.D., and Blasco, R. (2008) Characterization of the *Pseudomonas pseudoalcaligenes* CECT5344 cyanase, an enzyme that is not essential for cyanide assimilation. *Appl. Environ. Microbiol.* **74**: 6280–6288.

Luque-Almagro, V.M., Moreno-Vivian, C., and Roldan, M.D. (2016) Biodegradation of cyanide wastes from mining and jewellery industries. *Curr. Opin. Biotechnol.* **38**: 9–13.

Luthy, R.G. (1981) Treatment of coal coking and coal-gasification wastewaters. *J. Water Pollut. Control Fed.* **53**: 325–339.

Luthy, R.G. and Bruce, S.G. (1979) Kinetics of reaction of cyanide and reduced sulfur species in aqueous solution. *Environ. Sci. Technol.* **13**: 1481–1487.

Anderson, P.M., and Little, A.R. (1986) Kinetic properties of cyanase. *Biochemistry* **25**: 1621–1626.

Ma, M., Zhang, Y., Yu, W., Shen, H., Zhang, H., and Gu, N. (2003) Preparation and characterization of magnetite nanoparticles coated by amino silane. *Colloids Surf. A Physicochem. Eng. Asp.* **212**: 219–226.

Machingura, M., Salomon, E., Jez, J.M., and Ebbs, S.D. (2016) The β-cyanoalanine synthase pathway: Beyond cyanide detoxification. *Plant Cell Environ.* **39**: 2329–2341.

Maderbocus, R., Fields, B.L., Hamilton, K., Luo, S., Tran, T.H., Dietrich, L.E.P., and Tong, L. (2017) Crystal structure of a *Pseudomonas* malonate decarboxylase holoenzyme hetero-tetramer. *Nat. Commun.* **8**: 1–12.

Madhavan, A., Sindhu, R., Binod, P., Sukumaran, R.K., and Pandey, A. (2017) Strategies for design of improved biocatalysts for industrial applications. *Bioresour. Technol.* **245**: 1304–1313.

Magnan, E., Catarino, I., Paolucci-Jeanjean, D., Preziosi-Belloy, L., and Belleville, M.P. (2004) Immobilization of lipase on a ceramic membrane: Activity and stability. *J. Memb. Sci.* **241**: 161–166.

Malhotra, S., Pandit, M., Kapoor, J.C., and Tyagi, D.K. (2005) Photo-oxidation of cyanide in aqueous solution by the UV/H_2O_2 process. *J. Chem. Technol. Biotechnol.* **80**: 13–19.

Man, Y., Han, Y., Hu, Y., Yang, S., and Yang, S. (2016) Synthetic natural gas as an alternative to coal for power generation in China: Life cycle analysis of haze pollution, greenhouse gas emission, and resource consumption. *J. Clean. Prod.* **172**: 2503–2512.

Martínková, L. and Chmátal, M. (2016) The integration of cyanide hydratase and tyrosinase catalysts enables effective degradation of cyanide and phenol in coking wastewaters. *Water Res.* **102**: 90–95.

Mateo, C., Palomo, J.M., Fernandez-lorente, G., Guisan, J.M., and Fernandez-lafuente, R. (2007) Improvement of enzyme activity, stability and selectivity via immobilization techniques. *Enzyme Microb. Technol.* **40**: 1451–1463.

Matto, M. and Husain, Q. (2009) Calcium alginate-starch hybrid support for both surface immobilization and entrapment of bitter gourd (*Momordica charantia*) peroxidase. *J. Mol. Catal. B Enzym.* **57**: 164–170.

McCoy, A.J., Grosse-Kunstleve, R.W., Adams, P.D., Winn, M.D., Storoni, L.C., and Read, R.J. (2007) Phaser crystallographic software. *J. Appl. Crystallogr.* **40**: 658–674.

Mchunu, N.P., Permaul, K., Rahman, A.Y.A., Saito, J.A., Singh, S., and Alam, M. (2013) Xylanase superproducer: Genome sequence of a compost-loving thermophilic fungus, *Thermomyces lanuginosus* SSBP. *Genome Announc.* **1**: 4–5.

Merrikhpour, H. and Jalali, M. (2013) Comparative and competitive adsorption of cadmium, copper, nickel, and lead ions by Iranian natural zeolite. *Clean Technol. Environ. Policy* **15**: 303–316.

Mirizadeh, S., Yaghmaei, S., and Ghobadi Nejad, Z. (2014) Biodegradation of cyanide by a new isolated strain under alkaline conditions and optimization by response surface methodology (RSM). *J. Environ. Heal. Sci. Eng.* **12**: 85.

Modugno, G., Ksar, F., Battigelli, A., Russier, J., Soula, B., Lonchambon, P., da Silva, E.E., Ménard-Moyon, C., Soula, B., Galibert, A.M., Pinault, M., Flahaut, E., Mayne-L'Hermite, M., and Bianco, A. (2016) A comparative study on the enzymatic biodegradability of covalently functionalized double- and multi-walled carbon nanotubes. *Carbon.* **100**: 367–374.

Mohamad, N.R., Marzuki, N.H.C., Buang, N.A., Huyop, F., and Wahab, R.A. (2015) An overview of technologies for immobilization of enzymes and surface analysis techniques for immobilized enzymes. *Biotechnol. Biotechnol. Equip.* **29**: 205–220.

Mojsov, K. (2011) Application of enzymes in the textile industry: A review. *Eng. Ecol. Mater. Process. Ind.* **1**: 230–239.

Monteagudo, J.M., Rodriguez, L., and Villasenor, J. (2004) Advanced oxidation processes for destruction of cyanide from thermoelectric power station waste waters. *J. Chem. Technol. Biotechnol.* **79**: 117–125.

Montero, R., Guevara, A., and la Torre, E. (2012) Recovery of gold, silver, copper and niobium

from printed circuit boards using leaching column technique. *J. Earth Sci. Eng.* **2**: 6.

Morimoto, T., Yanal, H., and Nagao, M. (1976) Infrared spectra of ammonia adsorbed on zinc oxide. *J. Phys. Chem.* **80**: 471–475.

Morrow, K.J. (2007) Improving protein production processes. *Genet. Eng. Biotechnol. News* **27**: 50–54.

Mosher, J.B. and Figueroa, L. (1996) Biological oxidation of cyanide: A viable treatment option for the minerals processing industry. *Miner. Eng.* **9**: 573–581.

Mubarak, N.M., Wong, J.R., Tan, K.W., Sahu, J.N., Abdullah, E.C., Jayakumar, N.S., and Ganesan, P. (2014) Immobilization of cellulase enzyme on functionalized multiwall carbon nanotubes. *J. Mol. Catal. B Enzym.* **107**: 124–131.

Mudder, T., Botz, M.M., and Smith, A. (1991) Chemistry and treatment of cyanidation wastes. *Min. J. Books Ltd. London.* 373.

Mudder, T.I. and Botz, M.M. (2004) Cyanide and society: A critical review. *Eur. J. Miner. Process. Environ. Prot.* **4**: 62–74.

Mudliar, R., Umare, S.S., Ramteke, D.S., and Wate, S.R. (2009) Energy efficient-advanced oxidation process for treatment of cyanide containing automobile industry wastewater. *J. Hazard. Mater.* **164**: 1474–1479.

Murshudov, G.N., Vagin, A.A., and Dodson, E.J. (1997) Refinement of macromolecular structures by the maximum-likelihood method. *Acta Crystallogr. Sect. D Biol. Crystallogr.* **53**: 240–255.

Naim, R., Kisay, L., Park, J., Qaisar, M., Zulfiqar, A.B., Noshin, M., and Jamil, K. (2010) Precipitation chelation of cyanide complexes in electroplating industry wastewater. *Int. J. Environ. Res.* **4**: 735–740.

Nair, I.C. and Jayachandran, K. (2017) Enzymes for bioremediation and biocontrol. In: Sugathan S., Pradeep N., Abdulhameed S. (eds) *Bioresources and Bioprocess in Biotechnology*. Springer, Singapore., pp.75–97.

Nallapan Maniyam, M., Sjahrir, F., Latif Ibrahim, A., and Cass, A.E.G. (2015) Enzymatic cyanide

degradation by cell-free extract of *Rhodococcus* UKMP−5M. *J. Environ. Sci. Heal. Part A* **50**: 357–364.

Naveen, D., Majumder, C.B., Mondal, P., and Shubha, D. (2011) Biological treatment of cyanide containing wastewater. *Res. J. Chem. Sci.* **1**: 15–21.

Nawaz, K., Hussain, K., Choudary, N., Majeed, A., Ilyas, U., Ghani, A., Lin, F., Ali, K., Afghan, S., Raza, G., and Lashari, M.I. (2011) Eco-friendly role of biodegradation against agricultural pesticides hazards. *African J. Microbiol. Res.* **5**: 177–183.

Neifar, M., Maktouf, S., Ghorbel, R.E., Jaouani, A., and Cherif, A. (2015) Extremophiles as source of novel bioactive compounds with industrial potential. In, *Biotechnology of Bioactive Compounds: Sources and Applications*., pp. 245–267.

Nolan, L.M., Harnedy, P.A., Turner, P., Hearne, A.B., and O'Reilly, C. (2003) The cyanide hydratase enzyme of *Fusarium lateritium* also has nitrilase activity. *FEMS Microbiol. Lett.* **221**: 161–165.

Nwokoro, O. and Dibua, M.E.U. (2014) Degradation of soil cyanide by single and mixed cultures of *Pseudomonas stutzeri* and *Bacillus subtilis*. *Arch. Ind. Hyg. Toxicol.* **65**: 113–119.

O'Reilly, C. and Turner, P.D. (2003) The nitrilase family of CN hydrolysing enzymes- A comparative study. *J. Appl. Microbiol.* **95**: 1161–1174.

Ögütveren, Ü.B., Törü, E., and Koparal, S. (1999) Removal of cyanide by anodic oxidation for wastewater treatment. *Water Res.* **33**: 1851–1856.

Ohlen, M., Herfurth, A.M., and Wittstock, U. (2017) Herbivore adaptations to plant cyanide defenses. In, *Herbivores*., pp. 29–57.

Oliveira, S.F., Bisker, G., Bakh, N.A., Gibbs, S.L., Landry, M.P., and Strano, M.S. (2015) Protein functionalized carbon nanomaterials for biomedical applications. *Carbon.* **95**: 767–779.

Orescanin, V., Durgo, K., Mikelic, I.L., Halkijevic, I., and Kuspilic, M. (2018) Toxicity assessment of untreated/treated electroplating sludge using human and plant bioassay. *J. Environ. Sci. Health A Tox. Hazard Subst. Environ. Eng.* **30**: 1–6.

Orescanin, V., Mikulic, N., Mikelic, I.L., Posedi, M., Kampic, S., and Medunic, G. (2009) The

bulk composition and leaching properties of electroplating sludge prior/following the solidification/stabilization by calcium oxide. *J. Environ. Sci. Health A Tox. Hazard Subst. Environ. Eng.* **44**: 1282–1288.

Otwinowski, Z., Minor, W., and Mode, O. (1997) Processing of X-ray diffraction data collected in oscillation mode. *Methods Enzymol.* **276**: 307–326.

Outer, M. and Protein, M. (1987) Isolation and characterization of *Escherichia coli* mutants lacking inducible cyanase. *J. Gen. Microbiol.* **133**: 645–653.

Pahujani, S., Kanwar, S.S., Chauhan, G., and Gupta, R. (2008) Glutaraldehyde activation of polymer nylon-6 for lipase immobilization: Enzyme characteristics and stability. *Bioresour. Technol.* **99**: 2566–2570.

Pak, D. and Chang, W. (1997) Oxidation of aqueous cyanide solution using hydrogen peroxide in the presence of heterogeneous catalyst. *Environ. Technol.* **18**: 557–561.

Pal, P. and Kumar, R. (2013) Treatment of coke wastewater: A critical review for developing sustainable management strategies. *Sep. Purif. Rev.* **43**: 89–123.

Palatinszky, M., Herbold, C., Jehmlich, N., Pogoda, M., Han, P., von Bergen, M., Lagkouvardos, I., Karst, S.M., Galushko, A., Koch, H., Berry, D., Daims, H., and Wagner, M. (2015) Cyanate as an energy source for nitrifiers. *Nature* **524**: 105–8.

Papadimitriou, C.A., Dabou, X., Samaras, P., and Sakellaropoulos, G.P. (2006) Coke oven wastewater treatment by two activated sludge systems. *Glob. NEST* **8**: 16–22.

Papadimitriou, C.A., Samaras, P., and Sakellaropoulos, G.P. (2009) Comparative study of phenol and cyanide containing wastewater in CSTR and SBR activated sludge reactors. *Bioresour. Technol.* **100**: 31–37.

Parashar, D. and Satyanarayana, T. (2016) A chimeric α-amylase engineered from *Bacillus acidicola* and *Geobacillus thermoleovorans* with improved thermostability and catalytic efficiency. *J. Ind. Microbiol. Biotechnol.* **43**: 473–484.

Parga, J.R., Shukla, S.S., and Carrillo-Pedroza, F.R. (2003) Destruction of cyanide waste solutions using chlorine dioxide, ozone and titania sol. *Waste Manag.* **23**: 183–191.

Parker, W.L., Rathnum, M.L., Johnson, J.H., Wells, J.S., Principe, P.A., and Sykes, R.B. (1988) Aerocyanidin, a new antibiotic produced by *Chromobacterium violaceum*. *J. Antibiot.* **41**: 454–460.

Paschka, M.G., Ghosh, R.S., and Dzombak, D.A. (1999) Potential water-quality effects from iron cyanide anticaking agents in road salt. *Water Environ. Res.* **71**: 1235–1239.

Patil, Y.B. (2012) Development of a low-cost industrial waste treatment technology for resource conservation – An urban case study with gold-cyanide emanated from SMEs. *Procedia - Soc. Behav. Sci.* **37**: 379–388.

Patil, Y.B. and Paknikar, K.M. (2000) Development of a process for biodetoxification of metal cyanides from waste waters. *Process Biochem.* **35**: 1139–1151.

Patil, Y.B. and Paknikar, K.M. (1999) Removal and recovery of metal cyanides using a combination of biosorption and biodegradation processes. *Biotechnol. Lett.* **21**: 913–919.

Patila, M., Kouloumpis, A., Gournis, D., Rudolf, P., and Stamatis, H. (2016) Laccase-functionalized graphene oxide assemblies as efficient nanobiocatalysts for oxidation reactions. *Sensors* **16**: 1–14.

Pavlidis, I. V., Tsoufis, T., Enotiadis, A., Gournis, D., and Stamatis, H. (2010) Functionalized multi-wall carbon nanotubes for lipase immobilization. *Adv. Eng. Mater.* **12**: 179–183.

Pavlidis, I. V, Vorhaben, T., Tsoufis, T., Rudolf, P., Bornscheuer, U.T., Gournis, D., and Stamatis, H. (2012) Development of effective nanobiocatalytic systems through the immobilization of hydrolases on functionalized carbon-based nanomaterials. *Bioresour. Technol.* **115**: 164–171.

Pel, H.J., De Winde, J.H., Archer, D.B., Dyer, P.S., Hofmann, G., Schaap, P.J., Turner, G., de Vries, R.P., Albang, R., Albermann, K., Andersen, M.R., Bendtsen, J.D., Benen, J.A., van den Berg, M., Breestraat, S., Caddick, M.X., Contreras, R., Cornell, M., Coutinho, P.M., Danchin, E.G., Debets, A.J., Dekker, P., van Dijck, P.W., van Dijk, A., Dijkhuizen, L., Driessen, A.J., d'Enfert, C., Geysens, S., Goosen, C., Groot, G.S., de Groot, P.W., Guillemette, T., Henrissat, B., Herweijer, M., van den Hombergh, J.P., van den Hondel, C.A., van der Heijden, R.T., van der Kaaij, R.M., Klis, F.M., Kools, H.J., Kubicek, C.P., van Kuyk, P.A., Lauber, J., Lu, X., van der Maarel, M.J., Meulenberg, R., Menke, H., Mortimer, M.A.,

Nielsen, J., Oliver, S.G., Olsthoorn, M., Pal, K., van Peij, N.N., Ram, A.F., Rinas, U., Roubos, J.A., Sagt, C.M., Schmoll, M., Sun, J., Ussery, D., Varga, J., Vervecken, W., van de Vondervoort, P.J., Wedler, H., Wösten, H.A., Zeng, A.P., van Ooyen, A.J., Visser, J., and Stam, H. (2007) Genome sequencing and analysis of the versatile cell factory *Aspergillus niger* CBS 513.88. *Nat. Biotechnol.* **25**: 221–231.

Peral, J. and Domenech, X. (1992) Photocatalytic cyanide oxidation from aqueous copper cyanide solutions over TiO_2 and ZnO. *J. Chem. Technol. Biotechnol.* **53**: 93–96.

Pereira, L., Dias, P., Soares, O.S.G.P., Ramalho, P.S.F., Pereira, M.F.R., and Alves, M.M. (2017) Synthesis, characterization and application of magnetic carbon materials as electron shuttles for the biological and chemical reduction of the azo dye acid orange 10. *Appl. Catal. B Environ.* **212**: 175–184.

Peuke, A.D. and Rennenberg, H. (2005) Phytoremediation. *EMBO Rep.* **6**: 497–501.

Piccolino, M. (2000) Biological machines: From mills to molecules. *Nat. Rev. Mol. Cell Biol.* **1**: 149–153.

Pičmanová, M., Neilson, E.H., Motawia, M.S., Olsen, C.E., Agerbirk, N., Gray, C.J., Flitsch, S., Meier, S., Silvestro, D., Jørgensen, K., Sánchez-Pérez, R., Møller, B.L., and Bjarnholt, N. (2015) A recycling pathway for cyanogenic glycosides evidenced by the comparative metabolic profiling in three cyanogenic plant species. *Biochem. J.* **469**: 375–389.

Pogorilyi, R.P., Siletskaya, E.Y., Goncharik, V.P., Kozhara, L.I., and Zub, Y.L. (2007) Immobilization of urease on the silica gel surface by sol-gel method. *Russ. J. Appl. Chem.* **80**: 330–334.

Prabu, V. (2015) Integration of in-situ CO_2-oxy coal gasification with advanced power generating systems performing in a chemical looping approach of clean combustion. *Appl. Energy* **140**: 1–13.

Priestley, M., Le Breton, M., Bannan, T.J., Leather, K.E., Bacak, A., Reyes-Villegas, E., Vocht, F.D., Shallcross, B.M.A., Brazier, T., Khan, M.A., Allan, J., Shallcross, D.E., Coe, H., and Percival, C.J. (2018) Observations of isocyanate, amide, nitrate and nitro compounds from an anthropogenic biomass burning event using a ToF-CIMS. *J. Geophys. Res. Atmos.* Doi:

10.1002/2017JD027316.

Puchart, V., Katapodis, P., Biely, P., Kremnický, L., Christakopoulos, P., Vršanská, M., Kekos, D., Basil J.M., and Bhat, M.K. (1999) Production of xylanases, mannanases, and pectinases by the thermophilic fungus *Thermomyces lanuginosus*. *Enzyme Microb. Technol.* **24**: 355–361.

Pueyo, N., Miguel, N., Ovelleiro, J.L., and Ormad, M.P. (2016) Limitations of the removal of cyanide from coking wastewater by ozonation and by the hydrogen peroxideozone process. *Water, Air, Soil Pollut.* **74**: 482–490.

Punt, P.J., Van Biezen, N., Conesa, A., Albers, A., Mangnus, J., and Van Den Hondel, C. (2002) Filamentous fungi as cell factories for heterologous protein production. *Trends Biotechnol.* **20**: 200–206.

Purcarea, C., Ahuja, A., Lu, T., Kovari, L., Guy, H.I., and Evans, D.R. (2003) *Aquifex aeolicus* aspartate transcarbamoylase, an enzyme specialized for the efficient utilization of unstable carbamoyl phosphate at elevated temperature. *J. Biol. Chem.* **278**: 52924–52934.

Puri, M., Barrow, C.J., and Verma, M.L. (2013) Enzyme immobilization on nanomaterials for biofuel production. *Trends Biotechnol.* **31**: 215–216.

Puri, M., Kaur, H., and Kennedy, J.F. (2005) Covalent immobilization of naringinase for the transformation of a flavonoid. *J. Chem. Technol. Biotechnol.* **1165**: 1160–1165.

Qian, D., Jiang, L., Lu, L., Wei, C., and Li, Y. (2011) Biochemical and structural properties of cyanases from *Arabidopsis thaliana* and *Oryza sativa*. *PLoS One* **6**: 1–10.

Qian, M., Eaton, J.W., and Wolff, S.P. (1997) Cyanate-mediated inhibition of neutrophil myeloperoxidase activity. *Biochem. J.* **326**: 159–66.

Rajniak, J., Barco, B., Clay, N.K., and Sattely, E.S. (2015) A new cyanogenic metabolite in *Arabidopsis* required for inducible pathogen defence. *Nature* **525**: 376–379.

Ramani, K., Karthikeyan, S., Boopathy, R., Kennedy, L.J., Mandal, A.B., and Sekaran, G. (2012) Surface functionalized mesoporous activated carbon for the immobilization of acidic lipase and their application to hydrolysis of waste cooked oil: Isotherm and kinetic studies. *Process*

Biochem. **47**: 435–445.

Ran, N., Zhao, L., Chen, Z., and Tao, J. (2008) Recent applications of biocatalysis in developing green chemistry for chemical synthesis at the industrial scale. *Green Chem.* **10**: 361–372.

Rani, S., Das, M.L.M., and Satyanarayana, S. (2000) Preparation and characterization of amyloglucosidase adsorbed on activated charcoal. *J. Mol. Catal. B Enzym.* **10**: 471–476.

Ranjan, B. and Satyanarayana, T. (2016) Recombinant HAP phytase of the thermophilic mold *Sporotrichum thermophile*: Expression of the codon-optimized phytase gene in *Pichia pastoris* and applications. *Mol. Biotechnol.* **58**: 137–147.

Ranjan, B., Singh, B., and Satyanarayana, T. (2015) Characteristics of recombinant phytase (rSt-Phy) of the thermophilic mold *Sporotrichum thermophile* and its applicability in dephytinizing foods. *Appl. Biochem. Biotechnol.* **177**: 1753–1766.

Raybuck, S.A. (1992) Microbes and microbial enzymes for cyanide degradation. *Biodegradation* **3**: 3–18.

Rezende, R.P., Dias, J.C.T., Ferraz, V., and Linardi, V.R. (2000) Metabolism of benzonitrile by *Cryptococcus* sp. UFMG-Y28. *J. Basic Microbiol.* **40**: 389–392.

Rhodes, C.J. (2013) Feeding and healing the world: Through regenerative agriculture and permaculture. *Sci. Prog.* **95**: 345–446.

Rinágelová, A., Kaplan, O., Veselá, A.B., Chmátal, M., Křenková, A., Plíhal, O., Pasquarelli, F., Cantarella, M., and Martínková, L. (2014) Cyanide hydratase from *Aspergillus niger* K10: Overproduction in *Escherichia coli*, purification, characterization and use in continuous cyanide degradation. *Process Biochem.* **49**: 445–450.

Rocap, G., Larimer, F.W., Lamerdin, J., Malfatti, S., Chain, P., Ahlgren, N.A., Arellano, A., Coleman, M., Hauser, L., Hess, W.R., Johnson, Z.I., Land, M., Lindell, D., Post, A.F., Regala, W., Shah, M., Shaw, S.L., Steglich, C., Sullivan, M.B., Ting, C.S., Tolonen, A., Webb, E.A., Zinser, E.R., and Chisholm, S.W. (2003) Genome divergence in two *Prochlorococcus* ecotypes reflects oceanic niche differentiation. *Nature* **424**: 1042–1047.

Romanos, M. (1995) Advances in the use of *Pichia pastoris* for high-level gene expression. *Curr.*

Opin. Biotechnol. **6**: 527–533.

Romanos, M.A., Scorer, C.A., and Clare, J.J. (1992) Foreign gene expression in yeast: A review. *Yeast* **8**: 423–488.

Romaskevic, T., Viskantiene, E., Budriene, S., Ramanaviciene, A., and Dienys, G. (2010) Immobilization of maltogenase onto polyurethane microparticles from poly(vinyl alcohol) and hexamethylene diisocyanate. *J. Mol. Catal. B Enzym.* **64**: 172–176.

Rosa, C.C., Cruz, H.J., Vidal, M., and Oliva, A.G. (2002) Optical biosensor based on nitrite reductase immobilised in controlled pore glass. *Biosens. Bioelectron.* **17**: 45–52.

Ryu, B.G., Kim, J., Han, J.I., and Yang, J.W. (2017) Feasibility of using a microalgal-bacterial consortium for treatment of toxic coke wastewater with concomitant production of microbial lipids. *Bioresour. Technol.* **225**: 58–66.

Safder, I., Khan, S., Islam, I., and Kazim, M. (2018) *Pichia pastoris* expression system: A potential candidate to express protein in industrial and biopharmaceutical domains. *Biomed. Lett.* **4**: 1–13.

Sahney, R., Puri, B.K., and Anand, S. (2005) Enzyme coated glass pH-electrode: Its fabrication and applications in the determination of urea in blood samples. *Anal. Chim. Acta* **542**: 157–161.

Senanayake, G. (2008) A review of effects of silver, lead, sulfide and carbonaceous matter on gold cyanidation and mechanistic interpretation. *Hydrometallurgy* **90**: 46–73.

Senthilnathan, G.V.U. and Rajam, S. (2014) Cadmium removal from aqueous solutions using hybrid eucalyptus wood based activated carbon: Adsorption batch studies. *Clean Technol. Environ. Policy* **16**: 195–200.

Serralha, F.N., Lopes, J.M., Lemos, F., Prazeres, D.M.F., Aires-Barros, M.R., Cabral, J.M.S., and Ramôa Ribeiro, F. (1998) Zeolites as supports for an enzymatic alcoholysis reaction. *J. Mol. Catal. - B Enzym.* **4**: 303–311.

Sharma, N.K. and Philip, L. (2014) Effect of cyanide on phenolics and aromatic hydrocarbons biodegradation under anaerobic and anoxic conditions. *Chem. Eng. J.* **256**: 255–267.

Sharma, N.K., Philip, L., and Murty Bhallamudi, S. (2012) Aerobic degradation of phenolics and aromatic hydrocarbons in presence of cyanide. *Bioresour. Technol.* **121**: 263–273.

Sharma, V.K., Rivera, W., Smith, J.O., and Brien, B.O. (1998) Ferrate (VI) Oxidation of aqueous cyanide. *Environ. Sci. Technol.* **32**: 2608–2613.

Sheldon, R.A. (2007) Enzyme immobilization: The quest for optimum performance. *Adv. Synth. Catal.* **349**: 1289–1307.

Sheldon, R.A. and Woodley, J.M. (2017) Role of biocatalysis in sustainable chemistry. *Chem. Rev.* **118**: 801-838.

Shen, Q., Yang, R., Hua, X., Ye, F., Zhang, W., and Zhao, W. (2011) Gelatin-templated biomimetic calcification for β-galactosidase immobilization. *Process Biochem.* **46**: 1565–1571.

Shim, M., Kam, N.W.S., Chen, R.J., Li, Y., and Dai, H. (2002) Functionalization of carbon nanotubes for biocompatibility and biomolecular recognition. *Nano Lett.* **2**: 285–288.

Shrivastava, S., Shukla, P., Deepalakshmi, P.D., and Mukhopadhyay, K. (2013) Characterization, cloning and functional expression of novel xylanase from *Thermomyces lanuginosus* SS-8 isolated from self-heating plant wreckage material. *World J. Microbiol. Biotechnol.* **29**: 2407–2415.

Sikandar, S., Ujor, V.C., Ezeji, T.C., Rossington, J.L., Michel, F.C., McMahan, C.M., Ali, N., and Cornish, K. (2017) *Thermomyces lanuginosus* STm: A source of thermostable hydrolytic enzymes for novel application in extraction of high-quality natural rubber from Taraxacum kok-saghyz (*Rubber dandelion*). *Ind. Crops Prod.* **103**: 161–168.

Singh, N., Srivastava, G., Talat, M., Raghubanshi, H., Srivastava, O.N., and Kayastha, A.M. (2014) Cicer α-galactosidase immobilization onto functionalized graphene nanosheets using response surface method and its applications. *Food Chem.* **142**: 430–438.

Singh, R., Kumar, M., Mittal, A., and Mehta, P.K. (2016) Microbial enzymes: Industrial progress in 21st century. *3 Biotech* **6**: 1–15.

Singh, S., Madlala, A.M., and Prior, B.A. (2003) *Thermomyces lanuginosus*: Properties of strains

and their hemicellulases. *FEMS Microbiol. Rev.* **27**: 3–16.

Singh, S., Pillay, B., Dilsook, V., and Prior, B.A. (2000) Production and properties of hemicellulases by a *Thermomyces lanuginosus* strain. *J. Appl. Microbiol.* **88**: 975–982.

Śledź, P. and Caflisch, A. (2018) Protein structure-based drug design: From docking to molecular dynamics. *Curr. Opin. Struct. Biol.* **48**: 93–102.

Soleimani, M., Khani, A., and Najafzadeh, K. (2012) α-amylase immobilization on the silica nanoparticles for cleaning performance towards starch soils in laundry detergents. *J. Mol. Catal. B Enzym.* **74**: 1–5.

Song, W., Gao, B., Xu, X., Xing, L., Han, S., Duan, P., Song, W., and Jia, R. (2016) Adsorption-desorption behavior of magnetic amine/Fe_3O_4 functionalized biopolymer resin towards anionic dyes from wastewater. *Bioresour. Technol.* **210**: 123–130.

Sörensen, M.H., Ng, J.B.S., Bergström, L., and Alberius, P.C.A. (2010) Improved enzymatic activity of *Thermomyces lanuginosus* lipase immobilized in a hydrophobic particulate mesoporous carrier. *J. Colloid Interface Sci.* **343**: 359–365.

Spina, F., Cecchi, G., Landinez-Torres, A., Pecoraro, L., Russo, F., Wu, B., Cai, L., Liu, X.Z., Tosi, S., Varese, G.C., Zotti, M., and Persiani, A.M. (2018) Fungi as a toolbox for sustainable bioremediation of pesticides in soil and water. *Plant Biosyst.* **152**: 474–488.

Spiteller, P. (2015) Chemical ecology of fungi. *Nat. Prod. Rep.* **32**: 971–993.

Srikanth, P., Somasekhar, S.A., Babu, K.R., and Pradesh, A. (2013) Analysis of heavy metals by using atomic absorption spectroscopy from the samples taken around Visakhapatnam. *Int. J. Environ. Ecol. Famiy Urban Stud.* **3**: 127–132.

Stark, G.R. (1967) Modification of proteins with cyanate. *Methods Enzymol.* **11**: 590–594.

Staszczak, M. (2008) The role of the ubiquitin-proteasome system in the response of the ligninolytic fungus *Trametes versicolo*r to nitrogen deprivation. *Fungal Genet. Biol.* **45**: 328–337.

Subrizi, F., Crucianelli, M., Grossi, V., Passacantando, M., Botta, G., Antiochia, R., and Saladino, R. (2014) Versatile and efficient immobilization of 2-Deoxyribose-5-phosphate aldolase

(DERA) on multiwalled carbon nanotubes. *ACS Catal.* **4**: 3059–3068.

Subrizi, F., Crucianelli, M., Grossi, V., Passacantando, M., Pesci, L., and Saladino, R. (2014) Carbon nanotubes as activating tyrosinase supports for the selective synthesis of catechols. *ACS Catal.* **4**: 810–822.

Suh, Y.J., Park, J.M., and Yang, J.W. (1994) Biodegradation of cyanide compounds by *Pseudomonas fluorescens* immobilized on zeolite. *Enzyme Microb. Technol.* **16**: 529–533.

Sung, Y.C., Anderson, P.M., and Fuchs, J.A. (1987) Characterization of high-level expression and sequencing of the *Escherichia coli* K-12 *cynS* gene encoding cyanase. *J. Bacteriol.* **169**: 5224–5230.

Sung, Y.C. and Fuchs, J.A. (1988) Characterization of the cyn operon in *Escherichia coli* K12. *J. Biol. Chem.* **263**: 14769–75.

Sung, Y.C., Parsell, D., Anderson, P.M., and Fuchs, J.A. (1987) Identification, mapping, and cloning of the gene encoding cyanase in *Escherichia coli* K-12. *J. Bacteriol.* **169**: 2639–2642.

Supuran, C.T. (2016) Structure and function of carbonic anhydrases. *Biochem. J.* **473**: 2023–2032.

Sutherland, T.D., Horne, I., Weir, K.M., Coppin, C.W., Williams, M.R., Selleck, M., Russell, R.J., and Oakeshott, J.G. (2004) Enzymatic bioremediation: From enzyme discovery to applications. *Clin. Exp. Pharmacol. Physiol.* **31**: 817–821.

Tapia, J.S., Valde´s, J., Orrego, R., Tchernitchin, A., Dorador, C., Bolados, A., and Harrod, C. (2018) Geologic and anthropogenic sources of contamination in settled dust of a historic mining port city in northern Chile: Health risk implications. *PeerJ*. **6**: e4699.

Taylor, P., Lee, T., Kwon, Y., and Kim, D. (2004) Oxidative treatment of cyanide in wastewater using hydrogen peroxide and homogeneous catalyst. *J. Environ. Sci. Health A Tox. Hazard Subst. Environ. Eng.* **39**: 787–801.

Theron, C.W., Berrios, J., Delvigne, F., and Fickers, P. (2018) Integrating metabolic modeling and population heterogeneity analysis into optimizing recombinant protein production by *Komagataella* (*Pichia*) *pastoris*. *Appl. Microbiol. Biotechnol.* **102**: 63–80.

Tiong, B., Bahari, Z.M., Irwan Shah Lee, N.S., Jaafar, J., Ibrahim, Z., and Shahir, S. (2015)

Cyanide degradation by *Pseudomonas pseudoalcaligenes* W2 isolated from mining effluent. *Sains Malaysiana* **44**: 233–238.

Tran, D.N. and Balkus, K.J. (2011) Perspective of recent progress in immobilization of enzymes. *ACS Catal.* **1**: 956–968.

Tümtürk, H., Karaca, N., Demirel, G., and Şahin, F. (2007) Preparation and application of poly(N,N-dimethylacrylamide-co-acrylamide) and poly(N-isopropylacrylamide-co-acrylamide)/κ-carrageenan hydrogels for immobilization of lipase. *Int. J. Biol. Macromol.* **40**: 281–285.

Tutu, H., McCarthy, T.S., and Cukrowska, E. (2008) The chemical characteristics of acid mine drainage with particular reference to sources, distribution and remediation: The witwatersrand basin, South Africa as a case study. *Appl. Geochemistry* **23**: 3666–3684.

Tyagi, M., Rana, A., Kumari, S., and Jagadevan, S. (2018) Adsorptive removal of cyanide from coke oven wastewater onto zero-valent iron: Optimization through response surface methodology, isotherm and kinetic studies. *J. Clean. Prod.* **178**: 398–407.

Ubalua, A.O. (2010) Cyanogenic glycosides and the fate of cyanide in soil. *Aust. J. Crop Sci.* **4**: 223–237.

Umbuzeiro, G.A., Coluci, V.R., Honório, J.G., Giro, R., Morales, D.A., Lage, A.S.G., Mazzei, J.L., Felzenszwalb, I., SouzaFilho, A.G., Stéfani, D., and Alves, O.L. (2011) Understanding the interaction of multi-walled carbon nanotubes with mutagenic organic pollutants using computational modeling and biological experiments. *TrAC Trends Anal. Chem.* **30**: 437–446.

Uppal, H., Tripathy, S.S., Chawla, S., Sharma, B., Dalai, M.K., Singh, S.P., Singh, S., and Singh, N. (2017) Study of cyanide removal from contaminated water using zinc peroxide nanomaterial. *J. Environ. Sci. (China)* **55**: 76–85.

Georgakilas, V., Tzitzios, V., Gournis, D., and Petridis. D. (2005) Attachment of magnetic nanoparticles on carbon nanotubes and their soluble derivatives. *Chem. Mater.* **17**: 1613–1617.

Verma, M.L., Naebe, M., Barrow, C.J., and Puri, M. (2013) Enzyme immobilisation on amino-functionalised multi-walled carbon nanotubes: Structural and biocatalytic characterisation.

PLoS One **8**: 16–18.

Villa, S., Riani, P., Locardi, F., and Canepa, F. (2016) Functionalization of Fe_3O_4 NPs by silanization: Use of amine (APTES) and thiol (MPTMS) silanes and their physical characterization. *Materials (Basel).* **9**: 1–14.

Walsh, M.A., Otwinowski, Z., Perrakis, A., Anderson, P.M., and Joachimiak, A. (2000) Structure of cyanase reveals that a novel dimeric and decameric arrangement of subunits is required for formation of the enzyme active site. *Structure* **8**: 505–514.

Wang, P. (2006) Nanoscale biocatalyst systems. *Curr. Opin. Biotechnol.* **17**: 574–579.

Wang, Z., Xu, X., Gong, Z., and Yang, F. (2012) Removal of COD, phenols and ammonium from Lurgi coal gasification wastewater using A^2O-MBR system. *J. Hazard. Mater.* **236**: 78–84.

Watanabe, A., Yano, K., Ikebukuro, K., and Karube, I. (1998) Cyanide hydrolysis in a cyanide-degrading bacterium, *Pseudomonas stutzeri* AK61, by cyanidase. *Microbiology* **144**: 1677–1682.

Werten, M.W.T., Van Den Bosch, T.J., Wind, R.D., Mooibroek, H., and De Wolf, F.A. (1999) High-yield secretion of recombinant gelatins by *Pichia pastoris*. *Yeast* **15**: 1087–1096.

Whitlock, J.L. and Whitlock, C.W. (2001) Recent advances in technologies for biological treatment of thiocyanate, cyanide, heavy metals and nitrates. In, *Cyanide: Social, Industrial and Economic Aspects as held at the 2001 TMS Annual Meeting; New Orleans, LA; USA; 12-15 Feb. 2001.*, pp. 195–202.

Winger, A.M., Heazlewood, J.L., Chan, L.J., Petzold, C.J., Permaul, K., and Singh, S. (2014) Secretome analysis of the thermophilic xylanase hyper-producer *Thermomyces lanuginosus* SSBP cultivated on corn cobs. *J. Ind. Microbiol. Biotechnol.* **41**: 1687–1696.

Wolfe, G. V, Alstyne, K.L. Van, Wolfe, G. V, and Freidenburg, T.L. (2001) Activated defense systems in marine macroalgae: Evidence for an ecological role for DMSP cleavage. *Mar. Ecol. Prog. Ser.* **213**: 53–65.

Wong, D.E., Senecal, K.J., and Goddard, J.M. (2017) Immobilization of chymotrypsin on hierarchical nylon 6,6 nanofiber improves enzyme performance. *Colloids Surf. B*

Biointerfaces. **154**: 270–278.

Woodley, J.M., Breuer, M., and Mink, D. (2013) A future perspective on the role of industrial biotechnology for chemicals production. *Chem. Eng. Res. Des.* **91**: 2029–2036.

Wu, J., Kamaly, N., Shi, J., Zhao, L., Xiao, Z., Hollett, G., John, R., Ray, S., Xu, X., Zhang, X., Kantoff, P.W., and Farokhzad, O.C. (2014) Development of multinuclear polymeric nanoparticles as robust protein nanocarriers. *Angew. Chemie - Int. Ed.* **53**: 8975–8979.

Xiang, D., Jin, T., Lei, X., Liu, S., Jiang, Y., Dong, Z., Tao, Q., and Cao, Y. (2018) The high efficient synthesis of natural gas from a joint-feedstock of coke-oven gas and pulverized coke via a chemical looping combustion scheme. *Appl. Energy* **212**: 944–954.

Xing, G.W., Li, X.-W., Tian, G.L., and Ye, Y.H. (2000) Enzymatic peptide synthesis in organic solvent with different zeolites as immobilization matrixes. *Tetrahedron* **56**: 3517–3522.

Xiong, H., Nyyssölä, A., Jänis, J., Pastinen, O., Von Weymarn, N., Leisola, M., and Turunen, O. (2004) Characterization of the xylanase produced by submerged cultivation of *Thermomyces lanuginosus* DSM 10635. *Enzyme Microb. Technol.* **35**: 93–99.

Xiu-juan, F.A.N. and Xin, L.I. (2012) Preparation and magnetic property of multiwalled carbon nanotubes decorated by Fe_3O_4 nanoparticles. *New Carbon Mater.* **27**: 111–116.

Xu, L. and Wang, J. (2012) Environmental Fenton-like degradation of 2,4-dichlorophenol using Fe_3O_4 magnetic nanoparticles. *Applied Catal. B Environ.* **123**–**124**: 117–126.

Xu, X., Qi, X., Wang, X., Wang, X., Wang, Q., Yang, H., Fu, Y., and Yao, S. (2017) Highly efficient enzyme immobilization by nanocomposites of metal organic coordination polymers and carbon nanotubes for electrochemical biosensing. *Electrochem. commun.* **79**: 18–22.

Yadav, D., Ranjan, B., Mchunu, N., Roes-Hill, M. Le, and Kudanga, T. (2018) Secretory expression of recombinant small laccase from *Streptomyces coelicolor* A3(2) in *Pichia pastoris*. *Int. J. Biol. Macromol.* **108**: 642–649.

Young, C. and Jordan, T. (1995) Cyanide remediation: Current and past technologies. *Proc. 10th Annu. Conf. Hazard. Waste Res.* pp. 104–129.

Yu, L.J., Shukla, S.S., Dorris, K.L., Shukla, A., and Margrave, J.L. (2003) Adsorption of

chromium from aqueous solutions by maple sawdust. *J. Hazard. Mater.* **100**: 53–63.

Zagrobelny, M., Bak, S., and Møller, B.L. (2008) Cyanogenesis in plants and arthropods. *Phytochemistry* **69**: 1457–1468.

Zahrl, R.J., Peña, D.A., Mattanovich, D., and Gasser, B. (2017) Systems biotechnology for protein production in *Pichia pastoris*. *FEMS Yeast Res.* **17**: 1–15.

Zdarta, J., Meyer, A., Jesionowski, T., and Pinelo, M. (2018) A general overview of support materials for enzyme immobilization: Characteristics, properties, practical utility. *Catalysts* **8**: 92.

Zdor, R.E. (2015) Bacterial cyanogenesis: Impact on biotic interactions. *J. Appl. Microbiol.* **118**: 267–274.

Zhang, J.L., Srivastava, R.S., and Misra, R.D.K. (2007) Core-shell magnetite nanoparticles surface encapsulated with smart stimuli-responsive polymer: Synthesis, characterization, and LCST of viable drug-targeting delivery system. *Langmuir* **23**: 6342–6351.

Zhang, M., Puri, A.K., Govender, A., Wang, Z., Singh, S., and Permaul, K. (2015) The multi-chitinolytic enzyme system of the compost-dwelling thermophilic fungus *Thermomyces lanuginosus*. *Process Biochem.* **50**: 237–244.

Zhang, Y., Shan, C.-M., Wang, J., Bao, K., Tong, L., and Jia, S. (2017) Molecular basis for the role of oncogenic histone mutations in modulating H3K36 methylation. *Sci. Rep.* **7**: 43906.

Zhou, Y., Yu, S., Liu, Q., Yan, D., Wang, Y., Gao, L., and Han, J. (2017) Synchronized purification and immobilization of his-tagged β-glucosidase via Fe_3O_4/PMGcore/shell magnetic nanoparticles. *Sci. Rep.* **7**: 41741.

Zuldian, P., Fukuda, S., and Bustan, M.D. (2017) Economic analysis of coal gasification plant for electricity and thermal energy supplies in Indonesia. *J. Clean Energy Technol.* **5**: 193–198.

Bioresource Technology 238 (2017) 582–588

Contents lists available at ScienceDirect

Bioresource Technology

journal homepage: www.elsevier.com/locate/biortech

Expression of a novel recombinant cyanate hydratase (rTl-Cyn) in *Pichia pastoris*, characteristics and applicability in the detoxification of cyanate

Bibhuti Ranjan, Santhosh Pillai, Kugenthiren Permaul, Suren Singh *

Department of Biotechnology and Food Technology, Faculty of Applied Sciences, Durban University of Technology, Durban 4000, South Africa

HIGHLIGHTS

- First report on cloning of cyanate hydratase in *P. pastoris*.
- First report of thermostable cyanate hydratase with a high catalytic efficiency.
- First report of thermodynamic characteristics of the cyanate hydratase are being reported.
- First report on cyanate detoxification in wastewater sample by rTl-Cyn.
- Detection of ammonia from cyanate after treatment with rTl-Cyn.

ARTICLE INFO

Article history:
Received 21 March 2017
Received in revised form 19 April 2017
Accepted 22 April 2017
Available online 27 April 2017

Keywords:
T. lanuginosus SSBP
P. pastoris
Recombinant cyanate hydratase
Cyanate detoxification
Ammonia

ABSTRACT

A recombinant *Pichia pastoris* harbouring the cyanate hydratase gene (*rTl-Cyn*) from the thermophilic fungus *Thermomyces lanuginosus* SSBP yielded a high titre of extracellular cyanate hydratase (100 ± 13 U mL^{-1}) which was ~10-fold higher than the native fungal strain. The purified rTl-Cyn had a molecular mass of ~20 kDa on SDS-PAGE, with K_m, V_{max}, k_{cat} and k_{cat}/K_m values of 0.34 mM, 2857.14 μmoles mg^{-1} min^{-1}, 2.14×10^4 s^{-1} and 6.3×10^7 M^{-1} s^{-1}, respectively. Its properties of thermostability, pH stability, and heavy metals insensitivity, make it a suitable candidate for bioremediation in extreme environments. The rTl-Cyn was able to degrade toxic cyanate completely with the liberation of ammonia, which was confirmed by FTIR analysis. This is the first report of any known cyanate hydratase that has been expressed in *P. pastoris*, characterized and effectively evaluated for cyanate detoxification.

© 2017 Elsevier Ltd. All rights reserved.

1. Introduction

Cyanate is a toxic compound produced by industry, but it is also produced from some metabolites, such as urea and carbamoylphosphate (Outer and Protein, 1987). Cyanate hydratase is an enzyme that catalyzes the breakdown of cyanate into CO_2 and ammonium in a bicarbonate dependent reaction. Bicarbonate acts as a nucleophilic reactant which attacks and breaks down cyanate, with carbamate as an unstable intermediate (Anderson, 1980). Cyanate has been hypothesised to serve as a nitrogen source for the growth of certain marine cyanobacteria under nitrogen limitation (Kamennaya and Post, 2013; Rocap et al., 2003). At least three biological roles have been associated with cyanate hydratase activity, i.e., nitrogen assimilation, cyanate detoxification, and metabolism regulation (Luque-Almagro et al., 2008). Since the enzyme catalyzes the direct formation of ammonium from cyanate, cyanate hydratase activity allows some bacteria to utilize cyanate as a nitrogen source (Luque-Almagro et al., 2008). For the assimilation of cyanate, these phototrophic bacteria transform it to ammonium and CO_2 with the enzyme cyanate hydratase (also known as cyanate lyase and cyanase) (Palatinszky et al., 2015). Cyanate hydratase are also found in a variety of other bacteria and archaea, where they have been confirmed to play a role in nitrogen assimilation or detoxification, as cyanate chemically alters proteins through carbamylation (Kamennaya et al., 2008; Luque-Almagro et al., 2008). Nitrifying microorganisms are generally considered to be highly dedicated chemolithoautotrophs that oxidize either ammonia or nitrite to generate energy and reductant for growth, and use CO_2 as a carbon source (Palatinszky et al., 2015). Among living organisms, cyanate hydratase plays a role in the detoxification of cyanate and cyanide (Ebbs, 2004). Since cyanase directly yields ammonia and CO_2 from cyanate, therefore, it is utilised as a nitrogen and carbon source in some organisms (Espie et al.,

* Corresponding author.
E-mail address: singhs@dut.ac.za (S. Singh).

http://dx.doi.org/10.1016/j.biortech.2017.04.091
0960-8524/© 2017 Elsevier Ltd. All rights reserved.

2007; Kunz and Nagappan, 1989). However, the growth of microorganisms and plants which lack cyanate hydratase is inhibited in the presence of cyanate (Qian et al., 2011).

Whole genome sequencing and secretome analysis of the thermophilic fungus *T. lanuginosus* SSBP has revealed the presence of a cyanate hydratase gene in them (Mchunu et al., 2013; Winger et al., 2014). Since *T. lanuginosus* SSBP is a potent xylanase producer with good pH and temperature stability, this prompted us to further investigate the presence of cyanate hydratase as well. Since cyanate hydratase production levels by *T. lanuginosus* SSBP is low, it would be beneficial to clone the cyanate hydratase encoding genes and overexpress them heterologously in *P. pastoris*. *P. pastoris* is a methylotrophic yeast, in which heterologous proteins can be expressed either constitutively or inducibly. By using an expression plasmid with the secretory signal sequence of α-factor, heterologous proteins are secreted into the medium (Ranjan and Satyanarayana, 2016). A large number of genes have been successfully expressed in *P. pastoris* (Cregg et al., 2000), however, no attempts have been made to clone and express *Tl-Cyn* gene in them. In this study, we have investigated cloning and expression of cyanate hydratase heterologously in *P. pastoris*, characterization of the recombinant cyanate hydratase (rTl-Cyn) and testing its applicability in the detoxification of cyanate.

2. Materials and methods

2.1. P. pastoris strain and vectors

Pichia pastoris GS 115 (Invitrogen, USA) was used as the host to express recombinant cyanate hydratase (rTl-Cyn) protein. The expression cassette with the inducible promoter (*AOX1*) was used for protein expression. The plasmid pPICZαA was used to construct the methanol-inducible *Tl-Cyn* expression vector. *Eco*RI and *Kpn*I restriction sites were added to sense and antisense primers, respectively, for cloning *Tl-Cyn* in the pPICZαA vector. Cloning steps were performed in *Escherichia coli* (DH5α).

2.2. Suitability of the rTl-Cyn gene for expression in P. pastoris

Before commencing rTl-Cyn expression studies in the eukaryotic host *P. pastoris*, cyanate hydratase ORF of *T. lanuginosus* SSBP was analysed for codon bias. The percentage usage of different codons for a particular amino acid was calculated and compared with that of a codon usage in the highly expressed proteins in *P. pastoris* (Ranjan and Satyanarayana, 2016).

2.3. RNA isolation

RNA was isolated from *T. lanuginosus* SSBP mycelium after 5 days incubation, at the time of maximum cyanase activity. The mycelium was frozen in liquid nitrogen and ground in a mortar until a floury consistency was obtained. The RNA was extracted using a RNeasy Mini Kit (Qiagen, Germany) according to the manufacturer's protocol.

2.4. cDNA synthesis

cDNA synthesis was carried out using the Maxima H Minus First Strand cDNA Synthesis Kit (Thermo Fisher Scientific, USA) according to the manufacturer's instructions.

2.5. Construction of rTl-Cyn

The cyanate hydratase gene was amplified from cDNA using the primers P1 and P2 having flanking regions of *Eco*RI and *Kpn*I restriction sites. PCR conditions: denaturation at 95 °C for 5 min; 25 cycles (denaturation at 95 °C for 30 s, annealing 58 °C for 30 s, elongation 72 °C for 70 s) and final elongation at 72 °C for 5 min was used for *Tl-Cyn* amplification. The primers used in this investigations are given in [Table 1]. The final 500 bp PCR product thus obtained was digested with *Eco*RI and *Kpn*I and cloned into the plasmid pPICZαA vector to make the *rTl-Cyn*-pPICZαA construct. In this construct, the *rTl-Cyn* ORF was fused in-frame with the secretory signal sequence of α-factor, and the *myc* epitope and 6 x His-tag from the vector at the N- and C-termini, respectively. Confirmation of the construct was done by double digestion with *Eco*RI and *Kpn*I. The presence and precise positioning of the insert was confirmed by DNA sequencing.

2.6. Bioinformatic analysis

The nucleotide and protein sequences were compared with the NCBI nucleotide/protein database using BLASTN and BLASTP programs, respectively. Multiple sequence alignment of catalytic domains was performed at http://www.ebi.ac.uk/Tools/msa/clustalw2/ with the proteins available in the databases using ClustalW2.

2.7. Transformation of P. pastoris with Tl-Cyn

The *rTl-Cyn*-pPICZαA was linearized with *Sac*I for the transformation of *P. pastoris*. Competent *P. pastoris* cells were prepared by combining chemical transformation with electroporation. Approximately 10 μg of linearized plasmid was mixed with competent cells and the mixture was directly transferred to a 0.2 cm prechilled electroporation cuvette and incubated on ice for 5 min. The electroporation was accomplished with a voltage of 1.5 kV, capacitance of 25 μF and resistance of 200 Ω. To 1.0 mL aliquot, 1.0 M ice-cold sorbitol was immediately added to the cuvette after electroporation, and the mixture was spread on YPD agar (g L^{-1}: yeast extract 10, peptone 20 and dextrose 20, agar 15) medium supplemented with 1.0 M sorbitol containing different concentrations of Zeocin (100, 200, 500, 1000 and 1500 μg mL^{-1}). The plates were incubated at 30 °C until single distinct colonies appeared and colony PCR was further performed to identify positive clones harbouring cyanate hydratase gene. Spheroplasting of the *P. pastoris* was done before proceeding to colony PCR by spinning single yeast colony in 30 μL buffer containing 1 U of lyticase (Sigma, USA). After spheroplasting, 5 μL of the suspension was used as a template in PCR mix and PCR was performed using primers P1 and P2 as described above. The transformants with fastest growth rate on YPD agar plates (supplemented with 1.0 M sorbitol) containing the highest concentration of Zeocin were screened for the production of rTl-Cyn. These clones were first grown in YPD broth and then biomass was transferred to Yeast extract-Peptone (YP) medium containing 0.5% (v/v) methanol (Ranjan and Satyanarayana, 2016). The production of rTl-Cyn was confirmed by quantitative assays.

2.8. rTl-Cyn assay

Cyanate hydratase assay was performed according to the modified method of Anderson (Anderson, 1980). The reaction mixture

Table 1
Primers used in this study.

Primers	Oligonucleotide sequence (5′-3′)
P1	CGGAATTCATGGCTGATATCGCAACCC
P2	GGTTGGTACCTTGAATCGACTGTATGGCAA

GAATTC- restriction site for *Eco*RI; GGTACC- restriction site for *Kpn*I.

containing 0.1 mL appropriately diluted rTl-Cyn, 0.5 mL Tris-HCl buffer (50 mM, pH 8.0), 0.2 mL of potassium cyanate and 0.2 mL of sodium bicarbonate and was incubated at 60 °C for 10 min. One mL of Nessler's reagent was added to the reaction mixture to terminate the reaction. The amount of ammonia released was determined by measuring the absorbance at 420 nm after the addition of Nessler's reagent. One unit (U) of cyanate hydratase is defined as the amount of enzyme that liberates 1 μmol of ammonium per minute under the defined assay conditions.

2.9. Purification of rTl-Cyn

The cell-free culture supernatant was passed through 10 kDa ultrafiltration membrane cartridge (Millipore); desalting and reconcentration was carried out for three cycles using the same membrane cartridge with 20 mM Tris-HCl buffer (pH 8.0). The concentrated enzyme was then purified by fast protein liquid chromatography (FPLC) system [ÄKTApurifier 100, GE Healthcare, Bio-Sciences, Uppsala, Sweden] using HiTrap Capto Q column (GE Healthcare, Bio-Sciences, Uppsala, Sweden) and eluting the bound protein with a linear gradient of 0–1 M NaCl in Tris-HCl buffer (20 mM, pH 8.0) at 1.0 mL min^{-1}. The fractions with cyanate hydratase activity were pooled and dialyzed against Tris-HCl buffer (20 mM, pH 8.0) and concentrated using a vacuum concentrator [Eppendorf, Germany]. The concentrated enzyme was loaded on a gel filtration chromatography column [Sephacryl S-200HR (16/60)] and eluted with 20 mM Tris-HCl buffer (pH 8.0) containing 50 mM NaCl at a flow rate of 0.4 mL min^{-1}.The fractions having cyanate hydratase activity were collected, purity checked on SDS-PAGE and characterized.

2.10. Biochemical characterization of rTl-Cyn

The optimum pH for the activity of rTl-Cyn was determined by conducting enzyme assays at different pH (4–8) [Sodium acetate buffer 20 mM (pH 4.0, 5.0), Tris-HCl buffer 20 mM (pH 6.0–8.0) and glycine-NaOH buffer 20 mM (pH 9.0–10.0)] at 60 °C. Similarly, the optimum reaction temperature was determined by performing rTl-Cyn assays at various temperatures (40–80 °C) at pH 8.0. The effect of various modulators on recombinant cyanate hydratase activity was assessed by performing enzyme assays in the presence of modulators in the reaction mixtures.

2.11. Enzyme kinetics and thermal deactivation of rTl-Cyn

The enzyme was assayed at different concentrations of potassium cyanate (0.1 to 3.0 mM). The K_m and V_{max} values were graphically determined from the Lineweaver-Burk plot. Activation energy (E_a) was calculated according to Ranjan et al. (2015). The efficiency of ammonia liberation by the enzyme action was calculated as V_{max}/K_m ratio. The energy of deactivation (E_d) of the enzyme was calculated from residual activity at different temperatures by incubating the enzyme solution in 20 mM Tris-HCl buffer (pH 8.0) at various temperatures (60–80 °C) in the absence of substrate. From the incubated samples, aliquots were drawn at specific intervals, cooled on ice for 30 min and cyanate hydratase assays were performed for calculating the residual activity. Calculations for determining inactivation rate constants (K_d) and energy of deactivation (E_d) were calculated according to Ranjan and Satyanarayana (Ranjan and Satyanarayana, 2016).

The effect of temperature on the rate of reaction was expressed in terms of temperature quotient (Q_{10}), which is the factor by which the rate increases when the temperature is raised by 10 °C. Temperature quotient (Q_{10}) was calculated by rearranging the equation of Dixon and Webb (Dixon and Webb, 1979):

$$Q_{10} = \text{antilog}(E_a \times 10/RT^2) \quad (1)$$

where E_a = activation energy, R is universal gas constant and T is absolute temperature.

2.12. Thermodynamic parameters of rTl-Cyn

Thermodynamics of irreversible inactivation of the rTl-Cyn was determined by rearranging the Eyring's absolute rate equation derived from the transition state theory:

$$K_d = (K_bT/h)\ e^{(-\Delta H/RT)} e^{(-\Delta S/RT)} \quad (2)$$

ΔH (change in enthalpy of deactivation), ΔG (change in free energy of inactivation), and ΔS (change in entropy of inactivation) for irreversible inactivation were calculated as follows:

$$\Delta H = E_d - RT \quad (3)$$

$$\Delta G = -RT \ln(K_d h/K_b T) \quad (4)$$

$$\Delta S = (\Delta H - \Delta G)/T \quad (5)$$

where K_b is the Boltzmann's constant (R/N)=1.38 × 10–23 J K^{-1}, T is the absolute temperature (K), h the Planck's constant = 6.626 × 10^{-34} J s, N is the Avogadro's number = 6.02 × 10^{23} - mol^{-1}, R is the gas constant = 8.314 J K^{-1} mol^{-1}.

2.13. Fourier transform infrared (FTIR) spectroscopy analysis to check the degradation of cyanate using rTl-Cyn

Samples for FTIR spectroscopy analysis were prepared according to Program and Studies (Program and Studies, 1994). The reaction mixture containing 0.1 mL of appropriately diluted rTl-Cyn, 0.5 mL Tris-HCl buffer (50 mM, pH 8.0), 0.2 mL of potassium cyanate and 0.2 mL of sodium bicarbonate was incubated at 60 °C for 10 min. Reaction mixture without rTl-Cyn served as control. Absorbance measurements were taken on KBr sample pellets prepared using samples with and without rTl-Cyn to check the degradation of cyanate and liberation of ammonia.

2.14. Cyanate detoxification by rTl-Cyn in wastewater sample

Samples were collected from the influent of an industrial wastewater treatment plant in KwaZulu Natal Province, South Africa. rTl-Cyn (30 U) was added to 1 mL of wastewater sample supplemented with varying concentrations of cyanate (5–20 mM) and the reaction was carried out for 10 min at 60 °C, in a reciprocating water bath at 100 rpm. Similarly, a control experiment was also performed, except that the wastewater sample was replaced with Tris-HCl buffer (50 mM, pH 8.0). After 10 min, the samples were centrifuged and analysed for cyanate degradation via, release of product (ammonia). In a separate experiment, heavy metals (Ag, Au, Cd, Cr, Cu, Fe, Pb and Zn) were added to both wastewater samples and the control, and thereafter observed for cyanate degradation by rTl-Cyn. In addition, the presence of heavy metals in wastewater samples (spiked and un-spiked) were analysed using atomic absorption spectroscopy (Srikanth et al., 2013).

3. Results and discussion

3.1. Construction of rTl-Cyn

To achieve the expression of cyanate hydratase, differences in the relative codon frequency between *T. lanuginosus* SSBP and *P. pastoris* were analysed. The optimized cyanate hydratase gene was compared with the wild type and the sequence alignment was tested [data not shown]. Codon usage by the host *P. pastoris*

for the wild type gene and optimized gene has been compared, and found to be 46 and 38%, respectively (Ranjan and Satyanarayana, 2016). The value of 100 is set for the codon with the maximum usage frequency for a given amino acid in *P. pastoris*. Since codon usage of the optimized gene was lower than the native gene for expression in *P. pastoris*, this native gene was used in the present investigation. The construction of *rTl-Cyn*-pPICZαA [Fig. S1] was confirmed by colony PCR [Fig. 1a] and double digestion with *Eco*RI and *Kpn*I [Fig. 1b].

3.2. Bioinformatic analysis

Multiple amino acid sequence alignment of the catalytic domain of rTl-Cyn with known cyanases from NCBI showed an identity of 84, 84, 82, 82, 83, 83, 82 and 83% to the cyanases from *Rasamsonia emersonii* CBS 393.64 (KKA17850.1), *Talaromyces cellulolyticus* (GAM35076.1), *Talaromyces stipitatus* ATCC 10500 (XP_002486940.1), *Talaromyces marneffei* ATCC 18224 (XP_002145582.1), *Aspergillus oryzae* RIB40 (XP_001822419.1), *Aspergillus flavus* NRRL3357 (XP_002382512.1), *Penicillium oxalicum* (EPS32828.1), and *Neosartorya fischeri* NRRL 181 (XP_001261116.1), respectively [Fig. S2].

3.3. rTl-Cyn activity and Purification

Among the 100 clones screened, clone 26 produced the highest extracellular rTl-Cyn titre of 100 ± 13 U mL^{-1} and was therefore selected for further investigations. No cell bound cyanate hydratase activity was observed in clone 26 which showed the efficient functioning of the secretory signal sequence of α-factor. A ~10-fold enhancement in cyanate hydratase production was achieved by the recombinant *P. pastoris*, as compared to the native host [data not shown]. The rTl-Cyn was purified to homogeneity, in three steps viz., ultrafiltration, ion-exchange chromatography and gel filtration chromatography. The purity was confirmed by SDS-PAGE, showing a single band corresponding to ~20 kDa [Fig. 2]. Purification also resulted in a 34.66-fold increase in activity with a specific activity of 84545.45 U mg^{-1} [Table 2].

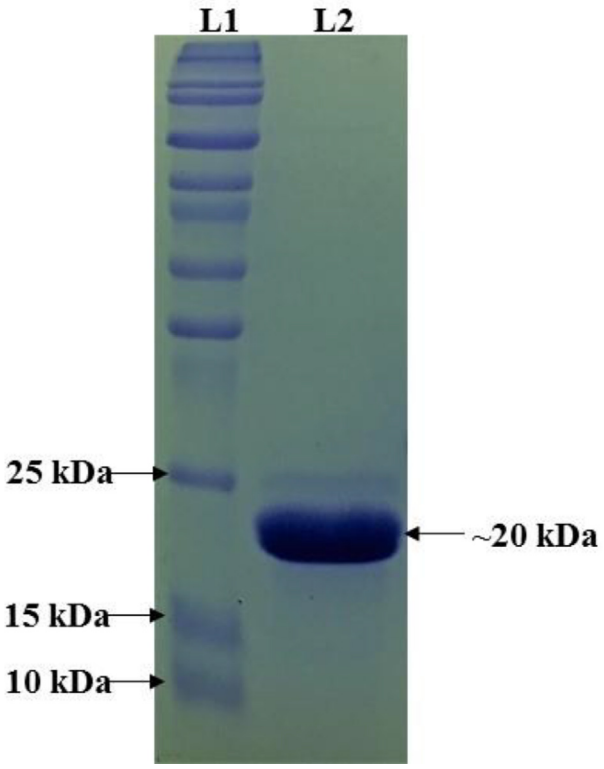

Fig. 2. SDS-PAGE analysis profile of rTl-Cyn: L1 protein marker, L2 purified rTl-Cyn.

3.4. Biochemical characterization of rTl-Cyn

The optimum temperature and pH for rTl-Cyn activity were 60 °C and pH 8, respectively. The optimum pH of rTl-Cyn was similar to that of the other known cyanases (Elleuche and Pöggeler, 2008; Luque-Almagro et al., 2008). The enzyme activity was marginally stimulated by Na^+ while other metal ions slightly inhibited or did not influence the activity [Table 3]. rTl-Cyn activity was inhibited by 44% in the presence of azide, which is remarkable, since azide is a cyanide and cyanate analog. In contrast, the

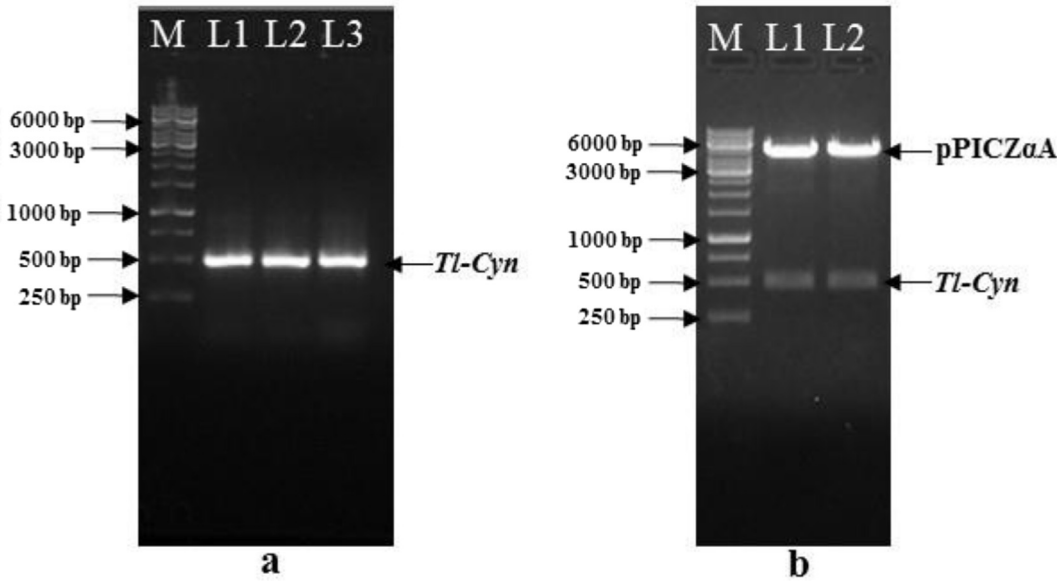

Fig. 1. Confirmation of pPICZαA-*Tl-Cyn* construction by (a) colony PCR and (b) double digestion; M- 1 kb ladder, Lane 1,2 double digested pPICZαA-*Tl-Cyn*.

Table 2
Summary of rTl-Cyn purification from *Pichia pastoris*.

Purification step	Total activity ($U\ mL^{-1}$)	Total Protein ($mg\ mL^{-1}$)	Specific activity ($U\ mg^{-1}$)	Purification fold
Cell-free supernatant	100	0.041	2439	1
Ultrafiltration (10 kDa)	209	0.076	2750	1.13
Anion exchange	185	0.0038	48684.21	19.96
Gel filtration	93	0.0011	84545.45	34.66

Table 3
Effect of different metal ions on rTl-Cyn.

Metal ions	Relative enzyme activity	
Control	100 ± 0.87	
	2 mM	5 mM
As	96 ± 0.93	93 ± 0.79
Cr	92.6 ± 0.82	88.8 ± 0.84
Cd	98 ± 0.72	97 ± 0.79
Cu	97 ± 0.92	95 ± 0.86
Hg	92 ± 0.89	89 ± 0.90
Na	102 ± 0.63	106 ± 0.68
Ni	99.2 ± 0.82	97.4 ± 0.79
Pb	93 ± 0.94	89 ± 0.83
Zn	100 ± 0.39	99.8 ± 0.48

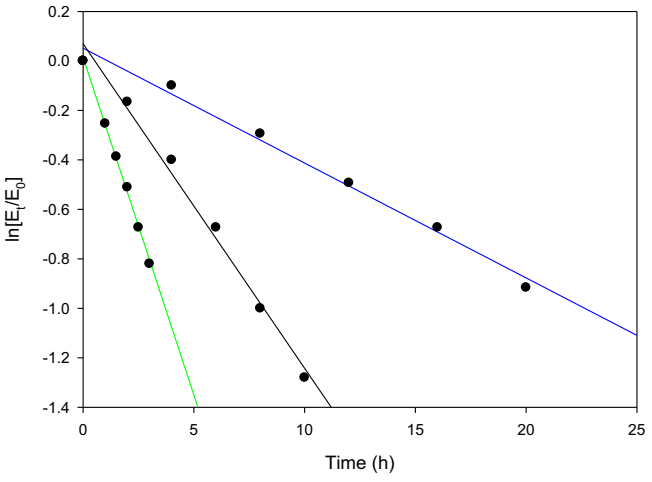

Fig. 3. Plot of $\ln[E_t/E_0]$ vs time (h) for the calculation of deactivation constant (K_d) and $T_{1/2}$ of rTl-Cyn at different temperature [60 °C (blue line), 70 °C (black line), 80 °C (green line)]. (For interpretation of the references to colour in this figure legend, the reader is referred to the web version of this article.)

enzyme activity was not inhibited by cyanide, urea, nitrite, EDTA, dithioerythritol up to 10 mM concentrations (data not shown). Similar results were observed with *Pseudomonas pseudoalcaligenes* CECT5344 Cyanase (Luque-Almagro et al., 2008). Reducing agents such as β-mercaptoethanol had no effect on the enzyme activity, signifying that –SH groups had no role in the catalytic activity or these enzymes do not have any free and accessible -SH groups. The chelating agent EDTA also has no effect on the activity of rTl-Cyn, indicating that it did not require any cations for activity (Ranjan and Satyanarayana, 2016).

3.5. Kinetic parameters and thermodynamics of rTl-Cyn

The K_m and V_{max} of rTl-Cyn were 0.34 mM and 2857.14 μmoles $mg^{-1}\ min^{-1}$. The k_{cat} and k_{cat}/K_m of the rTl-Cyn was $2.14 \times 10^4\ s^{-1}$ and $6.3 \times 10^7\ M^{-1}\ s^{-1}$, respectively, which was significantly higher than that of the other known cyanase (Anderson et al., 1994). A larger k_{cat} value signified that the least amount of enzyme was required for its applications (Ranjan and Satyanarayana, 2016).

The deactivation constant (K_d) of rTl-Cyn was calculated from the plot of ln[Et/Eo] vs time [Fig. 3]. This value of K_d was substituted in Eq. (2) to calculate $T_{1/2}$ of the rTl-Cyn. The $T_{1/2}$ values of the rTl-Cyn at 60 °C and 80 °C were 16.16 and 2.6 h, respectively. Arrhenius plot of the deactivation constant at different temperatures were plotted for calculating the deactivation energy (E_d) of rTl-Cyn, which was 91.73 KJ mol^{-1}. The activation energy of rTl-Cyn was 41.5 KJ mol^{-1}, and this value was substituted in Eq. (1) to calculate the temperature quotient (Q_{10}), was 1.57.

Thermodynamic parameters of thermal inactivation of rTl-Cyn have been calculated by applying the first order kinetics to the thermal inactivation data. The overall ΔG, ΔH and ΔS values for thermal inactivation of rTl-Cyn were positive [Table 4]. The enthalpy change (ΔH) represented the energy required for thermal denaturation of the protein. A large ΔH value signifies that high energy was required for breaking covalent bonds in the thermal inactivation of rTl-Cyn. Free energy change (ΔG) was positive for rTl-Cyn, which indicated that the thermal denaturation of recombinant enzyme was non-spontaneous as reported for other enzymes (Parashar and Satyanarayana, 2016; Ranjan and Satyanarayana, 2016; Ranjan et al., 2015). Denaturation of the enzyme was accompanied by an increase in the disorder of the enzyme structure which can be measured as entropy change (ΔS) which decreases with increasing enzyme stability.

3.6. FTIR spectroscopy analysis

FTIR analysis showed the complete degradation of cyanate and liberation of ammonia after the addition of rTl-Cyn in the reaction mixture. This was confirmed by a peak observed in the range of 3400 and 3320 cm^{-1} for ammonia and in contrast to the control, a peak in the range of 2300–2100 cm^{-1} was observed for cyanate [data not shown]. Similar peaks were observed by Morimoto et al. (1976) for ammonia and by Alwis et al. for cyanate (Alwis et al., 2015) respectively.

3.7. Cyanate detoxification by rTl-Cyn

The degradation potential of rTl-Cyn was evaluated in wastewater as well as in control samples supplemented with 5–20 mM cyanate. Complete degradation of cyanate (up to 10 mM concentration) was achieved in control and 90% of the wastewater samples within 10 min of incubation. Moreover, more than 80% cyanate degradation, (up to 20 mM cyanate) was achieved in wastewater and control samples under similar conditions [Fig. 4]. A similar study showed 80% cyanide (20 mM, KCN) degradation using cell-free extracts of *Rhodococcus* UKMP-5 M in 80 min (Nallapan Maniyam et al., 2015).

The effect of heavy metals on rTl-Cyn was also studied during cyanate degradation. Further, heavy metal levels present in wastewater samples under un-spiked and spiked conditions were also analysed [Table S1]. Our findings showed that heavy metals had no significant effect on rTl-Cyn activity achieving approxi-

Table 4
The thermodynamic parameters of rTl-Cyn measured during thermal deactivation at various temperatures.

Temp (K)	K_d (h^{-1})	$T_{1/2}$ (h)	ΔH (KJ mol^{-1})	ΔG (KJ mol^{-1})	ΔS (J mol^{-1} K^{-1})
333.15	0.043	16.16	88.96	52.33	110.00
343.15	0.113	6.14	88.88	51.23	109.78
353.15	0.266	2.6	88.79	50.29	109.07

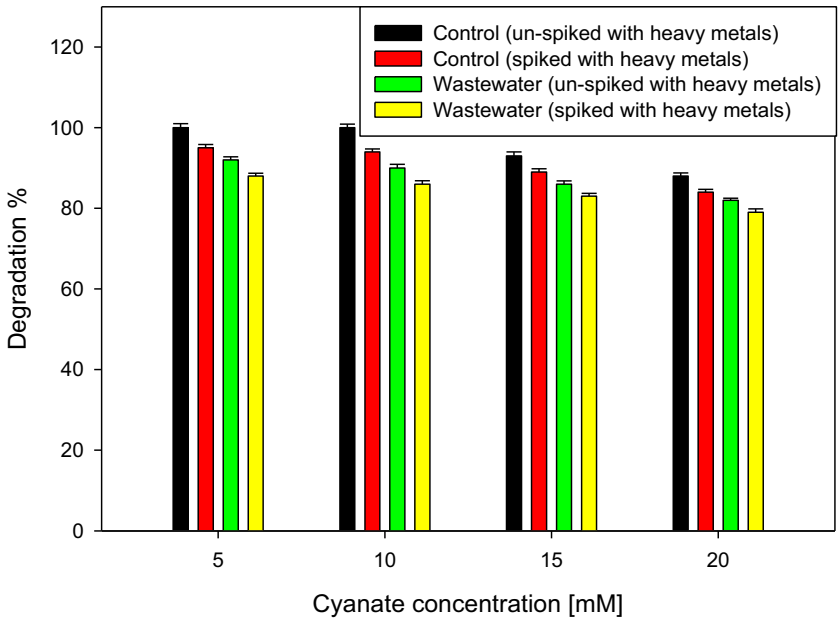

Fig. 4. Degradation of cyanate in wastewater sample and control* using rTl-Cyn. *Control: Tris-HCl buffer (50 mM, pH-8).

mately 95% cyanate degradation compared to un-spiked samples. Further, we observed that cyanate degradation was lower in wastewater samples compared to control. This could be due to fact that wastewater contains many impurities which might prevent rTl-Cyn from binding with cyanate.

4. Conclusions

The cyanate hydratase gene of *T. lanuginosus* SSBP was expressed in *P. pastoris*. The recombinant *P. pastoris* secreted ~10-fold higher cyanate hydratase than the native fungal strain. The thermostability, high catalytic efficiency and metal tolerance makes rTl-Cyn, a good biocatalyst for application in cyanate detoxification.

Acknowledgements

Authors are grateful to the National Research Foundation (UID 98725), Technology Innovation Agency (TIA) and the Durban University of Technology, Durban, South Africa for financial support during the course of this investigation.

Appendix A. Supplementary data

Supplementary data associated with this article can be found, in the online version, at http://dx.doi.org/10.1016/j.biortech.2017.04.091.

References

Alwis, L.K.H.K., Mucalo, M.R., Ingham, B., Kappen, P., 2015. A combined SNIFTIRS and XANES study of electrically polarized copper electrodes in DMSO and DMF solutions of cyanate (NCO-), thiocyanate (NCS-) and selenocyanate (NCSe-) ions. J. Electrochem. Soc. 162, H434–H448. http://dx.doi.org/10.1149/2.0321507jes.

Anderson, P.M., 1980. Purification and properties of the inducible enzyme cyanase. Biochemistry 19, 2882–2888.

Anderson, P.M., Korte, J.J., Holcomb, T.A., Cho, Y.G., Son, C.M., Sung, Y.C., 1994. Formation of intersubunit disulfide bonds and properties of the single histidine and cysteine residues in each subunit relative to the decameric structure of cyanase. J. Biol. Chem. 269, 15036–15045.

Cregg, J.M., Cereghino, J.L., Shi, J., Higgins, D.R., 2000. Recombinant protein expression in *Pichia pastoris*. Mol. Biotechnol. 16, 23–52. http://dx.doi.org/10.1385/MB:16:1:23.

Dixon, M., Webb, E.C., 1979. Enzyme kinetics. In: Dixon, M., Webb, E.C. (Eds.), Enzymes. Academic Press, New York.

Ebbs, S., 2004. Biological degradation of cyanide compounds. Curr. Opin. Biotechnol. 15, 231–236. http://dx.doi.org/10.1016/j.copbio.2004.03.006.

Elleuche, S., Pöggeler, S., 2008. A cyanase is transcriptionally regulated by arginine and involved in cyanate decomposition in *Sordaria macrospora*. Fungal Genet. Biol. 45, 1458–1469. http://dx.doi.org/10.1016/j.fgb.2008.08.005.

Espie, G.S., Jalali, F., Tong, T., Zacal, N.J., So, A.K.C., 2007. Involvement of the cynABDS operon and the CO_2-concentrating mechanism in the light-dependent transport and metabolism of cyanate by cyanobacteria. J. Bacteriol. 189, 1013–1024. http://dx.doi.org/10.1128/JB.01328-06.

Kamennaya, N.A., Chernihovsky, M., Post, A.F., 2008. The cyanate utilization capacity of marine unicellular Cyanobacteria. Limnol. Oceanogr. 53, 2485–2494. http://dx.doi.org/10.4319/lo.2008.53.6.2485.

Kamennaya, N.A., Post, A.F., 2013. Distribution and expression of the cyanate acquisition potential among cyanobacterial populations in oligotrophic marine waters. Limnol. Oceanogr. 58, 1959–1971. http://dx.doi.org/10.4319/lo.2013.58.6.1959.

Kunz, D.A., Nagappan, O., 1989. Cyanase-mediated utilization of cyanate in *Pseudomonas fluorescens* NCIB 11764. Appl. Environ. Microbiol. 55, 256–258.

Luque-Almagro, V.M., Huertas, M.J., Sáez, L.P., Luque-Romero, M.M., Moreno-Vivián, C., Castillo, F., Roldán, M.D., Blasco, R., 2008. Characterization of the *Pseudomonas pseudoalcaligenes* CECT5344 cyanase, an enzyme that is not essential for cyanide assimilation. Appl. Environ. Microbiol. 74, 6280–6288. http://dx.doi.org/10.1128/AEM.00916-08.

Mchunu, N.P., Permaul, K., Rahman, A.Y.A., Saito, J.A., Singh, S., Alam, M., 2013. Xylanase superproducer: genome sequence of a compost-loving thermophilic fungus, *Thermomyces lanuginosus* Strain SSBP. Genome Announc. 1, 4–5. http://dx.doi.org/10.1128/genomeA.00388-13.Copyright.

Morimoto, T., Yanal, H., Nagao, M., 1976. Infrared spectra of ammonia adsorbed on zinc oxide. J. Phys. Chem. 80, 471–475.

Nallapan Maniyam, M., Sjahrir, F., Latif Ibrahim, A., Cass, A.E.G., 2015. Enzymatic cyanide degradation by cell-free extract of *Rhodococcus* UKMP−5M. J. Environ. Sci. Health Part A 50, 357–364. http://dx.doi.org/10.1080/10934529.2015.987524.

Outer, M., Protein, M., 1987. Isolation and Characterization of *Escherichia coli* Mutants Lacking Inducible Cyanase. J. Gen. Microbiol. 133, 645–653.

Palatinszky, M., Herbold, C., Jehmlich, N., Pogoda, M., Han, P., von Bergen, M., Lagkouvardos, I., Karst, S.M., Galushko, A., Koch, H., Berry, D., Daims, H., Wagner, M., 2015. Cyanate as an energy source for nitrifiers. Nature 524, 105–108. http://dx.doi.org/10.1038/nature14856.

Parashar, D., Satyanarayana, T., 2016. A chimeric α-amylase engineered from *Bacillus acidicola* and *Geobacillus thermoleovorans* with improved thermostability and catalytic efficiency. J. Ind. Microbiol. Biotechnol. 43, 473–484. http://dx.doi.org/10.1007/s10295-015-1721-7.

Program, F.S., Studies, C.S., 1994. Ferrocyanide Safety Program Cyanide Speciation Studies FY 1994 Annual Report.

Qian, D., Jiang, L., Lu, L., Wei, C., Li, Y., 2011. Biochemical and structural properties of cyanases from *Arabidopsis thaliana* and *Oryza sativa*. PLoS One 6, 1–10. http://dx.doi.org/10.1371/journal.pone.0018300.

Ranjan, B., Satyanarayana, T., 2016. Recombinant HAP phytase of the thermophilic mold sporotrichum thermophile: expression of the codon-optimized phytase gene in *Pichia pastoris* and applications. Mol. Biotechnol. 58, 137–147. http://dx.doi.org/10.1007/s12033-015-9909-7.

Ranjan, B., Singh, B., Satyanarayana, T., 2015. Characteristics of Recombinant Phytase (rSt-Phy) of the Thermophilic mold *Sporotrichum thermophile* and its applicability in dephytinizing foods. Appl. Biochem. Biotechnol. 177, 1753–1766. http://dx.doi.org/10.1007/s12010-015-1851-4.

Rocap, G., Larimer, F.W., Lamerdin, J., Malfatti, S., Chain, P., Ahlgren, N.A., Arellano, A., Coleman, M., Hauser, L., Hess, W.R., Johnson, Z.I., Land, M., Lindell, D., Post, A. F., Regala, W., Shah, M., Shaw, S.L., Steglich, C., Sullivan, M.B., Ting, C.S., Tolonen, A., Webb, E.a., Zinser, E.R., Chisholm, S.W., 2003. Genome divergence in two *Prochlorococcus* ecotypes reflects oceanic niche differentiation. Nature 424, 1042–1047. http://dx.doi.org/10.1038/nature01947.

Srikanth, P., Somasekhar, S.A., Babu, K.R., Pradesh, A., 2013. Analysis of heavy metals by using atomic absorption spectro-scopy from the samples taken around Visakhapatnam. Int. J. Environ. Ecol. Family Urban Stud. 3, 127–132.

Winger, A.M., Heazlewood, J.L., Chan, L.J.G., Petzold, C.J., Permaul, K., Singh, S., 2014. Secretome analysis of the thermophilic xylanase hyper-producer *Thermomyces lanuginosus* SSBP cultivated on corn cobs. J. Ind. Microbiol. Biotechnol. 41, 1687–1696. http://dx.doi.org/10.1007/s10295-014-1509-1.

Bioresource Technology 253 (2018) 105–111

Contents lists available at ScienceDirect

Bioresource Technology

journal homepage: www.elsevier.com/locate/biortech

A novel strategy for the efficient removal of toxic cyanate by the combinatorial use of recombinant enzymes immobilized on aminosilane modified magnetic nanoparticles

Bibhuti Ranjan, Santhosh Pillai, Kugenthiren Permaul, Suren Singh*

Department of Biotechnology and Food Technology, Faculty of Applied Sciences, Durban University of Technology, Durban 4001, South Africa

GRAPHICAL ABSTRACT

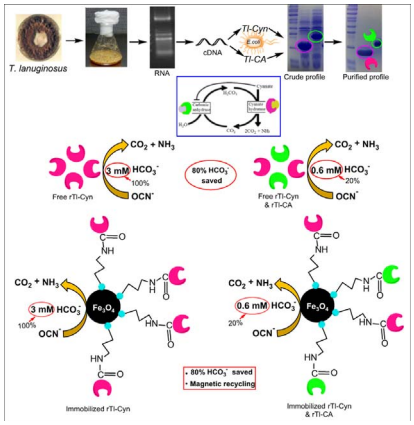

ARTICLE INFO

Keywords:
Cyanate
Carbonic anhydrase
Cyanase
Wastewater
Magnetic nanoparticles

ABSTRACT

Cyanase detoxifies cyanate by transforming it to ammonia and carbon dioxide in a bicarbonate-dependent reaction, however, dependence on bicarbonate limits its utilization in large-scale applications. A novel strategy was therefore developed for overcoming this bottleneck by the combined application of cyanase (rTl-Cyn) and carbonic anhydrase (rTl-CA). The synergistic effect of rTl-Cyn and rTl-CA could reduce the dependence of bicarbonate by 80%, compared to using rTl-Cyn alone. Complete degradation of cyanate (4 mM) was achieved with buffered conditions and 85 ± 5% degradation with industrial wastewater sample, when 20 U of rTl-Cyn was applied. Furthermore, a similar percentage of degradation was achieved using 80% less bicarbonate, when rTl-Cyn and rTl-CA were used together under identical conditions. In addition, rTl-Cyn and rTl-CA were immobilized onto the magnetic nanoparticles and their catalytic activity, stability and reusability were also evaluated. This is the first report on the synergistic biocatalysis by rTl-Cyn and rTl-CA, for cyanate detoxification.

* Corresponding author.
E-mail address: singhs@dut.ac.za (S. Singh).

https://doi.org/10.1016/j.biortech.2017.12.087
Received 3 November 2017; Received in revised form 21 December 2017; Accepted 22 December 2017
Available online 29 December 2017
0960-8524/ © 2018 Elsevier Ltd. All rights reserved.

1. Introduction

Cyanide, one of the most toxic chemicals, is extensively used in mining industries for the extraction of metals and electroplating (Barakat et al., 2004; Luque-Almagro et al., 2016). The mining industry discharges several billion pounds of toxic wastewaters, which in addition to cyanide, contains silver, gold, cadmium, chromium, copper, iron, lead, zinc etc. (Luque-almagro et al., 2011). Cyanate (OCN^-), an important cyanide derivative formed by cyanide oxidation (Luque-Almagro et al., 2016) is present in cyanide contaminated environments. The application of pesticides and fungicides in agriculture also results in the accumulation of cyanate in the environment (Elmore et al., 2015).

The treatment of cyanurated wastewaters has been performed using various physical, chemical and biological methods or combinations of them (Glanpracha and Annachhatre, 2016; Pal and Kumar, 2013; Papadimitriou et al., 2006; Sharma et al., 2012). Alkaline breakpoint chlorination is a commonly used chemical oxidation method for cyanide removal (Barakat et al., 2004; Baxter and Cummings, 2006). However, this method has significant disadvantages as it needs special requirements for waste disposal, releases more toxic chemical agents (such as OCN^-) and the potential formation of chlorinated organic compounds (Huertas et al., 2010). Similarly, some other alternative chemical treatments, such as, SO_2/air (INCO) process and hydrogen peroxide have been used, which also resulted in the formation of cyanate (Baxter and Cummings, 2006). Due to the several disadvantages associated with chemical treatments for cyanide removal, eco-friendly technologies using activated sludge (Papadimitriou et al., 2009; Ryu et al., 2017) or microbes (Ebbs, 2004) have been employed. However, the complex nature of polluted wastewaters, primarily the high concentrations of cyanide or cyanate in industrial effluents, may weaken the viability and activity of microorganisms (Papadimitriou et al., 2009; Sharma and Philip, 2014). Conversely, the cyanate hydrolyzing enzyme (rTl-Cyn), which is environmentally safe, selective and resistant to high concentrations of cyanate and other metals, is a promising alternative (Ranjan et al., 2017). Cyanase (cyanate hydratase) detoxifies cyanate by transforming it to ammonium (NH_4^+) and carbon dioxide (CO_2) in a bicarbonate dependent reaction (Johnson and Anderson, 1987). Since bicarbonate is required to facilitate the reaction, we have developed a strategy for the efficient removal of toxic cyanate by the combinatorial use of the rTl-Cyn and rTl-CA, in order to limit the dependence of bicarbonate.

Nevertheless, free enzymes have some limitations: large consumption, difficulty in separation and recycling, which are key factors for the effective utilization of enzymes at industrial scale (Madhavan et al., 2017). Enzyme immobilization offers an alternative to resolve the challenges associated with the reusability of enzymes coupled with the several advantages, such as, enhanced thermal stability and ease of separation (Dehnavi et al., 2015; Zhou et al., 2017). Various carriers have been used for the immobilization of enzymes, among them, Fe_3O_4 nanoparticles are deemed appropriate, owing to their small size and high surface area for the attachment of enzymes, superparamagnetism, low toxicity and good catalytic properties (Pereira et al., 2017; Xu and Wang, 2012).

In this work, the detoxification of cyanate has been evaluated by the combinatorial use of the rTl-Cyn and rTl-CA. As the efficacy for detoxification of cyanate has already been shown (Ranjan et al., 2017), this study focused mainly on two key objectives: (i) to evaluate the synergistic effect of rTl-Cyn and rTl-CA on the degradation efficiency of cyanate at varying concentrations of bicarbonate; (ii) to determine the influence of rTl-CA on the efficiency of cyanate degradation under the same conditions. Further, rTl-Cyn and rTl-CA were immobilized on silanized MNPs and their reusability in cyanate degradation was assessed. FT-IR; FE-SEM; and XRD analyses were also carried out on free and immobilized MNPs. Stability and reusability of immobilized MNPs were also assessed.

2. Materials and methods

2.1. Strains and reagents

E. coli DH5α was used as the host strain for all plasmid constructions and *E. coli* BL21 (DE3) (Invitrogen) was used as the expression host. The pJET1.2/blunt vector (Thermo Scientific) was used as the cloning vector for nucleotide sequence determination. Vector pET28a(+) (Novagen) was used for the cloning and expression of *Tl-Cyn* and *Tl-CA* genes. Ni^{2+}-NTA agarose resin for protein purification was purchased from Qiagen and restriction enzymes were procured from New England Biolabs. The primers used in this investigation were supplied by Integrated DNA Technologies. Wastewater samples were collected from the influent of an industrial wastewater treatment plant in KwaZulu-Natal, South Africa. The thermophilic fungus *Thermomyces lanuginosus* SSBP used in this study was deposited in the Industrial Biotechnology MIRCEN Culture Collection, Bloemfontein, South Africa (Accession number PRI 0226) (Singh et al., 2000).

2.2. RNA isolation, cDNA synthesis and construction of Tl-Cyn and Tl-CA plasmids

RNA isolation from *T. lanuginosus* SSBP and cDNA synthesis were performed as described previously (Ranjan et al., 2017). Cyanate hydratase and carbonic anhydrase genes were amplified from cDNA using the primers P1, P2 and P3, P4, respectively (Table 1), with flanking regions of *Eco*RI and *Hin*dIII restriction sites. PCR conditions: denaturation at 95 °C for 1 min; 25 cycles (denaturation at 95 °C for 40 s, annealing at 58 °C for 30 s, elongation 72 °C for 60 s) and final elongation at 72 °C for 8 min, were used for the amplification of *Tl-Cyn* and *Tl*-CA. Finally, 500 bp and 583 bp PCR products of *Tl-Cyn* and *Tl-CA* were obtained and digested with *Eco*RI and *Hin*dIII and cloned into the plasmid pET28a(+) vector to make pET28a-*Tl-Cyn* and pET28a-*Tl-CA* constructs. Confirmation of the constructs was performed by double digestion with *Eco*RI and *Hin*dIII. The presence and precise positioning of the inserts were confirmed by DNA sequencing.

2.3. Expression and purification of rTl-Cyn and rTl-CA

Plasmids isolated from both the positive clones, pET28a-*Tl-Cyn* and pET28a-*Tl-CA* were transformed into *E. coli* BL21 (DE3), and the transformed cells were cultured at 37 °C for 16–18 h in LB medium supplemented with kanamycin (50 μg/mL). LB-kanamycin medium was inoculated with *E. coli* BL21 (DE3) as the primary inoculum and cultivation was continued at 37 °C until the absorbance (A_{600}) reached 0.5–0.7 (Ranjan et al., 2015). The expression of *Tl-Cyn* and *Tl-CA* genes under the control of the T7 promoter was induced by adding 0.8 mM isopropyl-β-D-thiogalactopyranoside (IPTG) and further incubation was carried out at 25 °C for 8 h. The culture was then harvested and re-suspended in 50 mM Tris-HCl buffer, pH 8.0 and sonicated using a Ultrasonic Sonicator (Sonics Vibra-cell) using 2 s pulses for 10 min to release the intracellular proteins. The sonicated samples were then centrifuged at 13,000 × *g* for 20 min to remove cell debris, and the supernatant was assessed for enzyme activity. Recombinant cyanate hydratase and carbonic anhydrase were further purified using Ni-NTA

Table 1
Primers used in this study.

Primers	Oligonucleotide sequence (5′–3′)
P1	CGGAATTCATGGCTGATATCGCAACCC
P2	GGTTAAGCTTTTAGAATCGACTGTATGGC
P3	CGGAATTCATGGGTTTCCGCATTTATGGC
P4	GGTTAAGCTTTTATGTGCACACCTCCGGATCAAC

GAATTC-restriction site for *Eco*RI; AAGCTT-restriction site for *Hin*dIII.

columns (Parashar and Satyanarayana, 2016).

2.4. Enzyme assays

rTl-Cyn activity was determined as previously described by Ranjan et al. (2017). One unit (U) of cyanate hydratase was defined as the amount of enzyme that liberates 1 μmol of ammonium per minute under the standard assay conditions.

rTl-CA activity was assayed by a modified protocol of Khalifah (1971). The assay was performed at 4 °C by adding 0.1 mL of rTl-CA to 3.0 mL of 20 mM Tris–HCl buffer, pH 8.0. The reaction was then initiated by the addition of 2.0 mL ice cold CO_2-saturated water. The time interval for the pH to drop by 1 unit (from 8.0 to 7.0) due to the release of protons during CO_2 hydration was measured. One unit of rTl-CA activity was defined as the amount of enzyme required to reduce the pH of the buffer from 8.0 to 7.0, and expressed as Wilbur-Anderson (WA) units per unit volume.

2.5. Biodegradation of cyanate by rTl-Cyn

rTl-Cyn (20 U) was added to reaction mixtures (1 mL total volume) containing 50 mM Tris-HCl buffer (pH 8.0), 3 mM $NaHCO_3$, 4 mM KOCN and was incubated for 10 min at 60 °C in a shaking water bath at 100 rpm. The stability of rTl-Cyn in the presence of heavy metals such as Ag, Au, Cd, Cr, Cu, Fe, Pb and Zn was also evaluated. Additionally, the buffer was replaced with industrial wastewater (1 mL total volume) spiked with 4 mM cyanate. After incubation for 10 min, the samples were centrifuged and the supernatants were analysed by a colorimetric method via product analysis, using a UV-vis spectrophotometer and also assessed for the presence of ammonia and cyanate by Fourier transform infrared spectroscopy as previously described (Ranjan et al., 2017). The concentration of different heavy metals in the wastewater sample was analysed using atomic absorption spectroscopy (AAS) (Srikanth et al., 2013).

2.6. Biodegradation of cyanate by rTl-Cyn and rTl-CA and optimization of their concentrations

rTl-Cyn (20 U) was added to reaction mixtures (1 mL total volume) containing 50 mM Tris-HCl buffer (pH 8.0), 3 mM $NaHCO_3$ and 4 mM KOCN. Incubation of the reaction mixtures was carried out for 10 min at 60 °C in a shaking water bath at 100 rpm, and the liberation of ammonia was measured by colorimetric method. Varying concentrations of $NaHCO_3$ (0.3–3.0 mM) were also added to the buffered mixtures at the above conditions for measurement of the release of ammonia. rTl-Cyn and rTl-CA were also added together, and incubated at the above conditions in the presence of different concentrations of $NaHCO_3$ and was assessed for the degradation of cyanate. Buffered mixtures were also replaced with industrial wastewater and the reaction was carried out under the same conditions.

Varying concentrations of rTl-CA were used in combination with rTl-Cyn, together with different concentrations of $NaHCO_3$, to assess the minimum amount of rTl-CA required for cyanate degradation.

2.7. Synthesis of MNPs

MNPs were prepared by a chemical co-precipitation method (Can et al., 2009), wherein a 1.75:1 molar ratio of Fe^{3+}:Fe^{2+} was dissolved in 320 mL of Milli-Q water. The mixture was stirred vigorously under N_2 at 80 °C for 1 h. Aqueous ammonia solution (25%) was added to the mixture to raise the pH to ~10, and stirred under N_2 sparging for another 1 h and cooled to room temperature. The black magnetic slurry was collected by applying a magnetic field and thereafter washed several times with ethanol followed by Milli-Q water. Finally, MNPs were dispersed by sonication for 15 min and the precipitates were removed and dried under vacuum at 60 °C overnight.

2.8. Silanization of MNPs by (3-aminopropyl)-triethoxysilane (APTES)

The MNPs obtained from co-precipitation (1.0 g) were dispersed in a solution of APTES (20%) and glycerol (4.0 mL) and the mixture was heated for 2 h at 90 °C with simultaneous nitrogen sparging and mechanical stirring (Faridi et al., 2017). The solution was cooled to room temperature, and the modified MNPs were sonicated for 10 min and collected with a magnet followed by washing with ethanol (3 times) and Milli-Q water and dried under vacuum at 60 °C overnight.

2.9. Immobilization of rTl-Cyn and rTl-CA on modified MNPs

Prior to immobilization on modified MNPs, carboxyl groups of rTl-Cyn and rTl-CA were treated with 3-(3 dimethylaminopropyl) N′-ethylcarbodiimide (EDC) and N-hydroxysuccinimide (NHS) as described by Faridi et al. (2017). EDC (4 mg) was added to 10 mL solution of rTl-Cyn:rTl-CA (1:0.75; v/v), incubated at room temperature for 1 h with shaking followed by the addition of 5 mg of NHS. The solution was then added to 20 mg of MNPs and incubated at room temperature for 3 h with gentle shaking.

A schematic illustration of the MNPs synthesis, modification and immobilization of enzyme is shown in Fig. S1.

2.10. Determination of the binding efficiency of rTl-Cyn and rTl-CA onto silanized MNPs

MNPs (5 mg) were mixed with 1–10 mg of the recombinant enzyme for 3 h. After immobilization, the amount of free enzyme in the supernatant was measured by the Lowry method (Lowry et al., 1951), using bovine serum albumin as the standard. The binding capacity of the MNPs against varied enzyme concentrations was determined by the difference in concentration of the free enzyme after immobilization against the initial enzyme concentration (Faridi et al., 2017).

2.11. Characterization of nanoparticles

Adsorption of functional groups on the surface of Fe_3O_4 MNPs was confirmed by infrared spectra of the nanoparticles recorded on FT-IR (Perkin Elmer). Field emission scanning electron microscopy (FE-SEM) was performed using a Zeiss Gemini instrument to study the morphology of MNPs. The crystalline structure and phase purity of the Fe_3O_4 MNPs prepared were identified by X-ray diffraction (Philips PW1830).

2.12. Reusability of the immobilized enzyme

To investigate the reusability of Fe_3O_4/APTES-rTl-Cyn-rTl-CA, the immobilized enzyme was recovered by magnetic separation after each batch and washed several times with Tris–HCl buffer (20 mM, pH 8.0) to prepare it for the subsequent batch.

3. Results and discussion

3.1. Construction, expression and purification of rTl-Cyn and rTl-CA

Tl-Cyn and *Tl-CA* genes were constructed from the cDNA of *T. laniginosus* SSBP and the construction of pET28a-*Tl-Cyn* and pET28a-*Tl-CA* was confirmed by colony PCR and double digestion with *Eco*RI and *Hin*dIII.

The expression of rTl-Cyn and rTl-CA were confirmed by analysing the whole-cell protein profiles of the induced cultures (Fig. 1A). rTl-Cyn and rTl-CA were further purified to homogeneity, and the purity was confirmed by SDS-PAGE, where bands of ~18 kDa and ~22 kDa corresponded to rTl-Cyn and rTl-CA respectively (Fig. 1B). The sizes of rTl-Cyn and rTl-CA were similar to those reported for *E. coli* K12 (17 kDa) (Sung and Fuchs, 1988) and *E. coli* (24 kDa) (Guilloton et al., 1992),

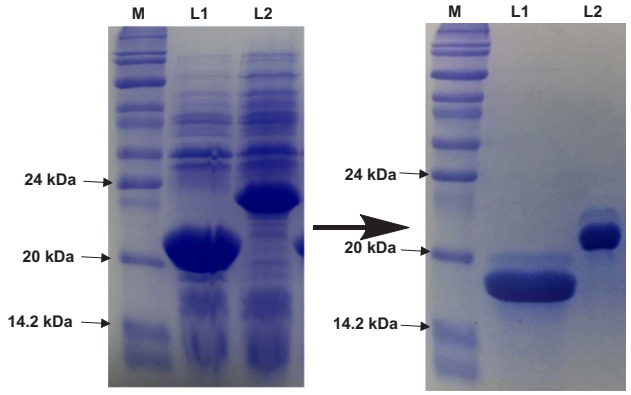

Fig. 1. SDS-PAGE profile of rTl-Cyn and rTl-CA (A) whole-cell protein profile, (B) purified protein profile: M-protein marker; L1-rTl-Cyn; L2-rTl-CA.

respectively.

3.2. Effect of industrial wastewater components on cyanate degradation

The effect of industrial wastewater components, especially heavy metals was tested with purified rTl-Cyn in 50 mM Tris-HCl buffer (pH 8.0) containing 4 mM cyanate. A 100% cyanate degradation was achieved in the buffered condition (without the addition of heavy metals) with 20 U of rTl-Cyn after 10 min, which was confirmed by UV-vis spectrophotometric analysis and also by FT-IR analysis. In other study, approximately 60% of cyanide degradation was observed using the enzyme, cyanide hydratase (Martínková and Chmátal, 2016) and cell free extracts of *Rhodococcus* UKMP-5M decreased the concentration of cyanide by 50% (Nallapan Maniyam et al., 2015). The impact of individual heavy metals (Ag, Au, Cd, Cr, Cu, Fe, Pb or Zn; their concentrations are shown in Table S1) on rTl-Cyn activity in a spiked industrial wastewater sample showed > 91% retention of its initial activity (data not shown). A 10% decrease in enzyme activity was observed when all the heavy metals were applied together. The concentration of cyanate did not decrease in control experiments without rTl-Cyn. Since, cyanate degradation by rTI-Cyn was not significantly affected by the addition of heavy metals which confirmed that the enzyme was relatively robust.

3.3. Application of rTl-Cyn in industrial wastewaters

rTl-Cyn was able to degrade 90% of cyanate in industrial wastewater and similarly 85% of cyanate was degraded when spiked with heavy metals. In buffered conditions, cyanate was completely degraded within 10 min following the addition of rTl-Cyn. FT-IR analysis also confirmed the degradation of cyanate, with peaks in the range of 3400–3320 cm^{-1} for ammonia and 2300–2100 cm^{-1} for cyanate in control experiments (Fig. S2). Hitherto, rTl-Cyn was only used for the removal of cyanate from the industrial wastewater (Ranjan et al., 2017), moreover, other close comparison is the cyanide hydratase expressed in *E. coli* from *Aspergillus niger* K10 which confirms a 80% degradation of cyanide (Rinágelová et al., 2014). Although, rTl-Cyn is able to degrade cyanate in wastewater samples (Ranjan et al., 2017), there is a major dependence on bicarbonate for its effective degradation and this is a complication for any large scale application. To overcome this bottleneck we combined rTl-Cyn and rTl-CA from *T. lanuginosus* SSBP.

3.4. Combinatorial effect of rTl-Cyn and rTl-CA in industrial wastewater bioremediation

Degradation of cyanate by rTl-Cyn was increased from 30 to 100% with increasing concentrations of $NaHCO_3$ from 0.3 to 3 mM (Fig. 2A). In comparison, the combined application of rTl-Cyn and rTl-CA resulted in the complete degradation of cyanate with 0.6 mM $NaHCO_3$ (Fig. 2B). The combined effect of rTl-Cyn and rTl-CA resulted in an enhanced cyanate degradation of ~3-fold in the presence of 0.6 mM $NaHCO_3$ with rTl-CA contributing to an overall enhancement of 64%. Consequently, this synergistic combination enhanced the degradation of cyanate even in the presence of a low concentrations of bicarbonate in comparison to rTl-Cyn alone. Similarly, in another study the integrative system has increased phenol removal from wastewater by ~22% (Jiang et al., 2016a). Although, other cyanases have been reported (Elleuche and Pöggeler, 2008; Luque-Almagro et al., 2008; Qian et al., 2011), however, their potential for the bioremediation of cyanurated wastewaters have not been investigated. The closest comparison to our study was the application of cyanide hydratase and tyrosinase in a two-step process for phenol degradation (Martínková and Chmátal, 2016). Therefore, the combinatorial use of rTl-Cyn and rTl-CA opens up new possibilities for the efficient biodegradation of cyanurated industrial wastes. We also tested 3 different ratios of rTl-CA, while keeping rTl-Cyn concentration constant, for the efficient degradation of cyanate in the presence of different $NaHCO_3$ concentrations (Fig. 2B–D) and found that rTl-Cyn:rTl-CA of 1.0:0.75 was the best ratio (Fig. 2C). This optimized enzyme combination was further used for cyanate degradation as well as immobilization. A schematic representation of the process for the expression of rTl-Cyn and rTl-CA and their combinatorial use to reduce bicarbonate utilization in cyanate removal is shown in Fig. S3.

3.5. Characterization of nanoparticles

FE-SEM images of Fe_3O_4 and Fe_3O_4/APTES nanoparticles revealed that the Fe_3O_4 nanoparticles had a diameter in the range of 50–200 nm (data not shown). No morphological changes were evident for the APTES grafted samples when compared to their bare counterparts (data not shown). Further, FT-IR spectra of the Fe_3O_4, Fe_3O_4/APTES and Fe_3O_4/APTES-rTl-Cyn-rTl-CA nanoparticles showed characteristic peaks (Fig. S4). A peak at 589 cm^{-1} was related to the Fe–O functional groups (Fig. S4A) as evidenced by the characteristic peak for Fe_3O_4 (Zhang et al., 2007). The introduction of APTES to the surface of Fe_3O_4 nanoparticles were confirmed by the band around 1055 cm^{-1} assigned to the Si–O groups (Faridi et al., 2017; Kumar and Cabana, 2016). The peak observed near 1637 cm^{-1} for the Fe_3O_4 nanoparticles was due to the adsorption of water molecules to the surface via hydrogen bonds (Faridi et al., 2017). A broad peak obtained at 3200–3500 cm^{-1} in all of the spectra, originated from the hydroxyl group present on the surface of the particles, uncondensed silanol groups present in the coating layer, and water on the surfaces of the Fe_3O_4 nanoparticles adsorbed physically and chemically (Ma et al., 2003). Thus, peaks shown by FT-IR confirmed the synthesis of Fe_3O_4 nanoparticles and the presence of APTES on its surface. Some peaks were common in Fe_3O_4, Fe_3O_4/APTES and Fe_3O_4/APTES-rTl-Cyn-rTl-CA nanoparticles, however, the peak intensity of Fe_3O_4 grafted with APTES or APTES/enzymes were increased distinctly, which confirmed that functional groups and enzymes were successfully introduced on the nanoparticles. Similar results were observed in with the functionalization of Fe_3O_4 nanoparticles, as reported by Song et al. (2016). XRD analysis confirmed the crystalline structure and phase purity of the Fe_3O_4 nanoparticles, which had six characteristic peaks $2\theta = 35.25°, 41.55°, 50.62°, 63.11°, 67.57°$ and 74.49 (Fig. S5), that matched well with the standard data of Fe_3O_4 (JCPDS 19-629).

3.6. Application of immobilized enzyme in cyanate remediation

Approximately 90% cyanate degradation by Fe_3O_4/APTES-rTl-Cyn was observed in industrial wastewater and complete degradation was achieved with buffered condition at a $NaHCO_3$ concentration of 3 mM. Decreasing concentrations of $NaHCO_3$ resulted in less cyanate degradation (Fig. 3A). Surprisingly, the combination of rTl-Cyn and rTl-

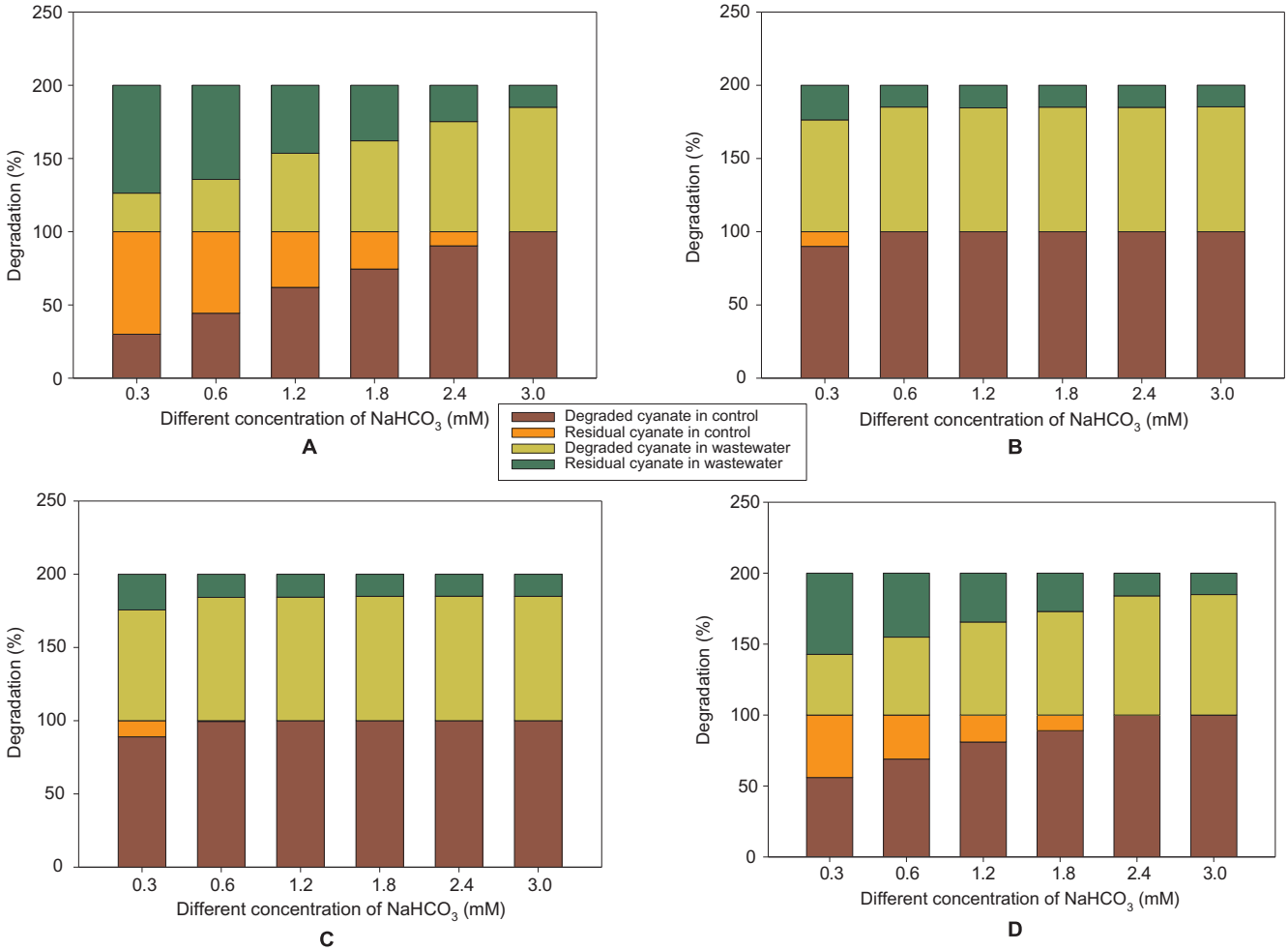

Fig. 2. Degradation of cyanate in control[α] and industrial wastewater[β] at different concentrations of $NaHCO_3$ by using (A) rTl-Cyn, (B) rTl-Cyn:rTl-CA (1:1), (C) rTl-Cyn:rTl-CA (1:0.75), (D) rTl-Cyn:rTl-CA (1:0.5). [[α]buffered conditions without heavy metals. [β]industrial wastewater sample spiked with cyanate and different heavy metals].

CA nanoparticles also achieved a 100% degradation at 0.6 mM concentration of $NaHCO_3$ (Fig. 3B).

3.7. Determination of binding and storage stability of the immobilized enzyme

The economics of industrial applications for enzymes are affected by the cost of enzyme production, therefore, enzymes with long-term

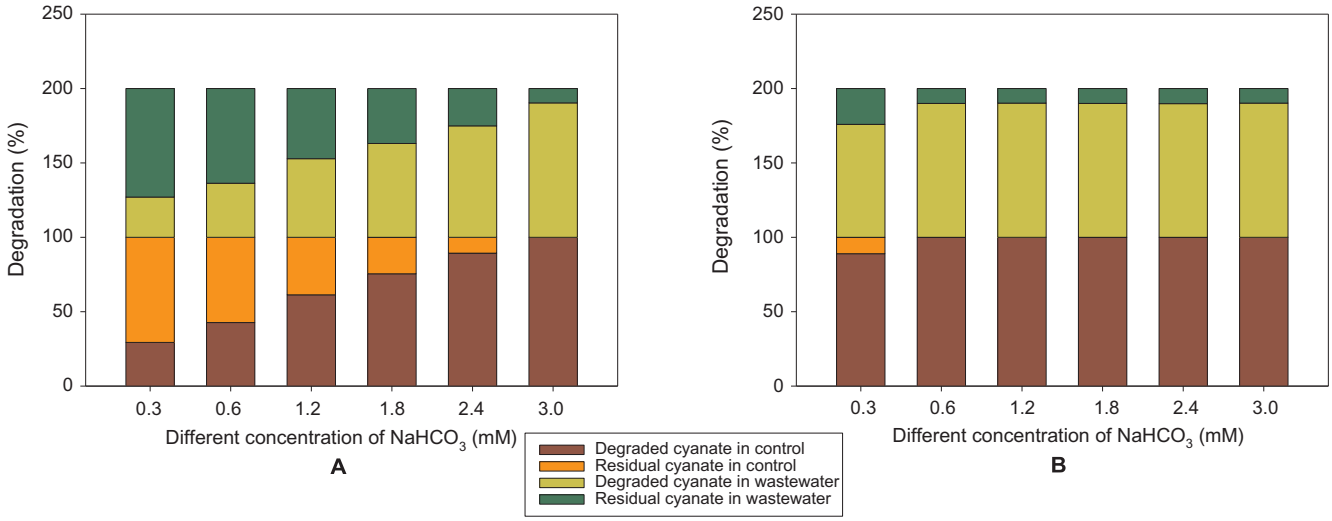

Fig. 3. Degradation of cyanate in control[α] and industrial wastewater[β] at different concentration of $NaHCO_3$ by using (A) Fe_3O_4/APTES-rTl-Cyn, (B) Fe_3O_4/APTES-rTl-Cyn-rTl-CA. [[α]buffered conditions without heavy metals. [β]industrial wastewater sample spiked with cyanate and different heavy metals].

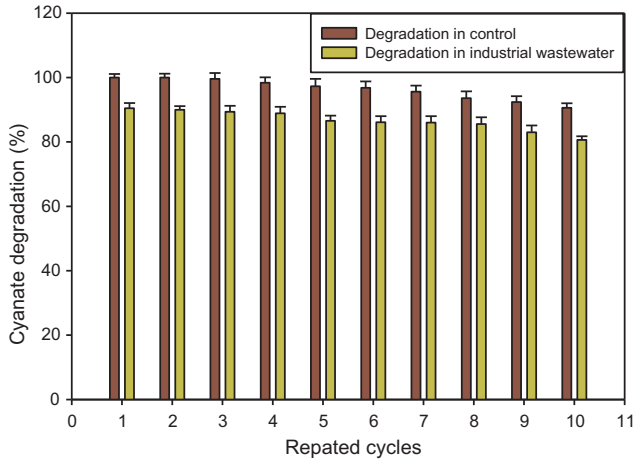

Fig. 4. Reusability of Fe_3O_4/APTES-rTl-Cyn-rTl-CA in cyanate degradation.

reusability and storage stability are preferred (Alex et al., 2014; Faridi et al., 2017). To this end immobilization and storage stability of Fe_3O_4/APTES-rTl-Cyn and Fe_3O_4/APTES-rTl-Cyn-rTl-CA was assessed by incubating them in Tris-HCl buffer (20 mM, pH 8.0) at 4 °C, and evaluated for the release of free enzyme into the supernatant after magnetic settlement. No free enzymes in the supernatant were detected over a 30-day incubation period from Fe_3O_4/APTES-rTl-Cyn and Fe_3O_4/APTES-rTl-Cyn-rTl-CA (data not shown). Similarly, enzymes stored at 4 °C were used for the detection of enzymatic activity every 5 days over a period of 30 days. The storage stability of the immobilized enzymes were sufficiently stable and retained almost 100% of their activity at 4 °C (data not shown), which highlighted its potential for large-scale application.

3.8. Reusability of immobilized enzyme

In an industrial bioremediation process, the reusability of the immobilized enzyme is critical as it determines the biodegradation potential over successive reuses (Jiang et al., 2016b). Thus, one of our goals was to use an immobilized enzyme with efficient bio-catalytic properties and that can be easily recovered and reused. Reusability of immobilized enzymes in this study was evidenced by the presence of more than 80% of residual activity in wastewater and 90% in buffered samples after 10 cycles (Fig. 4).

4. Conclusions

This study revealed that the combinatorial use of rTl-Cyn and rTl-CA reduced the dependence for $NaHCO_3$ by 80% as compared to the rTl-Cyn alone for cyanate remediation. In addition, the enzymes were successfully co-immobilized, with excellent stability retaining 100% of the catalytic activity over a period of 30-days. Of significance is that more than 80% of residual activity in wastewater and buffered samples were retained after 10 cycles with this co-immobilized system. This clearly demonstrates a unique and novel enzyme combination with great potential for the bioremediation of cyanurated wastes on a large-scale.

Acknowledgements

Authors are grateful to the National Research Foundation (NRF–UID 103232), Technology Innovation Agency and the Durban University of Technology, Durban, South Africa for financial support during the course of this investigation.

Conflict of interest

The authors declare that they have no conflict of interest.

Appendix A. Supplementary data

Supplementary data associated with this article can be found, in the online version, at http://dx.doi.org/10.1016/j.biortech.2017.12.087.

References

Alex, D., Mathew, A., Sukumaran, R.K., 2014. Esterases immobilized on aminosilane modified magnetic nanoparticles as a catalyst for biotransformation reactions. Bioresour. Technol. 167, 547–550. http://dx.doi.org/10.1016/j.biortech.2014.05.110.

Barakat, M.A., Chen, Y.T., Huang, C.P., 2004. Removal of toxic cyanide and Cu(II) ions from water by illuminated TiO_2 catalyst. Appl. Catal. B Environ. 53, 13–20. http://dx.doi.org/10.1016/j.apcatb.2004.05.003.

Baxter, J., Cummings, S.P., 2006. The current and future applications of microorganism in the bioremediation of cyanide contamination. Antonie van Leeuwenhoek. Int. J. Gen. Mol. Microbiol. 90, 1–17. http://dx.doi.org/10.1007/s10482-006-9057-y.

Can, K., Ozmen, M., Ersoz, M., 2009. Immobilization of albumin on aminosilane modified superparamagnetic magnetite nanoparticles and its characterization. Colloids Surf. B Biointerfaces 71, 154–159. http://dx.doi.org/10.1016/j.colsurfb.2009.01.021.

Dehnavi, S.M., Pazuki, G., Vossoughi, M., 2015. PEGylated silica-enzyme nanoconjugates: a new frontier in large scale separation of α-amylase. Sci. Rep. 5, 18221. http://dx.doi.org/10.1038/srep18221.

Ebbs, S., 2004. Biological degradation of cyanide compounds. Curr. Opin. Biotechnol. 15, 231–236. http://dx.doi.org/10.1016/j.copbio.2004.03.006.

Elleuche, S., Pöggeler, S., 2008. A cyanase is transcriptionally regulated by arginine and involved in cyanate decomposition in *Sordaria macrospora*. Fungal Genet. Biol. 45, 1458–1469. http://dx.doi.org/10.1016/j.fgb.2008.08.005.

Elmore, M.H., McGary, K.L., Wisecaver, J.H., Slot, J.C., Geiser, D.M., Sink, S., O'Donnell, K., Rokas, A., 2015. Clustering of two genes putatively involved in cyanate detoxification evolved recently and independently in multiple fungal lineages. Genome Biol. Evol. 7, 789–800. http://dx.doi.org/10.1093/gbe/evv025.

Faridi, S., Bose, H., Satyanarayana, T., 2017. Utility of immobilized recombinant carbonic anhydrase of *Bacillus halodurans* TSLV1 on the surface of modified iron magnetic nanoparticles in carbon sequestration. Energy Fuels 31, 3002–3009. http://dx.doi.org/10.1021/acs.energyfuels.6b02777.

Glanpracha, N., Annachhatre, A.P., 2016. Anaerobic co-digestion of cyanide containing cassava pulp with pig manure. Bioresour. Technol. 214, 112–121. http://dx.doi.org/10.1016/j.biortech.2016.04.079.

Guilloton, M.B., Korte, J.J., Lamblin, A.F., Fuchs, J.A., Anderson, P.M., 1992. Carbonic anhydrase in *Escherichia coli*. J. Biol. Chem. 267, 3731–3734.

Huertas, M.J., Sáez, L.P., Roldán, M.D., Luque-Almagro, V.M., Martínez-Luque, M., Blasco, R., Castillo, F., Moreno-Vivián, C., García-García, I., 2010. Alkaline cyanide degradation by *Pseudomonas pseudoalcaligenes* CECT5344 in a batch reactor Influence of pH. J. Hazard. Mater. 179, 72–78. http://dx.doi.org/10.1016/j.jhazmat.2010.02.059.

Jiang, B., Shi, S., Song, L., Tan, L., Li, M., Liu, J., Xue, L., 2016a. Efficient treatment of phenolic wastewater with high salinity using a novel integrated system of magnetically immobilized cells coupling with electrodes. Bioresour. Technol. 218, 108–114. http://dx.doi.org/10.1016/j.biortech.2016.06.080.

Jiang, B., Tan, L., Ning, S., Shi, S., 2016b. A novel integration system of magnetically immobilized cells and a pair of graphite plate-stainless iron mesh electrodes for the bioremediation of coking wastewater. Bioresour. Technol. 216, 684–690. http://dx.doi.org/10.1016/j.biortech.2016.06.009.

Johnson, W.V., Anderson, P.M., 1987. Bicarbonate is a recycling substrate for cyanase. J. Biol. Chem. 262, 9021–9025.

Khalifah, R.G., 1971. The carbon dioxide hydration activity of carbonic anhydrase. J. Biol. Chem. 246, 2561–2573.

Kumar, V.V., Cabana, H., 2016. Towards high potential magnetic biocatalysts for on-demand elimination of pharmaceuticals. Bioresour. Technol. 200, 81–89. http://dx.doi.org/10.1016/j.biortech.2015.09.100.

Lowry, O.H., Rosebrough, N.J., Farr, A.L., Randall, R.J., 1951. Protein measurement with the Folin phenol reagent. J. Biol. Chem. 193, 265–275. http://dx.doi.org/10.1016/0304-3894(92)87011-4.

Luque-almagro, V.M., Blasco, R., Mart, M., Moreno-vivi, C., Rold, M.D., 2011. Bacterial cyanide degradation is under review: *Pseudomonas pseudoalcaligenes* CECT5344, a case of an alkaliphilic cyanotroph. Biochem. Soc. Trans. 39, 269–274. http://dx.doi.org/10.1042/BST0390269.

Luque-Almagro, V.M., Huertas, M.J., Sáez, L.P., Luque-Romero, M.M., Moreno-Vivián, C., Castillo, F., Roldán, M.D., Blasco, R., 2008. Characterization of the *Pseudomonas pseudoalcaligenes* CECT5344 cyanase, an enzyme that is not essential for cyanide assimilation. Appl. Environ. Microbiol. 74, 6280–6288. http://dx.doi.org/10.1128/AEM.00916-08.

Luque-Almagro, V.M., Moreno-Vivián, C., Roldán, M.D., 2016. Biodegradation of cyanide wastes from mining and jewellery industries. Curr. Opin. Biotechnol. 38, 9–13. http://dx.doi.org/10.1016/j.copbio.2015.12.004.

Ma, M., Zhang, Y., Yu, W., Shen, H., Zhang, H., Gu, N., 2003. Preparation and characterization of magnetite nanoparticles coated by amino silane. Colloids Surf. A

Physicochem. Eng. Asp. 212, 219–226.
Madhavan, A., Sindhu, R., Binod, P., Sukumaran, R.K., Pandey, A., 2017. Strategies for design of improved biocatalysts for industrial applications. Bioresour. Technol. 245, 1304–1313. http://dx.doi.org/10.1016/j.biortech.2017.05.031.
Martínková, L., Chmátal, M., 2016. The integration of cyanide hydratase and tyrosinase catalysts enables effective degradation of cyanide and phenol in coking wastewaters. Water Res. 102, 90–95. http://dx.doi.org/10.1016/j.watres.2016.06.016.
Nallapan Maniyam, M., Sjahrir, F., Latif Ibrahim, A., Cass, A.E.G., 2015. Enzymatic cyanide degradation by cell-free extract of *Rhodococcus* UKMP − 5M. J. Environ. Sci. Health Part A 50, 357–364. http://dx.doi.org/10.1080/10934529.2015.987524.
Pal, P., Kumar, R., 2013. Treatment of coke wastewater: a critical review for developing sustainable management strategies. Sep. Purif. Rev. 43, 89–123. http://dx.doi.org/10.1080/15422119.2012.717161.
Papadimitriou, C.A., Dabou, X., Samaras, P., Sakellaropoulos, G.P., 2006. Coke oven wastewater treatment by two activated sludge systems. Glob. NEST 8, 16–22.
Papadimitriou, C.A., Samaras, P., Sakellaropoulos, G.P., 2009. Comparative study of phenol and cyanide containing wastewater in CSTR and SBR activated sludge reactors. Bioresour. Technol. 100, 31–37. http://dx.doi.org/10.1016/j.biortech.2008.06.004.
Parashar, D., Satyanarayana, T., 2016. A chimeric α-amylase engineered from *Bacillus acidicola* and *Geobacillus thermoleovorans* with improved thermostability and catalytic efficiency. J. Ind. Microbiol. Biotechnol. 43, 473–484. http://dx.doi.org/10.1007/s10295-015-1721-7.
Pereira, L., Dias, P., Soares, O.S.G.P., Ramalho, P.S.F., Pereira, M.F.R., Alves, M.M., 2017. Synthesis, characterization and application of magnetic carbon materials as electron shuttles for the biological and chemical reduction of the azo dye acid orange 10. Appl. Catal. B Environ. 212, 175–184. http://dx.doi.org/10.1016/j.apcatb.2017.04.060.
Qian, D., Jiang, L., Lu, L., Wei, C., Li, Y., 2011. Biochemical and structural properties of cyanases from *Arabidopsis thaliana* and *Oryza sativa*. PLoS One 6, 1–10. http://dx.doi.org/10.1371/journal.pone.0018300.
Ranjan, B., Pillai, S., Permaul, K., Singh, S., 2017. Expression of a novel recombinant cyanate hydratase (rTl-Cyn) in *Pichia pastoris*, characteristics and applicability in the detoxification of cyanate. Bioresour. Technol. 238, 582–588. http://dx.doi.org/10.1016/j.biortech.2017.04.091.
Ranjan, B., Singh, B., Satyanarayana, T., 2015. Characteristics of recombinant phytase (rSt-Phy) of the thermophilic mold *Sporotrichum thermophile* and its applicability in dephytinizing foods. Appl. Biochem. Biotechnol. 177, 1753–1766. http://dx.doi.org/10.1007/s12010-015-1851-4.
Rinágelová, A., Kaplan, O., Veselá, A.B., Chmátal, M., Křenková, A., Plíhal, O., Pasquarelli, F., Cantarella, M., Martínková, L., 2014. Cyanide hydratase from *Aspergillus niger* K10: overproduction in *Escherichia coli*, purification, characterization and use in continuous cyanide degradation. Process Biochem. 49, 445–450. http://dx.doi.org/10.1016/j.procbio.2013.12.008.
Ryu, B.G., Kim, J., Han, J.I., Yang, J.W., 2017. Feasibility of using a microalgal-bacterial consortium for treatment of toxic coke wastewater with concomitant production of microbial lipids. Bioresour. Technol. 225, 58–66. http://dx.doi.org/10.1016/j.biortech.2016.11.029.
Sharma, N.K., Philip, L., 2014. Effect of cyanide on phenolics and aromatic hydrocarbons biodegradation under anaerobic and anoxic conditions. Chem. Eng. J. 256, 255–267. http://dx.doi.org/10.1016/j.cej.2014.06.070.
Sharma, N.K., Philip, L., Murty Bhallamudi, S., 2012. Aerobic degradation of phenolics and aromatic hydrocarbons in presence of cyanide. Bioresour. Technol. 121, 263–273. http://dx.doi.org/10.1016/j.biortech.2012.06.039.
Singh, S., Pillay, B., Dilsook, V., Prior, B.A., 2000. Production and properties of hemicellulases by a *Thermomyces lanuginosus* strain. J. Appl. Microbiol. 88, 975–982. http://dx.doi.org/10.1046/j.1365-2672.2000.01063.x.
Song, W., Gao, B., Xu, X., Xing, L., Han, S., Duan, P., Song, W., Jia, R., 2016. Adsorption-desorption behavior of magnetic amine/Fe_3O_4 functionalized biopolymer resin towards anionic dyes from wastewater. Bioresour. Technol. 210, 123–130. http://dx.doi.org/10.1016/j.biortech.2016.01.078.
Srikanth, P., Somasekhar, S.A., Babu, K.R., Pradesh, A., 2013. Analysis of heavy metals by using atomic absorption spectroscopy from the samples taken around Visakhapatnam. Int. J. Environ. Ecol. Famiy Urban Stud. 3, 127–132.
Sung, Y.C., Fuchs, J.A., 1988. Characterization of the cyn operon in *Escherichia coli* K12. J. Biol. Chem. 263, 14769–14775.
Xu, L., Wang, J., 2012. Environmental fenton-like degradation of 2,4-dichlorophenol using Fe_3O_4 magnetic nanoparticles. Appl. Catal. B Environ. 123–124, 117–126. http://dx.doi.org/10.1016/j.apcatb.2012.04.028.
Zhang, J.L., Srivastava, R.S., Misra, R.D.K., 2007. Core-shell magnetite nanoparticles surface encapsulated with smart stimuli-responsive polymer: synthesis, characterization, and LCST of viable drug-targeting delivery system. Langmuir 23, 6342–6351. http://dx.doi.org/10.1021/la0636199.
Zhou, Y., Yu, S., Liu, Q., Yan, D., Wang, Y., Gao, L., Han, J., 2017. Synchronized purification and immobilization of his-tagged β-glucosidase via Fe_3O_4/PMG core/shell magnetic nanoparticles. Sci. Rep. 7, 41741. http://dx.doi.org/10.1038/srep41741.